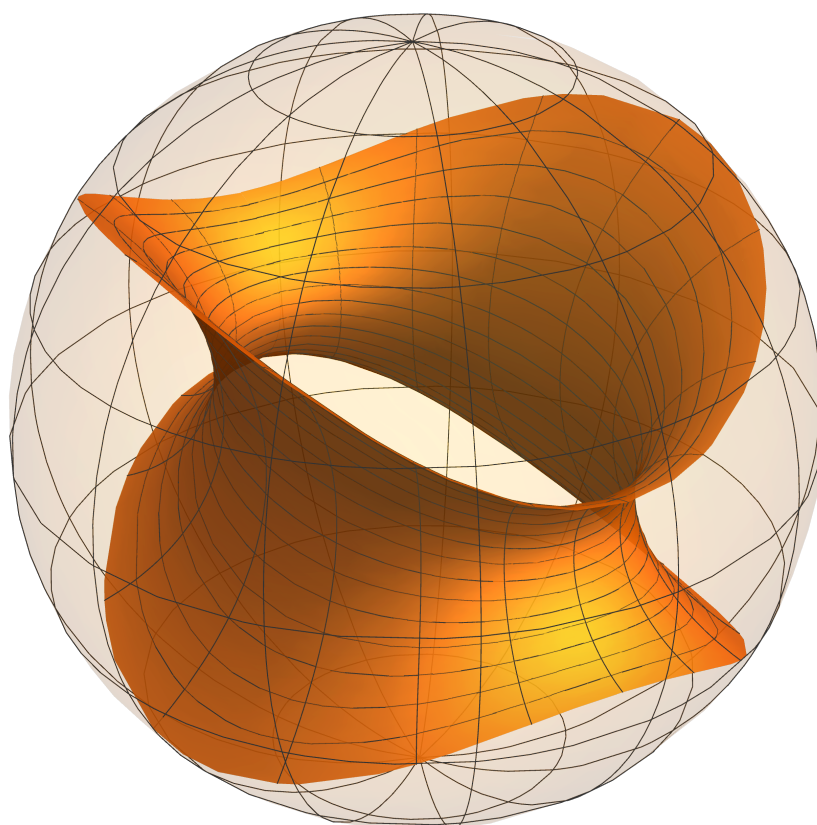


CONSTANT MEAN CURVATURE ANNULI WITH FREE BOUNDARY



ALBERTO CEREZO CID

Sevilla, July 2025

Supervisors: Isabel Fernández Delgado and Pablo Mira Carrillo

Agradecimientos

Una tarde de noviembre de 2018, y a raíz de la recomendación de un profesor de la carrera, decidí escribirle un correo a Isabel Fernández. Por aquel entonces, estaba en tercero de carrera, tenía cierto interés por saber algo más sobre análisis y geometría, y una idea algo vaga de lo que podía ser la investigación en matemáticas. Tras la primera reunión con Isa, salí con dos certezas: por un lado, que tenía que leerme el *do Carmo* de curvas y superficies; y por otro, que había conocido a mi primera referente en el mundo de la investigación. Mi segundo referente, Pablo, llegó un poco después, en 2021.

Os estoy profundamente agradecido por todo lo que he aprendido de vosotros, tanto en lo académico como lo personal. También por vuestro apoyo incondicional, dedicación, tiempo y paciencia. Debo destacar asimismo la constante motivación y todas las ideas que me habéis transmitido. Me siento muy afortunado por haber tenido la oportunidad de haberos conocido y trabajar con vosotros, y espero y deseo seguir haciéndolo en el futuro. Como persona con vocación docente e investigadora, me gustaría poder inspirar a otros estudiantes de la misma forma que lo habéis hecho conmigo.

Eu também gostaria de agradecer ao Professor Lucas Ambrozio por ter me recebido durante os 3 meses de estadia no Instituto de Matemática Pura e Aplicada. Foi uma experiência profundamente enriquecedora para mim. Queria também agradecer aos estudantes do IMPA, especialmente ao meu *parce* Carlos, por terem me acolhido. Senti-me em casa desde a primeira semana, e só estou desejando voltar a passar mais uma temporada na Cidade Maravilhosa.

En estos agradecimientos no podía olvidarme de mi gente del IMUS, ni de todo lo que me habéis regalado en este tiempo: vivencias, metrolíos, todo un diccionario de palabras en clave, y por supuesto, muchas amistades que guardo con especial cariño. Habéis hecho que estos tres años se pasen rapidísimo. Sin lugar a dudas, parte de lo que soy a día de hoy se explica gracias a vosotros. Nos vemos en la quedá de Triana, en una casa rural, en la media maratón de Sevilla, en la próxima feria de Mairena, o donde sea. *De nada*.

Por último, y aunque cualquier cosa que pueda decir de ellos va a resultar insuficiente, gracias a mis padres, Andrés y María. Por vuestro infinito cariño, dedicación constante, y sobre todo por haberme otorgado el privilegio de que estudiar haya sido mi única preocupación durante todos estos años. Aunque lo neguéis, soy consciente del esfuerzo que os ha supuesto, y de que estoy en deuda con vosotros. Y finalmente, gracias por haber cultivado desde edades muy tempranas mi curiosidad por aprender. Esta tesis es el fruto de ello, y también es vuestra.

This thesis has been financially supported by Grant PID2020-118137GB-I00 funded by MICIU/AEI/10.13039/501100011033 and by ESF+.

Resumen

En esta tesis se estudia la existencia de superficies de curvatura media constante no rotacionales, difeomorfas a anillos, que tienen borde libre en una bola de un espacio tridimensional de curvatura constante. Estas superficies aparecen de forma natural en el problema de la partición, consistente en encontrar puntos críticos del funcional área en la familia de superficies que dividen la bola en dos piezas de volúmenes dados. En este contexto, la condición de borde libre se refiere a que la superficie y la bola se intersecan ortogonalmente a lo largo de su frontera.

Las construcciones realizadas se basan en el estudio del conjunto de superficies de curvatura media constante foliadas por líneas de curvatura esféricas. Esto es, cada curva de la foliación pertenece a una superficie totalmente umbílica del espacio ambiente, y ambas superficies se intersecan con ángulo constante a lo largo de la curva. En el Capítulo 2 presentamos un estudio general de estas superficies.

En el Capítulo 3 construimos anillos no rotacionales de curvatura media constante con borde libre en la bola unidad del espacio euclídeo tridimensional. Además, estos ejemplos son embebidos, es decir, no tienen autointersecciones. La existencia de estos anillos resuelve un problema abierto planteado por Henry C. Wente en 1995.

En el Capítulo 4 extendemos este resultado al caso general de anillos con curvatura media constante y borde libre en bolas geodésicas de los espacios esférico e hiperbólico tridimensional. En este caso, los anillos obtenidos son embebidos bajo una restricción sobre la curvatura media. En particular, para el caso de superficies mínimas en la 3-esfera, construimos anillos de borde libre con autointersecciones.

En el Capítulo 5 construimos anillos mínimos de borde libre en bolas geodésicas del espacio hiperbólico. En este caso, los ejemplos obtenidos no son embebidos.

En el Capítulo 6 estudiamos superficies capilares en la bola unidad del espacio euclídeo. La hipótesis de capilaridad significa que el ángulo de intersección entre la superficie y el borde de la bola es constante, pero no necesariamente ortogonal. En este caso, construimos familias de anillos mínimos no rotacionales y embebidos que presentan un patrón de tipo Delaunay, interpolando entre un trozo de catenoide y una

cadena de discos verticales. Finalmente, al estudiar las imágenes de estos anillos por la aplicación de Gauss, damos contraejemplos a una conjetura de 2005 de Souam sobre la simetría radial de las soluciones a un problema tipo Schiffer sobredeterminado en la esfera 2-dimensional.

Abstract

In this thesis we investigate the existence of non-rotational compact surfaces of constant mean curvature, diffeomorphic to an annulus, that have free boundary in a ball of a 3-dimensional space of constant curvature. Such surfaces appear naturally when one considers the classical partitioning problem of finding critical points of the area functional among surfaces that divide the ball into two pieces of prescribed volumes. The free boundary condition means, in this context, that the surface and the ball intersect orthogonally along the boundary.

Our constructions are based on the ansatz of studying surfaces of constant mean curvature that are foliated by spherical curvature lines. This means that each curve of the foliation lies in a totally umbilical surface of the ambient manifold, and both surfaces meet at a constant angle along the curve. A general study of such surfaces is presented in Chapter 2.

In Chapter 3 we construct non-rotational free boundary constant mean curvature annuli in the unit ball of Euclidean 3-space that are embedded, i.e., they do not self-intersect. This solves in the negative a 1995 open problem by Wente.

In Chapter 4 we extend this theorem to free boundary constant mean curvature annuli in geodesic balls of the 3-dimensional sphere and the 3-dimensional hyperbolic space. This time, the embeddedness property of the examples is only true for some values of the mean curvature. For other values, like the case of minimal surfaces in the 3-sphere, we construct free boundary annuli with self intersections.

In Chapter 5 we use a deformation procedure to obtain free boundary minimal annuli in geodesic balls of the hyperbolic space. All of them are non-embedded.

In Chapter 6 we study capillary minimal surfaces, where the capillarity assumption means here that the intersection angle with the ball is constant along the boundary, but not necessarily orthogonal. In that situation, we find families of non-rotational embedded capillary minimal annuli in the unit ball that present a Delaunay-type pattern, interpolating between a piece of a catenoid and a chain of vertical flat disks. Finally, by studying the images of these annuli via the Gauss map, we give a counterexample

to a 2005 conjecture by Souam regarding the radial symmetry of solutions to an overdetermined Schiffer-type problem in the 2-dimensional sphere.

Contents

1	Introduction	1
2	Preliminaries	13
2.1	Summary	13
2.2	CMC surfaces immersed in space forms	13
2.3	Umbilics and topology of CMC surfaces	15
2.4	Enneper-type surfaces in \mathbb{R}^3	16
2.5	Enneper-type surfaces in space forms	23
2.5.1	A model for the space forms $\mathbb{M}^3(\kappa)$	23
2.5.2	Enneper-type surfaces in $\mathbb{M}^3(\kappa)$	25
2.6	Rotational free boundary CMC annuli in geodesic balls	28
2.6.1	Rotational CMC surfaces in $\mathbb{M}^3(\kappa)$	28
2.6.2	Existence of rotational free boundary CMC surfaces	32
2.7	Final notes	44
3	Free boundary CMC annuli in \mathbb{B}^3	49
3.1	Summary and main result	49
3.2	A family of Enneper-type CMC surfaces in \mathbb{R}^3	50
3.2.1	Constructing solutions to the sinh-Gordon equation	50
3.2.2	Construction of CMC $H = \frac{1}{2}$ immersions in \mathbb{R}^3	53
3.2.3	The case $a = 1, c > 1$: nodoids	55
3.3	Geometric properties of the surfaces $\Sigma(a, b, c)$	57
3.4	The orthogonality condition	60
3.4.1	The system (s, t)	60
3.4.2	The map $\tau(a, b, c)$	64
3.5	The period map	66
3.6	CMC annuli with spherical free boundary	68
3.7	Proof of Theorem 3.1.1	73

3.8	Final notes	76
4	Free boundary annuli in geodesic balls of space forms	79
4.1	Summary and main result	79
4.2	A family of Enneper-type surfaces in $\mathbb{M}^3(\kappa)$	82
4.3	Geometric properties of $\Sigma(a, b, c)$	85
4.4	The period map in $\mathbb{M}^3(\kappa)$	87
4.5	Construction of CMC annuli in $\mathbb{M}^3(\kappa)$	90
4.6	The case $a = 1$: rotational surfaces	92
4.7	The period map for rotational surfaces	94
4.8	Detecting critical rotational annuli	97
4.9	Proof of the main theorems	105
4.9.1	Proof of Theorem 4.1.1	105
4.9.2	Proof of Theorem 4.1.2	110
4.10	Embedded capillary minimal and CMC annuli in \mathbb{S}^3	111
4.10.1	Proof of Theorem 4.10.1	112
4.11	Final notes	114
5	Free boundary minimal annuli in hyperbolic balls	117
5.1	Summary and main result	117
5.2	A family of minimal immersions of Enneper type in $\mathbb{M}^3(\kappa)$	120
5.2.1	Constructing solutions to an overdetermined system	120
5.2.2	Construction of minimal immersions in $\mathbb{M}^3(\kappa)$	123
5.3	Geometric properties of $\Sigma(a, b, \kappa)$	126
5.3.1	The period map	127
5.3.2	Constructing minimal annuli	128
5.3.3	The geometry of the surfaces $\Sigma(1, b, \kappa)$	129
5.4	The period map for rotational immersions	131
5.5	The map $\tau(a, b, \kappa)$	133
5.5.1	Case $\kappa > 0$	135
5.5.2	Case $\kappa = 0$	138
5.6	Detecting the Euclidean free boundary catenoid	142
5.6.1	The case $(1, 1, 0) \in \mathcal{O}$	143
5.6.2	The orthogonal radius	144
5.7	Proof of the main theorem	148
5.7.1	The curve μ and the period map	149

5.7.2	The height map	151
5.7.3	Proof of Theorem 5.1.1	152
5.8	Final notes	154
6	Capillary minimal annuli in \mathbb{B}^3	157
6.1	Summary and main results	157
6.2	A family of minimal immersions of Enneper type in \mathbb{R}^3	159
6.2.1	A set of solutions to (2.14)	159
6.2.2	The induced minimal immersions	162
6.2.3	The limit case $a = 0$	163
6.2.4	The limit case $a = 1$: catenoids	165
6.3	The period map	166
6.4	The embeddedness property	170
6.4.1	The family of embedded capillary annuli	170
6.4.2	The limit $a = 0$	178
6.5	Proof of the main theorems	183
6.5.1	Proof of Theorem 6.1.1	183
6.5.2	Proof of Theorem 6.1.2	183
6.6	Preliminary lemmas	185
6.6.1	The system (s, t)	186
6.6.2	Proof of preliminary lemmas	191
6.7	An application to an overdetermined problem in \mathbb{S}^2	194
6.7.1	Proof of Theorem 6.7.1	198
6.7.2	Proof of Theorem 6.7.2	199
6.8	Final notes	200

Chapter 1

Introduction

The study of minimal and constant mean curvature surfaces is a classical area in differential geometry whose origins are closely related to physics and variational problems. To better understand this connection, let Σ be an interface separating two static fluids. The equilibrium configuration of Σ depends on the balance between surface tension and the difference in pressures Δp between fluids. This relation is made precise by Young-Laplace's law,

$$\Delta p = 2\gamma H. \quad (1.1)$$

Here, γ is the surface tension coefficient and H is the mean curvature of the surface, given by

$$H = \frac{\kappa_1 + \kappa_2}{2}, \quad (1.2)$$

where κ_1, κ_2 are the principal curvatures of the surface. Thus, it follows from (1.1) that when the pressure difference Δp is uniform across the interface, the mean curvature must be constant. This motivates the following definition:

Definition 1.1. *We say that a surface Σ in Euclidean 3-space has constant mean curvature (CMC) if $H = \text{const}$. In particular, if $H \equiv 0$, we say that Σ is minimal.*

According to (1.1), minimal surfaces appear when the pressure difference is zero across the interface. A physical example of this situation occurs when one considers a soap film bounded by a wire frame. In this case, the surface tension drives the film toward a configuration of minimal area. This establishes a connection between minimal surfaces and calculus of variations, which we detail next.

From a variational point of view, minimal surfaces (that is, surfaces whose mean curvature vanishes) can be characterized as critical points of the area functional. This mathematical equivalence aligns with the physical phenomenon observed in soap films

due to surface tension. More generally, CMC surfaces with $H \neq 0$ can be seen as critical points of the area subject to volume constraints, establishing a strong connection between calculus of variations and the concept of mean curvature.

We consider next a smooth bounded 3-dimensional domain W in \mathbb{R}^3 , and restrict ourselves to compact smooth surfaces Σ in \mathbb{R}^3 with boundary $\partial\Sigma$, so that $\text{int}\Sigma \subset \text{int}W$ and $\partial\Sigma \subset \partial W$. In this situation we can consider the *partitioning problem* of finding the critical points of the area functional among all such surfaces Σ that divide W into two pieces of prescribed volumes. See [62, 66, 67]. The resulting critical points are constant mean curvature surfaces that intersect ∂W orthogonally along $\partial\Sigma$. This motivates the following definition:

Definition 1.2. A free boundary CMC surface in $W \subset \mathbb{R}^3$ is a compact CMC surface Σ with $\text{int}\Sigma \subset \text{int}W$, non-empty boundary $\partial\Sigma \subset \partial W$, and so that Σ intersects ∂W orthogonally along $\partial\Sigma$.

In a similar way, we say that a surface $\Sigma \subset W$ defines a *capillary CMC surface* in W if it has constant mean curvature and it intersects ∂W along $\partial\Sigma$ with a constant angle θ . Capillary surfaces are also solutions to a natural variational problem related to the area functional, see [66]. The study of free boundary minimal surfaces goes back, at least, to the work of Courant in the 1940s, [20].

A particular case of special importance takes place when the container W is the unit ball \mathbb{B}^3 of \mathbb{R}^3 , since in that symmetric case it is possible to develop a more detailed geometric theory associated to it. The pioneer work in this direction is the 1985 paper [62] by Nitsche, who proved that any immersed capillary CMC surface in \mathbb{B}^3 homomorphic to a disk should be totally umbilical, and hence a flat disk (if $H = 0$) or a spherical cap (if $H \neq 0$). This theorem is the natural boundary analogue of the famous Hopf theorem in [42], according to which any CMC surface in \mathbb{R}^3 homeomorphic to \mathbb{S}^2 should be a *round* totally umbilic sphere. Nitsche also discussed in [62] how certain compact pieces of catenoids and rotational CMC surfaces (unduloids and nodoids) produced free boundary CMC surfaces in \mathbb{B}^3 with the topology of an annulus. In the minimal case, there is only one such example, which receives the name of *critical catenoid*; see Figure 1.1. For several decades, the only known examples of embedded (i.e. without self-intersections) free boundary CMC surfaces in \mathbb{B}^3 were these rotational examples we just discussed.

This situation changed around 10 years ago, due to the seminal work by Fraser and Schoen [34, 35]. These authors established a deep connection between free boundary minimal surfaces in \mathbb{B}^3 and the theory of eigenvalue optimization for the Steklov

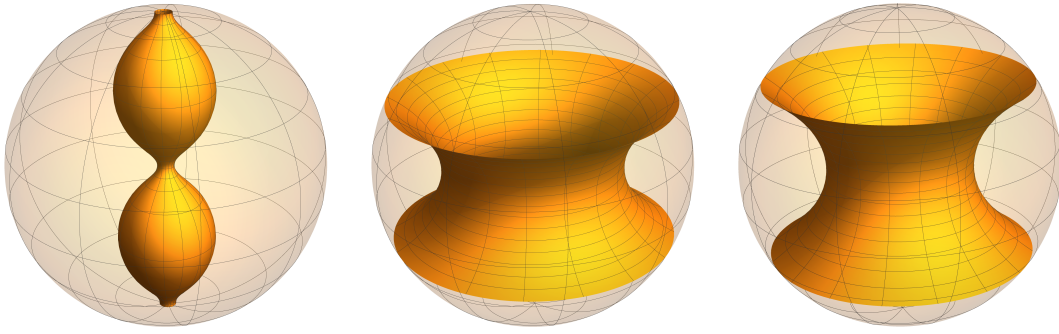


Figure 1.1: Example of a free boundary unduloid (left), nodoid (center) and the critical catenoid (right) in \mathbb{B}^3 .

problem in Riemannian surfaces. Motivated by these works, the theory of free boundary minimal surfaces in \mathbb{B}^3 experienced a revolution, flourishing in several directions. One of them was the construction of new embedded free boundary minimal surfaces in \mathbb{B}^3 , via perturbative arguments (gluing) [36, 43, 44, 45, 46, 47], variational theory (min-max) [10, 11, 30, 31, 50] or eigenvalue optimization [34, 35, 48, 49]. Recently, Karpukhin, Kusner, McGrath and Stern [48] solved the general problem of topological realization of such surfaces: *there exist embedded free boundary minimal surfaces in \mathbb{B}^3 of all possible orientable topologies, i.e. with any genus g and any number $k \geq 1$ of boundary components*. An account of many numerical simulations of all these new examples in the theory can be found in Schulz's gallery [69].

Once the general topological existence theorem has been obtained, one is naturally led to the problem of topological uniqueness, that is: *is any embedded free boundary minimal surface in \mathbb{B}^3 uniquely determined (up to ambient isometries) by its topology?* Note that the answer is affirmative in the simplest topological case (disks) by Nitsche's theorem in [62] mentioned above. However, for more complicated topologies, the answer is negative, see [11, 48]. These results put the focus on the case of annular topology, and more specifically on the following famous conjecture:

Conjecture 1.3 (Critical catenoid conjecture). *The critical catenoid is, up to ambient isometry, the only free boundary minimal annulus embedded in \mathbb{B}^3 .*

The conjecture is commonly associated to the names of Fraser and Li after [33], see also [32, 55], but the problem of the topological uniqueness of the critical catenoid is much older, and was already discussed in the original work of Nitsche [62]. In that work, Nitsche claimed without a proof that any free boundary minimal or CMC annulus in \mathbb{B}^3 , embedded or not, should be a rotational example. Recently, Fernández, Hauswirth and Mira [29] constructed counterexamples to Nitsche's claim, in the form

of *immersed* (non-embedded) free boundary minimal annuli in \mathbb{B}^3 . For that, they used the Weierstrass representation of minimal surfaces as a fundamental tool. Later on, Kapouleas-McGrath [43] presented an alternative, more analytical construction via doubling. Still, the critical catenoid conjecture remains open, despite several partial affirmative answers to it obtained by different authors under additional hypotheses, see [3, 22, 27, 29, 35, 43, 59, 65].

Conjecture 1.3 is commonly conceived as the natural boundary analogue of the famous Lawson conjecture [54], according to which the Clifford torus $\mathbb{S}^1(1/\sqrt{2}) \times \mathbb{S}^1(1/\sqrt{2}) \subset \mathbb{S}^3$ is, up to isometry, the only embedded minimal torus in the unit 3-sphere \mathbb{S}^3 . This conjecture was proved by Brendle [6], using an argument based on a maximum principle for a two-point function that, up to now, does not seem to work in the free boundary case. Later on, Andrews and Li [4] adapted Brendle's argument to the general CMC case and proved the Pinkall-Sterling conjecture in [63]: *any embedded CMC torus in \mathbb{S}^3 is rotational*.

In view of the previous discussion, the following problem, which was proposed by Wente [77] in 1995, comes up in a natural way.

Open problem 1.4 ([77]). *Are all embedded free boundary CMC annuli in \mathbb{B}^3 rotational?*

We note that this problem is the extension of the critical catenoid conjecture to the general CMC case, and also the natural boundary version of the Pinkall-Sterling conjecture for CMC tori in \mathbb{S}^3 mentioned above. The embeddedness assumption here is necessary, since Wente constructed in [77] examples of immersed free boundary CMC annuli with very large mean curvature in the unit ball of \mathbb{R}^3 .

The first main theorem of this thesis gives a negative answer to Wente's problem. Specifically, we prove (see Theorem 3.1.1):

For each $n \geq 2$ there exists a real analytic, one-parameter family of free boundary CMC annuli $\mathbb{A}_n(\tau)$, $\tau \in (0, \varepsilon)$, embedded in \mathbb{B}^3 , with a prismatic symmetry group of order $4n$. In particular, these annuli are not rotational; see Figure 1.2.

In this construction, the mean curvature of the examples is not fixed, that is, given n , each $\mathbb{A}_n(\tau)$ has in general a different constant mean curvature value. When $\tau \rightarrow 0$, the annuli $\mathbb{A}_n(\tau)$ converge to an embedded free boundary piece in \mathbb{B}^3 of an adequate nodoid.

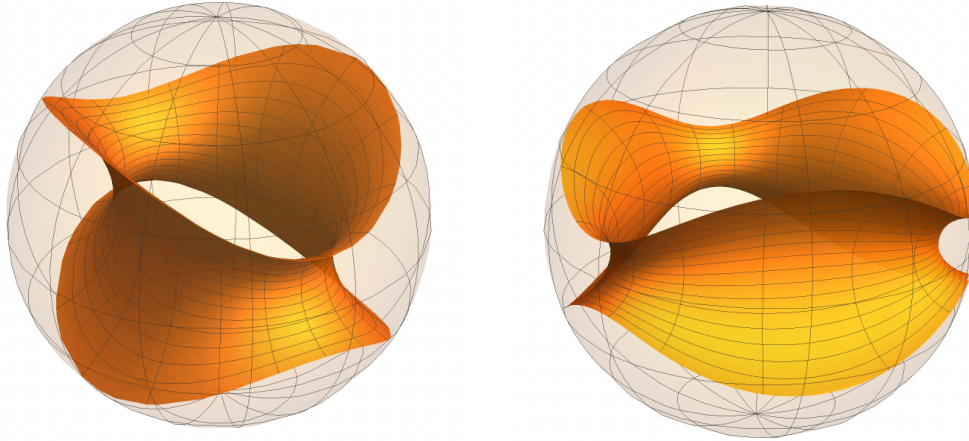


Figure 1.2: Examples of non-rotational free boundary CMC annuli $\mathbb{A}_n(\tau)$ with $n = 2$ (left) and $n = 3$ (right).

We remark that the CMC annuli $\mathbb{A}_n(\tau)$ that we construct constitute, up to now, the only known examples of non-rotational embedded free boundary CMC surfaces in \mathbb{B}^3 with non-zero mean curvature (of any topology). They also show that the Andrews-Li uniqueness theorem for embedded CMC tori in \mathbb{S}^3 does not hold in the free boundary case.

The construction method for these embedded annuli $\mathbb{A}_n(\tau)$ is via the study of the CMC surfaces in \mathbb{R}^3 with the special property of being *foliated by spherical curvature lines*. This means that, after choosing adequate conformal parameters (u, v) on the CMC surface Σ , the image of each parametric curve $v \mapsto (u_0, v)$ in Σ is contained in some sphere (or plane) $\mathbb{S}^2(c(u_0), R(u_0))$ of \mathbb{R}^3 , and Σ intersect this sphere with a constant angle $\theta(u_0)$ along that curve. Analytically, these surfaces are obtained by solving the following overdetermined problem for the classical sinh-Gordon equation:

$$\begin{cases} \Delta\omega + \sinh \omega \cosh \omega = 0, \\ 2\omega_u = \alpha(u)e^\omega + \beta(u)e^{-\omega} \end{cases} \quad (1.3)$$

Here, $e^{2\omega}(du^2 + dv^2)$ denotes the metric of Σ after being conformally parametrized by curvature lines, and $\alpha(u), \beta(u)$ are real functions. The first equation appears as the Gauss equation for Σ in these parameters, while the second one reflects the foliation structure by spherical curvature lines. This type of CMC surfaces were already considered by some differential geometers of the 19th century such as Enneper, Darboux or Dobriner, and their basic geometry was put into a more modern form by Wente in [76].

The idea of the construction is inspired in the work [29] by Fernández, Hauswirth and Mira in the minimal case, which also considered surfaces foliated by spherical curvature lines. However, in our CMC case there is no Weierstrass representation available, and so many of the ideas in [29] do not work here.

The basic problems regarding the geometry of free boundary and capillary CMC surfaces in the unit ball of \mathbb{R}^3 can also be formulated naturally in the context of metric balls in the space forms $\mathbb{M}^3(\kappa)$ of constant curvature κ , that is, the sphere $\mathbb{S}^3(\kappa)$ or the hyperbolic space $\mathbb{H}^3(\kappa)$ depending on the sign of κ . For example, Ros and Souam [66, 71] extended Nitsche's results in [62], proving that any simply connected capillary CMC surface in a metric ball of \mathbb{S}^3 or \mathbb{H}^3 is totally umbilic.

The problem of whether the only embedded free boundary minimal annulus in a geodesic ball of \mathbb{S}^3 is a (spherical) critical catenoid has been studied in two interesting recent works by Lima-Menezes [57] and Medvedev [60]. In [57], the uniqueness of this critical catenoid is obtained among immersed annuli by imposing that its coordinate functions are first eigenfunctions of a suitable Steklov problem. In [60] it is shown that the Morse index of the critical catenoid is 4, that its spectral index is 1, and that any free boundary minimal annulus with spectral index 1 is a (spherical) critical catenoid. See e.g. [5, 14, 38, 56, 61, 71, 74] for other results on free boundary CMC surfaces in spherical or hyperbolic balls. In particular, it has been conjectured in [57, 60] that the only embedded free boundary minimal annuli in metric balls of \mathbb{S}^3 or \mathbb{H}^3 are rotational. This is an extension of the critical catenoid conjecture to spherical and hyperbolic balls (see Conjecture 1.3).

Another main line of research in the present thesis regards the existence of free boundary minimal and CMC annuli in metric balls of \mathbb{S}^3 and \mathbb{H}^3 . In many situations we will also be able to control the embeddedness of these annuli; see Theorems 4.1.1 and 4.1.2. First, for the case of \mathbb{S}^3 we have:

In \mathbb{S}^3 there exist immersed, non-rotational free boundary H -annuli in metric balls $\mathbf{B} \subset \mathbb{S}^3$, for any $H \in \mathbb{R}$. In particular, there exist free boundary minimal annuli in \mathbb{S}^3 with a finite, prismatic, symmetry group.

For $H \geq 1/\sqrt{3}$, some of these free boundary CMC annuli in \mathbb{S}^3 are embedded.

We note that the existence of non-rotational immersed free boundary minimal annuli in metric balls of \mathbb{S}^3 solves a problem proposed by Medvedev [60].

Regarding the hyperbolic 3-space, we first focus on the case where the mean curvature H is *super-critical*, that is, $H > 1$. In that situation, we are able to have a good

additional control on the embeddedness of the examples (see Theorem 4.1.2):

In \mathbb{H}^3 , there exist embedded non-rotational free boundary H -annuli in metric balls $\mathbf{B} \subset \mathbb{H}^3$, for any $H > 1$. These annuli have a finite, prismatic, symmetry group.

The proofs of these results both in \mathbb{S}^3 and \mathbb{H}^3 follow the strategy used for our previous construction of embedded free boundary CMC annuli in the Euclidean unit ball \mathbb{B}^3 . Specifically, we will use that the sinh-Gordon equation appears as the Gauss equation for CMC surfaces in \mathbb{S}^3 , and for CMC surfaces in \mathbb{H}^3 with $H > 1$. In particular, we will use the special solutions to the overdetermined system (1.3) that we had previously constructed. The resulting CMC surfaces that we construct also have a *spherical curvatures line foliation* structure, where this time *spherical* means that each curvature line of the foliation lies in a totally umbilic surface \mathcal{Q} of $\mathbb{M}^3(\kappa)$. However, despite these analogies, the proofs need several new ideas, since some of the technical arguments used in Chapter 3 do not extend to \mathbb{S}^3 or \mathbb{H}^3 .

When one considers CMC surfaces in \mathbb{H}^3 with $|H| < 1$, the Gauss equation is equivalent to the cosh-Gordon equation $\Delta\omega + \cosh\omega = 0$. In this situation, the condition that provides a foliation by spherical curvature lines is equivalent to the second equation in (1.3), but the change of the accompanying elliptic equation changes in a very fundamental way the analysis of the possible solutions. This raises substantial difficulties to our approach, and our previous techniques cannot be easily adapted to prove existence of free boundary minimal or CMC annuli in that *subcritical case*. Nonetheless, by using a different strategy, based on a deformation of the space forms $\mathbb{M}^3(\kappa)$ and their associated Gauss-Codazzi equations, we can still construct non-rotational free boundary minimal annuli in \mathbb{H}^3 , see Theorem 5.1.1.

For any irreducible $q = m/n \in \mathbb{Q}$ of an interval $\mathcal{J} \subseteq (-1/\sqrt{2}, -1/\sqrt{3})$ there exists a real analytic family of immersed free boundary minimal annuli $\mathbb{A}_q(\eta)$, $\eta \in (0, \varepsilon)$, in geodesic balls $\mathbf{B} = \mathbf{B}(\eta)$ of \mathbb{H}^3 , with a finite prismatic symmetry group of order $4n$.

We remark that all these minimal annuli are of Enneper type, they are non-embedded, and the radii of the geodesic balls in which they lie vary with the parameter η .

The strategy to prove the previous theorem relies on using an adequate model for the spaces $\mathbb{M}^3(\kappa)$, so that both the ambient space and the system for minimal surfaces of Enneper type when $\kappa < 0$ appear as a finite real analytic continuation of the corresponding situation when $\kappa \geq 0$.

Coming back to minimal surfaces in the unit ball \mathbb{B}^3 of \mathbb{R}^3 , it is an interesting problem to replace the free boundary condition by the more flexible *capillary condition* in which the minimal surface Σ intersects $\partial\mathbb{B}^3$ along $\partial\Sigma$ at a constant angle θ , not necessarily $\theta = \pi/2$. By Nitsche's theorem [62], the only simply connected capillary minimal surfaces in \mathbb{B}^3 are flat disks, but in the annular case, the situation is much more interesting. First, one has again the obvious examples of *capillary catenoids* in \mathbb{B}^3 . Thus, the critical catenoid conjecture admits a natural capillary extension, already formulated by Went in 1995, see [77]: *are pieces of catenoids the only embedded capillary minimal annuli in \mathbb{B}^3 ?*

This question was answered in the negative by Fernández, Hauswirth and Mira [29], through the construction of non-rotational embedded minimal annuli in \mathbb{B}^3 foliated by spherical curvature lines. We remark that none of these embedded annuli has intersection angle $\theta = \pi/2$, since it was shown in [29] that the only free boundary embedded minimal annulus in \mathbb{B}^3 foliated by spherical curvature lines is the critical catenoid.

Nonetheless, this construction in [29] left several interesting questions open. For instance, while the examples in [29] were only obtained very close to a catenoid, it was conjectured there that the family branches of such capillary minimal annuli in \mathbb{B}^3 should remain embedded throughout the whole deformation, and converge at the other side of the moduli space to a necklace of n flat vertical disks in \mathbb{B}^3 ; see Figure 1.3.

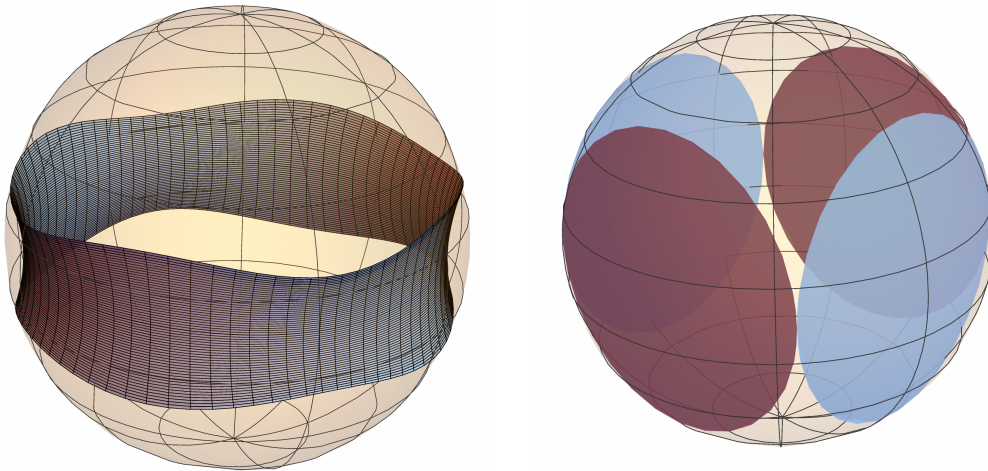


Figure 1.3: Example of a non-rotational capillary minimal annulus in \mathbb{B}^3 (left) and the conjectured limit of $n = 4$ vertical disks (right).

Our main result in Chapter 6 gives an affirmative answer to this conjecture in [29], see Theorem 6.1.1.

For each $n \geq 2$ there exists a real analytic family $\{\mathbb{A}_n(a) : a \in (0, 1)\}$ of embedded capillary minimal annuli in \mathbb{B}^3 with a prismatic symmetry group of order $4n$ (in particular, non-rotational), and such that:

1. When $a \rightarrow 1$, $\mathbb{A}_n(a)$ converges analytically to a capillary catenoid $\mathbb{A}_n(1)$.
2. When $a \rightarrow 0$, $\mathbb{A}_n(a)$ converges uniformly to a chain of n vertical disks meeting tangentially along the equator $\mathbb{B}^3 \cap \{x_3 = 0\}$.

The convergence in item (2) above is analytic only away from the *vertices* of the limit configuration where two different disks intersect. As one approaches such vertices, the curvature of the annuli $\mathbb{A}_n(a)$ blows up as $a \rightarrow 0$.

An interesting corollary of the previous result is that the critical catenoid conjecture does not hold when we replace the free boundary condition $\theta = \pi/2$ by other values of θ arbitrarily close to $\pi/2$, see Corollary 6.1.3 and Figure 1.4.

There exists $\theta_1 \in (0, \pi/2)$ such that for any $\theta \in (\theta_1, \pi/2)$ there exist embedded, non-rotational minimal annuli in \mathbb{B}^3 with capillary angle θ .

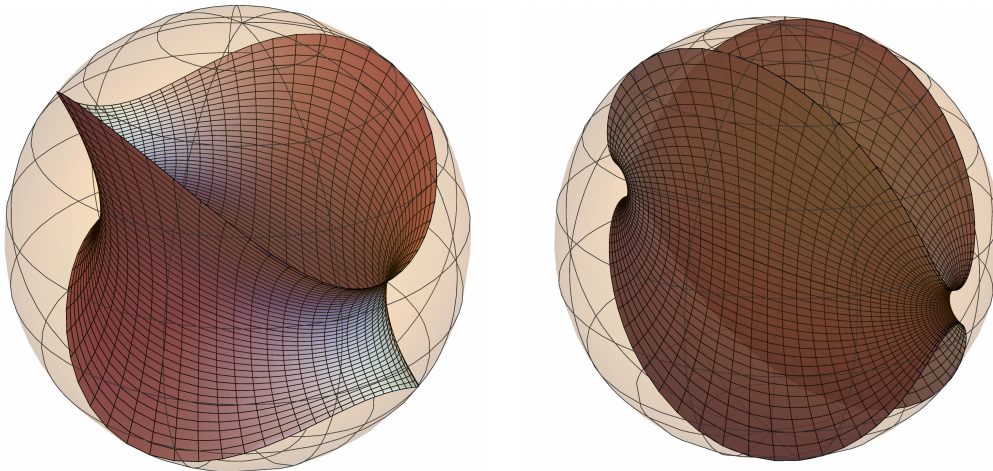


Figure 1.4: Examples of non-rotational capillary minimal annuli $\mathbb{A}_2(a)$ with $n = 2$. On the left, the parameter a is closer to 1, while the figure on the right has parameter a near zero. As a approaches zero, the contact angle between the annulus and $\partial\mathbb{B}^3$ approaches $\frac{\pi}{2}$.

The minimal annuli $\mathbb{A}_n(a)$ in Theorem 6.1.1 are foliated by spherical curvature lines. The main idea of the proof is based on making the Hopf differential act as an element of the space of parameters in the analysis of minimal surfaces with spherical curvature lines. The implementation of this idea avoids the use of Weierstrass

\wp -functions in [29] and results in a sharper control of the minimal annuli. It is interesting that this new way of parametrizing the space of minimal annuli with spherical curvature lines seems to have applications beyond this particular theory.

One of such applications concerns a counterexample to a conjecture by Souam [70] in the context of overdetermined elliptic problems that we explain next. First, we recall an important conjecture of elliptic PDE analysis and spectral theory, asserting that if a smooth bounded domain Ω in \mathbb{R}^n admits a non-constant solution u to the overdetermined problem

$$\begin{cases} \Delta u + \lambda u = 0 & \text{in } \Omega, \\ u = c, \quad \frac{\partial u}{\partial \nu} = d & \text{on } \partial\Omega, \end{cases} \quad (1.4)$$

for constants $c, d \in \mathbb{R}$, then Ω is a ball and u is radial with respect to its center. Here, ν denotes the exterior unit normal to $\partial\Omega$. When $d = 0$ and $n = 2$, problem (1.4) is the classical *Schiffer conjecture*, see Yau [78, Problem 80], which is of special importance due to its connection with the Pompeiu problem of integral geometry. An updated discussion on Schiffer's conjecture can be found in the recent work [25].

Problem (1.4) has also been studied in detail in the 2-sphere \mathbb{S}^2 , see e.g. [27, 28, 53]. In [28], Fall, Mindlind and Werth showed that there exist non-rotational ring domains in \mathbb{S}^2 that admit a solution to (1.4) with $d = 0$ for infinitely many $\lambda \in \mathbb{R}$. In particular, this gave a counterexample to a conjecture by Souam [70, p. 342], and showed that Schiffer's uniqueness is not true in the spherical setting. The proof uses Crandall-Rabinowitz bifurcation starting from geodesic bands of constant width in \mathbb{S}^2 .

Among all possible choices for the eigenvalue λ in \mathbb{S}^2 for (1.4), the most fundamental one from several viewpoints is $\lambda = 2$. The first obvious reason is that $\lambda = 2$ is the first non-zero eigenvalue of \mathbb{S}^2 . But also, the equation $\Delta u + 2u = 0$ is of importance in minimal surface theory, as it is classically known to describe Jacobi functions on branched minimal surfaces in \mathbb{R}^3 with injective Gauss map, see e.g. [27, 70]. This motivates the study of the Schiffer-type problem

$$\begin{cases} \Delta u + 2u = 0 & \text{in } \Omega \subset \mathbb{S}^2, \\ u = c, \quad \frac{\partial u}{\partial \nu} = d & \text{on } \partial\Omega, \end{cases} \quad (1.5)$$

for $c, d \in \mathbb{R}$. To this respect, we mention the following conjecture by Souam [70, p. 347]):

Conjecture 1.5 ([70]). *The only domains $\Omega \subset \mathbb{S}^2$ where problem (1.5) can be solved are geodesic balls and radial bands of constant width around a geodesic of \mathbb{S}^2 .*

As an application of our construction of the families of embedded capillary minimal annuli $\mathbb{A}_n(a)$ in Theorem 6.1.1, we can provide counterexamples to Conjecture 1.5; see Figure 1.5. Specifically, we prove (Theorem 6.7.1):

For any $n \geq 2$ there exists a real analytic family of regular ring domains $\{\Omega_n(a) : a \in (0, 1]\}$ in \mathbb{S}^2 , with the following properties:

1. *Each $\Omega = \Omega_n(a)$ admits a solution u to (1.5) with respect to constants $c = c(a, n) > 0$ and $d = d(a, n) < 0$.*
2. *When $a \in (0, 1)$, $\Omega_n(a)$ has a finite prismatic symmetry group of order $2n$. In particular, it is not radially symmetric.*
3. *For $a = 1$, $\Omega_n(1)$ is a rotational band of constant width around the equator of \mathbb{S}^2 .*
4. *When $a \rightarrow 0$, the domains $\Omega_n(a)$ converge to a chain of n vertical spherical caps of \mathbb{S}^2 of the same radius meeting tangentially along the equator; see Figure 1.6.*

The domains $\Omega_n(a) \subset \mathbb{S}^2$ are constructed as the spherical images of the capillary minimal annuli $\mathbb{A}_n(a)$ of Theorem 6.1.1. For this, we need to prove that the Gauss maps of all the annuli $\mathbb{A}_n(a)$ provide diffeomorphisms onto their spherical images.

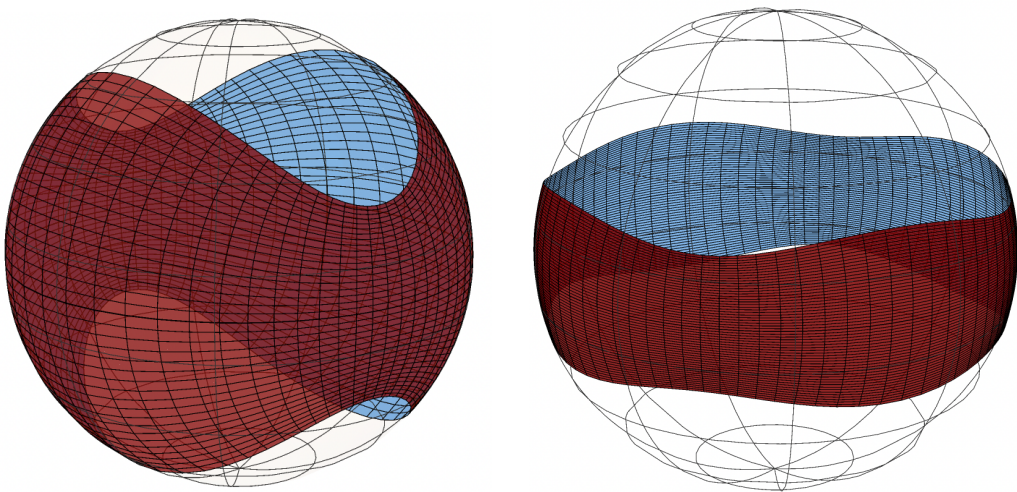


Figure 1.5: Examples of annular domains $\Omega_n(a)$, $a \in (0, 1)$, with $n = 2$ (left) and $n = 4$ (right).

We remark that the ring domains $\Omega_n(a) \subset \mathbb{S}^2$ of the above theorem can be seen as bifurcation of rotational bands of constant width, following a similar pattern to the annular Schiffer-type regions in \mathbb{S}^2 obtained by Fall, Mindlind and Werth in [28]. But in our situation, in contrast, we can control the whole bifurcation branches, not only near the radial situation where the bifurcation takes place, but up to the degenerate situation of a chain of vertical spherical caps at the other endpoint of the moduli space. This seems to be a new feature of our approach that is not present in previous works in the literature that construct solutions to overdetermined elliptic problems via bifurcation.

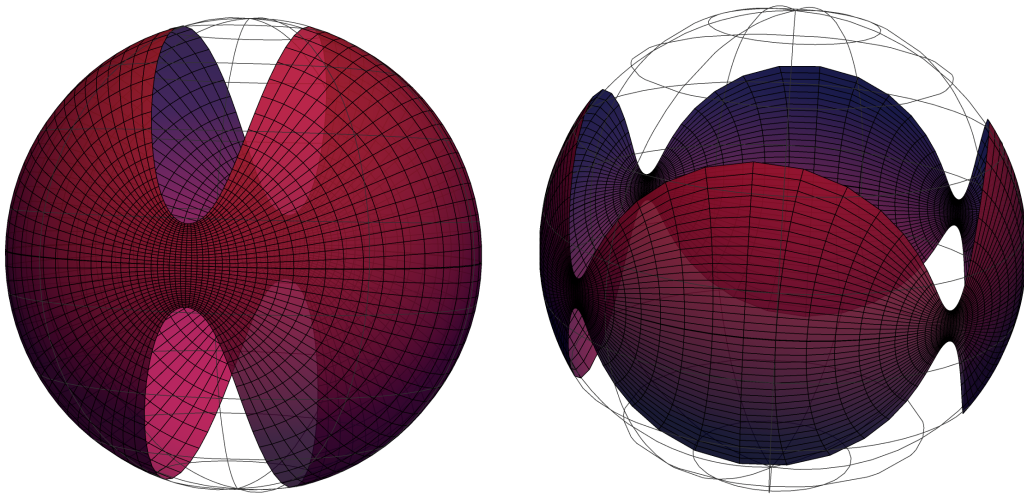


Figure 1.6: Examples of annular domains $\Omega_n(a)$ with a near 0 for $n = 2$ (left) and $n = 4$ (right). The domains $\Omega_n(a)$ converge to a chain of n spherical caps as $a \rightarrow 0$. In particular, if $n = 2$, $\Omega_2(a)$ converges to a pair of hemispheres.

Chapter 2

Preliminaries

2.1 Summary

In this chapter we introduce the surfaces of Enneper type as constant mean curvature surfaces in \mathbb{R}^3 foliated by spherical curvature lines. Following Wente [76], we show how the space of such surfaces can be parametrized by the solutions of a second order autonomous differential system, and study their basic properties. Then, we extend the concept of Enneper surface to the case of CMC surfaces in $\mathbb{S}^3(\kappa)$ and $\mathbb{H}^3(\kappa)$. Finally, we carry out a detailed discussion of the rotational CMC surfaces in spaces of constant curvature $\mathbb{M}^3(\kappa)$, and prove that a large family of such examples have a compact embedded annular piece that is free boundary in a geodesic ball of $\mathbb{M}^3(\kappa)$.

2.2 CMC surfaces immersed in space forms

Given a simply connected open set $\mathcal{D} \subset \mathbb{R}^2$, let $\psi(u, v) : \mathcal{D} \mapsto \mathbb{M}^3(\kappa)$ be a conformal immersion of a constant mean curvature $H \geq 0$ surface in a space form of constant sectional curvature $\kappa \in \mathbb{R}$. The first and second fundamental forms I, II of the immersion can be expressed as

$$\begin{aligned} I &= e^{2\omega(u,v)} (du^2 + dv^2), \\ II &= l_{11}(u, v)du^2 + 2l_{12}(u, v)dudv + l_{22}(u, v)dv^2, \end{aligned} \tag{2.1}$$

for certain functions $\omega, l_{11}, l_{12}, l_{22} : \mathcal{D} \rightarrow \mathbb{R}$. If we set $\zeta = u + iv$ and let $N(u, v)$ be the Gauss map of the immersion, it is possible to prove that the *Hopf differential* $Qd\zeta^2$,

where $Q(\zeta)$ is defined as

$$Q(\zeta) := 2\langle \psi_{\zeta\zeta}, N \rangle = \frac{1}{2} (l_{11}(\zeta) - l_{22}(\zeta)) - il_{12}(\zeta), \quad (2.2)$$

is holomorphic. This holds since the Codazzi equation for the surface can be expressed as

$$Q_{\bar{\zeta}} = e^{2\omega} H_{\zeta} = 0. \quad (2.3)$$

On the other hand, the Gauss equation of the surface is given by

$$\Delta\omega + (H^2 + \kappa)e^{2\omega} - |Q|^2 e^{-2\omega} = 0. \quad (2.4)$$

The principal curvatures of the immersion, $\kappa_1 \geq \kappa_2$, can be written in terms of the data H, Q, ω as

$$\kappa_1 = H + |Q|e^{-2\omega}, \quad \kappa_2 = H - |Q|e^{-2\omega}. \quad (2.5)$$

In particular, $|Q| = \frac{e^{2\omega}}{2} (\kappa_1 - \kappa_2)$, which indicates that the zeros of Q correspond with the set of umbilical points of the immersion. In particular, if $\psi(u, v)$ is assumed to have no umbilical points, then there exists a conformal reparametrization of the immersion such that Q is a real, positive constant. In other words, it follows from (2.1), (2.2) that the fundamental forms of the immersion reduce to

$$I = e^{2\omega(u,v)} (du^2 + dv^2), \quad II = (Q + He^{2\omega}) du^2 + (He^{2\omega} - Q) dv^2. \quad (2.6)$$

As a consequence, the u -lines and v -lines of $\psi(u, v)$ are curvature lines of the immersion. Conversely, the fundamental theorem of surfaces states that the Gauss and Codazzi equations (2.3)-(2.4), are *sufficient* integrability conditions for immersions in space forms. In other words,

Theorem 2.2.1. *Let $\omega(u, v) : \mathcal{D} \rightarrow \mathbb{R}$ be a solution to (2.4) defined on an open, simply connected domain $\mathcal{D} \subset \mathbb{R}^2$, where $H, Q, \kappa \in \mathbb{R}$ are constants satisfying $H \geq 0$, $Q > 0$. Then, there exists a conformal immersion $\psi(u, v) : \mathcal{D} \rightarrow \mathbb{M}^3(\kappa)$ with constant mean curvature H , Hopf differential $Qd\zeta^2$ and first and second fundamental forms I, II given by (2.6). In particular, the u -lines and v -lines of the immersion are lines of curvature. Moreover, $\psi(u, v)$ is unique up to an orientation-preserving isometry of $\mathbb{M}^3(\kappa)$, and $\psi(u, v)$ has no umbilical points.*

Remark 2.2.2. *The previous theorem also holds in the limit case $Q = 0$. In this situation, the induced immersion $\psi(u, v)$ is totally umbilical.*

2.3 Umbilics and topology of CMC surfaces

Let Σ be an immersed CMC surface in $\mathbb{M}^3(\kappa)$. Then, we can consider the Hopf differential as a holomorphic 2-form $\mathcal{Q} := Q(\zeta)d\zeta^2$ globally defined on Σ , where $Q(\zeta)$ was defined in (2.2) with respect to an arbitrary local conformal parameter $\zeta = u + iv$ on Σ . The umbilics of Σ are the points where $\mathcal{Q} = 0$, and the principal directions of Σ are those given by

$$\operatorname{Im}(\mathcal{Q}) = 0. \quad (2.7)$$

Around every non-umbilical point, the equation (2.7) determines two *principal* line fields $\mathcal{L}_1, \mathcal{L}_2$ that are orthogonal with respect to the induced metric of Σ . Moreover, since $Q(\zeta)$ is holomorphic, the umbilical points of Σ , given by the zeros of \mathcal{Q} , are isolated, and hence both principal line fields \mathcal{L}_j , $j = 1, 2$, have an isolated singularity at the umbilic point. If $n \geq 1$ denotes the order of the zero of $Q(\zeta)$ at an umbilic point of Σ , then it is a direct consequence of the holomorphicity of $Q(\zeta)$ that the *topological index* of the principal line fields \mathcal{L}_j are both equal to $-n/2 < 0$.

On the other hand, let Σ be a compact surface with boundary $\partial\Sigma$. Let $g \geq 0$ denote the genus of Σ and $k \geq 1$ the number of boundary components. Let \mathcal{L} denote a continuous line field in Σ that is either tangent or orthogonal to $\partial\Sigma$ along each boundary component of $\partial\Sigma$, and assume that \mathcal{L} only has a finite number of singularities, that is, \mathcal{L} is defined on $\Sigma \setminus \{p_1, \dots, p_n\}$. Let $\operatorname{Ind}(\mathcal{L})$ denote the sum of all indices of \mathcal{L} at the singularities p_j . In these conditions, \mathcal{L} can be extended by reflection to the *topological double* $\tilde{\Sigma}$ of Σ , and this extended line field on $\tilde{\Sigma}$ has index $2\operatorname{Ind}(\mathcal{L})$. Let \tilde{g} denote the genus of $\tilde{\Sigma}$. Then, by the Poincaré-Hopf theorem (see [41]), we have $2\operatorname{Ind}(\mathcal{L}) = 2 - 2\tilde{g}$. Therefore,

$$\operatorname{Ind}(\mathcal{L}) = 2 - 2g - k. \quad (2.8)$$

We now assume again that Σ is an immersed CMC surface with (smooth) boundary in $\mathbb{M}^3(\kappa)$. We also suppose that all connected components of $\partial\Sigma$ are curvature lines of Σ . Then, $\operatorname{Im}(\mathcal{Q}) \equiv 0$ along $\partial\Sigma$. Let us further assume that Σ is not totally umbilical, i.e., \mathcal{Q} is not identically zero, and let \mathcal{L} denote one of the two principal line fields of Σ . Recall that \mathcal{L} only has then, at the interior of Σ , a finite number of singularities, all of them of negative index. At the points in $\partial\Sigma$ the same is true, see [62, 66]. Then, equation (2.8) holds in this context, and we have the following consequences:

1. Let Σ be a compact CMC disk in $\mathbb{M}^3(\kappa)$ such that $\partial\Sigma$ is a line of curvature of Σ . Then Σ is totally umbilical.

2. Let Σ be a compact CMC annulus in $\mathbb{M}^3(\kappa)$ such that both components of $\partial\Sigma$ are lines of curvature of Σ . Then Σ does not have umbilic points.

Indeed, for the disk case, the total index of \mathcal{L} according to (2.8) is 1, which is impossible since all singularities have negative index. For the annulus case the total index of \mathcal{L} is zero, and the same argument shows that there are no umbilic points.

This result is relevant for the study of capillary CMC surfaces. Indeed, it is a consequence of Joachimsthal's classical theorem that if $\partial\Sigma$ lies in a totally umbilic surface M of $\mathbb{M}^3(\kappa)$, then $\partial\Sigma$ is a curvature line of Σ if and only if Σ intersects M along $\partial\Sigma$ at a constant angle. As a consequence, we obtain the theorem of Nitsche and Ros-Souam [62, 66] according to which any capillary CMC disk in a geodesic ball B of $\mathbb{M}^3(\kappa)$ must be totally umbilic. In the same way, capillary CMC annuli in geodesic balls of $\mathbb{M}^3(\kappa)$ cannot have umbilic points.

We finally discuss briefly the non-orientable case. First, we observe that any CMC surface in $\mathbb{M}^3(\kappa)$ with non-zero mean curvature H is trivially orientable. On the other hand, there are no topological obstructions for the existence of non-orientable minimal surfaces in $\mathbb{M}^3(\kappa)$. Nonetheless, in the free boundary case there is one topological constraint for non-orientability, recently obtained by C.T. Cardona [9]:

Theorem 2.3.1 ([9]). *There are no immersed free boundary minimal Möbius strips in a ball of \mathbb{R}^3 .*

As a matter of fact, the proof in [9] shows that there are no immersed minimal Möbius strips Σ in \mathbb{R}^3 whose boundary curve $\partial\Sigma$ is a line of curvature of Σ .

2.4 Enneper-type surfaces in \mathbb{R}^3

Throughout this section, let $\psi(u, v) : \mathcal{D} \subset \mathbb{R}^2 \mapsto \mathbb{R}^3$ be a constant mean curvature $H \geq 0$ immersion in \mathbb{R}^3 parametrized as in Theorem 2.2.1. Suppose that $(0, 0) \in \mathcal{D}$. Up to an orientation preserving isometry, we can assume that the immersion $\psi(u, v)$ satisfies

$$\psi(0, 0) = 0, \quad e^{-\omega(0,0)}\psi_u(0, 0) = \mathbf{e}_3, \quad e^{-\omega(0,0)}\psi_v(0, 0) = -\mathbf{e}_2, \quad N(0, 0) = \mathbf{e}_1, \quad (2.9)$$

where $\{\mathbf{e}_1, \mathbf{e}_2, \mathbf{e}_3\}$ is the canonical basis in \mathbb{R}^3 . By Theorem 2.2.1, these conditions determine $\psi(u, v)$ uniquely. According to (2.6), the Gauss-Weingarten equations for $\psi(u, v)$ are given by

$$\begin{cases} \psi_{uu} = \omega_u \psi_u - \omega_v \psi_v + (He^{2\omega} + Q) N, \\ \psi_{uv} = \omega_v \psi_u + \omega_u \psi_v, \\ \psi_{vv} = -\omega_u \psi_u + \omega_v \psi_v + (He^{2\omega} - Q) N, \\ N_u = -(H + Qe^{-2\omega}) \psi_u, \\ N_v = -(H - Qe^{-2\omega}) \psi_v. \end{cases} \quad (2.10)$$

We note that the v -lines are associated with the smaller principal curvature κ_2 in (2.5). We will now study a class of constant mean curvature surfaces of \mathbb{R}^3 that satisfy a special geometric condition: the immersion is foliated by *spherical curvature lines*. In the literature, these surfaces are commonly referred to as Enneper-type surfaces; see for example [76]. Let us define this concept:

Definition 2.4.1. *Let $u_0 \in \mathbb{R}$. We say that the v -curvature line $v \mapsto \psi(u_0, v)$ is spherical if it lies entirely in a sphere or a plane of \mathbb{R}^3 . Furthermore, the CMC H immersion $\psi(u, v)$ is said to be of Enneper type if every v -curve $v \mapsto \psi(u, v)$ is spherical.*

By construction, Enneper surfaces are either free of umbilical points or totally umbilical. Note that we are defining Enneper-type surfaces as those CMC immersions for which the v -curvature lines are spherical. While one might, in principle, consider surfaces such that the u -curvature lines are spherical instead, a detailed analysis of both families shows that the examples relevant to our study arise precisely when the spherical curvature line condition is imposed on the family associated with the smaller principal curvature κ_2 ; see (2.5). For $H = 0$, a change of orientation transforms u -curves into v -curves so both families agree in this case.

Remark 2.4.2. *By Joachimsthal's theorem [12, p. 152], if a v -curvature line $v \mapsto \psi(u, v)$ lies in a sphere or plane $\mathcal{Q} \subset \mathbb{R}^3$, the intersection angle between the immersion and \mathcal{Q} must be constant along the v -line.*

Apart from the Gauss equation (2.4), the set of Enneper-type surfaces in \mathbb{R}^3 satisfy a certain overdetermined condition, as observed by Wente:

Proposition 2.4.3 ([76]). *For each fixed $u \in \mathbb{R}$, the v -curvature line $v \mapsto \psi(u, v)$ is spherical if and only if there exist $\alpha = \alpha(u)$, $\beta = \beta(u)$ such that the function $\omega(u, v)$ in (2.6) satisfies*

$$2\omega_u = \alpha e^\omega + 2Q\beta e^{-\omega} \quad (2.11)$$

along the v -line. More precisely, if $\alpha(u) + 2H\beta(u) \neq 0$ and $Q \neq 0$, then $\psi(u, v)$ intersects a sphere $\mathcal{Q}(u)$ of radius $R(u)$ along $v \mapsto \psi(u, v)$ with angle $\theta(u)$, where

$$R^2 = \frac{4 + 4\beta^2}{(\alpha + 2H\beta)^2}, \quad \tan \theta = -\frac{1}{\beta}. \quad (2.12)$$

Furthermore, the center $\widehat{c}(u) \in \mathbb{R}^3$ of the sphere satisfies

$$\widehat{c}(u) = \psi - \frac{2}{\alpha + 2H\beta} \psi_u e^{-\omega} + \frac{2\beta}{\alpha + 2H\beta} N \quad (2.13)$$

In a similar way, if $\alpha(u) + 2H\beta(u) = 0$ and $Q \neq 0$, then the v -line $\psi(u, v)$ lies in a plane which intersects the immersion with angle $\theta(u)$ as above.

Proof. We will first deal with the planar case. Suppose that (2.11) holds for some $u \in \mathbb{R}$ such that $\alpha(u) + 2H\beta(u) = 0$. We deduce then from (2.10), (2.11) that the vector $\mathbf{t} := e^{-\omega} \psi_u - \beta N$ is constant along the v -line, since the partial derivative \mathbf{t}_v vanishes identically. As an immediate consequence, it follows that $d := \langle \mathbf{t}, \psi \rangle$ is also constant, showing that the v -line lies in the plane $P := \{ \langle x, \mathbf{t} \rangle = d : x \in \mathbb{R}^3 \}$. We note further that the angle θ between the immersion and the plane P satisfies (2.12). Conversely, let us assume that the v -line $v \mapsto \psi(u, v)$ lies in a plane P . This means that there exist $d \in \mathbb{R}, \mathbf{t} \in \mathbb{R}^3$ such that $d \equiv \langle \psi, \mathbf{t} \rangle$ along the v -line. Differentiating this expression with respect to v , we deduce that $0 = \langle \mathbf{t}, \psi_v \rangle$. By Joachimsthal's theorem, the intersection angle between P and the immersion is constant, which means that \mathbf{t} can be written as $\mathbf{t} = Ae^{-\omega} \psi_u + BN$ for some constants A, B ; see Remark 2.4.2. Differentiating \mathbf{t} with respect to v and using (2.10), it follows that (2.11) holds for a pair $\alpha, \beta \in \mathbb{R}$ with $\alpha + 2H\beta = 0$.

We will now consider the spherical case. Suppose that (2.11) holds with $\alpha(u) + 2H\beta(u) \neq 0$. It can then be proven that the map $\widehat{c}(u, v)$ defined as in (2.13) does not depend on v , that is, $\widehat{c} = \widehat{c}(u)$. In particular, $v \mapsto \|\widehat{c}(u) - \psi(u, v)\|$ is constant, which indicates that the v -line $v \mapsto \psi(u, v)$ lies in a sphere with center $\widehat{c}(u)$. It is straightforward to check that the radius and intersection angle of ψ with the sphere satisfy (2.12).

Finally, let us assume that the v -line $v \mapsto \psi(u, v)$ lies in a sphere of radius R and center $\widehat{c} \in \mathbb{R}^3$. By Joachimsthal's theorem, the intersection angle θ between the sphere and ψ must be constant. Since $R^2 = \|\widehat{c} - \psi(u, v)\|^2$, we can differentiate with respect to v and deduce that $0 = \langle \widehat{c} - \psi, \psi_v \rangle$, which implies that

$$\widehat{c} = \psi + R \sin \theta e^{-\omega} \psi_u + R \cos \theta N.$$

The fact that $\widehat{c}_v = 0$ implies that $2\omega_u = \alpha e^\omega + 2Q\beta e^{-\omega}$ for some pair α, β which are related to R, θ by (2.12). \square

As an immediate consequence of Theorem 2.2.1 and Proposition 2.4.3, we deduce the following result:

Theorem 2.4.4 ([76]). *Let $\mathcal{D} \subset \mathbb{R}^2$ be a simply connected domain on which the system*

$$\Delta\omega + Ae^{2\omega} - Q^2e^{-2\omega} = 0, \quad (2.14a)$$

$$2\omega_u = \alpha(u)e^\omega + 2Q\beta(u)e^{-\omega}, \quad (2.14b)$$

admits a solution $\omega(u, v) : \mathcal{D} \rightarrow \mathbb{R}$ for some real constants $A \geq 0, Q > 0$ and a pair of functions $(\alpha(u), \beta(u))$. Then, there exists a CMC $H \geq 0$ immersion $\psi(u, v) : \mathcal{D} \rightarrow \mathbb{R}^3$, where $H^2 = A$. This immersion has first and second fundamental forms given by (2.6), and it is unique once we fix the initial conditions (2.9). Moreover, the immersion is of Enneper type.

We note that the system (2.14) is overdetermined, so in order for it to have solutions, we must ask the pair $(\alpha(u), \beta(u))$ to satisfy a certain compatibility condition. We do this next.

Theorem 2.4.5 ([76]). *Let $\omega(u, v) : \mathcal{D} \rightarrow \mathbb{R}$ be a solution to (2.14) associated to a pair $(\alpha(u), \beta(u))$ for some constants $A \in \mathbb{R}, Q > 0$. If $\omega_v \not\equiv 0$, the partial derivative $\omega_v(u, v)$ satisfies*

$$4\omega_v^2(u, v) = \phi(u, \omega(u, v)), \quad (2.15)$$

where

$$\phi(u, \omega) = -(4A + \alpha^2)e^{2\omega} - 4Q^2(1 + \beta^2)e^{-2\omega} - 4\alpha'e^\omega + 8Q\beta'e^{-\omega} + C(u), \quad (2.16)$$

and $C(u) := 12Q\alpha(u)\beta(u) - 4\widehat{a}$, $\widehat{a} \in \mathbb{R}$ being a real constant. Moreover, $(\alpha(u), \beta(u))$ must be a solution to the autonomous differential system

$$\begin{cases} \alpha'' = \widehat{a}\alpha - 4Q\alpha^2\beta - 4AQ\beta, \\ \beta'' = \widehat{a}\beta - 4Q\alpha\beta^2 - Q\alpha. \end{cases} \quad (2.17)$$

Conversely, let $(\alpha(u), \beta(u)) : I \subset \mathbb{R} \rightarrow \mathbb{R}^2$ with $0 \in I$ be a solution to (2.17) for some constants $A, \widehat{a} \in \mathbb{R}, Q \geq 0$. Then, for any value $\omega_0 \in \mathbb{R}$ such that $\phi(0, \omega_0) \geq 0$,

there exists a unique solution $\omega(u, v)$ to system (2.14) defined on a neighbourhood \mathcal{D} of $(0, 0)$ satisfying $\omega(0, 0) = \omega_0$, $\omega_v(0, 0) = \frac{1}{2}\sqrt{\phi(0, \omega_0)}$.

Proof. Let us first show (2.15). The partial derivative ω_{uu} can be computed using (2.14b). Substituting this in (2.14a), one gets

$$4\omega_{vv} = -(4A + \alpha^2)e^{2\omega} + 4Q^2(1 + \beta^2)e^{-2\omega} - 2\alpha'e^\omega - 4Q\beta'e^{-\omega}. \quad (2.18)$$

Multiplying both sides by $2\omega_v$ and integrating in v , we get (2.15) for some integration constant $C(u)$ in (2.16) to be determined.

In order to obtain (2.17) and the expression for $C(u)$, we may compute the derivative ω_{uv} in two ways: first, we can differentiate ω_{vv} in (2.18) with respect to u . Alternatively, one can differentiate ω_u in (2.11) twice with respect to v , yielding

$$\omega_{uvv} = (\alpha e^\omega - 2Q\beta e^{-\omega})\omega_{vv} + (\alpha e^\omega + 2Q\beta e^{-\omega})\omega_v^2.$$

Using (2.15) and (2.18), we can substitute the expressions for ω_v and ω_{vv} in the above formula. Either computation shows that the quantity $e^{3\omega}\omega_{uvv}$ can be expressed as a degree-six polynomial in e^ω whose coefficients are functions of u alone. These coefficients take different forms depending on how ω_{uvv} is computed. By comparing the resulting expressions, we obtain (2.17) as well as the identity $C = 12Q\alpha\beta - 4\hat{a}$.

We will now show the converse implication, i.e., that a pair (α, β) satisfying (2.17) induces a solution $\omega(u, v)$ to the system (2.14). Let (α, β) be a solution to (2.17) and $\omega_0 \in \mathbb{R}$ such that $\phi(0, \omega_0)$ in (2.16) is non-negative. Let $x(v)$ be the (unique) solution to the ordinary differential equation

$$4x'' = -(4A + \alpha(0)^2)e^{2x} + 4Q^2(1 + \beta(0)^2)e^{-2x} - 2\alpha'(0)e^x - 4Q\beta'(0)e^{-x} \quad (2.19)$$

with $x(0) = \omega_0$, $x'(0) = \frac{1}{2}\sqrt{\phi(0, \omega_0)}$. Similarly, for every v_0 , we define $\omega(u, v_0)$ as the solution of the differential equation $2\omega_u = \alpha e^\omega + 2Q\beta e^{-\omega}$ with initial condition $\omega(0, v_0) = x(v_0)$.

By construction, the function $\omega(u, v)$ is real analytic and satisfies (2.14b), so we just need to check that (2.14a) holds. We will consider two cases depending on whether $x(v)$ is constant or not. Suppose first that $x'(v) \not\equiv 0$. Then, one can obtain from (2.19) the first integral

$$x'(v)^2 = \frac{1}{4}\phi(0, x(v)). \quad (2.20)$$

Now, by (2.14b), it holds

$$2\omega_{vu} = (\alpha e^\omega - 2Q\beta e^{-\omega}) \omega_v. \quad (2.21)$$

Similarly, from (2.16) it follows that $\phi(u, \omega(u, v))$ satisfies

$$\phi_u = (\alpha e^\omega - 2Q\beta e^{-\omega}) \phi. \quad (2.22)$$

In particular, we can integrate both ω_{vu} and ϕ_u in u to obtain $\omega_v^2 = \widehat{C}(v)\phi$ for some function $\widehat{C}(v)$. We will show that actually $\widehat{C}(v) \equiv \frac{1}{4}$: indeed, at $u = 0$, it holds $\omega(0, v) = x(v)$, and so

$$\omega_v(0, v)^2 = x'(v)^2 = \frac{1}{4}\phi(0, x(v)) = \frac{1}{4}\phi(0, \omega(0, v)).$$

In particular, we deduce that $\widehat{C}(v) \equiv \frac{1}{4}$, i.e., the function $\omega(u, v)$ satisfies (2.15). Now, a direct computation using (2.14b) and (2.15) yields

$$\Delta\omega = \omega_{uu} + \omega_{vv} = Q^2 e^{-2\omega} - A e^{2\omega},$$

proving (2.14a) in this case.

Finally, assume that $x'(v) \equiv 0$. Since $x(v) = \omega_0$ is a constant, it follows that $\omega = \omega(u)$ does not depend on v . Consider the function $\phi(u) \equiv \phi(u, \omega(u))$ defined in (2.16). By construction, it holds $\phi(0) \equiv \phi(0, \omega_0) = 4x_v(0)^2 = 0$, and by (2.22), we conclude that $\phi(u) \equiv 0$. Let us define next

$$\widetilde{\phi}(u) = -2(4A + \alpha^2)e^{2\omega} + 8Q^2(1 + \beta^2)e^{-2\omega} - 4\alpha'e^\omega - 8Q\beta'e^{-\omega}.$$

We note that $\widetilde{\phi}(0) = 8x''(0) = 0$ by (2.19). Moreover, it follows from (2.14b) and (2.16) that

$$\widetilde{\phi}_u = (\alpha e^\omega + \beta e^{-\omega})\phi + \frac{1}{2}(\alpha e^\omega - \beta e^{-\omega})\widetilde{\phi} = \frac{1}{2}(\alpha e^\omega - \beta e^{-\omega})\widetilde{\phi}.$$

Since $\widetilde{\phi}(0) = 0$, we deduce that $\widetilde{\phi}(u) \equiv 0$. Finally, it can be checked that

$$\Delta\omega - Q^2 e^{-2\omega} + A e^{2\omega} = \omega_{uu} - Q^2 e^{-2\omega} + A e^{2\omega} = -\frac{1}{8}\widetilde{\phi} = 0,$$

proving (2.14a). □

Remark 2.4.6. Let $X(u, v) := e^{\omega(u, v)}$. For technical purposes, it is more convenient to rewrite (2.15) as

$$4X_v^2 = p(u, X), \quad (2.23)$$

where $p(u, x)$ is the following fourth order polynomial whose coefficients depend on u :

$$p(u, x) = -(4A + \alpha^2)x^4 - 4\alpha'x^3 + (12Q\alpha\beta - 4\hat{a})x^2 + 8Q\beta'x - 4Q^2(1 + \beta^2). \quad (2.24)$$

It can be shown that the discriminant of $p(u, x)$ is independent of u ; we refer the reader to [76, p. 11] for further details.

Wente observed [76, p. 12-14] that the system (2.17) has a Hamiltonian nature. In particular, it admits a first integral, namely

$$\mathcal{K}_1 = \alpha'\beta' - \hat{a}\alpha\beta + 2Q\alpha^2\beta^2 + 2AQ\beta^2 + \frac{Q}{2}\alpha^2. \quad (2.25)$$

If, moreover, $A > 0$, then the system admits an additional first integral:

$$\mathcal{K}_2 = (\alpha\beta' - \alpha'\beta)^2 + \left(2\sqrt{A}\beta' - \alpha'\right)^2 + \left(2Q\alpha\beta - \hat{a} - 2\sqrt{A}Q\right) \left(\alpha - 2\sqrt{A}\beta\right)^2. \quad (2.26)$$

We emphasize that Theorem 2.4.5 provides a natural way to study the moduli space of Enneper-type immersions in \mathbb{R}^3 : indeed, any solution $(\alpha(u), \beta(u))$ to the system of differential equations (2.17) such that $\phi(0, \omega_0)$ in (2.16) is non-negative for some $\omega_0 \in \mathbb{R}$ yields a solution $\omega(u, v)$ to the overdetermined problem (2.14). According to Theorem 2.4.4, $\omega(u, v)$ induces an Enneper-type immersion. This process can be reversed under the additional assumption that the partial derivative ω_v does not vanish identically, i.e., $\omega(u, v)$ depends on v . Nevertheless, we note that any immersion $\psi(u, v)$ of Enneper type such that $\omega_v \equiv 0$ corresponds to a rotational CMC surface in \mathbb{R}^3 . These rotational examples appear as a degenerate family within the set of Enneper-type immersions, as will be seen throughout Chapters 3 and 6.

We will finish this section highlighting an interesting geometric property of the center map $\widehat{c}(u)$ defined in Proposition 2.4.3:

Proposition 2.4.7 ([76]). *The center map $\widehat{c}(u)$ in (2.13) takes its values on a line $L \subset \mathbb{R}^3$. More precisely, it holds*

$$\widehat{c}''(u) = -2 \frac{\alpha'(u) + 2H\beta'(u)}{\alpha(u) + 2H\beta(u)} \widehat{c}'(u). \quad (2.27)$$

Proof. The identity (2.27) is the result of a long but straightforward computation obtained using (2.10), (2.11), (2.13) and (2.17). If $\omega_v \neq 0$, one additionally needs to use (2.15) as well as (2.21).

From (2.27), it can be deduced that the center map $\widehat{c}(u)$ lies in a line of \mathbb{R}^3 : indeed, let $\mathbf{t}_1, \mathbf{t}_2$ be two unit vectors orthogonal to $\widehat{c}'(0)$, and $f_i(u) := \langle \widehat{c}'(u), \mathbf{t}_i \rangle$, $i = 1, 2$. Clearly, $f_i(0) = 0$, and it follows from (2.27) that

$$f'_i(u) = -2 \frac{\alpha'(u) + 2H\beta'(u)}{\alpha(u) + 2H\beta(u)} f_i(u).$$

In particular, $f_i(u)$ satisfies a first order linear differential equation with $f_i(0) = 0$, which implies by uniqueness that $f_i(u) \equiv 0$. As a consequence, $\widehat{c}'(u)$ is orthogonal to \mathbf{t}_1 and \mathbf{t}_2 for all u , which implies that $\widehat{c}(u)$ lies in a line $L \subset \mathbb{R}^3$. \square

2.5 Enneper-type surfaces in space forms

In this section, we will deal with the extension of Enneper-type surfaces within the broader framework of space forms $\mathbb{M}^3(\kappa)$ of constant sectional curvature $\kappa \in \mathbb{R}$.

In Euclidean space, Enneper-type immersions are defined as CMC surfaces which admit a foliation by curvature lines that are *spherical*, i.e., each of such curvature lines lie in a certain sphere (or plane) of \mathbb{R}^3 ; see Definition 2.4.1. We note that both spheres and planes are the only *totally umbilical* surfaces of \mathbb{R}^3 . From this perspective, it is natural to define Enneper-type immersions in $\mathbb{M}^3(\kappa)$ as CMC surfaces admitting a foliation by curvature lines that belong to totally umbilical examples. A precise definition will be given in Subsection 2.5.2. We will first introduce a model for the spaces $\mathbb{M}^3(\kappa)$, $\kappa \in \mathbb{R}$.

2.5.1 A model for the space forms $\mathbb{M}^3(\kappa)$

Let $\mathbb{R}^4_\kappa = (\mathbb{R}^4, \langle \cdot, \cdot \rangle_\kappa)$, $\kappa \neq 0$, be the pseudo-Riemannian manifold which consists of \mathbb{R}^4 equipped with the metric

$$\langle \cdot, \cdot \rangle_\kappa := dx_1^2 + dx_2^2 + dx_3^2 + \frac{1}{\kappa} dx_4^2. \quad (2.28)$$

Up to a homothety in the x_4 coordinate, we can identify \mathbb{R}^4_κ with either the Euclidean space (if $\kappa > 0$) or the Lorentz space \mathbb{L}^4 (if $\kappa < 0$). For $\kappa = 0$, we define $\mathbb{R}^4_0 := (\mathbb{R}^4, \langle \cdot, \cdot \rangle_0)$, where $\langle \cdot, \cdot \rangle_0$ is the usual canonical metric in \mathbb{R}^4 .

Definition 2.5.1. For any $\kappa \neq 0$, we define the 3-manifold $\mathbb{M}^3(\kappa) \subset \mathbb{R}_\kappa^4$ as

$$\mathbb{M}^3(\kappa) := \{(x_1, x_2, x_3, x_4) : \kappa(x_1^2 + x_2^2 + x_3^2) + x_4^2 = 1, x_4 > 0 \text{ if } \kappa < 0\}. \quad (2.29)$$

Similarly, for $\kappa = 0$, we define $\mathbb{M}^3(0)$ as the hyperplane $\{x_4 = 1\} \subset \mathbb{R}_0^4$.

Remark 2.5.2. Observe that for every $\kappa \in \mathbb{R}$, $\mathbb{M}^3(\kappa) \subset \mathbb{R}_\kappa^4$ is a Riemannian space form of constant sectional curvature κ . This is immediate for $\kappa = 0$, as $\mathbb{M}^3(0)$ is just the affine hyperplane $\{x_4 = 1\}$ of \mathbb{R}^4 , while for $\kappa \neq 0$ it suffices to observe that $\mathbb{M}^3(\kappa)$ is a standard 3-sphere (resp. 3-dimensional hyperboloid) in \mathbb{R}^4 (resp. \mathbb{L}^4) after applying the change $x_4 \mapsto \sqrt{|\kappa|}x_4$.

As mentioned at the beginning of the current section, totally umbilical surfaces in $\mathbb{M}^3(\kappa)$ will be essential for introducing the concept of Enneper-type surfaces in space forms; see Definition 2.5.4. We do this next. In the Euclidean case $\kappa = 0$, we recall that spheres and planes are the only totally umbilical surfaces in \mathbb{R}^3 . Now, if $\kappa \neq 0$, totally umbilical surfaces appear as the intersection of $\mathbb{M}^3(\kappa) \subset \mathbb{R}_\kappa^4$ with a hyperplane of \mathbb{R}_κ^4 , that is, they correspond with sets

$$S[m, d] := \{x \in \mathbb{M}^3(\kappa) : \langle x, m \rangle_\kappa = d\} \quad (2.30)$$

for some $m \in \mathbb{R}^4 \setminus \{0\}$, $d \in \mathbb{R}$. The values m, d are determined up to a common multiplicative constant. A necessary condition for $S[m, d]$ to be a (non-empty) surface is that

$$\langle m, m \rangle_\kappa - \kappa d^2 > 0.$$

This condition is also sufficient except when $\kappa < 0$ and $\langle m, m \rangle_\kappa \leq 0$, in which case it is additionally required that d and the fourth coordinate of m have opposite signs.

Remark 2.5.3. If $\kappa > 0$, any surface $S[m, d]$ must be a sphere. For $\kappa < 0$, $S[m, d]$ will be a sphere (resp. horosphere, pseudosphere) if and only if $\langle m, m \rangle_\kappa$ is negative (resp. zero, positive). We also note that $S[m, d]$ is totally geodesic if and only if $d = 0$.

Whenever $S[m, d]$ is a sphere, the value $m \in \mathbb{R}_\kappa^4$ admits a rescaling such that m belongs to $\mathbb{M}^3(\kappa)$, and in fact $m \in \mathbb{M}^3(\kappa)$ corresponds to the geodesic center of $S[m, d]$. We note also that in this case $S[m, d]$ can be defined alternatively as the boundary of the geodesic ball $B[m, d] \subset \mathbb{M}^3(\kappa)$, where

$$B[m, d] := \{x \in \mathbb{M}^3(\kappa) : \langle x, m \rangle_\kappa \geq d\}. \quad (2.31)$$

2.5.2 Enneper-type surfaces in $\mathbb{M}^3(\kappa)$

We will now extend the concept of Enneper-type surfaces introduced in Definition 2.4.1 for the general case of space forms. For the rest of this section, we let $\psi(u, v) : \mathcal{D} \subset \mathbb{R}^2 \rightarrow \mathbb{M}^3(\kappa)$ be an immersion with constant mean curvature $H \geq 0$ in $\mathbb{M}^3(\kappa)$, $\kappa \in \mathbb{R}$ parametrized as in Theorem 2.2.1. Suppose that $(0, 0) \in \mathcal{D}$. Up to an orientation preserving isometry, we can assume $\psi(u, v)$ to satisfy the *initial conditions*

$$\psi(0, 0) = \mathbf{e}_4, \quad e^{-\omega(0,0)}\psi_u(0, 0) = \mathbf{e}_3, \quad e^{-\omega(0,0)}\psi_v(0, 0) = -\mathbf{e}_2, \quad N(0, 0) = \mathbf{e}_1, \quad (2.32)$$

where $\{\mathbf{e}_1, \mathbf{e}_2, \mathbf{e}_3, \mathbf{e}_4\}$ is the canonical basis in \mathbb{R}^4 . We remark that $\psi(0, 0) = \mathbf{e}_4$ belongs to $\mathbb{M}^3(\kappa)$ and that the vectors $\psi_u(0, 0)$, $\psi_v(0, 0)$, $N(0, 0)$ belong to $T_{\mathbf{e}_4}\mathbb{M}^3(\kappa)$ for all $\kappa \in \mathbb{R}$. In this context, the Gauss-Weingarten equations for $\psi(u, v)$ can be written as

$$\begin{cases} \psi_{uu} = \omega_u \psi_u - \omega_v \psi_v + (He^{2\omega} + Q)N - \kappa e^{2\omega} \psi, \\ \psi_{uv} = \omega_v \psi_u + \omega_u \psi_v, \\ \psi_{vv} = -\omega_u \psi_u + \omega_v \psi_v + (He^{2\omega} - Q)N - \kappa e^{2\omega} \psi, \\ N_u = -(H + Qe^{-2\omega})\psi_u, \\ N_v = -(H - Qe^{-2\omega})\psi_v. \end{cases} \quad (2.33)$$

We now define the concept of Enneper-type surfaces in space forms:

Definition 2.5.4. Given $u_0 \in \mathbb{R}$, we say that a v -curve $v \mapsto \psi(u_0, v)$ is spherical if it lies in a totally umbilical surface of $\mathbb{M}^3(\kappa)$. Moreover, we say that $\psi(u, v)$ is of Enneper type if every v -curve $v \mapsto \psi(u, v)$ is spherical.

Remark 2.5.5. By Joachimsthal's theorem, if a v -curvature line $v \mapsto \psi(u, v)$ lies in some totally umbilical surface $\mathcal{Q} \subset \mathbb{M}^3(\kappa)$, then the intersection angle θ between the immersion and \mathcal{Q} is constant.

Proposition 2.4.3 admits a natural extension in the non-Euclidean case $\kappa \neq 0$:

Proposition 2.5.6 ([76]). Let $\kappa \in \mathbb{R}$, $\kappa \neq 0$ and $u \in \mathbb{R}$. A v -curvature line $v \mapsto \psi(u, v)$ lies in a totally umbilical surface $\mathcal{Q} = \mathcal{Q}(u) \subset \mathbb{M}^3(\kappa)$ if and only if there exist $\alpha = \alpha(u)$, $\beta = \beta(u)$ such that the function $\omega(u, v)$ in (2.6) satisfies

$$2\omega_u = \alpha e^\omega + 2Q\beta e^{-\omega} \quad (2.34)$$

along the v -line. More specifically, the immersion meets $\mathcal{Q}(u) = S[\tilde{m}(u), \tilde{d}(u)]$ with angle $\theta(u)$ along $v \mapsto \psi(u, v)$, where

$$\alpha = -2H\beta - \frac{2\kappa\tilde{d}}{\sin\theta\sqrt{\langle\tilde{m}, \tilde{m}\rangle_\kappa - \kappa\tilde{d}^2}}, \quad \beta = -\cot\theta, \quad (2.35)$$

and

$$\tilde{m}(u) = -2e^{-\omega}\psi_u + 2\beta N + (\alpha + 2H\beta)\psi. \quad (2.36)$$

Proof. Suppose first that for some fixed $u \in \mathbb{R}$ the curve $v \mapsto \psi(u, v)$ lies in a totally umbilical surface $\mathcal{Q} = S[\hat{m}, \hat{d}]$, that is, $v \mapsto \langle\hat{m}, \psi(u, v)\rangle_\kappa \equiv \hat{d}$ for all $v \in \mathbb{R}$. As a consequence, the partial derivative $(\langle\hat{m}, \psi\rangle_\kappa)_v = \langle\hat{m}, \psi_v\rangle_\kappa$ vanishes identically, i.e., $\langle\hat{m}, \psi_v\rangle_\kappa \equiv 0$. We deduce from these properties that

$$\hat{N}(v) := \hat{m} - \kappa\hat{d}\psi(u, v)$$

lies in $T_{\psi(u, v)}\mathbb{M}^3(\kappa)$ for all v . Moreover, $\hat{N}(v)$ is orthogonal to $S[\hat{m}, \hat{d}]$ along the v -line $v \mapsto \psi(u, v)$, as $\langle\hat{N}, \mathbf{t}\rangle_\kappa = 0$ for every $\mathbf{t} \in T_{\psi(u, v)}\mathbb{M}^3(\kappa)$ tangent to $S[\hat{m}, \hat{d}]$. In other words, $\hat{N}(v)$ is (up to a multiplicative factor) the unit normal of $\mathcal{Q} \subset \mathbb{M}^3(\kappa)$. As a consequence of Joachimsthal's theorem, the angle θ between $\hat{N}(v)$ and the unit normal $N(u, v)$ of the immersion $\psi(u, v)$ is constant along the v -line, i.e., $\langle N, \hat{N}\rangle_\kappa = \|\hat{N}\|_\kappa \cos\theta$. In this way, it can be deduced that

$$\hat{m} = \|\hat{N}\|_\kappa \sin\theta e^{-\omega}\psi_u + \|\hat{N}\|_\kappa \cos\theta N + \kappa\hat{d}\psi.$$

The fact that $\hat{m}_v \equiv 0$ implies (2.34) for some pair $\alpha, \beta \in \mathbb{R}$ as in (2.35).

Conversely, assume that (2.34) holds for some fixed $u \in \mathbb{R}$. Combining (2.33) and (2.34), we deduce that the value $\tilde{m}(u, v)$ defined as in (2.36) does not depend on v , that is, $\tilde{m} = \tilde{m}(u)$. Note also that $\tilde{d} := \langle\tilde{m}, \psi(u, v)\rangle = \frac{1}{\kappa}(\alpha + 2H\beta)$ does not depend on v either. Consequently, the v -line $v \mapsto \psi(u, v)$ is contained in the totally umbilical surface $\mathcal{Q} := S[\tilde{m}, \tilde{d}]$. The unit normal of \mathcal{Q} is (up to a multiplicative factor) given by $\hat{N}(v) = \tilde{m} - \kappa\tilde{d}\psi(u, v)$. From this, it can be checked that the pair (\tilde{m}, \tilde{d}) and the intersection angle θ between $\psi(u, v)$ and \mathcal{Q} are related to the pair (α, β) by (2.35). \square

Remark 2.5.7. We note that the map $\tilde{m}(u)$ in (2.36) is well defined in the Euclidean case $\kappa = 0$. In fact, if $\alpha(u) + 2H\beta(u) \neq 0$, the rescaling

$$\hat{c}(u) := \frac{1}{\alpha(u) + 2H\beta(u)}\tilde{m}(u)$$

lies in $\mathbb{M}^3(0) = \mathbb{R}_0^4 \cap \{x_4 = 1\}$, and this expression coincides with the center map $\widehat{c}(u)$ introduced in (2.13).

Combining Theorem 2.2.1 and Proposition 2.5.6, we can extend Theorem 2.4.4 in this context.

Theorem 2.5.8. *Let $\mathcal{D} \subset \mathbb{R}^2$ be a simply connected open set. Any solution $\omega(u, v) : \mathcal{D} \mapsto \mathbb{R}$ to the overdetermined system (2.14) with $Q > 0$ and $A = H^2 + \kappa$, induces an Enneper-type immersion $\psi(u, v) : \mathcal{D} \rightarrow \mathbb{M}^3(\kappa)$ with first and second fundamental forms given by (2.6). In particular, $\psi(u, v)$ does not have umbilical points.*

Remark 2.5.9. *We note that the statement of Theorem 2.4.5 is purely analytical, so the result can also be applied in space forms. Hence, it is possible to study the moduli space of Enneper type immersions in $\mathbb{M}^3(\kappa)$ in terms of the set of solutions $(\alpha(u), \beta(u))$ to (2.17).*

In the study of Enneper surfaces in \mathbb{R}^3 , it was proved that the center map $\widehat{c}(u)$ in (2.13) takes its values on line of the Euclidean space; see Proposition 2.4.7. The geometric analogue of this property also holds in the context of space forms, as shown by the following proposition and remark.

Proposition 2.5.10. *The map $\widetilde{m}(u)$ in (2.36) takes its values on a 2-dimensional linear subspace \mathcal{P}_0 of \mathbb{R}_κ^4 such that $\widetilde{m}(0), \widetilde{m}'(0) \in \mathcal{P}_0$. Moreover, $\widetilde{m}(u)$ satisfies the second order differential equation*

$$\widetilde{m}''(u) = (\widehat{a} - 2QH - 4Q\alpha(u)\beta(u))\widetilde{m}(u). \quad (2.37)$$

Proof. The identity (2.37) follows from a straightforward computation using (2.15), (2.17), (2.21), (2.33), (2.34) and (2.36). Now, let \mathcal{P}_0 be any 2-dimensional linear subspace containing the vectors $\widetilde{m}(0), \widetilde{m}'(0)$. Moreover, denote by $f(u)$ the orthogonal projection of the map $\widetilde{m}(u)$ in \mathcal{P}_0 with respect to the canonical Euclidean metric in \mathbb{R}^4 . It is clear by (2.37) that $f'' = (\widehat{a} - 2QH - 4Q\alpha\beta)f$, and that $f(0) = \widetilde{m}(0)$, $f'(0) = \widetilde{m}'(0)$. By uniqueness of solutions to ordinary differential equations, we deduce that $f(u) \equiv \widetilde{m}(u)$, so $\widetilde{m}(u) \in \mathcal{P}_0$ for all u . \square

Remark 2.5.11. *Let $\kappa \neq 0$ and $u \in \mathbb{R}$ so that the surface $\mathcal{Q}(u) = S[\widetilde{m}(u), \widetilde{d}(u)]$ is a sphere in $\mathbb{M}^3(\kappa)$. In such a case, it follows from Remark 2.5.3 that $\widetilde{m}(u)$ admits a rescaling $m(u) \in \mathbb{M}^3(\kappa)$ such that $m(u)$ is the geodesic center of $\mathcal{Q}(u)$. This implies that $m(u) \in \mathcal{P}_0 \cap \mathbb{M}^3(\kappa)$, and so the intersection $\mathcal{L} := \mathcal{P}_0 \cap \mathbb{M}^3(\kappa)$ cannot be empty. In particular, \mathcal{L} is a geodesic of $\mathbb{M}^3(\kappa)$.*

2.6 Rotational free boundary CMC annuli in geodesic balls

This section is devoted to the study of rotational CMC H surfaces in $\mathbb{M}^3(\kappa)$, $H \geq 0$, $\kappa \in \mathbb{R}$. More precisely, our goal is to show that a wide family of these rotational examples admit a compact, embedded annular piece which is free boundary in some geodesic ball of $\mathbb{M}^3(\kappa)$. This will be achieved in Theorem 2.6.9.

A detailed study of rotational CMC surfaces in space forms was carried out by do Carmo and Dajczer [13]. The existence of rotational surfaces with free boundary has also been studied by several authors [5, 56, 68] using different methods. However, we will need a more general existence result which has not been covered on previous works.

We will first present a general parametrization for the set of rotational CMC surfaces in our model of the spaces $\mathbb{M}^3(\kappa)$; see (2.29). We will restrict to the set of surfaces which are not totally umbilical. We remark that in the Euclidean case $\kappa = 0$, these surfaces are either catenoids (if $H = 0$) or nodoids, unduloids and cylinders (if $H > 0$).

2.6.1 Rotational CMC surfaces in $\mathbb{M}^3(\kappa)$

We consider different cases, depending on the sign of the curvature of the space $\mathbb{M}^3(\kappa)$.

Rotational CMC surfaces in spherical space. In what follows, we let $\kappa > 0$. Up to isometries, any rotational immersion in $\mathbb{M}^3(\kappa)$, viewed in the model (2.29), can be expressed as

$$\psi(\mathfrak{s}, \theta) = (x \cos \theta, -x \sin \theta, \sqrt{1/\kappa - x^2} \sin \phi, \sqrt{1 - \kappa x^2} \cos \phi), \quad (2.38)$$

for some functions $x = x(\mathfrak{s})$, $\phi = \phi(\mathfrak{s})$, where $\mathfrak{s} \in \mathbb{R}$ is the arclength parameter of the profile curve of the immersion. We note that the geodesic

$$\mathcal{X} := \{x_1 = x_2 = 0\} \cap \mathbb{M}^3(\kappa)$$

is the *rotation axis* of $\psi(\mathfrak{s}, \theta)$. If the immersion has CMC $H \geq 0$ and it is not totally umbilic, it can be shown that $x(\mathfrak{s})$ must be an analytic function satisfying the following

differential equation:

$$x'^2 = \frac{h(x)}{x^2} := \frac{x^2 - \kappa x^4 - (Hx^2 - \delta)^2}{x^2} \quad (2.39)$$

for some constant $\delta \neq 0$. In order for (2.39) to have solutions, it is necessary that the polynomial $h(x)$ be non-negative for some $x \in \mathbb{R}$. This will happen if and only if δ satisfies the condition

$$\delta \in \left[\frac{H - \mu}{2\kappa}, \frac{H + \mu}{2\kappa} \right], \quad (2.40)$$

where $\mu = \sqrt{H^2 + \kappa}$. If $\delta = \frac{H \pm \mu}{2\kappa}$, the polynomial $h(x)$ is non-positive, having roots at the values $x = \pm \sqrt{|\delta|/\mu}$. Hence, the only solutions to (2.39) in this case are the constants given by the roots of $h(x)$. Otherwise, if $\delta \in (\frac{H - \mu}{2\kappa}, \frac{H + \mu}{2\kappa})$ and $\delta \neq 0$, then $h(x)$ has four simple roots $-x_M < -x_m < 0 < x_m < x_M$. The differential equation (2.39) has two types of analytic solutions: the constants $x = \pm x_m$, $x = \pm x_M$, and a set of non-constant functions $x(\mathfrak{s})$ which oscillate either on the interval $[-x_M, -x_m]$ or on $[x_m, x_M]$. In this case, the only solutions $x(\mathfrak{s})$ that yield actual CMC surfaces in $\mathbb{M}^3(\kappa)$ are the oscillating ones. Up to isometries, we can always assume that $x(0) = x_m$.

Proposition 2.6.1. ([13]) *Let $\kappa > 0$, $H \geq 0$ and $\delta \neq 0$ satisfying (2.40). If $\delta = \frac{H \pm \mu}{2\kappa}$, set $x(\mathfrak{s}) := \sqrt{|\delta|/\mu}$. Otherwise, let $x(\mathfrak{s})$ be the unique non-constant solution of (2.39) with initial condition $x(0) = x_m$. Additionally, let*

$$\phi(\mathfrak{s}) := \int_0^{\mathfrak{s}} \frac{\delta - Hx^2}{\sqrt{\kappa}x(1/\kappa - x^2)} ds. \quad (2.41)$$

Denoting $\mathbb{S}^1 \equiv \mathbb{R}/(2\pi\mathbb{Z})$, the immersion $\psi : \mathbb{R} \times \mathbb{S}^1 \rightarrow \mathbb{M}^3(\kappa)$ given by (2.38) defines a rotational CMC- H surface, where \mathfrak{s} is the arclength parameter of the profile curve of the immersion. The \mathfrak{s} -curves and θ -curves are curvature lines with principal curvatures

$$\kappa_{\mathfrak{s}} = H + \frac{\delta}{x^2}, \quad \kappa_{\theta} = H - \frac{\delta}{x^2}. \quad (2.42)$$

Conversely, any rotational CMC surface in $\mathbb{M}^3(\kappa)$ must be an open piece of either one of these examples, or of a totally umbilical surface.

Definition 2.6.2 (Spherical nodoids, unduloids and catenoids). *Let $\kappa > 0$. For any $H \geq 0$ and $\delta \neq 0$ such that (2.40) holds, let $\mathcal{S} = \mathcal{S}(\kappa, H, \delta)$ be the rotational CMC surface in $\mathbb{M}^3(\kappa)$ of Proposition 2.6.1.*

- *If $H > 0$ and $0 < \delta < \frac{H + \mu}{2\kappa}$ we will say that \mathcal{S} is a spherical nodoid.*

- If $H > 0$ and $\frac{H-\mu}{2\kappa} < \delta < 0$ we will say that \mathcal{S} is a spherical unduloid.
- If $H = 0$ we will say that \mathcal{S} is a spherical catenoid. Since the change $\delta \mapsto -\delta$ just gives a reparameterization of \mathcal{S} , we can assume in this case that $\delta > 0$.
- If $\delta = \frac{H \pm \mu}{2\kappa}$, \mathcal{S} covers a flat torus. For $H = 0$, it is a Clifford torus.

Rotational CMC surfaces in hyperbolic space. In the hyperbolic case, in which we assume $\kappa < 0$, we will focus on rotational surfaces of *elliptic* type, that is, surfaces which are invariant by a compact, continuous 1-parameter subgroup of isometries of $\mathbb{M}^3(\kappa)$. Arguing as in the spherical case, up to an isometry, any rotational surface of elliptic type in $\mathbb{M}^3(\kappa)$ can be expressed in the model (2.29) as

$$\psi(\mathfrak{s}, \theta) = (x \cos \theta, -x \sin \theta, \sqrt{x^2 - 1/\kappa} \sinh \phi, \sqrt{1 - \kappa x^2} \cosh \phi), \quad (2.43)$$

where \mathfrak{s} is the arclength parameter of the profile curve of the immersion. The geodesic

$$\mathcal{X} = \{x_1 = x_2 = 0\} \cap \mathbb{M}^3(\kappa)$$

is the *rotation axis* of the immersion. It can be shown that if $\psi(\mathfrak{s}, \theta)$ has constant mean curvature $H \geq 0$ and no umbilical points, then $x(\mathfrak{s})$ must be a solution of (2.39) for some $\delta \in \mathbb{R}$, $\delta \neq 0$. In particular, $h(x)$ must be non-negative for some $x \in \mathbb{R}$. This will happen in any of these situations:

1. $H^2 + \kappa < 0$,
2. $H^2 + \kappa = 0$ and $\delta > -\frac{1}{2\sqrt{|\kappa|}}$,
3. $H^2 + \kappa > 0$ and $\delta \geq \frac{\mu-H}{|\kappa|}$.

In cases (1) and (2), the polynomial $h(x)$ has two roots $-x_m < 0 < x_m$, and $h(x) \geq 0$ for all $x \in (-\infty, -x_m] \cup [x_m, \infty)$. In case (3), $h(x)$ has four roots $-x_M \leq -x_m < 0 < x_m \leq x_M$, with equality $x_m = x_M$ if and only if $\delta = \frac{\mu-H}{2|\kappa|}$. In this third case, $h(x) \geq 0$ for every $x \in [-x_M, -x_m] \cup [x_m, x_M]$.

If $H^2 + \kappa > 0$ and $\delta = \frac{\mu-H}{2|\kappa|}$, then $x_m = x_M = \sqrt{\frac{|\delta|}{\mu}}$ and the only analytic solutions of (2.39) are the constants $x = \pm x_m$. The resulting surfaces are flat hyperbolic cylinders in $\mathbb{M}^3(\kappa)$.

In the rest of cases, (2.39) has two types of analytic solutions: the constants given by the roots of $h(x)$, and non-constant solutions. The only ones that give rise to actual CMC immersions are those which are not constant. More specifically, if $H^2 + \kappa > 0$,

then $x(\mathfrak{s})$ oscillates on either $[-x_M, -x_m]$ or $[x_m, x_M]$. If $H^2 + \kappa \leq 0$, $x(\mathfrak{s})$ is unbounded, taking values on either $(-\infty, -x_m]$ or $[x_m, \infty)$. In either case, up to isometries in $\mathbb{M}^3(\kappa)$, we can always assume that $x(0) = x_m$.

Proposition 2.6.3 ([13]). *Let $\kappa < 0$, $H \geq 0$, $\delta \neq 0$. If $H^2 + \kappa > 0$ and $\delta = \frac{\mu-H}{2|\kappa|}$, let $x(\mathfrak{s}) \equiv x_m$. Otherwise, let $x(\mathfrak{s})$ be the unique nonconstant solution of (2.39) with initial condition $x(0) = x_m$. We define*

$$\phi(\mathfrak{s}) := \int_0^{\mathfrak{s}} \frac{\delta - Hx^2}{\sqrt{|\kappa|x(x^2 - 1/\kappa)}} ds. \quad (2.44)$$

Under these conditions, the immersion $\psi : \mathbb{R} \times \mathbb{S}^1 \rightarrow \mathbb{M}^3(\kappa)$ in (2.43) is a rotational surface in $\mathbb{M}^3(\kappa)$ of elliptic type with constant mean curvature $H \geq 0$ parametrized by curvature lines. In particular, \mathfrak{s} is the arclength parameter of the profile curve of the immersion, and the principal curvatures are given by (2.42).

Conversely, any rotational CMC surface of elliptic type in $\mathbb{M}^3(\kappa)$ must be an open piece of either one of these examples, or of a totally umbilical surface of $\mathbb{M}^3(\kappa)$.

Definition 2.6.4 (Hyperbolic nodoids, unduloids and catenoids). *We will say that the immersion $\psi(\mathfrak{s}, \theta)$ in Proposition 2.6.3 is a hyperbolic nodoid (resp. unduloid) if $H^2 + \kappa > 0$ and $\delta > 0$ (resp. $\frac{\mu-H}{2|\kappa|} < \delta < 0$), and denote it by $\mathcal{S} = \mathcal{S}(\kappa, H, \delta)$.*

Similarly, if $H = 0$, we will say that $\psi(\mathfrak{s}, \theta)$ is a hyperbolic catenoid. In this case, the change $\delta \mapsto -\delta$ just gives a reparametrization of the same surface, so we may assume that $\delta > 0$ in this case.

Rotational CMC surfaces in Euclidean space. We finally deal with the Euclidean case $\kappa = 0$. As pointed out in Section 2.5.1, $\mathbb{M}^3(0) \equiv \mathbb{R}^3$ is just the hyperplane $\mathbb{R}^4 \cap \{x_4 = 1\}$. Hence, any rotational surface in the $\mathbb{M}^3(0)$ model can be expressed as

$$\psi(\mathfrak{s}, \theta) = (x \cos \theta, -x \sin \theta, x_3, 1), \quad (2.45)$$

where $x = x(\mathfrak{s})$, $x_3 = x_3(\mathfrak{s})$ are functions of \mathfrak{s} , the arclength parameter of the profile curve. The rotation axis of the immersion is the line $\mathcal{X} = \{x_1 = x_2 = 0\} \cap \mathbb{M}^3(0)$. If $\psi(\mathfrak{s}, \theta)$ has CMC $H \geq 0$, then $x(\mathfrak{s})$ must be a solution of (2.39). In this case, the polynomial $h(x)$ will be non-negative for some $x \in \mathbb{R}$ if one of the following conditions hold:

1. $H > 0$ and $\delta \geq -\frac{1}{4H}$,
2. $H = 0$.

In case (1), if $\delta = -\frac{1}{4H}$, the polynomial $h(x)$ is non-positive and has two roots $x = \pm\frac{1}{2H}$ of multiplicity 2. Hence, the only solutions to (2.39) are precisely the constants $x(\mathfrak{s}) = \pm\frac{1}{2H}$. Otherwise, if $\delta > -\frac{1}{4H}$, $h(x)$ has four roots $-x_M < -x_m < 0 < x_m < x_M$, and $h(x) \geq 0$ if $x \in [-x_M, -x_m] \cup [x_m, x_M]$. As in the previous cases, the only solutions $x(\mathfrak{s})$ to (2.39) associated to CMC immersions are the non-constant ones, which take values in one of the intervals $[-x_M, -x_m]$ or $[x_m, x_M]$.

In case (2), the polynomial $h(x)$ is non-negative on the intervals $(-\infty, -x_m] \cup [x_m, \infty)$, where $x_m = |\delta|$. The solutions $x(\mathfrak{s})$ that induce actual immersions in $\mathbb{M}^3(0)$ are unbounded and take values in one of the intervals $(-\infty, -x_m]$ or $[x_m, \infty)$.

Proposition 2.6.5. ([13]) *Let $H \geq 0$, $\delta \neq 0$. If $H > 0$ and $\delta = -\frac{1}{4H}$, let $x(\mathfrak{s}) = \frac{1}{2H}$. Otherwise, let $x(\mathfrak{s})$ be the unique non-constant solution of (2.39) with $x(0) = x_m$. Let us also define $x_3(\mathfrak{s})$ as*

$$x_3(\mathfrak{s}) := \int_0^{\mathfrak{s}} \frac{\delta - Hx^2}{x} ds. \quad (2.46)$$

Then, the immersion $\psi(\mathfrak{s}, \theta) : \mathbb{R} \times \mathbb{S}^1 \mapsto \mathbb{M}^3(0)$ given in (2.45) is a CMC H surface in $\mathbb{M}^3(0)$ parametrized by curvature lines, with principal curvatures given by (2.42). Moreover, \mathfrak{s} corresponds to the arclength parameter of the profile curve of surface.

According to the values of H and δ , the immersion $\mathcal{S} = \mathcal{S}(0, H, \delta)$ in (2.45) can be classified as follows:

- \mathcal{S} is a cylinder if $H > 0$ and $\delta = -\frac{1}{4H}$.
- \mathcal{S} is an unduloid if $H > 0$ and $-\frac{1}{4H} < \delta < 0$,
- \mathcal{S} is a nodoid if $H > 0$ and $\delta > 0$.
- \mathcal{S} is a catenoid if $H = 0$.

2.6.2 Existence of rotational free boundary CMC surfaces

We will now show that every rotational CMC surface $\mathcal{S}(\kappa, H, \delta)$ with $\delta > 0$ constructed in Section 2.6.1 admits a compact, annular piece with free boundary in some geodesic ball of $\mathbb{M}^3(\kappa)$.

Definition 2.6.6. *For every $\mathfrak{s}_0 > 0$, we define $\mathfrak{A} = \mathfrak{A}(\mathfrak{s}_0)$ as the compact annulus contained in $\mathcal{S}(\kappa, H, \delta)$ given by the restriction of $\psi(\mathfrak{s}, \theta)$ to $[-\mathfrak{s}_0, \mathfrak{s}_0] \times \mathbb{S}^1$, where we identify the points $(\mathfrak{s}, \theta + 2\pi) \sim (\mathfrak{s}, \theta)$.*

Remark 2.6.7. Let $x_3(\mathfrak{s})$ denote the third coordinate of the immersion $\psi(\mathfrak{s}, \theta)$ in (2.38), (2.43) or (2.45). The fact that $x(0) = x_m$ and $x_3(0) = 0$ along with (2.39), (2.41), (2.44), (2.46) imply that the function $x(\mathfrak{s})$ is symmetric, while $x_3(\mathfrak{s})$ is antisymmetric. A geometric consequence of this is that for every $\mathfrak{s}_0 > 0$, the annulus $\mathfrak{A}(\mathfrak{s}_0)$ is symmetric with respect to the totally geodesic surface

$$\mathbf{S} := \{x_3 = 0\} \cap \mathbb{M}^3(\kappa) \quad (2.47)$$

of $\mathbb{M}^3(\kappa)$. We note that the geodesic balls centered at the point $\mathbf{e}_4 \in \mathbb{M}^3(\kappa)$ are also symmetric with respect to \mathbf{S} and invariant under rotations with axis $\mathcal{X} := \{x_1 = x_2 = 0\} \cap \mathbb{M}^3(\kappa)$.

We will now state the main result of this section. In order to do so, we must introduce first the following concept:

Definition 2.6.8. For every $\mathfrak{s}_0 > 0$, we define $\zeta_{\mathfrak{s}_0} \subset \mathbb{M}^3(\kappa)$ as the unique geodesic of $\mathbb{M}^3(\kappa)$ passing through $\psi(\mathfrak{s}_0, 0)$ with tangent vector $\psi_{\mathfrak{s}}(\mathfrak{s}_0, 0)$.

Theorem 2.6.9. Let $(\kappa, H, \delta) \in \Omega$, where

$$\Omega := \{(\kappa, H, \delta) \in \mathbb{R}^3 : H \geq 0, \delta > 0, 2\kappa\delta < H + \mu \text{ if } \kappa > 0\} \quad (2.48)$$

and $\mu = \sqrt{H^2 + \kappa}$. Then, the following properties hold:

1. There exists a map $\tilde{\mathfrak{s}} = \tilde{\mathfrak{s}}(\kappa, H, \delta) > 0$ such that the compact annulus $\mathfrak{A}(\tilde{\mathfrak{s}}) \subset \mathbb{M}^3(\kappa)$ in Definition 2.6.6 is embedded and free boundary in a geodesic ball $B = B(\kappa, H, \delta) \subset \mathbb{M}^3(\kappa)$ centered at \mathbf{e}_4 . Additionally, B is contained in the half-space $\{x_4 > 0\}$, and the principal curvature $\kappa_{\mathfrak{s}}(\mathfrak{s})$ associated to the profile curve of the annulus is decreasing for all $\mathfrak{s} \in [0, \tilde{\mathfrak{s}}]$.
2. There exists a neighbourhood $I_1 \subset \mathbb{R}$ of $\tilde{\mathfrak{s}} = \tilde{\mathfrak{s}}(\kappa, H, \delta)$ such that, for every $\mathfrak{s} \in I_1$, the rotation axis \mathcal{X} of $\mathfrak{A}(\mathfrak{s})$ and the geodesic $\zeta_{\mathfrak{s}}$ in Definition 2.6.8 meet at a unique point $\hat{p}(\mathfrak{s})$ with $\hat{p}_4(\mathfrak{s}) > 0$. Moreover, the function $\hat{p} : I_1 \rightarrow \mathcal{X}$ is analytic with $\hat{p}_3(\tilde{\mathfrak{s}}) = 0$ and $\hat{p}_3'(\tilde{\mathfrak{s}}) > 0$. Here, $\hat{p}_3(\mathfrak{s}), \hat{p}_4(\mathfrak{s})$ denote the third and fourth coordinates of $\hat{p}(\mathfrak{s})$ respectively.
3. $\tilde{\mathfrak{s}} : \Omega \rightarrow (0, \infty)$ is a real analytic function.
4. $\tilde{\mathfrak{s}}(\kappa, H, \delta)$ extends continuously to the boundary surface

$$\partial\Omega_1 := \{\kappa > 0, H \geq 0, \delta > 0, 2\kappa\delta = H + \mu\} \subset \partial\Omega. \quad (2.49)$$

In fact,

$$\tilde{\mathfrak{s}}(\kappa, H, \delta)|_{\partial\Omega_1} = \frac{\pi}{2\sqrt{2\mu(H+\mu)}}. \quad (2.50)$$

Remark 2.6.10. *The previous Theorem does not ensure that the annuli $\mathfrak{A}(\tilde{\mathfrak{s}})$ associated to surfaces $\mathcal{S}(\kappa, H, \delta)$ with $(\kappa, H, \delta) \in \partial\Omega_1$ admit embedded, free boundary annular pieces. However, these surfaces are rotational flat tori, and the functions $x(\mathfrak{s})$, $x_3(\mathfrak{s})$ can be computed explicitly:*

$$x(\mathfrak{s}) \equiv \sqrt{\frac{\mu+H}{2\kappa\mu}}, \quad x_3(\mathfrak{s}) = \sqrt{\frac{\mu-H}{2\kappa\mu}} \sin\left(\sqrt{2\mu(H+\mu)}\mathfrak{s}\right). \quad (2.51)$$

It is then possible to check that the annulus $\mathfrak{A}(\tilde{\mathfrak{s}})$, with $\tilde{\mathfrak{s}}$ defined as in (2.50), is embedded and free boundary in $B[\mathbf{e}_4, 0]$; see (2.31).

The rest of this section is devoted to showing Theorem 2.6.9. The proof of this result is lengthy and technically involved; therefore, we will prove items (1), (2), (3) and (4) separately.

Proof of item (1) of Theorem 2.6.9.

Let $(\kappa, H, \delta) \in \Omega$. By Remark 2.6.7, if an annulus $\mathfrak{A}(\mathfrak{s}_0)$ were free boundary in a geodesic ball $B \subset \mathbb{M}^3(\kappa)$, the following properties should hold:

1. B must be invariant under symmetry with respect to the totally geodesic surface \mathbf{S} and rotations with respect to the geodesic \mathcal{X} . In particular, the geodesic center of B has to be the point \mathbf{e}_4 where \mathcal{X} and \mathbf{S} meet.
2. The profile curve $\mathfrak{s} \mapsto \psi(\mathfrak{s}, 0)$ must meet the boundary of B orthogonally at $\mathfrak{s} = \mathfrak{s}_0$. Since B is a geodesic ball, this is equivalent to the fact that the geodesic $\zeta_{\mathfrak{s}_0}$ in Definition 2.6.8 meets \mathbf{e}_4 , i.e. the center of B .

As we will see in Lemma 2.6.12, these two geometric properties can be reduced to studying whether the function

$$F(\mathfrak{s}) := x_3(\mathfrak{s})x'(\mathfrak{s}) - x'_3(\mathfrak{s})x(\mathfrak{s}) \quad (2.52)$$

vanishes at $\mathfrak{s} = \mathfrak{s}_0$. Here, $x(\mathfrak{s})$ and $x_3(\mathfrak{s})$ denote the first and third coordinates of the profile curve $\psi(\mathfrak{s}, 0)$ in (2.38), (2.43), (2.45). In the following lemma, we will show that $F(\mathfrak{s})$ has a first positive root $\tilde{\mathfrak{s}}(\kappa, H, \delta)$ for every $(\kappa, H, \delta) \in \Omega$. Later, in Lemma

2.6.12, we will show that this root of $F(\mathfrak{s})$ is indeed related to a free boundary annular piece $\mathfrak{A}(\tilde{\mathfrak{s}})$, showing item (1) of Theorem 2.6.9.

Lemma 2.6.11. *For any $(\kappa, H, \delta) \in \Omega$, the function $F(\mathfrak{s})$ in (2.52) has a first positive root $\tilde{\mathfrak{s}} = \tilde{\mathfrak{s}}(\kappa, H, \delta) > 0$ such that $F(\mathfrak{s}) < 0$ for all $\mathfrak{s} \in [0, \tilde{\mathfrak{s}})$. In addition,*

1. *$x(\mathfrak{s})$ is strictly increasing on $[0, \tilde{\mathfrak{s}}]$, while the principal curvature $\kappa_{\mathfrak{s}}$ in (2.42) is decreasing. Moreover, $x'(\tilde{\mathfrak{s}}) > 0$, and $\delta - Hx(\tilde{\mathfrak{s}})^2 > 0$.*
2. *$x'_3(\mathfrak{s}) > 0$ for every $\mathfrak{s} \in [-\tilde{\mathfrak{s}}, \tilde{\mathfrak{s}}]$. In particular, $x_3(\mathfrak{s})$ is strictly positive in $(0, \tilde{\mathfrak{s}}]$.*
3. *If $\kappa \neq 0$, $\kappa x'_4(\mathfrak{s}) < 0$ for all $\mathfrak{s} \in (0, \tilde{\mathfrak{s}}]$ and $x_4(\tilde{\mathfrak{s}}) > 0$, where $x_4(\mathfrak{s})$ is the fourth coordinate of the profile curve $\psi(\mathfrak{s}, 0)$.*

Proof. We will prove that $F(0) < 0$ and that $F(\mathfrak{s}_0) > 0$ for some $\mathfrak{s}_0 > 0$, deducing the existence of a first positive root $\tilde{\mathfrak{s}} \in (0, \mathfrak{s}_0)$. The properties on the functions $x(\mathfrak{s})$, $x_3(\mathfrak{s})$, $x_4(\mathfrak{s})$ will appear naturally in the process.

It is possible to check that $F(0) < 0$ using (2.38), (2.39), (2.41), (2.43), (2.44), (2.45) and (2.46): indeed, for all $(\kappa, H, \delta) \in \Omega$, it holds $x_3(0) = 0$, $x(0) = x_m > 0$ and $\delta - Hx_m^2 > 0$, which implies that $x'_3(0) > 0$. Hence, it just remains to prove that $F(\mathfrak{s}_0) > 0$ for some $\mathfrak{s}_0 > 0$. We will deal with seven cases depending on the sign of κ .

Case 1: $\kappa > 0$ and $H > \kappa\delta$.

In this case, the polynomial $h(x)$ in (2.39) has two positive roots $0 < x_m < x_M$. According to (2.39), $x(\mathfrak{s})$ is increasing on an interval $\mathfrak{s} \in (0, \mathfrak{s}_2)$, where $\mathfrak{s}_2 > 0$ is the first positive value such that $x(\mathfrak{s}_2) = x_M$. Furthermore, $x_0 = \sqrt{\delta/H}$ satisfies $x_m < x_0 < x_M$, so the function $\mathfrak{s} \mapsto \delta - Hx(\mathfrak{s})^2$, and consequently $\phi'(\mathfrak{s})$, changes sign on the interval $(0, \mathfrak{s}_2)$. Hence, there exists a first value $\mathfrak{s}_1 \in (0, \mathfrak{s}_2)$ such that $(\sin(\phi))'|_{\mathfrak{s}=\mathfrak{s}_1} = 0$, so in particular $\sin(\phi(\mathfrak{s}))$ is increasing on $[0, \mathfrak{s}_1]$. As a consequence, $\delta - Hx(\mathfrak{s})^2 \geq 0$ for all $\mathfrak{s} \in [0, \mathfrak{s}_1]$, and $x'_3(\mathfrak{s}_1) < 0$. If we define $\mathfrak{s}_0 < \mathfrak{s}_1$ as the first positive value for which $x'_3(\mathfrak{s}_0) = 0$, it is possible to deduce that $F(\mathfrak{s}_0) > 0$, as we wanted to show. Properties (1) and (2) of Lemma 2.6.11 follow from the fact that $\tilde{\mathfrak{s}} \in (0, \mathfrak{s}_0)$. We finally note that the function $x_4(\mathfrak{s})$ is strictly decreasing and positive for all $\mathfrak{s} \in [0, \mathfrak{s}_0)$, so property (3) of Lemma 2.6.11 also holds.

Case 2: $\kappa > 0$ and $H = \kappa\delta$.

In this situation, the polynomial $h(x)$ has two positive roots $0 < x_m < x_M$, with $x_M = 1/\sqrt{\kappa}$. As before, let us define $\mathfrak{s}_2 > 0$ as the first positive value such that $x(\mathfrak{s}_2) = 1/\sqrt{\kappa}$. This implies that $x_3(0) = x_3(\mathfrak{s}_2) = 0$, and since $x'_3(0) > 0$, there exists a first $\mathfrak{s}_0 \in (0, \mathfrak{s}_2)$ such that $x'_3(\mathfrak{s}_0) = 0$. Now, $x_3(\mathfrak{s})$ is increasing on $[0, \mathfrak{s}_0]$, so

in particular $x_3(\mathfrak{s}_0) > 0$, and hence $F(\mathfrak{s}_0) > 0$, deducing the existence of $\tilde{\mathfrak{s}} \in (0, \mathfrak{s}_0)$. Note also that the function $\phi(\mathfrak{s})$ must be increasing on $[0, \mathfrak{s}_0]$, and so $\delta - Hx^2(\mathfrak{s}) \geq 0$ for all $\mathfrak{s} \in [0, \mathfrak{s}_0]$. Properties (1) and (2) of Lemma 2.6.11 can be deduced from this. We also claim that $\phi(\mathfrak{s}_0) < \frac{\pi}{2}$: otherwise, there would be an intermediate value $\bar{\mathfrak{s}}$ such that $\phi(\bar{\mathfrak{s}}) = \frac{\pi}{2}$, and so $x'_3(\bar{\mathfrak{s}}) < 0$ at that point, reaching a contradiction. A consequence of this fact is that $x_4(\mathfrak{s})$ is decreasing and positive for all $\mathfrak{s} \in [0, \mathfrak{s}_0)$, proving property (3) of Lemma 2.6.11.

Case 3: $\kappa > 0$ and $H < \kappa\delta$.

Note that for all $x \in \left[0, \frac{1}{\sqrt{\kappa}}\right]$, it holds $\delta - Hx^2 > H(\frac{1}{\kappa} - x^2) \geq 0$, so $\phi(\mathfrak{s})$ is increasing for all $\mathfrak{s} \in \mathbb{R}$. As in the previous cases, let $\mathfrak{s}_2 > 0$ the first positive value for which $x(\mathfrak{s}_2) = x_M$, where x_M is the largest positive root of $h(x)$ in (2.39). We note that $x_M < \frac{1}{\sqrt{\kappa}}$. If we manage to prove that $\phi(\mathfrak{s}_2) > \pi/2$, then there must exist a unique $\mathfrak{s}_0 \in (0, \mathfrak{s}_2)$ such that $\phi(\mathfrak{s}_0) = \pi/2$. In particular, $x_3(\mathfrak{s}_0) > 0$, $x'_3(\mathfrak{s}_0) < 0$, and so $F(\mathfrak{s}_0) > 0$. Additionally, we deduce that $x_4(\mathfrak{s})$ is decreasing and positive for all $\mathfrak{s} \in [0, \mathfrak{s}_0)$. This would show Lemma 2.6.11 in this case.

Let us then show that $\phi(\mathfrak{s}_2) > \pi/2$. Consider the change of variables $w(\mathfrak{s}) = x(\mathfrak{s})^2$ on the integral that describes $\phi(\mathfrak{s}_2)$. Defining $w_m = w(0) = x_m^2$, $w_M = w(\mathfrak{s}_2) = x_M^2$, it follows from (2.39) that

$$\phi(\mathfrak{s}_2) = \int_{w_m}^{w_M} \frac{\delta - Hw}{2\sqrt{\kappa w}(1/\kappa - w)\sqrt{w - \kappa w^2 - (Hw - \delta)^2}} dw.$$

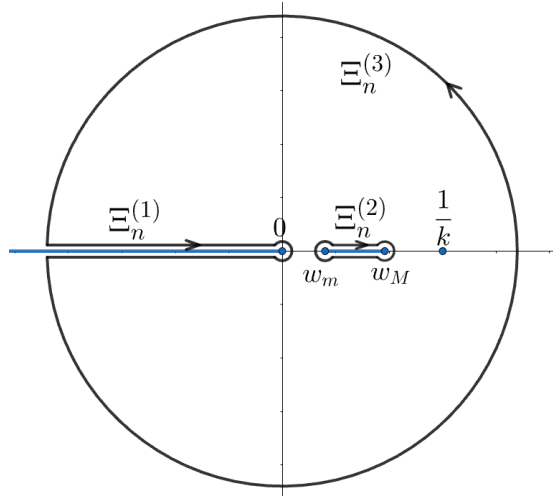
We analyze this integral via residues. Note that

$$z - \kappa z^2 - (Hz - \delta)^2 = -(H^2 + \kappa)(z - w_m)(z - w_M) \quad (2.53)$$

by definition of w_m, w_M . Consider now the meromorphic function

$$f(z) := i \frac{\delta - Hz}{2\sqrt{H^2 + \kappa}(1/\kappa - z)\sqrt{\kappa z}\sqrt{z - w_m}\sqrt{z - w_M}}$$

defined on $\mathbb{C} \setminus ((-\infty, 0] \cup [w_m, w_M])$ and with a pole at $z = 1/\kappa$. We will integrate along a sequence of closed paths Ξ_n shown in Figure 2.1. Each such path Ξ_n can be divided into three pieces: a circle arc $\Xi_n^{(1)}$ of radius n , a curve $\Xi_n^{(2)}$ enclosing the segment $[w_m, w_M]$ and another curve $\Xi_n^{(3)}$ around the interval $(-n, 0]$ with the same boundary points as $\Xi_n^{(1)}$. We take $\Xi_n^{(2)}$ and $\Xi_n^{(3)}$ so that they converge to the intervals $[w_m, w_M]$ and $(-\infty, 0]$ respectively as $n \rightarrow \infty$.

Figure 2.1: Integration path Ξ_n for $f(z)$.

By the residue theorem, and using (2.53),

$$\int_{\Xi_n} f(z) dz = 2\pi i \operatorname{Res} \left(f, \frac{1}{\kappa} \right) = \pi.$$

A careful analysis of $f(z)$ shows that

$$\lim_{n \rightarrow \infty} \int_{\Xi_n^{(1)}} f(z) dz = 0,$$

$$\begin{aligned} \lim_{n \rightarrow \infty} \int_{\Xi_n^{(2)}} f(z) dz &= 2 \int_{w_m}^{w_M} \frac{i(\delta - Hw)}{2i^3 \sqrt{H^2 + \kappa}(1/\kappa - w) \sqrt{\kappa w} \sqrt{w - w_m} \sqrt{w_M - w}} dw \\ &= 2\phi(\mathfrak{s}_2), \end{aligned}$$

$$\begin{aligned} \lim_{n \rightarrow \infty} \int_{\Xi_n^{(3)}} f(z) dz &= 2 \int_{-\infty}^0 \frac{i(\delta - Hw)}{2i^3 \sqrt{H^2 + \kappa}(1/\kappa - w) \sqrt{-\kappa w} \sqrt{w_m - w} \sqrt{w_M - w}} dw \\ &= -M, \end{aligned}$$

for some positive constant $M > 0$. Consequently,

$$\pi = 2\phi(\mathfrak{s}_2) - M < 2\phi(\mathfrak{s}_2),$$

as we wanted to prove.

Case 4: $\kappa < 0$, $H > 0$.

We define \mathfrak{s}_0 as the first value for which $x(\mathfrak{s}_0) = x_0$, where $x_0 = \sqrt{\delta/H}$. Let us prove that \mathfrak{s}_0 exists. First, if $\kappa + H^2 > 0$, then $h(x)$ in (2.39) has two positive roots $x_m < x_M$, and $x(\mathfrak{s})$ oscillates between the values x_m and x_M . Since $h(x_0) > 0$, it follows that $x_m < x_0 < x_M$, so \mathfrak{s}_0 exists indeed. In the case $\kappa + H^2 \leq 0$, the polynomial $h(x)$ has a unique positive root x_m such that $x_m < x_0$, and $h(x) > 0$ for all $x \in (x_m, \infty)$. This implies that $x(\mathfrak{s})$ is strictly increasing for all $\mathfrak{s} > 0$ with $\lim_{\mathfrak{s} \rightarrow \infty} x(\mathfrak{s}) = \infty$, so the value \mathfrak{s}_0 must exist. Now, notice that $\phi(\mathfrak{s})$ is an increasing function on the interval $[0, \mathfrak{s}_0]$, and $\phi'(\mathfrak{s}_0) = 0$. In particular, we deduce that $\delta - Hx(\mathfrak{s}) \geq 0$ for all $\mathfrak{s} \in [0, \mathfrak{s}_0]$ and that $\phi(\mathfrak{s}_0) > 0$. A direct computation using (2.43) shows that

$$F(\mathfrak{s}_0) = -x'(\mathfrak{s}_0) \frac{\sinh(\phi(\mathfrak{s}_0))}{\kappa \sqrt{x(\mathfrak{s}_0)^2 - 1/\kappa}} > 0,$$

as we wanted to prove. Additionally, it holds that $\kappa x_4(\mathfrak{s})$ is decreasing for all $\mathfrak{s} \in [0, \mathfrak{s}_0]$.

Case 5: $\kappa < 0$, $H = 0$.

The polynomial $h(x)$ in (2.39) has a unique positive root x_m . This implies that $x(\mathfrak{s})$ is strictly increasing for all $\mathfrak{s} > 0$ with $\lim_{\mathfrak{s} \rightarrow \infty} x(\mathfrak{s}) = \infty$. In particular, the function $\phi(\mathfrak{s})$ in (2.44) must be increasing as well. Nevertheless, $\phi(\mathfrak{s})$ is bounded: indeed, applying the change of variables $y = x(\mathfrak{s})$, it holds

$$\phi(\mathfrak{s}) < \lim_{\mathfrak{s} \rightarrow \infty} \phi(\mathfrak{s}) = \int_{x(0)}^{\infty} \frac{\delta}{\sqrt{-\kappa}(y^2 - 1/\kappa) \sqrt{-\kappa y^4 + y^2 - \delta^2}} dy < \infty.$$

We can now show that $F(\mathfrak{s}) > 0$ for \mathfrak{s} large enough. Consider the function

$$G(\mathfrak{s}) := \frac{F(\mathfrak{s}) \sqrt{x(\mathfrak{s})^2 - 1/\kappa}}{x'(\mathfrak{s})}.$$

If $\mathfrak{s} > 0$, the sign of $F(\mathfrak{s})$ coincides with that of $G(\mathfrak{s})$. A straightforward computation using (2.43), (2.44), (2.52) shows that

$$\lim_{\mathfrak{s} \rightarrow \infty} G(\mathfrak{s}) = -\frac{1}{\kappa} \sinh(\phi_M) > 0,$$

where $\phi_M := \lim_{\mathfrak{s} \rightarrow \infty} \phi(\mathfrak{s})$. In particular, $G(\mathfrak{s})$ is positive for large $\mathfrak{s} > 0$, and so is $F(\mathfrak{s})$. Items (1) and (3) of the lemma are immediate, while (2) is a consequence of the fact that $\phi(\mathfrak{s})$ is strictly increasing.

Case 6: $\kappa = 0, H > 0$.

The polynomial $h(x)$ has two positive roots $x_m < x_M$. Since $x_0 = \sqrt{\delta/H} \in (x_m, x_M)$, there exists a first value $\mathfrak{s}_0 > 0$ such that $x(\mathfrak{s}_0) = x_0$, and hence $x'_3(\mathfrak{s}_0) = 0$. In particular, $F(\mathfrak{s}_0) > 0$, from which we deduce the existence of $\tilde{\mathfrak{s}}$.

Case 7: $\kappa = 0, H = 0$.

In this particular case, it is possible to obtain explicit expressions for $x(\mathfrak{s})$ and $x_3(\mathfrak{s})$ by integrating (2.39) and (2.46). Specifically,

$$\begin{aligned} x(\mathfrak{s}) &= \sqrt{\mathfrak{s}^2 + \delta^2}, \\ x_3(\mathfrak{s}) &= \delta \operatorname{arcsinh}\left(\frac{\mathfrak{s}}{\delta}\right). \end{aligned} \quad (2.54)$$

The function $F(\mathfrak{s})$ can be computed explicitly. It is possible to check $F(\mathfrak{s})$ has a unique positive root $\tilde{\mathfrak{s}}$ given by the implicit equation

$$\operatorname{arcsinh}\left(\frac{\mathfrak{s}}{\delta}\right) = \frac{\sqrt{\mathfrak{s}^2 + \delta^2}}{\mathfrak{s}}.$$

This completes the proof of Lemma 2.6.11. □

We now show item (1) in Theorem 2.6.9. This follows from the next lemma:

Lemma 2.6.12. *For any $(\kappa, H, \delta) \in \Omega$, the compact minimal annulus*

$$\mathfrak{A}(\tilde{\mathfrak{s}}) = \mathfrak{A}(\tilde{\mathfrak{s}}; \kappa, H, \delta)$$

in Definition 2.6.6 is embedded and free boundary in a geodesic ball B centered at \mathbf{e}_4 . More specifically, for $\kappa \neq 0$,

$$B = B[\mathbf{e}_4, x_4(\tilde{\mathfrak{s}})/\kappa], \quad (2.55)$$

while for $\kappa = 0$, B is the ball centered at \mathbf{e}_4 with radius

$$R = \sqrt{x(\tilde{\mathfrak{s}})^2 + x_3(\tilde{\mathfrak{s}})^2}. \quad (2.56)$$

In any of the cases, B is contained in $\{x_4 > 0\} \cap \mathbb{M}^3(\kappa)$.

Proof. Fix $(\kappa, H, \delta) \in \Omega$, and let $\tilde{\mathfrak{s}} = \tilde{\mathfrak{s}}(\kappa, H, \delta)$. The embeddedness of the annulus $\mathfrak{A}(\tilde{\mathfrak{s}})$ follows from the fact that the third coordinate function, $x_3(\mathfrak{s})$, is strictly increasing on the interval $[-\tilde{\mathfrak{s}}, \tilde{\mathfrak{s}}]$; see Lemma 2.6.11.

According to the symmetries of $\mathfrak{A}(\tilde{\mathfrak{s}})$ (see Remark 2.6.7), if this annulus were free

boundary in a geodesic ball B , its geodesic center should necessarily be \mathbf{e}_4 . This will happen if the following conditions hold:

1. $\mathfrak{A}(\tilde{\mathfrak{s}})$ must be contained in B and its two boundary components $\psi(\{\tilde{\mathfrak{s}}\} \times \mathbb{R})$, $\psi(\{-\tilde{\mathfrak{s}}\} \times \mathbb{R})$, should lie in the geodesic sphere ∂B .
2. The geodesic $\zeta_{\tilde{\mathfrak{s}}}$ meets the point \mathbf{e}_4 ; see Definition 2.6.8. This ensures that the annulus $\mathfrak{A}(\tilde{\mathfrak{s}})$ meets the geodesic sphere ∂B orthogonally.

The first condition holds if we choose the balls given by (2.55), (2.56): indeed, if $\kappa \neq 0$ and $\mathfrak{s} \in [0, \tilde{\mathfrak{s}}]$,

$$\langle \mathbf{e}_4, \psi(\mathfrak{s}, \theta) \rangle_\kappa = \frac{x_4(\mathfrak{s})}{\kappa} \geq \frac{x_4(\tilde{\mathfrak{s}})}{\kappa},$$

since $\kappa x_4(\mathfrak{s})$ is decreasing by Lemma 2.6.11. The inequality also holds for $\mathfrak{s} \in [-\tilde{\mathfrak{s}}, 0]$, as $x_4(\mathfrak{s})$ is symmetric. This implies by (2.55) that $\mathfrak{A}(\tilde{\mathfrak{s}}) \subset B[\mathbf{e}_4, x_4(\tilde{\mathfrak{s}})/\kappa]$. Similarly, if $\kappa = 0$, we take the ball B centered at \mathbf{e}_4 of radius R as in (2.56). Since the function $\mathfrak{s} \mapsto \sqrt{x(\mathfrak{s})^2 + x_3(\mathfrak{s})^2}$ is strictly increasing on $\mathfrak{s} \in [0, \tilde{\mathfrak{s}}]$ (because $x(\mathfrak{s})$ and $x_3(\mathfrak{s})$ are), we deduce that the annulus $\mathfrak{A}(\tilde{\mathfrak{s}})$ is contained in B , as expected.

We will now show the second condition, i.e., that $\psi(\mathfrak{s}, 0)$ meets the geodesic sphere ∂B orthogonally. Given any $\kappa \in \mathbb{R}$, we define the totally geodesic surface $\mathbb{M}^2(\kappa) := \mathbb{M}^3(\kappa) \cap \{x_2 = 0\}$. This surface has constant sectional curvature κ , so it is isometric to either a 2-sphere (if $\kappa > 0$), a hyperbolic plane ($\kappa < 0$) or a Euclidean plane ($\kappa = 0$). Now, let $P : \mathbb{M}^2(\kappa) \cap \{x_4 > 0\} \rightarrow \mathbb{R}^2$ be the totally geodesic projection

$$(\bar{x}, \bar{y}) = P(x_1, x_3, x_4) := \left(\frac{x_1}{x_4}, \frac{x_3}{x_4} \right). \quad (2.57)$$

Observe that if $\kappa \leq 0$, P is defined on the whole surface $\mathbb{M}^2(\kappa)$, while for $\kappa > 0$ it is just defined on a hemisphere. Moreover, P sends the rotation axis \mathcal{X} of the annulus \mathfrak{A} to the line $\{\bar{x} = 0\}$, and $P(\mathbf{e}_4) = (0, 0)$. Now, let $\eta(\mathfrak{s}) = P(\psi(\mathfrak{s}, 0))$. Since P is totally geodesic, the projection of any geodesic $\zeta_{\mathfrak{s}_0}$ coincides with the tangent line $L_{\mathfrak{s}_0}$ to the curve $\eta(\mathfrak{s})$ at $\eta(\mathfrak{s}_0)$. This line will either be parallel to the axis $\{\bar{x} = 0\}$ or meet it at a single point $(0, \bar{y})$, where $\bar{y} = \bar{y}(\mathfrak{s}_0)$. The condition for $L_{\mathfrak{s}_0}$ not to be parallel to the axis is that $\left(\frac{x}{x_4} \right)' \Big|_{\mathfrak{s}_0} \neq 0$. In that case, it follows that

$$\bar{y}(\mathfrak{s}_0) = \frac{x_3(\mathfrak{s}_0)}{x_4(\mathfrak{s}_0)} - \frac{x(\mathfrak{s}_0) \left(\frac{x_3}{x_4} \right)' \Big|_{\mathfrak{s}_0}}{x_4(\mathfrak{s}_0) \left(\frac{x}{x_4} \right)' \Big|_{\mathfrak{s}_0}} = \frac{F(\mathfrak{s}_0)}{x'(\mathfrak{s}_0)x_4(\mathfrak{s}_0) - x(\mathfrak{s}_0)x_4'(\mathfrak{s}_0)}, \quad (2.58)$$

see (2.52). Let us assume for a moment that

$$\left(\frac{x}{x_4}\right)' = \frac{x'x_4 - xx_4'}{x_4^2} > 0 \quad (2.59)$$

holds on a neighbourhood of $\mathfrak{s} = \tilde{\mathfrak{s}}$. Then, (2.58) implies that $\bar{y}(\tilde{\mathfrak{s}}) = 0$, that is, the line $L_{\tilde{\mathfrak{s}}}$ passes through the origin of \mathbb{R}^2 , which means that $\zeta_{\tilde{\mathfrak{s}}} \subset \mathbb{M}^2(\kappa)$ meets \mathbf{e}_4 . This is exactly the condition that we were looking for. Hence, it just remains to check (2.59) to prove Lemma 2.6.12. Suppose by contradiction that

$$x'(\tilde{\mathfrak{s}})x_4(\tilde{\mathfrak{s}}) \leq x(\tilde{\mathfrak{s}})x_4'(\tilde{\mathfrak{s}}). \quad (2.60)$$

This is impossible if $\kappa \geq 0$ as $x(\tilde{\mathfrak{s}}), x'(\tilde{\mathfrak{s}}), x_4(\tilde{\mathfrak{s}}) > 0$ but $x_4'(\tilde{\mathfrak{s}}) \leq 0$; see Lemma 2.6.11. Assume then that $\kappa < 0$. The fact that $\psi(\mathfrak{s}, 0) \in \mathbb{M}^2(\kappa)$ implies that

$$x^2 + x_3^2 + \frac{x_4^2}{\kappa} = \frac{1}{\kappa} \quad (2.61)$$

for all \mathfrak{s} , so in particular

$$x(\tilde{\mathfrak{s}})x'(\tilde{\mathfrak{s}}) + x_3(\tilde{\mathfrak{s}})x_3'(\tilde{\mathfrak{s}}) = -\frac{x_4(\tilde{\mathfrak{s}})x_4'(\tilde{\mathfrak{s}})}{\kappa}. \quad (2.62)$$

By definition of $\tilde{\mathfrak{s}}$, it holds $x_3(\tilde{\mathfrak{s}})x'(\tilde{\mathfrak{s}}) = x(\tilde{\mathfrak{s}})x_3'(\tilde{\mathfrak{s}})$. Moreover, by (2.60), $x_4'(\tilde{\mathfrak{s}}) \geq \frac{x'(\tilde{\mathfrak{s}})x_4(\tilde{\mathfrak{s}})}{x(\tilde{\mathfrak{s}})}$. Substituting in (2.62) for $\mathfrak{s} = \tilde{\mathfrak{s}}$,

$$xx' + \frac{x_3^2 x'}{x} = -\frac{x_4 x_4'}{\kappa} \geq -\frac{x' x_4^2}{\kappa x} = -\frac{x'}{\kappa x} (1 - \kappa(x^2 + x_3^2)).$$

Multiplying both sides by $\frac{x}{x'} > 0$,

$$x^2 + x_3^2 \geq x^2 + x_3^2 - \frac{1}{\kappa}.$$

This implies that $\frac{1}{\kappa} > 0$, which is impossible by hypothesis. Hence, (2.59) holds, proving Lemma 2.6.12 and item (1) of Theorem 2.6.9. □

Proof of item (2) in Theorem 2.6.9.

In the proof of Lemma 2.6.12, we showed that (2.59) holds on a neighbourhood $I_0 \subset \mathbb{R}$ of $\tilde{\mathfrak{s}}$. In particular, by (2.58) we see that the function $\bar{y} = \bar{y}(\mathfrak{s}) : I_0 \rightarrow \mathbb{R}$ is analytic.

On the other hand, by definition of \bar{y} , the point $P^{-1}(0, \bar{y}(\mathfrak{s})) \in \mathbb{M}^2(\kappa)$ is the (unique) point in the half-space $\{x_4 > 0\}$ in which the geodesics \mathcal{X} and $\zeta_{\mathfrak{s}}$ meet. This shows that the map $\hat{p}(\mathfrak{s})$ introduced in item (2) of Theorem 2.6.9 is well defined and analytic on a neighbourhood $I_1 \subset I_0$ of $\tilde{\mathfrak{s}}$, as $\hat{p}(\mathfrak{s}) = P^{-1}(0, \bar{y}(\mathfrak{s}))$. The fact that $\hat{p}_3(\tilde{\mathfrak{s}}) = 0$ is immediate since $\bar{y}(\tilde{\mathfrak{s}}) = 0$. It is also clear by (2.58) that the sign of the derivative $\hat{p}'_3(\tilde{\mathfrak{s}})$ coincides with that of $F'(\tilde{\mathfrak{s}})$. We will show next that actually $F'(\tilde{\mathfrak{s}}) > 0$, completing the proof of item (2) of Theorem 2.6.9.

Proof of item (3) of Theorem 2.6.9

We will now prove that the map $\tilde{\mathfrak{s}} = \tilde{\mathfrak{s}}(\kappa, H, \delta) : \Omega \rightarrow (0, \infty)$ is analytic. By definition, $\tilde{\mathfrak{s}}$ is the first positive root of the function $F(\mathfrak{s})$ in (2.52). Hence, it suffices to show that

$$F'(\tilde{\mathfrak{s}}) > 0, \quad (2.63)$$

and that $F = F(\mathfrak{s}; \kappa, H, \delta)$ is analytic both as a function of \mathfrak{s} and (κ, H, δ) , so that we can apply the implicit function theorem. We first show that $F(\mathfrak{s}; \kappa, H, \delta)$ is analytic. According to (2.52), we just need to check that the coordinate functions $x(\mathfrak{s}; \kappa, H, \delta)$, $x_3(\mathfrak{s}; \kappa, H, \delta)$ are analytic. We emphasize that the analytic dependence on the parameter κ is not immediate, as the coordinate function x_3 adopts different expressions depending on the sign of κ ; see (2.38), (2.43), (2.45). Nevertheless, for any $(\kappa, H, \delta) \in \Omega$, the tuple (x, x_3, x_4) can be expressed as a solution of the following differential system:

$$\begin{cases} x'' &= -\kappa x - 2H \frac{(Hx^2 - \delta)}{x} + \frac{(Hx^2 - \delta)^2}{x^3}, \\ x'_3 &= \kappa \frac{xx'}{\kappa x^2 - 1} x_3 + \frac{(\delta - Hx^2)}{x(1 - \kappa x^2)} x_4, \\ x'_4 &= \kappa \frac{xx'}{\kappa x^2 - 1} x_4 + \kappa \frac{(\delta - Hx^2)}{x(\kappa x^2 - 1)} x_3, \end{cases} \quad (2.64)$$

where we set the initial conditions

$$\begin{aligned} x(0) &= \frac{\sqrt{2}\delta}{\sqrt{1 + 2\delta H + \sqrt{(1 + 2\delta H)^2 - 4\delta^2(H^2 + \kappa)}}}, \\ x'(0) &= 0, \\ x_3(0) &= 0, \\ x_4(0) &= \sqrt{1 - \kappa x(0)^2}. \end{aligned}$$

The equations in system (2.64) are immediate from (2.38), (2.43) and (2.45). We also note that the initial conditions are chosen so that $x(0)$ is the first positive root x_m

of $h(x)$ in (2.39). Both this system and its initial conditions depend analytically on $(\kappa, H, \delta) \in \Omega$: indeed, the fact that $(\kappa, H, \delta) \in \Omega$ ensures that the expressions for $x(0)$ and $x_4(0)$ are analytic. Hence, the solution (x, x_3, x_4) to (2.64) will be analytic in terms of $(\mathfrak{s}; \kappa, H, \delta)$, and so will be $F = F(\mathfrak{s}; \kappa, H, \delta)$.

Let us now prove (2.63). A direct computation using (2.39) and (2.64) shows that

$$F'(\mathfrak{s}) = \frac{(\delta + Hx^2)((\delta - Hx^2)x_3 + x^2x_4x')}{x^3(1 - \kappa x^2)} \quad (2.65)$$

for all $\mathfrak{s} \in \mathbb{R}$. At $\mathfrak{s} = \tilde{\mathfrak{s}}$, we have that $x(\tilde{\mathfrak{s}}), x'(\tilde{\mathfrak{s}}), x_3(\tilde{\mathfrak{s}}), x_4(\tilde{\mathfrak{s}}) > 0$ and $\delta - Hx(\tilde{\mathfrak{s}})^2 \geq 0$; see Lemma 2.6.11. Moreover, $1 - \kappa x(\tilde{\mathfrak{s}})^2 > 0$; this is trivial if $\kappa \leq 0$, while for $\kappa > 0$ is an immediate consequence of (2.61). In any case, (2.63) holds. This shows that $\tilde{\mathfrak{s}} : \Omega \rightarrow \mathbb{R}^+$ is an analytic function, and concludes the proof of item (3) in Theorem 2.6.9.

Proof of item (4) in Theorem 2.6.9.

We will finally prove that the extension of $\tilde{\mathfrak{s}}(\kappa, H, \delta)$ in (2.50) along the boundary component $\partial\Omega_1$ is continuous. Let us define the function $F(\mathfrak{s}; \kappa, H, \delta) : \mathbb{R} \times \Lambda \rightarrow \mathbb{R}$ in (2.52), where

$$\Lambda := \{(\kappa, H, \delta) : \kappa > 0, H \geq 0, \delta > 0, 2\kappa\delta \leq H + \mu\}.$$

Note that we can rewrite this set as $\Lambda = (\Omega \cap \{\kappa > 0\}) \sqcup \partial\Omega_1$; see (2.48), (2.49). In particular, by Lemma 2.6.11, the function $\tilde{\mathfrak{s}}(\kappa, H, \delta)$ is defined on $\Omega \cap \Lambda$. We can further define $\tilde{\mathfrak{s}}$ along $\partial\Omega_1$ as in (2.50), so that $\tilde{\mathfrak{s}}(\kappa, H, \delta)$ is defined on the whole set Λ . It remains to show that this function is continuous.

First, it is clear that F is continuous on $\mathbb{R} \times \Lambda$, since x, x_3 and their derivatives are. Moreover, the following properties hold for every $(\kappa, H, \delta) \in \Lambda$:

- (a) $F(\mathfrak{s}; \kappa, H, \delta) < 0$ for all $0 \leq \mathfrak{s} < \tilde{\mathfrak{s}}$,
- (b) $\mathfrak{s} \mapsto F(\mathfrak{s}; \kappa, H, \delta)$ changes sign at $\mathfrak{s} = \tilde{\mathfrak{s}}$.

Indeed, (a) and (b) hold for every $(\kappa, H, \delta) \in \Omega \cap \Lambda$; this is an immediate consequence of the definition of $\tilde{\mathfrak{s}}$, Lemma 2.6.11 and (2.63). On the other hand, for $(\kappa, H, \delta) \in \partial\Omega_1$, we may use the explicit expressions for $x(\mathfrak{s}), x_3(\mathfrak{s})$ in Remark 2.6.10 to show properties (a) and (b).

Let us now show that $\tilde{\mathfrak{s}}(\kappa, H, \delta)$ is continuous in Λ . This is clear for every $(\kappa, H, \delta) \in \Omega \cap \Lambda$, so we fix $(\kappa_0, H_0, \delta_0) \in \partial\Omega_1$. Continuity at the point $(\kappa_0, H_0, \delta_0)$ is equivalent

to showing that

$$\lim_{\substack{(\kappa, H, \delta) \rightarrow (\kappa_0, H_0, \delta_0) \\ (\kappa, H, \delta) \in \Omega}} \tilde{\mathfrak{s}}(\kappa, H, \delta) = \frac{\pi}{2\sqrt{2\mu_0(H_0 + \mu_0)}} =: \tilde{\mathfrak{s}}_0. \quad (2.66)$$

Hence, let $\mathfrak{s}_I \leq \mathfrak{s}_S$ denote respectively the limits inferior and superior of the left hand-side of (2.66). We need to prove that these limits coincide and are equal to $\tilde{\mathfrak{s}}_0$. First, by the continuity of F , it follows that $F(\mathfrak{s}; \kappa_0, H_0, \delta_0) \leq 0$ for all $\mathfrak{s} \in [0, \mathfrak{s}_S]$. Moreover, since $F(\mathfrak{s}; \kappa_0, H_0, \delta_0) > 0$ for any $\mathfrak{s} > \tilde{\mathfrak{s}}_0$ sufficiently close to $\tilde{\mathfrak{s}}_0$, we deduce that $\mathfrak{s}_S \leq \tilde{\mathfrak{s}}_0$.

We will now show that $\tilde{\mathfrak{s}}_0 \leq \mathfrak{s}_I$. Notice first that $\mathfrak{s}_I \geq 0$ since $\tilde{\mathfrak{s}}(\kappa, H, \delta)$ is positive in Ω . Moreover, the fact that $F(\tilde{\mathfrak{s}}(\kappa, H, \delta); \kappa, H, \delta) \equiv 0$ implies by continuity that $F(\mathfrak{s}_I; \kappa_0, H_0, \delta_0) = 0$. However, $\tilde{\mathfrak{s}}_0$ is the first positive root of $\mathfrak{s} \mapsto F(\mathfrak{s}; \kappa_0, H_0, \delta_0)$, so necessarily $\tilde{\mathfrak{s}}_0 \leq \mathfrak{s}_I$. As a consequence, $\mathfrak{s}_I = \mathfrak{s}_S = \tilde{\mathfrak{s}}_0$, and (2.66) holds. This shows item (4) in Theorem 2.6.9.

2.7 Final notes

The class of CMC surfaces with spherical lines was already studied extensively in the 19th century, for instance, in the books by Darboux [21] and Enneper [26], as well as the articles by Dobriner [23, 24]. Almost one century later, this class of surfaces played an important role in the solution to an old conjecture by Hopf, according to which the only *closed*, i.e., compact without boundary, CMC surfaces in Euclidean space \mathbb{R}^3 should be the round, totally umbilic spheres. This conjecture was unexpectedly solved in the negative by Wente [75] in 1986, by constructing CMC tori in \mathbb{R}^3 with self-intersections and a discrete symmetry group. Subsequently, Abresch [1] and Walter [72, 73] gave a more explicit construction of such tori, by prescribing that the CMC tori were foliated by *planar curvature lines*.

After this, Wente developed in [76] a more systematic study of the class of CMC surfaces of Enneper type, putting the old previous works into a more modern, global perspective. In particular, it follows from his studies that Enneper surfaces are complete, and that the moduli space of all Enneper surfaces is composed by several finite-dimensional connected components.

Using this study, Wente was able to produce new CMC tori of Enneper type [76], and he also used this class to construct immersed free boundary annuli with very large mean curvature in the unit ball [77]. In his studies, Wente focused on a special region

of the moduli space of Enneper surfaces, namely, those for which the associated polynomial of degree 4 in (2.24) has negative discriminant. Moreover, he assumed that the family of spherical curvature lines of the surface was the one associated with the *largest* principal curvature κ_1 , since this is the family where CMC tori are naturally produced. In contrast, in our study here we have chosen the spherical curvature lines of Enneper surfaces associated with the *smallest* principal curvature $\kappa_2 \leq \kappa_1$. This choice will be crucial for our construction of free boundary CMC annuli in later sections. We will also deviate from Wente's studies because we will work with polynomials of *positive* discriminant. Our studies suggest that, even though these examples do not close up to create CMC tori, one can only obtain *embedded* free boundary CMC annuli when working in the component of the parameter space with positive discriminant.

As we explained along the chapter, any Enneper surface in a space form $\mathbb{M}^3(\kappa)$ is constructed by the following process. First, integrate the Hamiltonian system (2.17) to obtain a pair $(\alpha(u), \beta(u))$ of real functions; then, plug this pair into the overdetermined system (2.14) to produce a function $\omega(u, v)$ that gives a solution to the Gauss-Codazzi equation for CMC surfaces in $\mathbb{M}^3(\kappa)$; and finally, use the fundamental theorem of surfaces to construct the desired Enneper surface. But despite this apparent homogeneity in the construction procedure, the situation changes substantially when considering different values for the mean curvature H and the ambient sectional curvature κ , in two different ways.

First, we note that the Gauss equation (2.14a) is equivalent after an adequate change, to either the sinh-Gordon equation $\Delta\omega + \sinh \omega = 0$ if $H^2 + \kappa > 0$, to the Liouville equation $\Delta\omega + e^\omega = 0$ if $H^2 + \kappa = 0$, or the cosh-Gordon equation $\Delta\omega + \cosh \omega = 0$ when $H^2 + \kappa < 0$. These elliptic equations have different analytic behaviors, as is well known. But moreover, the Hamiltonian system (2.17) for (α, β) also changes substantially in each of these three situations. For instance, when $H^2 + \kappa > 0$, the solutions are globally defined on \mathbb{R} , but this is not true in the rest of the cases. Moreover, it is explained in Wente [76] how in the case $H^2 + \kappa < 0$, the usual Hamilton-Jacobi procedure to solve system (2.17) by separation of variables requires a *complex* (i.e. not real) change of coordinates. This makes the study of this case much harder.

As we explained previously, the natural extension of Hopf's theorem to space forms states that any CMC 2-sphere Σ (i.e. Σ is diffeomorphic to \mathbb{S}^2) in $\mathbb{M}^3(\kappa)$ must be totally umbilical. For the case of minimal surfaces, this was noted by Almgren [2], namely: any minimal 2-sphere Σ in \mathbb{S}^3 is a totally geodesic equator of \mathbb{S}^3 . In [37], Gálvez, Mira and Tassi extended Almgren's theorem to a purely geometric context in which no elliptic equation is imposed on Σ , only saddleness. Here, we say that a surface Σ

is *saddle* if $\kappa_1 \kappa_2 \leq 0$ holds at every point of Σ . Specifically, they showed that *any immersed real analytic saddle 2-sphere in \mathbb{S}^3 is a totally geodesic equator of \mathbb{S}^3* . The result is not true for saddle C^∞ spheres.

In the view of this result, it is natural to ask if Nitsche's characterization of equatorial disks of \mathbb{B}^3 as the only free boundary minimal disks in \mathbb{B}^3 admits a similar extension to saddle surfaces. That is, if equatorial disks are the only real analytic free boundary saddle disks in \mathbb{B}^3 . We note that this time, and in contrast with the \mathbb{S}^3 case, it is far from obvious to show that the analyticity condition is needed, i.e., to show that there exist smooth free boundary saddle disks in \mathbb{B}^3 other than equators. The next result proves this:

Theorem 2.7.1 ([19]). *There exist compact C^∞ -smooth saddle immersions Σ from a disk $\mathcal{D} \subset \mathbb{R}^2$ into \mathbb{B}^3 that intersect $\partial\mathbb{B}^3$ orthogonally along $\partial\Sigma$, and are not flat disks.*

We will now sketch the construction of one of these immersions, and refer the reader to [19] for further details. Let $\gamma(u) : [-2, 2] \rightarrow \mathbb{D}$ be a planar curve contained in the horizontal unit disk

$$\mathbb{D} := \{(x_1, x_2, x_3) \in \mathbb{R}^3 : x_1^2 + x_2^2 \leq 1, x_3 = 0\}. \quad (2.67)$$

Assume that γ satisfies the following properties (see Figure 2.2):

Properties 2.7.2.

1. For $u \in [-2, -1]$, $\gamma(u)$ parametrizes the segment $[-1, a] \times \{0\} \times \{0\}$ for some $a \in (0, 1)$.
2. For $u \in [1, 2]$, $\gamma(u)$ parametrizes the segment $\{0\} \times [-1, a] \times \{0\}$.
3. For $u \in (-1, 1)$, $\gamma(u)$ is a strictly convex curve contained in the quadrant $(0, 1) \times (0, 1) \times \{0\} \cap \mathbb{D}$. The tangent vector $\gamma'(u)$ describes a rotation of angle $\frac{3\pi}{2}$ for $u \in (-1, 1)$. As a consequence, $\gamma'(u)$ is not collinear with $\gamma(u)$.
4. The curve γ is symmetric with respect to the line $\{x_1 = x_2\}$, so that $\gamma(0)$ passes through this line.

It is clear that there exist infinitely many C^∞ curves $\gamma(u)$ satisfying the properties above.

Now, given any $p \in \mathbb{D}$ with $p \neq (0, 0, 0)$, let Π_p be the unique plane containing the x_3 -axis and the point p . We then define $c_p \subset \Pi_p \cap \mathbb{B}^3$ as the unique piece of

circle passing through p that meets $\partial\mathbb{B}^3$ orthogonally; see Figure 2.2. Otherwise, if $p = (0, 0, 0)$, we define c_p as the vertical segment $\{0\} \times \{0\} \times [-1, 1] \subset \mathbb{B}^3$. In any case, we parametrize the curve $c_p = c_p(v)$ via the arc-length parameter, that is, $c_p(v) : [-v_0, v_0] \rightarrow \mathbb{B}^3$ for some $v_0 = v_0(p) > 0$. We note that the value $v_0(p)$ depends analytically on p .

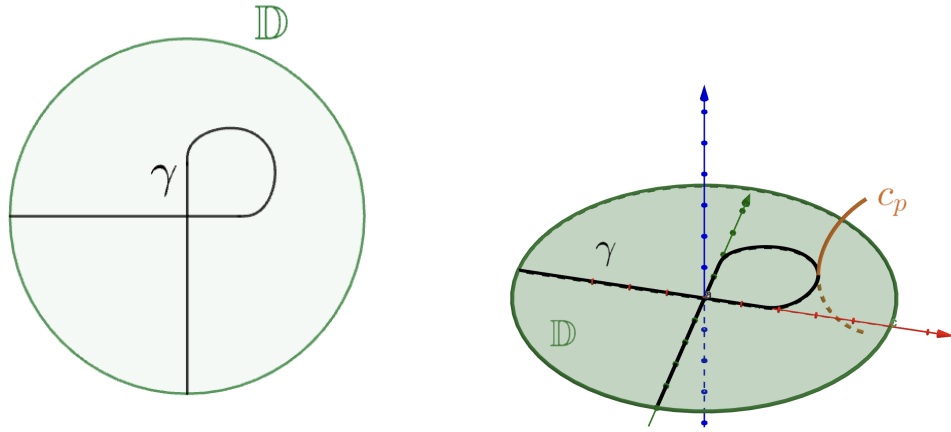


Figure 2.2: Left: curve γ in the conditions of Properties 2.7.2. Right: curve c_p associated to a point $p \in \gamma$.

We can then define the immersion $\psi(u, v) : \mathcal{D} \rightarrow \mathbb{B}^3$ as

$$\psi(u, v) := c_{\gamma(u)}(v), \quad (2.68)$$

where $\mathcal{D} \subset \mathbb{R}^2$ is the disk given by

$$\mathcal{D} = \{(u, v) : u \in [-2, 2], -v_0(\gamma(u)) \leq v \leq v_0(\gamma(u))\}.$$

It is shown in [19] that if $\gamma(u)$ is any C^∞ curve satisfying Properties 2.7.2, then the immersion $\psi(u, v)$ in (2.68) produces an example of an immersed free boundary saddle disk which is different from a planar example; see Figure 2.3.

We emphasize that, even though the immersion $\psi(u, v)$ in (2.68) is not totally geodesic, it contains a pair of totally geodesic pieces of disks which are joined in a C^∞ way.

Related to this construction, we also recall that there are no free boundary minimal surfaces in \mathbb{B}^3 homeomorphic to a Möbius strip; see [9]. Again, it is not obvious

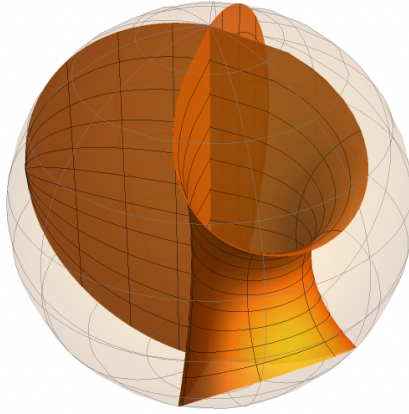


Figure 2.3: Saddle immersion of a disk associated to a curve γ in the conditions of Properties 2.7.2.

whether this result could be extended to free boundary saddle Möbius strips in \mathbb{B}^3 . The following theorem states that it does not hold within the class of C^∞ -smooth surfaces:

Theorem 2.7.3 ([19]). *There exist compact C^∞ -smooth saddle surfaces Σ immersed in \mathbb{B}^3 and homeomorphic to a Möbius strip, which intersect $\partial\mathbb{B}^3$ orthogonally along $\partial\Sigma$.*

The proof of this result is based on a similar construction to the one shown for Theorem 2.7.1. We refer to [19] for further details.

The existence of real analytic free boundary saddle surfaces in \mathbb{B}^3 that are homeomorphic to either a disk (other than flat equatorial disks in \mathbb{B}^3) or a Möbius strip remains as an open problem.

Chapter 3

Free boundary CMC annuli in \mathbb{B}^3

3.1 Summary and main result

In this chapter we construct, for any $n \in \mathbb{N}$, $n \geq 2$, a real analytic, one-parameter family of compact embedded CMC annuli with free boundary in the unit ball \mathbb{B}^3 of \mathbb{R}^3 . These CMC annuli are foliated by spherical curvature lines, and have a prismatic symmetry group of order $4n$, so in particular they are not rotational; see Figure 1.2. This chapter is based on [15]. Specifically, we prove the following result:

Theorem 3.1.1. *For any $n \in \mathbb{N}$, $n \geq 2$, there exists a real analytic family $\{\mathbb{A}_n(\eta) : \eta \in [0, \varepsilon_0)\}$ of embedded CMC annuli in \mathbb{R}^3 such that:*

1. $\mathbb{A}_n(\eta)$ is contained in the closed unit ball \mathbb{B}^3 with $\partial\mathbb{A}_n(\eta) \subset \partial\mathbb{B}^3$.
2. $\mathbb{A}_n(\eta)$ intersects $\partial\mathbb{B}^3$ along its boundary, so that $\mathbb{A}_n(\eta)$ is free boundary in \mathbb{B}^3 .
3. $\mathbb{A}_n(\eta)$ is of Enneper type, that is, $\mathbb{A}_n(\eta)$ has a family of spherical curvature lines.
4. Each $\mathbb{A}_n(\eta)$ is symmetric with respect to the horizontal plane $\{x_3 = 0\}$ and with respect to n equiangular vertical planes containing the x_3 -axis.
5. The annulus $\mathbb{A}_n(0)$ is a compact piece of a free boundary nodoid in \mathbb{B}^3 . If $\eta > 0$, $\mathbb{A}_n(\eta)$ is not rotational, and has a prismatic symmetry group of order $4n$; see Figure 1.2. This group is generated by the symmetries mentioned in item (4).

We remark that these embedded CMC annuli are not minimal, and that the analytic map $\eta \mapsto H(\eta)$ that assigns to each η the (constant) mean curvature of $\mathbb{A}_n(\eta)$ is not constant. Moreover, the mean curvature vector of $\mathbb{A}_n(\eta)$ points *outwards* along the horizontal planar geodesic $\mathbb{A}_n(\eta) \cap \{x_3 = 0\}$, and for $\eta > 0$ small enough, $\mathbb{A}_n(\eta)$ has

negative Gaussian curvature. The constant mean curvatures H_n of the embedded free boundary nodoids $\mathbb{A}_n(0)$ in \mathbb{B}^3 of Theorem 3.1.1 satisfy that $H_n \rightarrow \infty$ as $n \rightarrow \infty$.

A brief outline of the chapter is as follows. In Section 3.2 we construct a family of CMC surfaces Σ in \mathbb{R}^3 with a family of spherical curvature lines corresponding to the *smallest* principal curvature κ_2 of Σ , following the study in Chapter 2. In this construction, we end up with three free parameters (a, b, c) . In Section 3.3 we study the symmetry properties of this family of surfaces. In Section 3.4 we find a suitable region in the parameter space (a, b, c) where we can control the condition that Σ intersects orthogonally a sphere along each boundary curve. Then, in Section 3.5, we define a period map $\Theta = \Theta(a, b, c)$ whose rational values allow us to detect examples of immersed CMC annuli. Later, in Section 3.6, we show that each of these annuli admits a compact piece whose boundary components lie on the same sphere of \mathbb{R}^3 , and such that the intersection angle between the sphere and the annulus is constant. Finally, in Section 3.7 we complete the proof of Theorem 3.1.1, by controlling the embeddedness of the surface, and the property that both boundary curves intersect orthogonally the same sphere. Let us remark that our examples can be seen as suitable bifurcations of certain free boundary nodoids of \mathbb{B}^3 , although our approach does not use bifurcation theory.

3.2 A family of Enneper-type CMC surfaces in \mathbb{R}^3

In this section, we will construct a family of CMC $H = \frac{1}{2}$ surfaces of Enneper type in \mathbb{R}^3 ; see Definition 2.4.1. In order to do so, we will make use of Theorems 2.4.4 and 2.4.5, which allow us to obtain these examples in terms of solutions $(\alpha(u), \beta(u))$ of the differential system (2.17). Up to a conformal reparametization, we may assume that the constant Q associated to the Hopf differential satisfies $Q = \frac{1}{2}$.

3.2.1 Constructing solutions to the sinh-Gordon equation

Let us define the functions $(y(u), z(u))$ in terms of $(\alpha(u), \beta(u))$, where

$$y(u) := \frac{1}{2}(\alpha(u) + \beta(u)), \quad z(u) := \frac{1}{2}(\alpha(u) - \beta(u)). \quad (3.1)$$

According to (2.17) and the fact that we have set $A = H^2 = \frac{1}{4}$, $Q^2 = \frac{1}{4}$, if the pair $(\alpha(u), \beta(u))$ is a solution of (2.17), then $(y(u), z(u))$ must satisfy the second order differential system

$$\begin{cases} y'' = (\widehat{a} - 1)y - 2y(y^2 - z^2) \\ z'' = \widehat{a}z - 2z(y^2 - z^2). \end{cases} \quad (3.2)$$

We will now fix suitable initial conditions for the system (3.2). Let \mathcal{O} be the parameter domain

$$\mathcal{O} := \{(a, b, c) \in \mathbb{R}^3 : b \geq a \geq 1, c \geq 1\}. \quad (3.3)$$

Let us fix $(a, b, c) \in \mathcal{O}$. We define the constants

$$\mathcal{A} := \frac{1}{2}(a + a^{-1}), \quad \mathcal{B} := \frac{1}{2}(b + b^{-1}), \quad \mathcal{C} := \frac{1}{2}(c - c^{-1}). \quad (3.4)$$

Now, let $(y(u), z(u))$ be the unique solution to (3.2) with initial conditions

$$y(0) = z(0) = 0, \quad y'(0) = \frac{(\mathcal{A} + \mathcal{B})\mathcal{C}}{2}, \quad z'(0) = \frac{(\mathcal{B} - \mathcal{A})\sqrt{\mathcal{C}^2 + 1}}{2} \quad (3.5)$$

and constant $\widehat{a} := 1 - \mathcal{A}\mathcal{B} + \mathcal{C}^2$. We note that $y'(0), z'(0) \geq 0$ for every $(a, b, c) \in \mathcal{O}$. With these constants, at $u = 0$, the polynomial $p(x) \equiv p(0, x)$ in (2.24) can be rewritten as

$$p(x) \equiv p(0, x) = \left(x - \frac{a}{c}\right) \left(x - \frac{1}{ac}\right) (x + bc) \left(x + \frac{c}{b}\right). \quad (3.6)$$

Note that $p(x) \geq 0$ for every $x \in [\frac{1}{ac}, \frac{a}{c}]$. By Theorem 2.4.5, Remark 2.4.6 and (3.1), these will induce solutions $\omega(u, v)$ to the overdetermined system

$$\Delta\omega + \sinh \omega \cosh \omega = 0, \quad (3.7a)$$

$$\omega_u = y(u) \cosh \omega + z(u) \sinh \omega, \quad (3.7b)$$

We note that (3.7a) is also known as the classical sinh-Gordon equation, and it is obtained from (2.14a) for the particular case $A = Q^2 = \frac{1}{4}$.

Definition 3.2.1. For every $(a, b, c) \in \mathcal{O}$, we denote by $\omega(u, v) := \omega(u, v; a, b, c)$ the unique solution to (3.7) satisfying $\omega(0, 0) = -\log(ac)$.

Remark 3.2.2. Let $X(u, v) := e^{\omega(u, v)}$. It follows from Remark 2.4.6 that, at $u = 0$, the derivative $X_v(0, v)$ satisfies

$$4X_v(0, v)^2 = p(X), \quad (3.8)$$

where $p(X)$ is given by (3.6). If $a > 1$, this implies that $X(0, v)$ is a periodic function

taking values on the interval $[\frac{1}{ac}, \frac{a}{c}]$. If $a = 1$, it holds that $X(0, v)$ is constant, $X(0, v) \equiv \frac{1}{c}$. In either case, $X(0, v)$ is periodic in v , and so is $\omega(0, v)$.

As a consequence of the periodicity of $v \mapsto \omega(0, v)$ and (3.7b), we deduce that $\omega(u, v)$ can always be defined at least on an open strip $\mathcal{D} = (-u_{\mathcal{D}}, u_{\mathcal{D}}) \times \mathbb{R} \subset \mathbb{R}^2$ for some $u_{\mathcal{D}} > 0$. In fact, it is possible to show that these functions are globally defined:

Proposition 3.2.3. *The functions $\omega(u, v)$ in Definition 3.2.1 are defined on \mathbb{R}^2 .*

Proof. Let $(a, b, c) \in \mathcal{O}$. We will split the proof into two cases, depending on whether $a > 1$ or $a = 1$. Assume first that $a > 1$. We will show in Section 3.4.1 that the solutions $(y(u), z(u))$ to (3.2), (3.5) and its derivatives are defined for all $u \in \mathbb{R}$, and are uniformly bounded; see Remark 3.4.2. For each fixed $v_0 \in \mathbb{R}$, let I_{v_0} be the maximal interval in which the function $u \mapsto \omega(u, v_0)$ is defined. By (3.7b) and the aforementioned properties of $(y(u), z(u))$, we deduce that either $I_{v_0} = \mathbb{R}$ or $u \mapsto \omega(u, v_0)$ explodes in finite time.

Let us now consider the polynomial $x \mapsto p(u, x)$ in (2.24). This polynomial satisfies the following properties:

1. By Remark 2.4.6, the discriminant $\Delta = \Delta(u)$ of $p(u, x)$ does not depend on u . In particular, $\Delta(u) = \Delta(0)$.
2. By (3.6), $p(0, x)$ has four distinct real roots: two negative and two positive. In particular, $\Delta(0) > 0$.
3. The leading coefficient and the constant coefficient of $p(u, x)$ are both negative for all $u \in \mathbb{R}$; see (2.24).

These three properties allow us to conclude that for every $u \in \mathbb{R}$, the polynomial $x \mapsto p(u, x)$ has four distinct real roots

$$x_1(u) < x_2(u) < 0 < x_3(u) < x_4(u),$$

which are defined for all $u \in \mathbb{R}$. We note that at $u = 0$, it holds $x_3(0) = \frac{1}{ac}$, $x_4(0) = \frac{a}{c}$, and by (3.8), $x_3(0) \leq X(0, v_0) \leq x_4(0)$. It then follows from (2.23) that the bound

$$x_3(u) \leq X(u, v_0) \leq x_4(u)$$

holds for every $u \in I_{v_0}$. Consequently, since $x_3(u)$ and $x_4(u)$ are defined for all $u \in \mathbb{R}$, we deduce that $\omega(u, v_0) = \log(X(u, v_0))$ cannot explode in finite time, so $I_{v_0} = \mathbb{R}$ and $\omega(u, v)$ is globally defined.

Finally, consider the case $a = 1$. According to Remark 3.2.2, the function $v \mapsto \omega(0, v)$ is constant, so by (3.7b), it follows that $\omega = \omega(u)$ only depends on $u \in \mathbb{R}$. Notice that, by (3.7a), $\omega(u)$ satisfies the autonomous differential equation

$$\omega_{uu} = -\frac{1}{4} (e^{2\omega} - e^{-2\omega}).$$

Setting $X(u) := e^{\omega(u)}$, we find the first integral

$$X_u^2 = \frac{1}{4} \left(X^2 - \frac{1}{c^2} \right) (c^2 - X^2),$$

which shows that $X(u)$ is a periodic function satisfying $X(u) \in [\frac{1}{c}, c]$. In particular, $X(u)$ is defined for all $u \in \mathbb{R}$. \square

3.2.2 Construction of CMC $H = \frac{1}{2}$ immersions in \mathbb{R}^3

By Theorem 2.4.4, any solution $\omega(u, v)$ in the conditions of Definition 3.2.1 induces a CMC $H = \frac{1}{2}$ immersion $\psi(u, v) : \mathbb{R}^2 \rightarrow \mathbb{R}^3$ parametrized by curvature lines and with first and second fundamental forms given by

$$I = e^{2\omega}(du^2 + dv^2), \quad II = e^\omega (\cosh \omega du^2 + \sinh \omega dv^2). \quad (3.9)$$

The immersion $\psi(u, v)$ is unique once we fix the initial conditions on its moving frame at $(u, v) = (0, 0)$ as in (2.9). Let us note that the principal curvatures $\kappa_1 > \kappa_2$ of $\psi(u, v)$ are

$$\kappa_1 = e^{-\omega} \cosh \omega, \quad \kappa_2 = e^{-\omega} \sinh \omega. \quad (3.10)$$

Definition 3.2.4. For every $(a, b, c) \in \mathcal{O}$, we denote by $\Sigma = \Sigma(a, b, c)$ the unique surface given by the immersion $\psi(u, v) : \mathbb{R}^2 \rightarrow \mathbb{R}^3$ constructed above.

Remark 3.2.5. We note that both $\omega(u, v) = \omega(u, v; a, b, c)$ and the immersion $\psi(u, v) = \psi(u, v; a, b, c)$ depend analytically on the parameters $(a, b, c) \in \mathcal{O}$.

As an application of Proposition 2.4.3, (3.1) and (3.7b), we deduce that every v -curvature line $v \mapsto \psi(u, v)$ of the immersion lies in a sphere or plane $\mathcal{Q}(u)$ of \mathbb{R}^3 . By (2.12) and (3.1), we can write the radii $R(u)$ of these spheres and contact angles $\theta(u)$ with Σ as

$$R^2 = \frac{1 + (z - y)^2}{y^2}, \quad \tan \theta = \frac{-1}{y - z}. \quad (3.11)$$

Similarly, the center $\widehat{c}(u)$ of the spheres $\mathcal{Q}(u)$, given by (2.13), reduces to

$$\widehat{c}(u) = \psi - \frac{1}{y}\psi_u e^{-\omega} + \frac{y-z}{y}N. \quad (3.12)$$

Remark 3.2.6. We note that a v -line is planar (i.e. $R(u) = \infty$) if and only if $y(u) = 0$, and that $\cos(\theta(u)) = 0$ if and only if $y(u) = z(u)$. In particular, it follows from (2.9) and (3.5) that the curvature line $v \mapsto \psi(0, v)$ lies in the horizontal plane $\{x_3 = 0\}$, and that Σ intersects this plane orthogonally. As a consequence, we deduce from (3.2), (3.5) that the functions $y(u), z(u)$ are antisymmetric, so $\omega(u, v)$ in (3.7b) satisfies

$$\omega(u, v) = \omega(-u, v). \quad (3.13)$$

Hence, by (3.9) and the fundamental theorem of surfaces, Σ must be symmetric with respect to the plane $\{x_3 = 0\}$.

It was proven in Proposition 2.4.7 that the center map $\widehat{c}(u)$ takes values on a certain line $L \subset \mathbb{R}^3$. We prove below that this line is vertical:

Lemma 3.2.7. Let $u \in \mathbb{R}$ such that $y(u) \neq 0$. Then, $\widehat{c}(u)$ lies in a line L orthogonal to the horizontal plane $\{x_3 = 0\}$. More precisely, it holds

$$\widehat{c}'(u) = \frac{y'(0)}{y^2} \mathbf{e}_3. \quad (3.14)$$

Proof. We know from Proposition 2.4.7 that the center map lies in a line L of \mathbb{R}^3 . If we denote by $\mathbf{t} \in \mathbb{R}^3$ the unit vector tangent to L , then it holds $\mathbf{t} = \frac{\widehat{c}'(u)}{|\widehat{c}'(u)|}$ for every u such that $y(u) \neq 0$. By (3.5), it holds $y(0) = 0$ but $y(u) \neq 0$ for u close enough to 0. We may then use (2.9) and (3.12) to deduce that

$$\mathbf{t} = \lim_{u \rightarrow 0} \frac{\widehat{c}'(u)}{|\widehat{c}'(u)|} = \psi_u(0, 0) e^{-\omega(0,0)} = \mathbf{e}_3.$$

Hence, $\widehat{c}'(u) = \widehat{c}'_3(u) \mathbf{e}_3$, where $\widehat{c}'_3(u)$ denotes the third coordinate of $\widehat{c}'(u)$. By (2.27), $\widehat{c}'_3(u)$ satisfies the condition

$$\widehat{c}''_3(u) = -2 \frac{y'(u)}{y(u)} \widehat{c}'_3(u),$$

which we can integrate to obtain $\widehat{c}'_3(u) = \frac{M}{y^2(u)}$ for some constant $M \in \mathbb{R}$. Using again

(2.9) and (3.12), we see that

$$M = \lim_{u \rightarrow 0} y(u)^2 \mathcal{C}_3(u) = y'(0),$$

obtaining (3.14). □

3.2.3 The case $a = 1$, $c > 1$: nodoids

We finish this section by considering the set of CMC surfaces $\Sigma(a, b, c)$ given by $\psi(u, v)$ in Definition 3.2.4 with $a = 1$ and $c > 1$. We know from Remark 3.2.2 that in this case, $\omega(0, v) \equiv -\log(c)$ for all $v \in \mathbb{R}$. It then follows from (3.7b) that $\omega = \omega(u)$ only depends on u . Hence, the first and second fundamental forms of $\Sigma(1, b, c)$ only depend on u , which implies that Σ is invariant under a 1-parameter group \mathcal{G} of isometries in \mathbb{R}^3 , and in fact the v -lines $\psi(u_0, v)$ are the orbits of $\psi(u_0, 0)$ under the action of \mathcal{G} . Now, since $y(u) \not\equiv 0$ (see (3.5)), we deduce from Remark 3.2.6 that there exist v -lines $\psi(u_0, v)$ which lie in spheres of \mathbb{R}^3 . By compactness, this means that \mathcal{G} must be a rotation group in \mathbb{R}^3 . Hence, Σ must be a Delaunay surface. The v -lines $v \mapsto \psi(u, v)$ parametrize circles in horizontal planes, while the profile curve of the immersion is given by $u \mapsto \psi(u, 0)$.

The principal curvature κ_1 associated to the profile curve is $e^{-\omega} \cosh \omega > 0$ (see (3.10)). Since this curvature is always positive, $\Sigma(1, b, c)$ must be a nodoid \mathbf{N} . This nodoid depends exclusively on the value $c > 1$, i.e., $\mathbf{N} = \mathbf{N}(c)$: indeed, the v -curve $v \mapsto \psi(0, v)$ is a planar geodesic of $\Sigma(1, b, c)$ which has negative curvature $\kappa_2(0, v) = \frac{1-c^2}{2}$. This curve describes the *neck* of the nodoid, which is a circle in the plane $\{x_3 = 0\}$ with radius $r = \frac{2}{c^2-1}$.

It is known that every nodoid admits a compact, embedded piece $\mathfrak{N} = \mathfrak{N}(c)$ which is free boundary in some geodesic ball B of \mathbb{R}^3 ; see Figure 3.1. More specifically, with respect to the parametrization $\psi(u, v)$ constructed in this section, let $\widehat{u} > 0$ be the first positive value where the tangent vector of the profile curve $u \mapsto \psi(u, 0)$ is vertical; see Figure 3.2. This implies that $v \mapsto \psi(\widehat{u}, v)$ parametrizes a *bulge* of the nodoid. Since $\psi(u, 0)$ has positive curvature and $v \mapsto \psi(0, v)$ parametrizes the neck of the nodoid \mathbf{N} , it is clear that there exists a unique value $\bar{u} \in (0, \widehat{u})$ such that the tangent line to $\psi(u, 0)$ at $u = \bar{u}$ passes through the intersection point $p = p(c)$ of the rotation axis of \mathbf{N} and the horizontal plane $\{x_3 = 0\}$ where the neck of \mathbf{N} is contained. In this situation, the restriction of the image of $\psi(u, v)$ to $[-\bar{u}, \bar{u}] \times \mathbb{R}$ defines a compact, embedded rotational $H = \frac{1}{2}$ annulus $\mathfrak{N}(c)$ contained in a ball $B(c) \subset \mathbb{R}^3$ with center $p = p(c)$

and radius $R = |\psi(\bar{u}, 0) - p(c)|$, and moreover $\mathfrak{N}(c)$ intersects orthogonally $\partial B(c)$ orthogonally along its boundary.

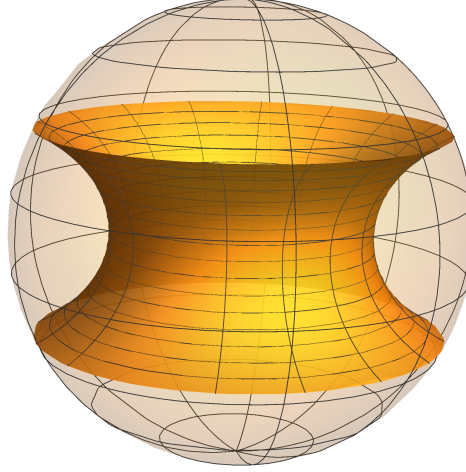


Figure 3.1: An embedded free boundary nodoid in \mathbb{B}^3 .

Definition 3.2.8. For every $c > 1$ we denote by $\mathfrak{N}(c)$ the embedded free boundary nodoid with $H = \frac{1}{2}$ and necksize $r = \frac{2}{c^2-1}$.

We emphasize that the unit normal of $\mathfrak{N}(c)$ points *outwards*, and that for every $r_0 > 0$ there exists a unique embedded free boundary nodoid with necksize $r = r_0$ and $H = \frac{1}{2}$. After a homothety, each nodoid $\mathfrak{N}(c)$ defines a rotational embedded free boundary annulus in \mathbb{B}^3 with constant mean curvature $H = H(c) = |\psi(\bar{u}, 0) - p(c)|/2$.

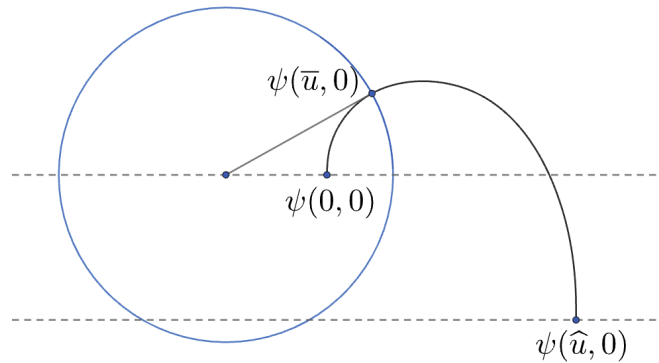


Figure 3.2: The values $\psi(\bar{u}, 0)$ and $\psi(\hat{u}, 0)$ in the profile curve of the nodoid.

3.3 Geometric properties of the surfaces $\Sigma(a, b, c)$

Let us now fix $(a, b, c) \in \mathcal{O}$ with $a > 1$ and consider the CMC surface $\Sigma(a, b, c)$ given by $\psi(u, v)$ in Definition 3.2.4. Our goal in this section is to show that Σ has several vertical planes of symmetry, which under certain conditions allow us to deduce that the spherical curvature lines $v \mapsto \psi(u, v)$ are closed. We first show the following:

Proposition 3.3.1. *There exists $\sigma = \sigma(a, b, c) > 0$ such that for each $j \in \mathbb{Z}$, the curvature line $u \mapsto \psi(u, j\sigma)$ lies in a vertical plane $\Omega_j \subset \mathbb{R}^3$, and Σ intersects Ω_j orthogonally along $\psi(u, j\sigma)$. The value σ is given by*

$$\sigma(a, b, c) = \int_{\frac{1}{ac}}^{\frac{a}{c}} \frac{2}{\sqrt{p(x)}} dx, \quad (3.15)$$

where $p(x)$ is the polynomial in (3.6). Moreover, the angle between consecutive planes Ω_j, Ω_{j+1} is independent of j . Specifically, this angle coincides with the variation of the unit tangent vector of the planar geodesic $\psi(0, v)$ of Σ between $v = j\sigma$ and $v = (j+1)\sigma$, given by

$$\chi(a, b, c) = \int_{\frac{1}{ac}}^{\frac{a}{c}} \frac{x - 1/x}{\sqrt{p(x)}} dx. \quad (3.16)$$

Additionally, $\chi(a, b, c) \in (-\pi, \pi)$.

Proof. Let $x(v) := e^{\omega(0, v)}$. Note that the values $\frac{1}{ac}$ and $\frac{a}{c}$ are the positive roots of the polynomial $p(x)$ in (3.6), and that $x(0) = \frac{1}{ac}$. According to Remark 3.2.2, $x(v)$ is a periodic function which reaches its minimum at $v = 0$. Hence, there exists a value $\sigma > 0$ such that $x(v)$ is increasing on $[0, \sigma]$, so that $x(v)$ reaches its maximum at $v = \sigma$, i.e., $x(\sigma) = \frac{a}{c}$. This value can be computed easily from (3.8), yielding (3.15). In particular, $x(v)$ is 2σ -symmetric. We also deduce from (3.8) the symmetry condition

$$\omega(0, j\sigma - v) = \omega(0, j\sigma + v) \quad (3.17)$$

for all $v \in \mathbb{R}$ and $j \in \mathbb{Z}$. Consequently, the derivative $\omega_v(0, v)$ vanishes if and only if $v = j\sigma$.

By differentiating (3.7b), we have

$$\omega_{vu} = (y \sinh \omega + z \cosh \omega) \omega_v,$$

which can be seen as an ODE for $\omega_v(\cdot, v_0)$ for every $v_0 \in \mathbb{R}$. By uniqueness of solutions

of the Cauchy problem and (3.17), we deduce that

$$\omega(u, j\sigma - v) = \omega(u, j\sigma + v) \quad (3.18)$$

holds for all u . By (3.9), it follows that there exist planes Ω_j in \mathbb{R}^3 such that:

1. The curvature line $u \mapsto \psi(u, j\sigma)$ is contained in Ω_j .
2. Ω_j intersects the surface Σ orthogonally along $\psi(u, j\sigma)$. In fact, if we denote by Ψ_j the symmetry with respect to the plane Ω_j in \mathbb{R}^3 , it holds

$$\psi(u, j\sigma - v) = \Psi_j \circ \psi(u, j\sigma + v). \quad (3.19)$$

In particular, the vectors $\nu_j := \psi_v(0, j\sigma)$ are orthogonal to the planes Ω_j . We recall that, by Remark 3.2.6, the v -line $\psi(0, v)$ is a geodesic lying in the horizontal plane $\{x_3 = 0\}$, so the planes Ω_j must be vertical.

Now, let $\Gamma(v) := \psi(0, v)$ be the horizontal geodesic of Σ , denote by $\mathbf{t}(v) := e^{-\omega(0,v)}\Gamma'(v)$ its tangent vector and let $n(v) = N(0, v)$ be the normal vector. If $\xi(v)$ denotes the angle between $\mathbf{t}(v)$ and a fixed horizontal direction, then the variation of $\xi(v)$ between $v = j\sigma$ and $v = (j+1)\sigma$, which we denote by χ , is given by

$$\chi = \int_{j\sigma}^{(j+1)\sigma} \langle \mathbf{t}', n \rangle dv.$$

Note that $\langle \mathbf{t}', n \rangle = e^{\omega(0,v)}k_2(0, v) = \sinh(\omega(0, v))$, so

$$\chi = \int_{j\sigma}^{(j+1)\sigma} \sinh \omega(0, v) dv. \quad (3.20)$$

We may now consider the change of variables $x(v) = e^{\omega(0,v)}$, since the function $v \mapsto x(v)$ defines a diffeomorphism between $[j\sigma, (j+1)\sigma]$ and $[\frac{1}{ac}, \frac{a}{c}]$, yielding (3.16).

We note that the (oriented) angle between Ω_j and Ω_{j+1} , when oriented by their normals ν_j, ν_{j+1} , coincides with the angle χ between $\mathbf{t}(j\sigma)$ and $\mathbf{t}((j+1)\sigma)$ modulo 2π . So, if we prove that χ in (3.16) satisfies $\chi \in (-\pi, \pi)$, we deduce that χ actually describes the angle between consecutive planes Ω_j . We do this next.

First, by (3.6) and (3.16), it holds

$$\chi = \int_{\frac{1}{ac}}^{\frac{a}{c}} \frac{f(x)}{\sqrt{(\frac{a}{c} - x)(x - \frac{1}{ac})}} dx,$$

where $f(x) = \frac{x-1/x}{\sqrt{(x+bc)(x+\frac{c}{b})}}$. It is not hard to prove that $|f(x)| < 1$ in $[\frac{1}{ac}, \frac{a}{c}]$: indeed, $f(x)$ is strictly increasing on this interval, and $-1 < f(\frac{1}{ac}) < f(\frac{a}{c}) < 1$. As a consequence,

$$|\chi| < \int_{\frac{1}{ac}}^{\frac{a}{c}} \frac{1}{\sqrt{(\frac{a}{c} - x)(x - \frac{1}{ac})}} dx = \pi,$$

as we wanted to prove. \square

Remark 3.3.2. We will prove in Proposition 3.5.1 that if $c = 1$ we have $\chi = 0$, and whenever $c > 1$, it holds $\chi < 0$.

Corollary 3.3.3. Let $(a, b, c) \in \mathcal{O}$, $a > 1$, such that $\chi(a, b, c)/\pi = m/n \in \mathbb{Q} \cap (-1, 1)$, with $\chi \neq 0$ and m/n irreducible. Then, $\psi(u, v + 2n\sigma) = \psi(u, v)$. In particular, by considering the quotient of \mathbb{R}^2 by the relation $(u, v) \sim (u, v + 2n\sigma)$, it holds:

1. For every $u_0 > 0$, the restriction $\psi : [-u_0, u_0] \times [0, 2n\sigma] \rightarrow \mathbb{R}^3$ defines a compact annulus.
2. The surface Σ is symmetric with respect to the horizontal plane $\{x_3 = 0\}$ and with respect to n different equiangular vertical planes $\Omega_1, \dots, \Omega_n$. These vertical planes intersect along a common vertical line, which is the line L of Lemma 3.2.7.
3. The planar geodesic $\psi(0, v) : [0, 2n\sigma] \rightarrow \{x_3 = 0\}$ is closed, with rotation index m ; see Figure 3.3.

Proof. By Proposition 3.3.1, Σ is symmetric with respect to, at least, n different vertical equiangular planes $\Omega_1, \dots, \Omega_n$. Note that $n \geq 2$, since χ/π is not an integer. Moreover, for any $u \in \mathbb{R}$ and any $j \in \{1, \dots, n\}$, the curve $\psi(u, j\sigma)$ lies in the symmetry plane Ω_j . Since $\chi \neq 0$, it follows from Remark 3.3.2 that $c > 1$, which implies by (3.5) that $y(u)$ is not identically zero. As a consequence, there must exist some u_0 for which (3.12) holds. From this equation we deduce that $\widehat{c}(u_0)$ lies in Ω_j . The planes Ω_j are vertical, so the vertical line L that contains the centers $\widehat{c}(u)$ must also lie in Ω_j . Therefore, $L \subset \cap_{j=1}^n \Omega_j$. Since $n \geq 2$ and the planes are different, we deduce that actually $L = \cap_{k=1}^n \Omega_k$.

In particular, we obtain directly from (3.19) that $\psi(u, v + 2\sigma) = \mathcal{R}(\psi(u, v))$, where \mathcal{R} is the rotation of angle 2χ around the vertical line L . Now, since $2\chi = 2\pi m/n$, we deduce that $\psi(u, v)$ is $2n\sigma$ -periodic in the v -direction, as stated. In particular, by considering the quotient of \mathbb{R}^2 by $(u, v) \sim (u, v + 2n\sigma)$, we deduce that the restrictions

$\psi : [-u_0, u_0] \times [0, 2n\sigma] \rightarrow \mathbb{R}^3$ define immersed, compact annuli in \mathbb{R}^3 . The fact that Σ is symmetric with respect to the horizontal plane $\{x_3 = 0\}$ was shown in Remark 3.2.6. Finally, item (3) follows directly from Proposition 3.3.1. \square

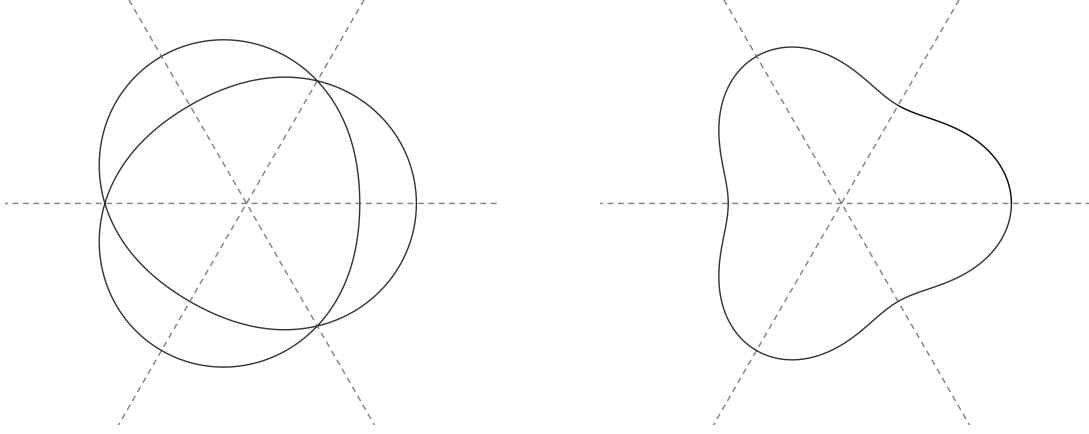


Figure 3.3: Examples of planar curves $v \mapsto \psi(0, v)$ with $\chi = \frac{2\pi}{3}$ (left) and $\chi = \frac{\pi}{3}$ (right).

3.4 The orthogonality condition

The goal of this section is to define a certain region \mathcal{W} of the parameter space $\mathcal{O} \subset \mathbb{R}^3$ such that for every $(a, b, c) \in \mathcal{W}$ we can control the orthogonality condition in the intersection of the spherical curvature lines of the surface $\Sigma = \Sigma(a, b, c)$ with the spheres that contain them. This will be accomplished by analyzing the system (3.2), which we now examine.

3.4.1 The system (s, t)

Given any $(a, b, c) \in \mathcal{O}$, let $(y(u), z(u))$ be the unique solution to (3.2), (3.5). Went observed [76, p. 17] that the system (3.2) has a Hamiltonian nature, and admits two first integrals, namely

$$\mathcal{K}_1 = y'^2 - z'^2 - (\hat{a} - 1)y^2 + \hat{a}z^2 + (y^2 - z^2)^2, \quad (3.21a)$$

$$\mathcal{K}_2 = 4(zy' - yz')^2 + 4z'^2 + 4z^2(y^2 - z^2 - \hat{a}), \quad (3.21b)$$

for some real constants $\mathcal{K}_1, \mathcal{K}_2 \in \mathbb{R}$. We note that these integrals correspond to (2.25), (2.26) under the substitution $A = H^2 = \frac{1}{4}$, $Q = \frac{1}{2}$, (3.1). These first integrals al-

low us to separate variables in system (3.2) following a classical procedure by Jacobi. Specifically, as detailed in [76, p. 17], we consider the change of variables

$$y^2 = -(1-s)(1-t), \quad z^2 = -st. \quad (3.22)$$

This defines a diffeomorphism from any of the four open quadrants of the (y, z) -plane onto the region of the (s, t) -plane given by $\{s > 1, t < 0\}$, which extends homeomorphically to the boundary. It can then be shown that any solution $(y(u), z(u))$ to (3.2) transforms into a solution $(s(\lambda), t(\lambda))$ to

$$\begin{cases} s'(\lambda)^2 = s(s-1)g(s), & (s \geq 1), \\ t'(\lambda)^2 = t(t-1)g(t), & (t \leq 0), \end{cases} \quad (3.23)$$

where $g(x)$ is the third-degree polynomial

$$g(x) = -x^3 + (\widehat{a} + 1)x^2 + (\mathcal{K}_1 - \widehat{a})x + \frac{1}{4}\mathcal{K}_2, \quad (3.24)$$

and λ is related to u by

$$2u'(\lambda) = s(\lambda) - t(\lambda) \geq 1. \quad (3.25)$$

The polynomial $g(x)$ in (3.24) has three real roots $r_1 \leq r_2 \leq 0 < 1 \leq r_3$ satisfying

$$\begin{aligned} r_1 &= -\frac{(ab-1)^2}{4ab}, \\ r_2 &= -\frac{(b-a)^2}{4ab}, \\ r_3 &= 1 + \mathcal{C}^2. \end{aligned} \quad (3.26)$$

Remark 3.4.1. We emphasize that $r_1 = r_2$ if and only if $a = 1$, that $r_2 = 0$ if and only if $a = b$ and that $r_3 = 1$ if and only if $c = 1$. Since $y(0) = z(0) = 0$, we deduce by (3.22) that $s(0) = 1$, $t(0) = 0$, after possibly a transformation in the λ -parameter. Note that (3.23) is a pair of first order ODEs that can be solved by integration. In fact, one can see that both $s(\lambda)$ and $t(\lambda)$ are defined for every $\lambda \in \mathbb{R}$. If $c = 1$, then $s(\lambda) \equiv 1$. However, if $c > 1$, $s(\lambda)$ is $2\mathcal{M}$ -periodic, where

$$\mathcal{M} := \int_1^{r_3} \frac{dx}{\sqrt{-x(x-1)(x-r_1)(x-r_2)(x-r_3)}} < \infty. \quad (3.27)$$

Similarly, if $r_1 < r_2 < 0$, then $t(\lambda)$ is $2\mathcal{N}$ -periodic, where the half-period \mathcal{N} is

$$\mathcal{N} := \int_{r_2}^0 \frac{dx}{\sqrt{-x(x-1)(x-r_1)(x-r_2)(x-r_3)}} < \infty. \quad (3.28)$$

If, however, $r_1 = r_2 < 0$, then the integral above diverges and $t(\lambda)$ is not periodic. Finally, $t(\lambda) \equiv 0$ whenever $r_2 = 0$.

As a consequence of Remark 3.4.1, we deduce that, whenever $c > 1$, it holds

$$s(0) = s(2\mathcal{M}) = 1, \quad s(\mathcal{M}) = r_3,$$

with $s(\lambda) \in (1, r_3]$ for every $\lambda \in (0, 2\mathcal{M})$. We emphasize that $r_3 > 1$ in this case and that $y'(0) > 0$; see (3.5). In a similar fashion, if $r_1 < r_2 < 0$, then

$$t(0) = t(2\mathcal{N}) = 0, \quad t(\mathcal{N}) = r_2,$$

and $t(\lambda) \in [r_2, 0)$ for all $\lambda \in (0, 2\mathcal{N})$. If $r_1 = r_2 < 0$, then $t(\lambda)$ is decreasing for all $\lambda \in (0, \infty)$, with $\lim_{\lambda \rightarrow \infty} t(\lambda) = r_2$. Finally, if $r_1 \leq r_2 = 0$, then $t(\lambda) \equiv 0$.

Remark 3.4.2. It follows from Remark 3.4.1 that the solutions $(s(\lambda), t(\lambda))$ are defined for all $\lambda \in \mathbb{R}$. Moreover, from (3.25) we deduce that

$$1 \leq 2u'(\lambda) \leq r_3 - r_2. \quad (3.29)$$

In particular, the solution $(y(u), z(u))$ to (3.2), (3.5) is defined for all $u \in \mathbb{R}$ as well. In fact, from (3.22) it follows that the functions $y(u), z(u)$ and their derivatives are uniformly bounded.

Lemma 3.4.3. Suppose that $r_1 \leq r_2 < 0$ and $1 < r_3$. Then, $\mathcal{M} < \mathcal{N}$.

Proof. If $r_1 = r_2$, then the integral that defines \mathcal{N} in (3.28) diverges, so the result holds trivially. Let us assume then that $r_1 < r_2$. In this case, let $h(x) := 1/(x - w_0)$, where $w_0 \in (0, 1)$ is a constant which will be determined later, and consider the change of variables $\mu = h(x)$ on (3.27) and (3.28). Observe that

$$x - a = -\frac{h(x) - h(a)}{h(x)h(a)} = -\frac{\mu - h(a)}{\mu h(a)}.$$

Using (3.24), (3.27) and (3.28), we obtain that \mathcal{M} and \mathcal{N} satisfy

$$\mathcal{M} = \int_{h(r_3)}^{h(1)} \Psi(\mu) d\mu, \quad \mathcal{N} = \int_{h(0)}^{h(r_2)} \Psi(\mu) d\mu, \quad (3.30)$$

where

$$\Psi(\mu) := \frac{\sqrt{h(r_2)h(0)h(1)h(r_3)}}{\sqrt{-(\mu - h(r_2))(\mu - h(0))(\mu - h(1))(\mu - h(r_3))} \sqrt{\frac{1}{\mu} + w_0 - r_1}}.$$

Since $\mu < 0$ for every $\mu \in (h(0), h(r_2))$, we have from (3.30) that $\mathcal{N} > T$, where

$$T := \int_{h(0)}^{h(r_2)} \frac{\sqrt{h(r_2)h(0)h(1)h(r_3)} d\mu}{\sqrt{-(\mu - h(r_2))(\mu - h(0))(\mu - h(1))(\mu - h(r_3))} \sqrt{w_0 - r_1}}.$$

Similarly, since $\mu > 0$ when $\mu \in (h(r_3), h(1))$, we obtain $\mathcal{M} < T'$, where

$$T' := \int_{h(r_3)}^{h(1)} \frac{\sqrt{h(r_2)h(0)h(1)h(r_3)} d\mu}{\sqrt{-(\mu - h(r_2))(\mu - h(0))(\mu - h(1))(\mu - h(r_3))} \sqrt{w_0 - r_1}}. \quad (3.31)$$

We next show that $T = T'$ for a certain choice of $w_0 \in (0, 1)$. Consider the function $f(x, w) := 1/(x - w)$, where $w \in (0, 1)$, and define

$$F(w) := f(1, w) - f(r_3, w) - (f(r_2, w) - f(0, w)) : (0, 1) \rightarrow \mathbb{R}.$$

Since $F(w) \rightarrow -\infty$ (resp. $F(w) \rightarrow \infty$) as $w \rightarrow 0$ (resp. $w \rightarrow 1$), there exists some $w_0 \in (0, 1)$ for which $F(w_0) = 0$, by continuity of F . If we define w_0 in this way, we get

$$h(1) - h(r_3) = h(r_2) - h(0) > 0.$$

From this expression, we obtain by applying the change of variable $\xi = -\mu + h(1) + h(0)$ in (3.31) that

$$T' = - \int_{h(r_2)}^{h(0)} \frac{\sqrt{h(r_2)h(0)h(1)h(r_3)} d\xi}{\sqrt{-(\xi - h(r_2))(\xi - h(0))(\xi - h(1))(\xi - h(r_3))} \sqrt{w_0 - r_1}} = T.$$

Thus, $\mathcal{M} < T' = T < \mathcal{N}$, completing the proof of the lemma. \square

3.4.2 The map $\tau(a, b, c)$

We will now use the results of Section 3.4.1 to study the conditions under which a surface $\Sigma(a, b, c)$ intersects orthogonally a certain sphere $\mathcal{Q}(u_0)$ along the v -line $v \mapsto \psi(u_0, v)$. According to (3.11), this will happen whenever

$$y(u_0) = z(u_0). \quad (3.32)$$

To control this condition, we first show the following result.

Proposition 3.4.4. *For every $(a, b, c) \in \mathcal{O}$ with $c > 1$, there exists a unique $u_1 = u_1(a, b, c) > 0$ satisfying:*

1. $y(u) > 0$ for every $u \in (0, u_1)$ and $y(u_1) = 0$.
2. If $z(u)$ is not identically zero, then $z(u) > 0$ for every $u \in (0, u_1]$.

Moreover, the function $u_1 = u_1(a, b, c) : \mathcal{O} \cap \{c > 1\} \rightarrow \mathbb{R}$ is real analytic

Proof. We consider the solution $(y(u), z(u))$ to (3.2), (3.5) and the associated pair $(s(\lambda), t(\lambda))$ solving (3.23). First, the fact that $c > 1$ implies by (3.5) that $y'(0) > 0$, so $y(u) > 0$ for $u > 0$ small enough. On the other hand, it follows from (3.26) that $r_3 > 1$. Hence, by Remark 3.4.1, the function $s(\lambda)$ satisfies $s(\lambda) \in (1, r_3]$ for all $\lambda \in (0, 2\mathcal{M})$, where \mathcal{M} is given by (3.27). Now, the reparametrization $u = u(\lambda)$ satisfies (3.29), which implies that $u'(\lambda)$ is bounded between two positive constants, so there must exist a unique positive value $u_1 := u(2\mathcal{M})$ such that $u(\lambda)$ defines a diffeomorphism between $[0, 2\mathcal{M}]$ and $[0, u_1]$. By (3.22), it follows that u_1 must be the first positive root of $y(u)$. In particular, $y(u) > 0$ for all $u \in (0, u_1)$, proving item (1) of the Proposition. It also holds that the map $u_1(a, b, c)$ is analytic: this follows from the analyticity theorem of solutions of ODEs with respect to initial conditions, (3.25), (3.27), and the fact that $u_1 = u(2\mathcal{M})$.

Let us now prove item (2). Assume that $z(u) \not\equiv 0$. This implies that the derivative $z'(0)$ cannot be zero: otherwise, we would have $z(0) = z'(0) = 0$ and by (3.5), $z(u) \equiv 0$. Consequently, $z'(0) \neq 0$, which by (3.5) and the definition of the set \mathcal{O} in (3.3) implies that $b > a$, and thus $z'(0) > 0$. We also deduce that $r_2 < 0$. According to Remark 3.4.1, this implies that the function $t(\lambda)$ is either negative for all $\lambda > 0$ (if $r_1 = r_2$), or it is periodic and $t(\lambda) \in [r_2, 0)$ for all $\lambda \in (0, 2\mathcal{N})$. In any case, we conclude from Lemma 3.4.3 that $t(\lambda) < 0$ for every $\lambda \in (0, 2\mathcal{M}]$. By (3.22) and the definition of the value u_1 , we deduce that necessarily $z(u) > 0$ for every $u \in (0, u_1]$, which proves item (2). \square

In order to show that the orthogonality condition (3.32) holds, we define the set $\mathcal{W} \subset \mathcal{O}$ as

$$\mathcal{W} := \left\{ (a, b, c) \in \mathcal{O} : b \geq a \geq 1, c^2 > \frac{(\mathcal{A} - \mathcal{B})^2}{4\mathcal{A}\mathcal{B}} \right\}, \quad (3.33)$$

where $\mathcal{A}, \mathcal{B}, \mathcal{C}$ are given by (3.4). We note that $c > 1$ for all $(a, b, c) \in \mathcal{W}$.

Proposition 3.4.5. *For every $(a, b, c) \in \mathcal{W}$, there exists a unique $\tau = \tau(a, b, c) \in (0, u_1]$ such that $y(\tau) = z(\tau)$ and $y(u) > z(u) \geq 0$ for all $u \in (0, \tau)$. Moreover, the function $\tau(a, b, c) : \mathcal{W} \rightarrow \mathbb{R}$ is real analytic.*

Proof. Consider the function $\beta(u) = y(u) - z(u)$ in (3.1). By (3.5) and the fact that $(a, b, c) \in \mathcal{W}$, it follows that $\beta(0) = 0, \beta'(0) > 0$. By Proposition 3.4.4, we have $\beta(u_1) \leq 0$, with equality holding if and only if $z(u) \equiv 0$. Hence, there exists a unique value $\tau \in (0, u_1]$ satisfying the conditions of the Proposition.

Let us now prove that $\tau = \tau(a, b, c)$ is real analytic. We note that the solutions $(y(u), z(u))$ to (3.2) depend analytically on (a, b, c) . Thus, we can view β as a function depending on these parameters, $\beta = \beta(u; a, b, c)$. We will now prove that for every $(a, b, c) \in \mathcal{W}$ it holds $\beta_u(\tau; a, b, c) \neq 0$, where $\tau = \tau(a, b, c)$. This would imply by the implicit function theorem that $\tau(a, b, c)$ is real analytic, as stated in the Proposition.

Arguing by contradiction, assume that $\beta_u(\tau; a, b, c) = 0$. By definition of τ , we deduce that $y(\tau) = z(\tau), y'(\tau) = z'(\tau)$. It would then follow from (3.2) that $\beta''(\tau) = y''(\tau) - z''(\tau) = -y(\tau) \leq 0$. We treat two cases, depending on whether $\tau < u_1$ or $\tau = u_1$.

If $\tau < u_1$, then $y(\tau) > 0$ according to Proposition 3.4.4, and so $\beta''(\tau) < 0$, which implies that $\beta(u)$ has a local maximum at $u = \tau$. This is impossible since $\beta(\tau) = 0$ but $\beta(u) > 0$ for $u \in (0, \tau)$.

If $\tau = u_1$, then $z(u) \equiv 0$, according to item (2) in Proposition 3.4.4, so in particular $z'(\tau) = 0$. Since $y(\tau) = y(u_1) = 0$, we may use (2.25) to deduce that $y'(\tau)^2 = y'(0)^2 \neq 0$. However, it was assumed that $y'(\tau) = z'(\tau) = 0$, reaching a contradiction. \square

Corollary 3.4.6. *For every $(a, b, c) \in \mathcal{W}$, the surface $\Sigma(a, b, c)$ intersects the sphere $\mathcal{Q}(\tau)$ orthogonally along the v -line $v \mapsto \psi(\tau, v)$.*

Remark 3.4.7. *If $b \geq a \geq 1$ and $c > 1$ but, in contrast with (3.33), we assume*

$$c^2 \leq \frac{(\mathcal{A} - \mathcal{B})^2}{4\mathcal{A}\mathcal{B}}, \quad (3.34)$$

so that $(a, b, c) \in \mathcal{W}$, then, $y(u) < z(u)$ for every $u > 0$ small enough. Indeed, the inequality (3.34) is strict, then $\beta(u) = y(u) - z(u)$ satisfies $\beta(0) = 0$, $\beta'(0) < 0$. Similarly, if equality holds in (3.34), then one can prove using (3.2) that $\beta(0) = \beta'(0) = \beta''(0) = 0$ but $\beta'''(0) = -y'(0) < 0$, so $\beta(u) < 0$ for small u .

3.5 The period map

Given $(a, b, c) \in \mathcal{O}$ with $a > 1$, we consider the function $\chi(a, b, c)$ defined in (3.16). By Corollary 3.3.3, the v -lines $v \mapsto \psi(u, v)$ of the immersion will be closed if and only if the value $\Theta = \Theta(a, b, c)$ belongs to \mathbb{Q} , where

$$\Theta(a, b, c) := \frac{\chi}{\pi} = \frac{1}{\pi} \int_{\frac{1}{ac}}^{\frac{a}{c}} \frac{x - 1/x}{\sqrt{p(x)}} dx \quad (3.35)$$

where $p(x)$ is the polynomial in (3.6). We recall that $\frac{1}{ac}$, $\frac{a}{c}$ are the positive roots of $p(x)$. We will refer to (3.35) as the *period map*. We will devote this section to the study of this map, and more specifically to the analysis of the structure of the level sets of $\Theta(a, b, c)$. This will be achieved in Proposition 3.5.3.

It is clear from (3.35) that the period map is analytic for every $(a, b, c) \in \mathcal{O}$ provided that $a > 1$. We will now show that, actually, the period map can be analytically extended for the limit value $a = 1$.

Proposition 3.5.1. *The period map $\Theta(a, b, c)$ can be extended analytically to the set \mathcal{O} . Moreover, if $a = 1$,*

$$\Theta(1, b, c) = \frac{1 - c^2}{\sqrt{1 + (b + b^{-1})c^2 + c^4}}. \quad (3.36)$$

Proof. For every $a > 1$, let $h_a(t) := \left(\frac{a}{c} - \frac{1}{ac}\right)t + \frac{1}{ac}$. We can consider the change of variables $x = h_a(t)$ in (3.35), yielding

$$\Theta(a, b, c) = \frac{1}{\pi} \int_0^1 \frac{h_a(t) - \frac{1}{h_a(t)}}{\sqrt{t(1-t)} \sqrt{h_a(t)^2 + (b + b^{-1})h_a(t)c + c^2}} dt.$$

Note that this expression is well defined and analytic for $a = 1$, so it allows us to extend the period map for this limit value. In fact, we can explicitly compute $\Theta(1, b, c)$,

obtaining

$$\Theta(1, b, c) = \frac{1}{\pi} \int_0^1 \frac{c^{-1} - c}{\sqrt{t(1-t)} \sqrt{c^{-2} + (b + b^{-1}) + c^2}} dt = \frac{1 - c^2}{\sqrt{1 + (b + b^{-1})c^2 + c^4}}.$$

This completes the proof. \square

Remark 3.5.2. *The change of variables $x = h_a(t)$ may also be used in the integral that defines the value σ in (3.15). This shows that the map $\sigma(a, b, c)$ is also analytic in \mathcal{O} , and for the limit value $a = 1$, we get*

$$\sigma(1, b, c) = \frac{2\pi c}{\sqrt{1 + (b + b^{-1})c^2 + c^4}}. \quad (3.37)$$

Using (3.35), it is possible to show that the level sets of $\Theta(a, b, c)$ are given by analytic graphs. We do this next.

Proposition 3.5.3. *The period map $\Theta(a, b, c)$ satisfies the following properties:*

1. $\frac{\partial \Theta}{\partial c} < 0$.
2. $\Theta(a, b, 1) = 0$ and $\lim_{c \rightarrow \infty} \Theta(a, b, c) = -1$.
3. *For every $d \in (-1, 0]$, the non-empty level set $\Theta^{-1}(d)$ can be expressed as the graph $c_d = c_d(a, b)$ of an analytic map $c_d(a, b)$ defined for every $b \geq a \geq 1$. Moreover, $c_0(a, b) \equiv 1$ and $c_d < c_{d'}$ for every $d > d'$.*

Proof. Let us prove item (1) first. Let $f(x; l, m)$ be the function

$$f(x; l, m) := \frac{1 - x^2}{\sqrt{l + mx^2 + x^4}}.$$

We note that the derivative f_x is negative for every $x, l, m > 0$. If $a = 1$, it follows from (3.36) that

$$\Theta(1, b, c) = f(c; 1, b + b^{-1}), \quad (3.38)$$

so clearly $\frac{\partial \Theta}{\partial c}(1, b, c) < 0$. Similarly, if $a > 1$, we may consider the change of variables $\mu = \frac{1}{cx}$ in (3.35) to obtain

$$\Theta(a, b, c) = \frac{1}{\pi} \int_{a^{-1}}^a \frac{f(c\mu; \mu^2, (b + b^{-1})\mu)}{\sqrt{(a - \mu)(\mu - a^{-1})}} d\mu. \quad (3.39)$$

Thus, the derivative $\frac{\partial \Theta}{\partial c}(a, b, c)$ is the integral of a negative function, so $\frac{\partial \Theta}{\partial c} < 0$, showing item (1) of the proposition.

We will now show that $\Theta(a, b, 1) = 0$. This is clear if $a = 1$, so let us assume that $a > 1$. We observe that the polynomial $p(x)$ in (3.6) satisfies the relation $p(x) = x^4 p(1/x)$ whenever $c = 1$. Using this fact and the change of variables $\mu = \frac{1}{x}$, we see that

$$\Theta(a, b, 1) = \frac{1}{\pi} \int_{a^{-1}}^a \frac{x - 1/x}{\sqrt{p(x)}} dx = \frac{1}{\pi} \int_{a^{-1}}^a \frac{1/\mu - \mu}{\mu^4 \sqrt{p(1/\mu)}} d\mu = -\Theta(a, b, 1).$$

In particular, $\Theta(a, b, 1) = 0$, as claimed.

To complete the proof of item (2), it remains to show that $\Theta(a, b, c)$ converges to -1 as $c \rightarrow \infty$. The case $a = 1$ is immediate from (3.36), so let $a > 1$. By (3.39) and the fact that $\lim_{x \rightarrow \infty} f(x; l, m) = -1$, it follows that

$$\lim_{c \rightarrow \infty} \Theta(a, b, c) = \frac{1}{\pi} \int_{a^{-1}}^a \frac{-1}{\sqrt{(a - \mu)(\mu - a^{-1})}} d\mu = -1,$$

proving item (2).

We deduce from the previous assertions that $\Theta(a, b, c) \in (-1, 0]$ for every $(a, b, c) \in \mathcal{O}$. More precisely, for every $d \in (-1, 0]$, the level set $\Theta^{-1}(d)$ can be expressed as a graph $c = c_d(a, b)$, according to item (1). The real analyticity of $c_d(a, b)$ follows from the analyticity of the period map, proved in Proposition 3.5.1. The fact that $c_0(a, b) \equiv 1$ and the monotonicity of $c_d(a, b)$ with respect to the parameter d follows from item (2).

□

Remark 3.5.4. For every $d \in (-1, 0]$, let $\mathcal{C}_d := \frac{1}{2} \left(c_d(1, b) - \frac{1}{c_d(1, b)} \right)$ and define \mathcal{B} as in (3.4). Then, (3.36) can be rewritten as

$$\mathcal{C}_d^2 = \frac{d^2(\mathcal{B} + 1)}{2(1 - d^2)}. \quad (3.40)$$

3.6 CMC annuli with spherical free boundary

Let $(a, b, c) \in \mathcal{O}$ such that $\Theta(a, b, c) \in \mathbb{Q}$, $\Theta \neq 0$, where $\Theta(a, b, c)$ is the period map in Section 3.5, and consider the associated immersion $\psi(u, v) = \psi(u, v; a, b, c)$. In Corollary 3.3.3, it was shown that for every $u_0 > 0$ the restriction of $\psi(u, v)$ to $[-u_0, u_0] \times \mathbb{R}$ defines a compact annulus in \mathbb{R}^3 . We now aim to find a special value $u^* > 0$ with the additional property that both boundary components of the annulus lie in the same sphere of \mathbb{R}^3 . By the symmetry of $\Sigma(a, b, c)$ with respect to the plane $\{x_3 = 0\}$, this will happen if the center map $\hat{c}(u)$ lies in this plane at $u = u^*$.

Lemma 3.6.1. *For any $(a, b, c) \in \mathcal{O} \cap \{c > 1\}$, there exists a unique $u^* = u^*(a, b, c)$ such that $u^* \in (0, u_1)$ and $\widehat{c}_3(u^*) = 0$, where \widehat{c}_3 denotes the third coordinate of the center map $\widehat{c}(u)$ in (3.12). Additionally, $u^*(a, b, c) : \mathcal{O} \cap \{c > 1\} \rightarrow \mathbb{R}$ is real analytic.*

Proof. Let $(a, b, c) \in \mathcal{O} \cap \{c > 1\}$. By (3.5), $y(u)$ satisfies $y'(0) > 0$. By Lemma 3.2.7, we deduce that $\widehat{c}_3(u)$ is strictly increasing on $u \in (0, u_1)$. Note that in the limits $u \rightarrow 0^+$, $u \rightarrow u_1^-$, the radii $R(u)$ of the spheres go to infinity, as $y(0) = y(u_1) = 0$; see (3.11). In particular, by the monotonicity of $\widehat{c}_3(u)$, it follows that

$$\lim_{u \rightarrow 0^+} \widehat{c}_3(u) = -\infty, \quad \lim_{u \rightarrow u_1^-} \widehat{c}_3(u) = \infty.$$

Hence, there exists a unique $u^* \in (0, u_1)$ where $\widehat{c}_3(u)$ vanishes.

To prove that $u^* : \mathcal{O} \cap \{c > 1\}$ is analytic, we view $\widehat{c}_3(u) = \widehat{c}_3(u; a, b, c)$ as a function of both $u \in (0, u_1)$ and the parameters $(a, b, c) \in \mathcal{O} \cap \{c > 1\}$. The real analyticity of $\widehat{c}_3(u; a, b, c)$ follows from (3.12) and the fact that the immersion $\psi(u, v)$ and the solution $(y(u), z(u))$ to (3.2) depend analytically on u and (a, b, c) ; see Remark 3.2.5. Now, by (3.14), it holds $(\widehat{c}_3)_u(u^*; a, b, c) \neq 0$, which implies that $u^*(a, b, c)$ is real analytic using the implicit function theorem. \square

Definition 3.6.2. *For every $(a, b, c) \in \mathcal{O} \cap \{c > 1\}$, we denote by $\Sigma_0 = \Sigma_0(a, b, c)$ the restriction of the immersion $\psi(u, v)$ of Definition 3.2.4 to $[-u^*, u^*] \times \mathbb{R}$.*

We next summarize the properties of the surfaces $\Sigma_0(a, b, c)$ when $\Theta(a, b, c) = -1/n$.

Proposition 3.6.3. *Let $(a, b, c) \in \mathcal{O} \cap \{c > 1\}$ so that $\Theta(a, b, c) = -\frac{1}{n}$ for some $n \in \mathbb{N}$, $n \geq 2$. Then, $\psi(u, v + 2n\sigma) = \psi(u, v)$, where $\sigma = \sigma(a, b, c)$; see Proposition 3.3.1 and Remark 3.5.2. In particular, if we consider the relation $(u, v) \sim (u, v + 2n\sigma)$, we can view the surface Σ_0 in Definition 3.6.2 as a compact CMC $H = \frac{1}{2}$ annulus in \mathbb{R}^3 with the following properties:*

1. *Each v -line of Σ_0 is a closed spherical curvature line.*
2. *Σ_0 is symmetric with respect to the plane $\{x_3 = 0\}$ and with respect to n equiangular vertical planes of \mathbb{R}^3 that intersect along the vertical line L in which the center map $\widehat{c}(u)$ lies; see Lemma 3.2.7.*
3. *The closed planar geodesic $\Gamma(v) \equiv \psi(0, v) : [0, 2n\sigma] \rightarrow \{x_3 = 0\}$ has rotation index -1 .*

4. The boundary components $\partial\Sigma_0$ of Σ_0 , given by the v -lines $\psi(-u^*, v)$, $\psi(u^*, v)$, lie in the same sphere $\mathcal{Q} \subset \mathbb{R}^3$ of radius R . Moreover, Σ_0 intersects this sphere at a constant angle θ , where R and θ are given by

$$R^2 = \frac{1 + (z(u^*) - y(u^*))^2}{y^2(u^*)}, \quad \tan(\theta) = \frac{1}{z(u^*) - y(u^*)}.$$

5. If $a > 1$, Σ_0 is not rotational, and has a prismatic symmetry group of order $4n$. This group is generated by the symmetries in item (2).
6. If $a = 1$, Σ_0 is a compact piece of a nodoid, and in fact the line L of item (2) is the rotation axis of the annulus.

Proof. Let us first assume that $a > 1$. The equality $\psi(u, v) = \psi(u, v + 2n\sigma)$ and the first three items follow from Corollary 3.3.3. Item (4) follows from (3.11) and the fact that $\widehat{c}_3(u^*) = \widehat{c}_3(-u^*) = 0$, which implies that the spheres $\mathcal{Q}(u^*)$ and $\mathcal{Q}(-u^*)$ coincide.

We will now prove item (5). First, note that the curvature of the planar curve $\Gamma(v)$, given by

$$\kappa_2(0, v) = e^{-\omega(0, v)} \sinh \omega(0, v), \quad (3.41)$$

is not constant, so Γ is not a circle. In particular, the annulus Σ_0 cannot be rotational. Let us now show that the symmetry group of Σ_0 is actually generated by the symmetries described in item (2), which will allow us to prove item (5).

Let Φ be an isometry of \mathbb{R}^3 that leaves Σ_0 invariant. The fact that Γ is the only v -curvature line of Σ_0 which is planar implies that necessarily $\Phi(\Gamma) = \Gamma$. This implies that Φ must be a symmetry of the form $(\Psi, \pm Id)$, where Ψ is an isometry of the plane $\{x_3 = 0\}$ with $\Psi(\Gamma) = \Gamma$. In particular, Ψ belongs to the planar symmetry group of the curve Γ . By item (2), we know that Γ is symmetric with respect to n vertical planes $\{\Omega_1, \dots, \Omega_n\}$. In particular, the symmetry group of Γ must be a dihedral group $D_{n'}$ that contains at least the reflections with respect to n equiangular lines $\{L_1, \dots, L_n\}$, where $L_j = \Omega_j \cap \{x_3 = 0\}$. Hence, $n' \geq n$. Assume by contradiction that $n' > n$. In that case, there would exist an additional symmetry line L' for Γ . At the intersection points of Γ and L' , the curvature κ_2 of Γ should have a maximum or minimum. However, it was proved in Proposition 3.3.1 that the unique critical points of κ_2 appear in the intersection between Γ and any of the lines L_j . Hence, the additional line L' does not exist, so $n = n'$, and consequently the isometry group of Σ_0 is generated by the symmetries in item (2). This completes the proof of the proposition when $a > 1$.

Let us finally assume that $a = 1$. It follows from our analysis in Section 3.2.3 that Σ_0 must be a compact piece of a nodoid obtained by rotating the profile curve $u \mapsto \psi(u, 0)$, with $u \in [-u^*, u^*]$. We recall that the curves $v \mapsto \psi(u, v)$ are horizontal circles whose centers lie in the rotation axis of Σ_0 . The function $\omega(u, v)$ associated to the metric only depends on u , and in fact $e^{\omega(0, v)} = \frac{1}{c}$. This allows us to prove items (1) and (4). Item (6) follows after noting that if a horizontal circle $\psi(u_0, v)$ lies in a sphere, then the vertical line that passes through the center of the circle (i.e. the rotation axis of the nodoid) also passes through the center of the sphere. This ensures that the rotation axis of the nodoid coincides with L , so item (6) holds.

Let us now prove that $\psi(u, v) = \psi(u, v + 2n\sigma)$. Let $\mathbf{t}(v) := e^{-\omega(0, v)}\Gamma'(v) = c\Gamma'(v)$ be the unit tangent vector of $\Gamma(v)$. By (3.20), if we denote by $\xi(v)$ the angle between $\mathbf{t}(v)$ and a fixed direction of \mathbb{R}^2 , the variation of $\xi(v)$ between $v = 0$ and $v = 2n\sigma$ is given by

$$\widehat{\chi} = \int_0^{2n\sigma} \sinh \omega(0, v) dv = n\sigma \left(\frac{1}{c} - c \right).$$

It follows from (3.36) and (3.37) together with $\Theta(1, b, c) = -\frac{1}{n}$ that $\widehat{\chi} = -2\pi$. In particular, the values of the moving frame of $\psi(u, v)$ at $(u, v) = (0, 2n\sigma)$ agree with the ones at $(u, v) = (0, 0)$, given by (2.9). By (3.9) and the fundamental theorem of surfaces we deduce that $\psi(u, v) = \psi(u, v + 2n\sigma)$. This also proves item (3) of the proposition, since $\widehat{\chi} = -2\pi$.

It just remains to prove item (2). This is immediate: indeed, the piece of nodoid Σ_0 is symmetric with respect to the plane $\{x_3 = 0\}$ by Remark 3.2.6, and also with respect to any vertical plane that contains the axis L , as Σ_0 is rotational. This completes the proof. \square

Corollary 3.6.4. *In the conditions of the previous proposition, assume further that $(a, b, c) \in \mathcal{W}$ and that $u^*(a, b, c) = \tau(a, b, c)$, where \mathcal{W} and $\tau(a, b, c)$ are given by (3.33) and Proposition 3.4.5 respectively. Then, Σ_0 intersects orthogonally the sphere in which the boundary components $\partial\Sigma_0$ of Σ_0 lie.*

We remark that the previous corollary does not imply that Σ_0 is free boundary in the ball B bounded by the sphere in which $\partial\Sigma_0$ lies.

The next result will be essential to detect points $(a, b, c) \in \mathcal{W}$ in which the condition $u^*(a, b, c) = \tau(a, b, c)$ holds. For that purpose, we will show that the function $u^* - \tau$ changes sign along certain paths in \mathcal{W} .

Proposition 3.6.5. *Let $f : [0, 1) \rightarrow \mathbb{R}$ be the analytic map*

$$f(\rho) := u^*(\Upsilon(\rho)) - \tau(\Upsilon(\rho)),$$

where $\Upsilon : [0, 1] \rightarrow \overline{\mathcal{W}}$ is an analytic arc satisfying

1. $\Upsilon(0) = (a_0, a_0, c_0) \in \mathcal{W}$.
2. $\Upsilon(\rho) \in \mathcal{W}$ for all $\rho \in [0, 1)$.
3. $\Upsilon(1) = (a_1, b_1, c_1) \notin \mathcal{W}$, where $c_1 > 1$ and the values $(\mathcal{A}_1, \mathcal{B}_1, \mathcal{C}_1)$ defined in terms of Υ_1 by (3.4) satisfy

$$\mathcal{C}_1^2 = \frac{(\mathcal{A}_1 - \mathcal{B}_1)^2}{4\mathcal{A}_1\mathcal{B}_1}. \quad (3.42)$$

Then, there exists some $\rho^* \in (0, 1)$ and $\varepsilon > 0$ such that $f(\rho^*) = 0$, $f(\rho) < 0$ for $\rho \in (\rho^* - \varepsilon, \rho^*)$ and $f(\rho) > 0$ for $\rho \in (\rho^*, \rho^* + \varepsilon)$.

Proof. We will prove that $u^*(\Upsilon(0)) < u_1(\Upsilon(0)) = \tau(\Upsilon(0))$, where u_1 is defined in Proposition 3.4.4, and that

$$\lim_{\rho \rightarrow 1^-} \tau(\Upsilon(\rho)) = 0 < u^*(\Upsilon(1)).$$

This means that $f(\rho)$ changes sign at some point $\rho^* \in (0, 1)$. Since the function $f(\rho)$ is a non-constant analytic function, its zeros are isolated, and so we can choose ρ^*, ε so that the conditions in the proposition are satisfied.

First, we note that, by Lemma 3.6.1, it holds $0 < u^*(\Upsilon(\rho)) < u_1(\Upsilon(\rho))$. We also emphasize that $\tau(\Upsilon(\rho))$ is only defined for $\rho \in [0, 1)$, since the point $\Upsilon(1)$ does not belong to the set \mathcal{W} .

To prove that $u_1(\Upsilon(0)) = \tau(\Upsilon(0))$ we observe that, for $\Upsilon(0) = (a_0, a_0, c_0)$, the solution $(y(u), z(u))$ to (3.2), (3.5) satisfies $z(u) \equiv 0$ and $y(u) > 0$ for every $u \in (0, u_1)$; see Proposition 3.4.4. Consequently, the value τ for which $y(\tau) = z(\tau) = 0$ must be $\tau = u_1$. Hence, $u_1(\Upsilon(0)) = \tau(\Upsilon(0))$.

We now claim that $\lim_{\rho \rightarrow 1^-} \tau(\Upsilon(\rho)) = 0$. Assume by contradiction that there exists a sequence $\{\rho_n\}_n$ converging to 1 such that $\tau(\Upsilon(\rho_n)) > \epsilon$ for some $\epsilon > 0$. Let $(y_n(u), z_n(u))$ be the solutions to the system (3.2), (3.5) associated to the values $\Upsilon(\rho_n)$, and denote by $(y(u), z(u))$ the corresponding solution for $\Upsilon(1)$.

The continuity of solutions to ODEs with respect to initial conditions and parameters shows that $(y_n(u), z_n(u))$ converges pointwise to $(y(u), z(u))$. By hypothesis, we

would have that $y_n(u) - z_n(u) > 0$ for $u \in (0, \epsilon)$. Hence, $y(u) \geq z(u)$ for every $u \in [0, \epsilon]$. However, Remark 3.4.7 and (3.42) imply that $y(u) - z(u) < 0$ for $u > 0$ sufficiently small, leading to a contradiction. \square

3.7 Proof of Theorem 3.1.1

From now on, we fix $n \geq 2$ and $d := -1/n$, and consider the analytic map

$$G : (0, \infty) \times (0, \infty) \rightarrow \mathbb{R}^3$$

given by

$$G(a, b) := (a, b, c_d(a, b)),$$

where $c_d(a, b)$ is the analytic function in Proposition 3.5.3. We note that $G(a, b)$ is a parametrization of the level set $\Theta = -1/n$. We now define the curve

$$\Upsilon(b) := G(1, b) : [1, \infty) \rightarrow \mathbb{R}^3.$$

We will show that there exists some $\tilde{b} > 1$ such that $\Upsilon(b) \in \mathcal{W}$ for all $b \in [1, \tilde{b}]$ and $\Upsilon(\tilde{b})$ satisfies (3.42). To do so, we consider the auxiliary function $J(a, b, c)$ given by

$$J(a, b, c) = \mathcal{C}^2 - \frac{(\mathcal{A} - \mathcal{B})^2}{4\mathcal{A}\mathcal{B}},$$

where $(a, b, c) \in \mathcal{O}$ and $\mathcal{A}, \mathcal{B}, \mathcal{C}$ are defined in terms of these parameters by (3.4). According to the definition of J , it follows that $J > 0$ on \mathcal{W} . By (3.40), the composition $J(\Upsilon(b))$ can be written as

$$J(\Upsilon(b)) = \frac{d^2(\mathcal{B} + 1)}{2(1 - d^2)} - \frac{(\mathcal{B} - 1)^2}{4\mathcal{B}},$$

where $\mathcal{B} = \frac{1}{2}(b + b^{-1})$. Note that $J(\Upsilon(1)) = d^2/(1 - d^2) > 0$. Moreover, since $d^2 < 1$, we have

$$\frac{d^2}{2(1 - d^2)} < \frac{1}{4},$$

and we deduce that

$$\lim_{b \rightarrow \infty} J(\Upsilon(b)) = \lim_{\mathcal{B} \rightarrow \infty} \frac{d^2(\mathcal{B} + 1)}{2(1 - d^2)} - \frac{(\mathcal{B} - 1)^2}{4\mathcal{B}} = -\infty.$$

As a consequence, there exists some $\tilde{b} > 1$ verifying $J(\Upsilon(\tilde{b})) = 0$ and $J(\Upsilon(b)) > 0$ for all $b \in [1, \tilde{b})$. In other words, $\Upsilon(b) \in \mathcal{W}$ for all $b \in [1, \tilde{b})$ and $\Upsilon(\tilde{b}) =: (1, b_1, c_1) \notin \mathcal{W}$ satisfies (3.42). Applying Proposition 3.6.5 we deduce the existence of some $b^* \in (1, \tilde{b})$ such that $f(b) = u^*(\Upsilon(b)) - \tau(\Upsilon(b))$ changes sign at $b = b^*$. In particular, $u^*(\Upsilon(b^*)) = \tau(\Upsilon(b^*))$.

Let $(1, b^*, c^*) := \Upsilon(b^*) = G(1, b^*)$, and define the function

$$F(a, b) = u^*(G(a, b)) - \tau(G(a, b)).$$

This function satisfies $F(1, b^*) = 0$, and is analytic on a neighbourhood of $(1, b^*)$ since the maps u^*, τ are analytic at $(1, b^*, c^*)$; see Proposition 3.4.5 and Lemma 3.6.1. The fact that $b \mapsto F(1, b)$ changes sign at $b = b^*$ implies, by Lojasiewicz's Structure Theorem [52, Theorem 5.2.3], the existence of an analytic curve

$$C(\eta) := (a(\eta), b(\eta)) : [0, \varepsilon) \rightarrow \mathbb{R}^2$$

such that $C(0) = (1, b^*)$, with $F(C(\eta)) \equiv 0$ and $a(\eta) > 1$ for every $\eta \in (0, \varepsilon)$.

For each $\eta \in [0, \varepsilon)$, let $\Sigma(\eta)$ denote the complete $H = 1/2$ surface Σ of Definition 3.2.4 associated to the values $(a, b, c) = G(C(\eta))$. Also, as in Definition 3.6.2, we define $\Sigma_0(\eta)$ as the restriction of $\Sigma(\eta)$ to $[-u^*(\eta), u^*(\eta)] \times \mathbb{R}$, where $u^*(\eta) := u^*(G(C(\eta)))$. We will also denote $\tau(\eta) := \tau(G(C(\eta)))$. From this construction we can deduce the following assertions:

1. $\Sigma_0(\eta)$ is a compact $H = 1/2$ annulus once we identify $(u, v) \sim (u, v + 2n\sigma)$, where $\sigma = \sigma(G(C(\eta)))$. Moreover, $\Sigma_0(\eta)$ intersects orthogonally a sphere $\mathbb{S}^2 = \mathbb{S}^2(\eta)$ of some radius $R(\eta) > 0$ along $\partial\Sigma_0(\eta)$. This follows from Proposition 3.6.3. The fact that the angle of intersection θ between $\Sigma_0(\eta)$ and $\mathbb{S}^2(\eta)$ along the boundary is $\pi/2$ is a consequence of the condition $\tau(\eta) = u^*(\eta)$ satisfied by $\Sigma_0(\eta)$, which implies that $y(u^*) = z(u^*)$.
2. $\Sigma(0)$ is the universal cover of a nodoid. This follows from the discussion in Section 3.2.3 and the fact that $C(0) = (1, b^*)$. In particular, the annulus $\Sigma_0(0)$ is rotational.
3. If $\eta > 0$, $\Sigma_0(\eta)$ has a prismatic symmetry group of order $4n$. This follows directly from Proposition 3.6.3.
4. The family of compact annuli $\{\Sigma_0(\eta) : \eta \in [0, \varepsilon)\}$ is real analytic in terms of η . This is immediate from the analytic nature of the construction.

We will now prove that, maybe for a smaller $\varepsilon_0 > 0$, every annulus $\Sigma_0(\eta)$ with $\eta \in [0, \varepsilon_0)$ is contained in the ball $B = B(\eta)$ of \mathbb{R}^3 bounded by the sphere $\mathbb{S}^2(\eta)$, and is embedded.

To start, let $\psi_\eta(u, v) : I_\eta \times \mathbb{R} \rightarrow \mathbb{R}^3$, where $I_\eta := [-u^*(\eta), u^*(\eta)]$, denote our usual parametrization of the compact annulus $\Sigma_0(\eta)$; see Definition 3.6.2. Recall that, by Proposition 3.6.3, ψ_η is periodic in the v -direction, with a fundamental period $2n\sigma$ for some $\sigma = \sigma(\eta) = \sigma(G(C(\eta))) > 0$. Therefore, we will view $\psi_\eta(u, v)$ as a parametrization of $\Sigma_0(\eta)$ defined on $I_\eta \times \mathbb{S}^1$ after the identification $(u, v) \sim (u, v + 2n\sigma)$.

Claim 3.7.1. $\psi_0 : I_0 \times \mathbb{S}^1 \rightarrow \Sigma(0)$ is an injective parametrization of the embedded free boundary nodoid $\mathfrak{N}(c^*) \subset \Sigma(0)$ of Definition 3.2.8, where $c^* = c_d(1, b^*)$.

Proof. Recall from Section 3.2.3 that every curve $v \mapsto \psi_0(u_0, v)$ parametrizes a horizontal circle of the rotational surface $\Sigma(0)$. Since, by construction, the period map Θ on $\Sigma(0)$ is equal to $-1/n$, it follows from Proposition 3.6.3 that the rotation index of the planar geodesic $\psi(0, v) : \mathbb{S}^1 \rightarrow \{x_3 = 0\}$ is -1 . Therefore, for any $u_0 \in I_0$ we have that the closed curve $v \in \mathbb{S}^1 \mapsto \psi(u_0, v)$ is injective.

From now on, let us denote by Σ the nodoid $\Sigma(0)$. Also, we denote $\Sigma_0 := \Sigma_0(0)$ and $u^* := u^*(0) = \tau(0)$. Our goal will be to prove that u^* coincides with the free boundary value $\bar{u} > 0$ defined in Section 3.2.3. This will show that ψ_0 is an injective parametrization of $\mathfrak{N}(c^*)$, as stated.

Following the discussion in Section 3.2.3, the profile curve of the nodoid Σ is given by $u \mapsto \psi(u, 0)$. The curvature of this curve is $\kappa_1 = e^{-\omega} \cosh \omega$, where we recall that $\omega = \omega(u)$ depends only on u . We note that κ_1 is strictly decreasing on the interval $u \in [0, \hat{u}]$ and reaches its minimum at $u = \hat{u}$. This can be used to show that $u^* < \hat{u}$, as follows. First, by the definition of $u^* = \tau$, for every $u \in (0, \hat{u}]$ we have that $y(u) \geq z(u)$; see Proposition 3.4.5. Moreover, since $b^* > 1$, we have $z(u) > 0$ when restricted to that interval. As a consequence, by (3.7b),

$$\omega_u(u) = y(u) \cosh \omega + z(u) \sinh \omega \geq z(u)(\cosh \omega + \sinh \omega) = z(u)e^\omega > 0$$

for every $u \in (0, \hat{u}]$. Consequently, $\omega(u)$ is strictly increasing on an open interval \mathcal{J} containing $(0, u^*]$, which means that $\kappa_1(u)$ is strictly decreasing on \mathcal{J} . Thus $u^* < \hat{u}$.

According to Proposition 3.6.3, the fact that $u^* = u^*(0) = \tau(0)$ implies geometrically that the tangent line to the profile curve $\psi(u, 0)$ at the point $\psi(u^*, 0)$ passes through the intersection point of the rotation axis of the nodoid and the plane $\{x_3 = 0\}$.

We know that there is a unique $\bar{u} \in (0, \hat{u})$ satisfying this property (see Section 3.2.3), so \bar{u} must coincide with u^* . This completes the proof of the claim. \square

As a consequence of Claim 3.7.1, the compact CMC annulus $\Sigma_0(0) = \mathfrak{N}(c^*)$ is embedded and contained in the ball B_0 bounded by the sphere \mathbb{S}_0^2 where $\partial\Sigma_0(0)$ is contained. By the real analyticity of the family of compact annuli $\{\Sigma_0(\eta)\}_\eta$ we deduce that, for $\varepsilon_0 > 0$ small enough and any $\eta \in [0, \varepsilon_0)$, the annulus $\Sigma_0(\eta)$ is also embedded and contained in the ball B_η bounded by \mathbb{S}_η^2 .

Finally, for any $\eta \in [0, \varepsilon_0)$, let Ψ_η denote the homothety and translation of \mathbb{R}^3 that sends the sphere B_η to the unit ball \mathbb{B}^3 of \mathbb{R}^3 . Then, $\mathbb{A}_n(\eta) := \Psi_\eta(\Sigma_0(\eta))$ is an embedded free boundary CMC annulus in \mathbb{B}^3 with all the properties listed in Theorem 3.1.1. This completes the proof.

3.8 Final notes

The existence of the family $\mathbb{A}_n(\eta)$ of non-rotational embedded free boundary CMC annuli of Theorem 3.1.1 can be seen as a bifurcation of certain embedded free boundary nodoids in \mathbb{B}^3 . The bifurcation of complete nodoids in \mathbb{R}^3 was studied by Mazzeo and Pacard in [58], where they showed the existence of bifurcation branches of the family of nodoids in \mathbb{R}^3 that give rise to complete, properly immersed, cylindrically bounded CMC annuli in \mathbb{R}^3 with a finite symmetry group. Our annuli $\mathbb{A}_n(\eta)$ come, after a homothety, from compact pieces of complete $H = 1/2$ annuli with the same properties than the Mazzeo-Pacard examples. However, they are different, since they have different symmetry groups. We do not know if the Mazzeo-Pacard examples in [58] possess some compact portion that has free boundary in a ball of \mathbb{R}^3 .

Our construction gives a sequence of mean curvature values $\{H_n\}_n$ for which the embedded free boundary nodoid in \mathbb{B}^3 with mean curvature $H_n > 0$ bifurcates into our family of CMC annuli $\mathbb{A}_n(\eta)$. In that bifurcation, the free boundary condition is preserved, but the constant mean curvatures of the annuli $\mathbb{A}_n(\eta)$ are not equal to H_n , in general. The bifurcation values H_n tend to ∞ as $n \rightarrow \infty$ and can be estimated numerically following the construction process described in this chapter. We omit the details of this numerical estimation, since it is a bit involved, and not fundamental to our study.

It remains open to show if for any $H > 0$ there exists a non-rotational, embedded free boundary annulus in \mathbb{B}^3 with constant mean curvature H . We remark nonetheless that our construction does not work for $H = 0$. Indeed, it was shown in [29] that the only embedded free boundary minimal annulus in \mathbb{B}^3 foliated by spherical curvature

lines is the critical catenoid.

We also note that, if n is even, the annuli $\mathbb{A}_n(\eta)$ are symmetric with respect to three orthogonal planes of \mathbb{R}^3 . Thus, McGrath's characterization of the critical catenoid among embedded free boundary minimal annuli in \mathbb{B}^3 with three orthogonal symmetry planes (see [59]) does not hold in the general CMC case.

It seems interesting, in the view of Theorem 3.1.1, to update Wente's uniqueness problem as follows:

Open problem 3.8.1. *Does every embedded free boundary CMC annulus in \mathbb{B}^3 have a family of spherical curvature lines?*

Note that this seems to be the natural extension to the CMC case of the critical catenoid conjecture.

Our deformation process does not work in the embedded case if we try to bifurcate from a free boundary unduloid in \mathbb{B}^3 . However, it does work when we consider, for nodoids, the *free boundary bulges* instead of the *free boundary necks*; see Figure 3.4. In other words, each nodoid N in \mathbb{R}^3 has a compact embedded annular piece $\Sigma_1 \subset N$ that intersects a ball B orthogonally along its boundary, so that Σ lies in the *exterior* of B , and we take that compact piece as our starting surface. The proof we presented about the existence of non-rotational embedded free boundary CMC annuli in \mathbb{B}^3 can be easily adapted then to prove that an analogous result follows for embedded free boundary CMC annuli in the exterior of the unit ball; see Figure 3.5.

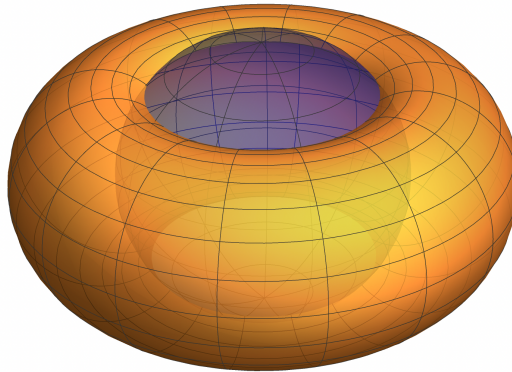


Figure 3.4: A free boundary nodoid *outside* the unit ball.

Theorem 3.8.2. *For every $n \geq 2$ there exist non-rotational compact embedded CMC annuli Σ with a prismatic symmetry group of order $4n$, that are contained in $\mathbb{R}^3 \setminus \mathbb{B}^3$, and intersect \mathbb{B}^3 orthogonally along $\partial\Sigma$.*

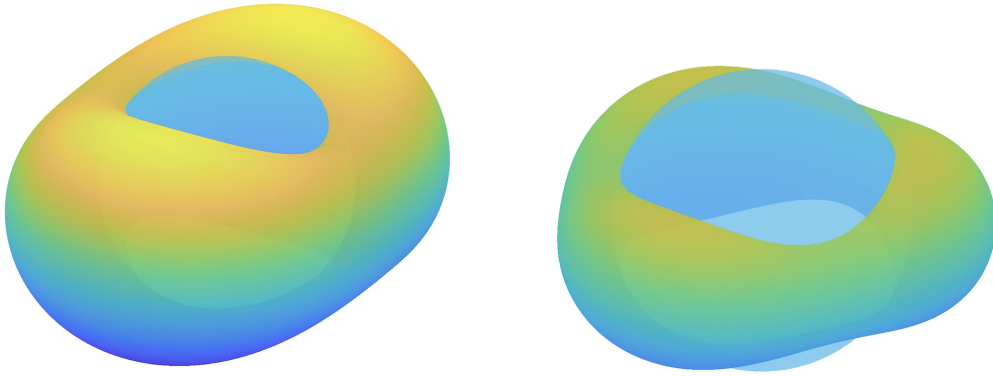


Figure 3.5: Examples of non-rotational free boundary CMC annuli of Theorem 3.8.2 with $n = 2$ (left) and $n = 3$ (right).

There is a simpler version of our construction procedure, in which we merely ask the curvature lines associated to the smallest principal curvature κ_2 to be *planar* instead of *spherical*. This is equivalent to imposing the condition $y(u) \equiv 0$ in our previous process. With that ansatz, we can no longer produce CMC annuli with spherical boundaries (unless they are rotational), but we can certainly produce them with planar boundaries. This suggests the possibility of finding embedded free boundary CMC annuli in the slab of \mathbb{R}^3 determined by two parallel planes. However, an easy application of Alexandrov's reflection principle (see [77]) shows that such examples do not exist. Yet, inspired by Theorem 3.8.2, one can ask whether there exist embedded free boundary CMC annuli in \mathbb{R}^3 such that $\partial\Sigma$ is contained in two parallel planes P_1, P_2 , and Σ intersects these planes orthogonally along $\partial\Sigma$. In such a case, Σ would not be contained in the slab between P_1 and P_2 . This simplified version of our construction works perfectly, with more explicit, direct computations, and the resulting CMC annuli can be seen, again, as bifurcations of suitable embedded compact pieces of nodoids of \mathbb{R}^3 . Nonetheless, we do not include here this construction, as these examples were already known in the literature. They had been constructed by Grosse-Brauckmann and He [39] using the conjugate Plateau technique, starting from adequate solutions to the Plateau problem for minimal surface in the 3-sphere \mathbb{S}^3 , and then using the Lawon correspondence to induce these examples into CMC surfaces in \mathbb{R}^3 .

Chapter 4

Free boundary minimal and CMC annuli in geodesic balls of space forms

4.1 Summary and main result

In this chapter we construct, for any $H \geq 0$, infinitely many free boundary annuli in geodesic balls of \mathbb{S}^3 with constant mean curvature H and a discrete, non-rotational, prismatic symmetry group. Some of these free boundary CMC annuli are actually embedded if $H \geq 1/\sqrt{3}$. We also construct embedded, non-rotational, free boundary CMC annuli in geodesic balls of \mathbb{H}^3 , for all values $H > 1$ of the mean curvature H . All these examples are of Enneper type in \mathbb{H}^3 or \mathbb{S}^3 . This chapter is based on [16].

We will use the model $\mathbb{M}^3(\kappa)$ introduced in Section 2.5.1 to work with the space forms $\mathbb{S}^3 = \mathbb{M}^3(1)$ and $\mathbb{H}^3 = \mathbb{M}^3(-1)$. We now state the main results of this chapter:

Theorem 4.1.1. *Let $H \geq 0$, $\kappa \in \{-1, 1\}$. Then, there exists an open interval $\mathcal{J} = \mathcal{J}(H, \kappa)$ contained in $(0, 1)$ such that, for any irreducible $q = m/n \in \mathcal{J} \cap \mathbb{Q}$, there exists a real analytic 1-parameter family $\{\mathbb{A}_q(\eta) : \eta \in [0, \varepsilon_0(q))\}$ of compact annuli in $\mathbb{M}^3(\kappa)$ with the following properties:*

1. *Each annulus $\mathbb{A}_q(\eta)$ has constant mean curvature H , and has free boundary in a geodesic ball $\mathbf{B} = \mathbf{B}(q, \eta) \subset \mathbb{M}^3(\kappa)$ centered at $\mathbf{e}_4 = (0, 0, 0, 1) \in \mathbb{M}^3(\kappa)$.*
2. *$\mathbb{A}_q(\eta)$ is symmetric with respect to the totally geodesic surface $\mathbf{S} := \mathbb{M}^3(\kappa) \cap \{x_3 = 0\}$.*
3. *The closed geodesic $\mathbf{S} \cap \mathbb{A}_q(\eta)$ of $\mathbb{A}_q(\eta)$ has rotation index $-m$ in \mathbf{S} .*

4. $\mathbb{A}_q(0)$ is a finite m -cover of a compact embedded piece of a rotational surface in $\mathbb{M}^3(\kappa)$.
5. If $\eta > 0$, then $\mathbb{A}_q(\eta)$ is not rotational, and its symmetry group is generated by the symmetry with respect to \mathbf{S} and the symmetries with respect to $n > 1$ equiangular totally geodesic surfaces of $\mathbb{M}^3(\kappa)$ orthogonal to \mathbf{S} . That is, the symmetry group of $\mathbb{A}_q(\eta)$ is prismatic of order $4n$.
6. Each annulus $\mathbb{A}_q(\eta)$ is of Enneper type; see Definition 2.5.4.

Under additional restrictions on the mean curvature, we can control the embeddedness of some of the examples in the previous theorem.

Theorem 4.1.2. *Assume in Theorem 4.1.1 that $\kappa = -1$ or that $\kappa = 1$ and $H \geq 1/\sqrt{3}$. Then, there exist elements in $\mathcal{J} \cap \mathbb{Q}$ of the form $q = 1/n$, and for any such q , the free boundary H -annuli $\mathbb{A}_q(\eta)$ are embedded, for η sufficiently small. When $\kappa = -1$, it actually holds $1/n \in \mathcal{J}$ for any $n \geq 2$.*

Organization of the chapter

The strategy to prove Theorems 4.1.1 and 4.1.2 is inspired by the construction of free boundary CMC annuli in \mathbb{R}^3 detailed in Chapter 3. We will start by constructing a family of immersions $\psi(u, v) : \mathbb{R}^2 \rightarrow \mathbb{M}^3(\kappa)$ with constant mean curvature H (with $H > 1$ if $\kappa = -1$) of Enneper type; see Definition 2.5.4. These surfaces will depend on three real parameters (a, b, c) , obtained through special solutions of the sinh-Gordon equation. Apart from being foliated by spherical curvature lines, these surfaces also satisfy $\psi(-u, v) = \Phi(\psi(u, v))$, where Φ denotes the symmetry with respect to the totally geodesic surface $\mathbb{M}^3(\kappa) \cap \{x_3 = 0\}$. The proof of Theorems 4.1.1 and 4.1.2 is then based on proving that there exist parameter values (a, b, c) such that:

1. ψ is periodic in the v -direction, and so ψ covers an annulus.
2. There exists $u_0 > 0$ such that $\theta(u_0) = \pi/2$ and $\mathcal{Q}(u_0)$ is a sphere invariant by Φ .
3. The annulus $\psi([-u_0, u_0] \times \mathbb{S}^1) \subset \mathbb{M}^3(\kappa)$ lies in the geodesic ball \mathbf{B} of $\mathbb{M}^3(\kappa)$ bounded by $\mathcal{Q}(u_0)$, and so, because of the properties above, it is a free boundary annulus in \mathbf{B} .

The idea of the proof will be to *bifurcate* from free boundary rotational examples (critical catenoids or nodoids) within the family associated to the (a, b, c) -parameters, to create some non-rotational examples, and to control their embeddedness.

Let us remark that there appear however several sources of complication in the process when we consider \mathbb{S}^3 or \mathbb{H}^3 instead of \mathbb{R}^3 as our ambient space, and their resolution requires new ideas. For instance, we cannot use the Weierstrass representation of minimal surfaces as in [29]. And, in contrast with the \mathbb{R}^3 case studied in Chapter 3, in our spherical or hyperbolic setting we do not have an explicit expression for the *period map* that controls the periodicity of the spherical curvature lines of our examples. Moreover, we cannot use CMC surfaces with *planar* curvature lines as a limit in order to control the centers of the spherical curvature lines, as we did in Chapter 3 for the Euclidean case, since such surfaces do not exist in \mathbb{S}^3 or \mathbb{H}^3 .

We next explain the basic steps of the proof.

In Section 4.2, we recall our construction in Chapter 3 of some special solutions to an overdetermined problem for the sinh-Gordon equation. This equation can be viewed as the Gauss equation of a CMC surface in \mathbb{S}^3 or \mathbb{H}^3 parametrized by curvature lines (with $H > 1$ in \mathbb{H}^3). Hence, these solutions yield complete CMC surfaces in $\mathbb{M}^3(\kappa)$ foliated by spherical curvature lines. Along such curvature lines, the surface intersects the corresponding totally umbilic surface at a constant angle, by Joachimsthal's theorem. In this way, we end up with a family of conformal CMC immersions $\psi(u, v) : \mathbb{R}^2 \rightarrow \mathbb{M}^3(\kappa)$ parametrized by curvature lines, which depends on three parameters (a, b, c) , and so that the curves $v \mapsto \psi(u, v)$ are spherical.

In Section 4.3 we study the geometry of the immersions $\psi(u, v)$. We prove that they are symmetric with respect to a *horizontal* totally geodesic surface $\mathbf{S} \subset \mathbb{M}^3(\kappa)$ and with respect to a number of *vertical* totally geodesic surfaces $\Omega_j \subset \mathbb{M}^3(\kappa)$ that, in adequate conditions, intersect along a vertical geodesic of $\mathbb{M}^3(\kappa)$ that contains all the *centers* of the totally umbilic surfaces where the spherical curvature lines $v \mapsto \psi(u, v)$ of the immersion lie.

Next, in Section 4.4, we define a real analytic *period map* $\Theta(a, b, c)$ with the property that, when $\Theta(a, b, c) = m/n \in \mathbb{Q}$, the spherical curvature lines $v \mapsto \psi(u, v)$ are periodic curves with rotation index m , while n gives the number of vertical symmetry surfaces Ω_j . In particular, when $\Theta(a, b, c) = m/n$, the restriction of ψ to $[-u_0, u_0] \times \mathbb{R}$ covers a CMC annulus $\Sigma_0 = \Sigma_0(a, b, c, u_0)$ in $\mathbb{M}^3(\kappa)$ that intersects with a constant angle two (isometric) totally umbilic surfaces of $\mathbb{M}^3(\kappa)$. This property is studied in Section 4.5.

In Section 4.6 we will show that, when $a = 1$, the immersion $\psi(u, v)$ parametrizes a compact piece of a rotational CMC surface. More specifically, of either a nodoid (in \mathbb{H}^3), or a nodoid, a (spherical) catenoid or a flat torus in \mathbb{S}^3 . The parameter c will control the necksize of this example. The parameter b is needed to account for the fact

that, in the rotational case, each curve $v \mapsto \psi(u, v)$ is a circle, and so there is a priori an infinite number of totally umbilic surfaces in $\mathbb{M}^3(\kappa)$ that contain it. The parameter b determines a choice for such umbilic surfaces.

In Section 4.7 we will give an explicit expression for the period map $\Theta(1, b, c)$ in the case $a = 1$ that allows for a good control on the periodicity of the parametrized curvature lines $v \mapsto \psi(u, v)$, which in this $a = 1$ case are merely circles.

In Section 4.8 we will restrict to a certain *free boundary region* of our parameter space, and control there, also for the case $a = 1$, the situation in which $\Sigma_0(1, b, c, u_0)$ covers a critical catenoid or nodoid in $\mathbb{M}^3(\kappa)$. We will show that these rotational free boundary surfaces must appear along certain curves of the parameter domain in that $a = 1$ case.

In Section 4.9 we prove Theorems 4.1.1 and 4.1.2. For that we use our study of the rotational $a = 1$ case in the previous sections in what regards the free boundary annulus structure of the examples, and induce it to the non-rotational $a > 1$ case. The embeddedness is obtained for values of the period $\Theta(a, b, c)$ of the form $-1/n$, with $a > 1$ close to 1.

Finally, in Section 4.10 we use some of the analysis of the previous sections to construct embedded capillary CMC surfaces in geodesic balls of \mathbb{S}^3 , for all values of H .

4.2 A family of Enneper-type surfaces in $\mathbb{M}^3(\kappa)$

The goal of this section is to define a family of CMC $H \geq 0$ surfaces of Enneper type in the space forms $\mathbb{M}^3(\kappa)$, where $\kappa \in \{-1, 1\}$, satisfying the additional property that $H^2 + \kappa > 0$. According to Theorem 2.5.8, these surfaces can be defined in terms of solutions $\rho(u, v)$ to the overdetermined system (2.14) for some constant $Q > 0$. The assumption that $H^2 + \kappa$ is positive allows to reduce (2.14) to the sinh-Gordon system in (3.7), as we will see in Lemma 4.2.1. We recall that in Section 3.2.1, we already constructed a wide family of solutions to the sinh-Gordon overdetermined system depending on three parameters $(a, b, c) \in \mathcal{O}$, where $\mathcal{O} \subset \mathbb{R}^3$ is given by (3.3).

Lemma 4.2.1. *Let $H \geq 0$, $\kappa \in \{-1, 1\}$ such that $H^2 + \kappa > 0$, and $\mu := \sqrt{H^2 + \kappa}$. For any $(a, b, c) \in \mathcal{O}$, let $(y(u), z(u))$ be the solution to (3.2), (3.5), where \mathcal{O} is given by (3.3), denote by $\omega(u, v) = \omega(u, v; a, b, c)$ the corresponding function in Definition 3.2.1. Then,*

$$\rho(u, v) := \omega(u, v) - \log(2\mu) \quad (4.1)$$

satisfies the overdetermined system

$$\Delta\rho + \mu^2 e^{2\rho} - \frac{1}{16\mu^2} e^{-2\rho} = 0, \quad (4.2a)$$

$$2\rho_u = \alpha(u)e^\rho + \frac{1}{2\mu}\beta e^{-\rho}, \quad (4.2b)$$

where $(\alpha(u), \beta(u))$ are given by

$$\alpha(u) = 2\mu(y(u) + z(u)), \quad \beta(u) = y(u) - z(u). \quad (4.3)$$

Proof. The proof is straightforward using (3.7): indeed, by (3.7a),

$$\Delta\rho = \Delta\omega = -\frac{1}{4}e^{2\omega} + \frac{1}{4}e^{-2\omega} = -\mu^2 e^{2\rho} + \frac{1}{16\mu^2} e^{-2\rho},$$

proving (4.2a). A similar argument using (3.7b) and (4.3) shows (4.2b). \square

We observe that (4.2) coincides with the system (2.14) for $A = H^2 + \kappa > 0$, $Q = \frac{1}{4\mu}$. Thus, by Theorem 2.5.8, for every $(a, b, c) \in \mathcal{O}$, the function $\rho(u, v) = \rho(u, v; a, b, c)$ in the previous lemma induces a CMC $H \geq 0$ surface $\psi(u, v) : \mathbb{R}^2 \rightarrow \mathbb{M}^3(\kappa)$ in the space form $\mathbb{M}^3(\kappa)$, which is unique once we fix the initial conditions (2.32) for $\psi(u, v)$. This surface is of Enneper type (see Definition 2.5.4) and has no umbilical points. The first and second fundamental forms of the immersion are given by

$$I = e^{2\rho}(du^2 + dv^2), \quad II = \left(He^{2\rho} + \frac{1}{4\mu}\right)du^2 + \left(He^{2\rho} - \frac{1}{4\mu}\right)dv^2. \quad (4.4)$$

In particular, the principal curvatures κ_1, κ_2 associated to the u and v -curves satisfy

$$\kappa_1 = H + \frac{1}{4\mu}e^{-2\rho}, \quad \kappa_2 = H - \frac{1}{4\mu}e^{-2\rho}. \quad (4.5)$$

Definition 4.2.2. We denote by $\Sigma = \Sigma(a, b, c)$ the surface given by the immersion $\psi(u, v)$ associated to system (4.2) satisfying the initial conditions (2.32).

Remark 4.2.3. It is clear from (4.1) that $\rho(u, v; a, b, c)$ inherits the same symmetry properties as the function $\omega(u, v; a, b, c)$ constructed in Section 3.2.1, that is,

$$\rho(u, v) = \rho(-u, v) \quad (4.6)$$

as well as

$$\rho(u, j\sigma + v) = \rho(u, j\sigma - v) \quad (4.7)$$

for all $j \in \mathbb{Z}$, where $\sigma = \sigma(a, b, c)$ is the value in Proposition 3.3.1; see also (3.13), (3.18).

We finally note that, as a consequence of Remark 3.2.2, the proof of Proposition 3.3.1 and (4.1), the function $v \mapsto \rho(0, v)$ is either the constant $\rho(0, v) \equiv -\log(2\mu c)$ (if $a = 1$) or attains its critical values only at the points $v = j\sigma$, $j \in \mathbb{Z}$ (when $a > 1$).

According to Proposition 2.5.6 and (4.2b), every v -line $v \mapsto \psi(u, v)$ of $\psi(u, v)$ lies in a totally umbilical surface $\mathcal{Q}(u) \subset \mathbb{M}^3(\kappa)$, $\mathcal{Q}(u) = S[\tilde{m}(u), \tilde{d}(u)]$. The values $\tilde{m}(u)$, $\tilde{d}(u)$ and the intersection angle $\theta(u)$ between $\psi(u, v)$ and $\mathcal{Q}(u)$ are related to the pair $(\alpha(u), \beta(u))$ by (2.35) and

$$\tilde{m}(u) = -2e^{-\rho}\psi_u + 2\beta N + (\alpha + 2H\beta)\psi. \quad (4.8)$$

We also recall that the pair $(\tilde{m}(u), \tilde{d}(u))$ is defined up to a common multiplicative constant. In fact, whenever the surface $S[\tilde{m}(u), \tilde{d}(u)]$ is a sphere, $\tilde{m}(u)$ admits a rescaling $m(u)$ which belongs to $\mathbb{M}^3(\kappa)$; see Remark 2.5.3. In such a case, $m(u)$ corresponds to the geodesic center of $\mathcal{Q}(u)$. According to (4.8), $\mathcal{Q}(u)$ will be a 2-sphere if and only if

$$(\alpha(u) + 2H\beta(u))^2 + 4\kappa(1 + \beta(u)^2) > 0. \quad (4.9)$$

Observe that (4.9) holds trivially when $\kappa = 1$.

Proposition 4.2.4. *Let $u_0 \in \mathbb{R}$ such that (4.9) holds. Then, there exists a neighbourhood I of $u = u_0$ such that $\mathcal{Q}(u)$ is a 2-sphere of $\mathbb{M}^3(\kappa)$ for every $u \in I$. The geodesic center of $\mathcal{Q}(u)$ is given by the analytic map*

$$m(u) := \epsilon \frac{\tilde{m}(u)}{\sqrt{\langle \tilde{m}(u), \tilde{m}(u) \rangle_\kappa}} = \epsilon \frac{-2e^{-\rho}\psi_u + 2\beta N + (\alpha + 2H\beta)\psi}{\sqrt{(\alpha + 2H\beta)^2 + 4\kappa(1 + \beta^2)}}, \quad (4.10)$$

where $\epsilon = \text{sgn}(\alpha(u_0) + 2H\beta(u_0))$ if $\kappa = -1$. If $\kappa = 1$, ϵ can be chosen to be 1 or -1 . Moreover, let

$$\mathcal{P} := \text{span}\{\tilde{m}(0), \tilde{m}'(0)\}. \quad (4.11)$$

Then, \mathcal{P} is a plane in \mathbb{R}_κ^4 such that $\mathcal{L} := \mathcal{P} \cap \mathbb{M}^3(\kappa)$ is a geodesic of $\mathbb{M}^3(\kappa)$, and $m(u) \in \mathcal{L}$ for all $u \in I$.

Proof. It is clear by (4.9) that the function $m(u)$ in (4.10) is well defined and analytic on a neighbourhood I of $u = u_0$. We note that if $\kappa = -1$, (4.9) implies $\alpha(u_0) +$

$2H\beta(u_0) \neq 0$, so the quantity $\text{sgn}(\alpha(u_0) + 2H\beta(u_0))$ is well defined and ϵ is constantly 1 or -1 on I .

Let us now prove that $m(u) \in \mathbb{M}^3(\kappa)$. If $\kappa = 1$, this is equivalent to the condition $\langle m, m \rangle_\kappa = 1$, which clearly holds in this case. If $\kappa = -1$, we must check that $\langle m, m \rangle_\kappa = -1$ and that $m(u)$ belongs to the half-space $\{x_4 > 0\}$; see (2.29). It is immediate from (4.10) that $\langle m, m \rangle_\kappa = -1$. This implies that either $m(u)$ or $-m(u)$ belongs to $\mathbb{M}^3(\kappa)$. The fact that we set ϵ to be $\text{sgn}(\alpha + 2H\beta)$ ensures that actually $m(u) \in \mathbb{M}^3(\kappa)$. In particular, this shows that $m(u)$ is the geodesic center of $\mathcal{Q}(u)$; see Remark 2.5.3.

Let us finally show that $m(u)$ belongs to the geodesic \mathcal{L} defined above. We already proved in Proposition 2.5.10 that $\tilde{m}(u)$ in (4.8) belongs to a certain plane \mathcal{P}_0 such that $\tilde{m}(0), \tilde{m}'(0) \in \mathcal{P}_0$, so the rescaling $m(u)$ satisfies $m(u) \in \mathcal{P}_0 \cap \mathbb{M}^3(\kappa)$. We also note that by (3.5), (4.3), (4.8), the vectors $\tilde{m}(0), \tilde{m}'(0)$ are linearly independent, so \mathcal{P}_0 must necessarily coincide with the plane \mathcal{P} defined in (4.11). \square

Remark 4.2.5. *It follows from (4.10) that $m(u)$ is not only analytic with respect to u , but also with respect to the parameters $(a, b, c) \in \mathcal{O}$.*

Remark 4.2.6. *We note that the map $\tilde{m}(u)$ in (4.8) always belongs to the plane \mathcal{P} in (4.11), even if the condition (4.9) is not satisfied.*

4.3 Geometric properties of $\Sigma(a, b, c)$

Let us fix $H \geq 0$, $\kappa \in \{-1, 1\}$ and $(a, b, c) \in \mathcal{O}$, and consider the immersion $\psi(u, v)$ associated to the surface $\Sigma(a, b, c; H, \kappa)$ in Definition 4.2.2. We recall that the first and second fundamental forms of $\psi(u, v)$ are given by (4.4), where $\rho(u, v)$ is the function defined in Lemma 4.2.1. The properties of $\rho(u, v)$, studied in Remark 4.2.3, will allow us to detect the symmetries of $\psi(u, v)$.

Lemma 4.3.1. *Let $\mathbf{S} \subset \mathbb{M}^3(\kappa)$ be the totally geodesic surface*

$$\mathbf{S} := \{x_3 = 0\} \cap \mathbb{M}^3(\kappa) \tag{4.12}$$

and $\Psi_{\mathbf{S}} : \mathbb{M}^3(\kappa) \rightarrow \mathbb{M}^3(\kappa)$ denote the reflection with respect to \mathbf{S} . Then, Σ is invariant under $\Psi_{\mathbf{S}}$; specifically, it holds

$$\psi(-u, v) = \Psi_{\mathbf{S}}(\psi(u, v)). \tag{4.13}$$

In particular, the v -curve $v \mapsto \psi(0, v)$ is a geodesic of Σ which lies in \mathbf{S} .

Proof. It is an immediate consequence of (4.6), the fundamental theorem for surfaces in $\mathbb{M}^3(\kappa)$ and the expressions for the first and second fundamental forms in (4.4). \square

The surface Σ actually has more symmetries, as we will see next.

Proposition 4.3.2. *For each $j \in \mathbb{Z}$, let $\nu_j = \psi_v(0, j\sigma)$, where σ is the value defined in Proposition 3.3.1, and define $\Omega_j \subset \mathbb{M}^3(\kappa)$ as the unique totally geodesic surface orthogonal to ν_j at the point $\psi(0, j\sigma)$. Then,*

- (1) *Each Ω_j is orthogonal to the totally geodesic surface $\mathbf{S} = \mathbb{M}^3(\kappa) \cap \{x_3 = 0\}$.*
- (2) *Let $\Psi_j : \mathbb{M}^3(\kappa) \rightarrow \mathbb{M}^3(\kappa)$ be the reflection with respect to Ω_j . Then,*

$$\psi(u, v + j\sigma) = \Psi_j(\psi(u, j\sigma - v)). \quad (4.14)$$

In particular, the u -curve $u \mapsto \psi(u, j\sigma)$ lies in Ω_j .

- (3) *The angle between two consecutive vectors ν_j, ν_{j+1} does not depend on j .*
- (4) *Assume that the vectors ν_0, ν_1 satisfy*

$$\langle \nu_0, \nu_0 \rangle_\kappa \langle \nu_1, \nu_1 \rangle_\kappa > \langle \nu_0, \nu_1 \rangle_\kappa^2. \quad (4.15)$$

Then, $\Lambda := \text{span}\{\nu_j : j \in \mathbb{Z}\} \subset \mathbb{R}_\kappa^4$ is a 2-dimensional subspace, which is spacelike if $\kappa < 0$.

- (5) *Assume that (4.15) holds. Setting $\mathcal{P} = \text{span}\{\tilde{m}(0), \tilde{m}'(0)\}$, then $\mathcal{L} = \mathcal{P} \cap \mathbb{M}^3(\kappa)$ is a geodesic of $\mathbb{M}^3(\kappa)$, and in fact*

$$\mathcal{L} = \bigcap_{j \in \mathbb{Z}} \Omega_j. \quad (4.16)$$

Proof. To prove (1) recall that the v -curve $v \mapsto \psi(0, v)$ is contained in \mathbf{S} . In particular, the vectors $\nu_j = \psi_v(0, j\sigma)$ are tangent to \mathbf{S} , so the surfaces Ω_j are orthogonal to \mathbf{S} . Item (2) is a direct consequence of (4.7), the fundamental theorem of surfaces and the expressions of the fundamental forms (4.4).

Let us now prove item (3). By item (2), notice that $\nu_j = -\Psi_j(\nu_j)$ and $\nu_{j+1} = -\Psi_j(\nu_{j+1})$, where we now view $\Psi_j : \mathbb{R}_\kappa^4 \rightarrow \mathbb{R}_\kappa^4$ as an isometry in \mathbb{R}_κ^4 . Thus,

$$\langle \nu_j, \nu_{j+1} \rangle_\kappa = \langle \Psi_j(\nu_j), \Psi_j(\nu_{j+1}) \rangle_\kappa = \langle \nu_j, \nu_{j-1} \rangle_\kappa.$$

By induction, it is immediate that $\langle \nu_j, \nu_{j+1} \rangle_\kappa = \langle \nu_0, \nu_1 \rangle_\kappa$ for all j , and so the angle between two consecutive vectors ν_j, ν_{j+1} is constant.

Regarding item (4), let us define $\Lambda_0 := \text{span}\{\nu_0, \nu_1\} \subset \Lambda$. By (4.15), Λ_0 is a 2-dimensional subspace which must be spacelike if $\kappa < 0$. Now, the fact that $\nu_{j+1} = -\Psi_j(\nu_{j-1})$ implies geometrically that ν_{j+1} can be expressed as a linear combination of ν_{j-1} and ν_j . By induction, this means that actually every ν_j is spanned by $\{\nu_0, \nu_1\}$, and hence $\Lambda = \Lambda_0$.

Let us prove item (5). For each j , define $P_j \subset \mathbb{R}_\kappa^4$ as the 3-dimensional linear subspace orthogonal to ν_j . We note that $\Omega_j = P_j \cap \mathbb{M}^3(\kappa)$: indeed, totally geodesic surfaces in $\mathbb{M}^3(\kappa)$ appear as intersections of $\mathbb{M}^3(\kappa)$ with linear subspaces of dimension 3, and P_j is the unique such subspace orthogonal to ν_j . Now, a direct computation using (4.8) shows that, for each j , the vector $\nu_j = \psi_v(0, j\sigma)$ is orthogonal to both $\tilde{m}(0)$ and $\tilde{m}'(0)$. In particular,

$$\mathcal{P} \subseteq \Lambda^\perp = \bigcap_{j \in \mathbb{Z}} P_j.$$

Note that actually $\mathcal{P} = \Lambda^\perp = \bigcap_{j \in \mathbb{Z}} P_j$, since both \mathcal{P} and Λ^\perp are 2-dimensional subspaces. Hence, it follows that \mathcal{P} is timelike in the case $\kappa < 0$, so the intersection $\mathcal{L} := \mathcal{P} \cap \mathbb{M}^3(\kappa)$ is a geodesic indeed. Now, intersecting the sets \mathcal{P} and $\bigcap_{j \in \mathbb{Z}} P_j$ with $\mathbb{M}^3(\kappa)$, we see that

$$\mathcal{L} = \mathcal{P} \cap \mathbb{M}^3(\kappa) = \bigcap_{j \in \mathbb{Z}} (P_j \cap \mathbb{M}^3(\kappa)) = \bigcap_{j \in \mathbb{Z}} \Omega_j,$$

as we wanted to prove. □

The proof of the previous proposition motivates the definition of the following set.

Definition 4.3.3. *We define \mathcal{O}^- as the open set of \mathcal{O} for which (4.15) holds; see also (3.3).*

We will see later that \mathcal{O}^- is not empty; see Proposition 4.7.4.

4.4 The period map in $\mathbb{M}^3(\kappa)$

Given $H \geq 0$, $\kappa \in \{-1, 1\}$ and $(a, b, c) \in \mathcal{O}^-$, let $\Sigma = \Sigma(a, b, c)$ be the surface associated to the immersion $\psi(u, v) : \mathbb{R}^2 \rightarrow \mathbb{M}^3(\kappa)$ of Definition 4.2.2; see also Definition

4.3.3. By Lemma 4.3.1, we know that Σ intersects orthogonally the totally geodesic slice $\mathbf{S} \subset \mathbb{M}^3(\kappa)$ in (4.12) along the geodesic $\Gamma(v) := \psi(0, v)$.

Our goal in this section is to characterize the periodicity of the curve $\Gamma(v)$, and to understand its rotation index and symmetry group when it is periodic. Note that the periodicity of $\Gamma(v)$ automatically implies that all the (spherical) v -curvature lines $v \mapsto \psi(u_0, v)$ of Σ are closed. In order to do so, we will introduce a period map $\Theta(a, b, c)$ such that $\Gamma(v)$ will be closed whenever $\Theta(a, b, c)$ is a rational number; see Definition 4.4.2. This extends the period map introduced in Chapter 3 to the general context of surfaces immersed in space forms $\mathbb{M}^3(\kappa)$.

Since $(a, b, c) \in \mathcal{O}^-$, it follows from Proposition 4.3.2 that the subspace $\Lambda \subset \mathbb{R}_\kappa^4$ is two-dimensional, and it is spacelike if $\kappa = -1$. Moreover, $\Lambda^\perp = \mathcal{P}$, where \mathcal{P} is given by (4.11). Note that $\mathbf{e}_3 \in \mathcal{P}$, since $\tilde{m}(0) = -2\mathbf{e}_3$; see (2.32), (4.8), (3.5), (4.3). Also, it holds $\mathcal{P} \subset \{x_2 = 0\}$, since $\nu_0 = \psi_v(0, 0)$ is collinear with \mathbf{e}_2 by (2.32). In this way, after a linear isometry of \mathbb{R}_κ^4 that fixes $\mathbf{e}_2, \mathbf{e}_3$, we can assume that

$$\mathcal{P} = \{x_1 = x_2 = 0\}. \quad (4.17)$$

Note that this isometry changes the initial conditions for $\psi(0, 0)$ and $N(0, 0)$ in (2.32), but it does so in a real analytic way, since $\mathcal{P} = \Lambda^\perp$ and $\sigma = \sigma(a, b, c)$ is real analytic (see Proposition 3.3.1).

Remark 4.4.1. *From now on, we will use the aforementioned initial conditions for any surface $\Sigma(a, b, c)$ with $(a, b, c) \in \mathcal{O}^-$.*

We will now project the space $\mathbb{M}^3(\kappa)$ into \mathbb{R}^3 via the stereographic map φ_κ from the point $-\mathbf{e}_4$. More precisely, for every $\kappa \in \{-1, 1\}$, φ_κ is the restriction to $\mathbb{M}^3(\kappa)$ of the map

$$\varphi : \mathbb{R}^4 \cap \{x_4 > -1\} \rightarrow \mathbb{R}^3$$

given by

$$\varphi(x_1, x_2, x_3, x_4) := \left(\frac{2x_1}{1+x_4}, \frac{2x_2}{1+x_4}, \frac{2x_3}{1+x_4} \right). \quad (4.18)$$

For $\kappa = 1$, the corresponding projection φ_κ sends $\mathbb{M}^3(\kappa) \setminus \{-\mathbf{e}_4\}$ to \mathbb{R}^3 . For $\kappa = -1$, the projection sends $\mathbb{M}^3(\kappa)$ to the Euclidean 3-ball of radius 2. In any case, φ_κ is a conformal map that sends the surface \mathbf{S} to the plane $\{z = 0\}$ and the geodesic \mathcal{L} to the line $\{x = y = 0\}$, where (x, y, z) denote the usual Euclidean coordinates on \mathbb{R}^3 . In particular, since Γ lies in \mathbf{S} , the curve $\gamma := \varphi \circ \Gamma$ is a planar curve in $\{z = 0\} \subset \mathbb{R}^3$.

Definition 4.4.2. Using the above notation, we define the period map as

$$\Theta : \mathcal{O}^- \rightarrow \mathbb{R},$$

$$\Theta := \frac{1}{\pi} \int_0^\sigma \kappa_\gamma \|\gamma'\| dv, \quad (4.19)$$

where κ_γ and $\|\gamma'\|$ denote the Euclidean curvature and the norm of the tangent vector γ' , respectively, and $\sigma = \sigma(a, b, c)$ is given by Proposition 3.3.1; see also Remark 3.5.2. Note that $\pi\Theta(a, b, c)$ represents the variation of the (Euclidean) unit tangent of $\gamma(v)$ along the interval $[0, \sigma]$.

Proposition 4.4.3. The map $\Theta = \Theta(a, b, c)$ in Definition 4.4.2 is real analytic in \mathcal{O}^- .

Proof. It is an immediate consequence of the real analyticity of $\sigma = \sigma(a, b, c)$ (Proposition 3.3.1) and $\rho = \rho(u, v; a, b, c)$, together with the analytic dependence of the Gauss-Weingarten system (2.33) with respect to initial conditions. \square

We explain next the geometry of the surface Σ when its associated period is a rational number. We start by describing the geometry of the geodesic $\Gamma(v) = \psi(0, v)$.

Proposition 4.4.4. Assume that $\Theta(a, b, c) = m/n \in \mathbb{Q}$, with $n \in \mathbb{N} \setminus \{0\}$ and m/n irreducible. Then $\Gamma(v + 2n\sigma) = \Gamma(v)$. In particular $\Gamma(v)$ is a closed curve. Moreover, $\Gamma(v)$ has rotation index $m \in \mathbb{Z}$ and, if $a > 1$, a dihedral symmetry group D_n with $n \geq 2$.

Proof. Let us see first that $\gamma = \varphi \circ \Gamma$ satisfies $\gamma(v + 2n\sigma) = \gamma(v)$, where φ is given by (4.18). Consider the totally geodesic surfaces Ω_j in Proposition 4.3.2. Then, φ maps Ω_j into vertical planes Π_j containing the z -axis. Let $L_j := \Pi_j \cap \{z = 0\}$. Then $\{L_j : j \in \mathbb{Z}\}$ is a family of equiangular lines in $\{z = 0\} \equiv \mathbb{R}^2$ passing through the origin. It follows from Proposition 4.3.2 and the fact that φ is conformal that the angle between L_j and L_{j+1} coincides with the angle between $\gamma'(0)$ and $\gamma'(\sigma)$. We denote this angle by ϑ . Note that $\gamma'(j\sigma)$ is orthogonal to L_j . This implies that

$$\pi\Theta(a, b, c) = 2\pi l + \vartheta \quad (4.20)$$

for some $l \in \mathbb{Z}$. In particular, $n\vartheta \in \pi\mathbb{Z}$. By (4.14), we have

$$\gamma(j\sigma - v) = T_j(\gamma(j\sigma + v)), \quad (4.21)$$

where T_j denotes the symmetry of \mathbb{R}^2 that fixes L_j . If \mathcal{R} denotes the rotation around the origin of angle 2ϑ , then we have by (4.21) that $\gamma(v + 2\sigma) = \mathcal{R}(\gamma(v))$. From here

and $n\vartheta \in \pi\mathbb{Z}$ we obtain $\gamma(v + 2n\sigma) = \gamma(v)$. Also from (4.21) we obtain that the function $f := \|\gamma'\|\kappa_\gamma$ satisfies $f(j\sigma - v) = f(j\sigma + v)$ for all $j \in \mathbb{Z}$. Observe that this implies that

$$\Theta(a, b, c) = \frac{1}{\pi} \int_{j\sigma}^{(j+1)\sigma} \kappa_\gamma \|\gamma'\| dv.$$

From here, $\Theta(a, b, c) = m/n$ and the $2\sigma n$ -periodicity of $\gamma(v)$, it follows that the rotation index of $\gamma(v)$ is equal to m .

Finally, we determine the symmetry group of $\Gamma(v)$ when $a > 1$. In that case we know that the only critical points of the function $v \mapsto \rho(0, v)$ are those of the form $j\sigma$, $j \in \mathbb{Z}$; see Remark 4.2.3. Also, by (4.5) and since $\psi(u, v)$ intersects \mathbf{S} orthogonally along $\Gamma(v)$, we have

$$\kappa_\Gamma(v) = \kappa_2(0, v) = H - \frac{1}{4\mu} e^{-2\rho(0, v)},$$

where κ_Γ is the geodesic curvature of Γ in \mathbf{S} . Since the stereographic projection φ preserves the critical points of the geodesic curvature of regular curves (because it preserves curves of constant curvature, and hence the contact order with these curves), we deduce that $\kappa_\gamma(v)$ only has critical points at the values $v = j\sigma$, $j \in \mathbb{Z}$.

In particular, $\gamma(v)$ has a (finite) dihedral symmetry group, as it is symmetric with respect to the reflections T_1, \dots, T_n . So, its isometry group is $D_{n'}$ for some $n' \geq n$, since m/n is irreducible. If $n' > n$, there would exist some additional symmetry line L' for $\gamma(v)$ different from all L_j . So, $\Gamma(v_0 - v) = \Phi'(\Gamma(v_0 + v))$ for some $v_0 \notin \{j\sigma : j \in \mathbb{Z}\}$, where Φ' is the symmetry with respect to L' . Thus, κ_γ would have a critical point at v_0 , what is a contradiction. Hence, the symmetry group of $\gamma(v)$ is D_n , and generated by the reflections T_1, \dots, T_n .

Finally, we show that $n \geq 2$. Indeed, if $n = 1$, then all the L_j 's agree, and this contradicts that $(a, b, c) \in \mathcal{O}^-$, since the vectors ν_0, ν_1 in (4.15) would be collinear. \square

As an immediate consequence of Propositions 4.3.2 and 4.4.4, we have:

Corollary 4.4.5. *Let $(a, b, c) \in \mathcal{O}^-$ so that $\Theta(a, b, c) = m/n \in \mathbb{Q}$, where $n \in \mathbb{N} \setminus \{0\}$, with m/n irreducible. Then, $\psi(u, v + 2n\sigma) = \psi(u, v)$.*

4.5 Construction of CMC annuli in $\mathbb{M}^3(\kappa)$

Following the results in Section 4.4, given $u_0 > 0$, we define $\Sigma_0 = \Sigma_0(a, b, c; u_0)$ as the surface given by the restriction of $\psi(u, v)$ to the band $[-u_0, u_0] \times \mathbb{R}$. By Corollary

4.4.5, if $\Theta(a, b, c) = m/n \in \mathbb{Q}$, we can view Σ_0 as a compact H -annulus in $\mathbb{M}^3(\kappa)$ under the identification $(u, v + 2n\sigma) \sim (u, v)$. With this, we have our main conclusion of this section:

Theorem 4.5.1. *Let $(a, b, c) \in \mathcal{O}^-$ so that $\Theta(a, b, c) = m/n \in \mathbb{Q}$, where $n \in \mathbb{N} \setminus \{0\}$, with m/n irreducible. Then, for any $u_0 > 0$, the following properties hold for the annulus $\Sigma_0 = \Sigma_0(a, b, c; u_0)$:*

1. Σ_0 is symmetric with respect to $\mathbf{S} = \mathbb{M}^3(\kappa) \cap \{x_3 = 0\}$, and with respect to $n \geq 2$ totally geodesic surfaces $\Omega_1, \dots, \Omega_n$ of $\mathbb{M}^3(\kappa)$ that intersect equiangularly along the geodesic $\mathcal{L} = \mathbb{M}^3(\kappa) \cap \mathcal{P}$; see Proposition 4.2.4.
2. Along each boundary component $\partial\Sigma_0^i$, $i = 1, 2$, Σ_0 intersects at a constant angle θ a totally umbilic surface \mathcal{Q}_i of $\mathbb{M}^3(\kappa)$. Specifically, the intersection angle θ is the same at both components, and $\mathcal{Q}_1 = \Psi_{\mathbf{S}}(\mathcal{Q}_2)$, where $\Psi_{\mathbf{S}}$ is the symmetry of $\mathbb{M}^3(\kappa)$ with respect to \mathbf{S} .
3. Assume that $\beta(u_0) = 0$ for some $u_0 > 0$. Then $\theta = \pi/2$, i.e., $\partial\Sigma_0^i$ intersects \mathcal{Q}_i orthogonally.
4. Assume that $\tilde{m}_3(u_0) = 0$, where \tilde{m}_3 denotes the third coordinate of the map $\tilde{m}(u)$ in (4.8). Then both boundary curves of Σ_0 lie in the same totally umbilic 2-sphere \mathcal{Q} of $\mathbb{M}^3(\kappa)$.
5. If $a > 1$, the symmetry group of Σ_0 is prismatic of order $4n$, and it is generated by the symmetries in item (1). In particular, Σ_0 is not rotational.

Proof. Item (1) is a direct consequence of Proposition 4.3.2. Item (2) follows from the symmetry of Σ_0 with respect to \mathbf{S} and the fact that the boundary curves of Σ_0 correspond to the spherical curvature lines $v \mapsto \psi(\pm u_0, v)$. Item (3) is immediate by (2.35).

Regarding item (4), we first note that the surface $S[\tilde{m}(u_0), \tilde{d}(u_0)]$ is one of $\mathcal{Q}_1, \mathcal{Q}_2$. If $\tilde{m}_3(u_0) = 0$, it follows that the *center* of this \mathcal{Q}_i lies in \mathbf{S} . Since $\mathcal{Q}_1 = \Psi_{\mathbf{S}}(\mathcal{Q}_2)$ by item (2), we have $\mathcal{Q}_1 = \mathcal{Q}_2 = S[m(u_0), d(u_0)]$. We show next that $S[\tilde{m}(u_0), \tilde{d}(u_0)]$ is a totally umbilic 2-sphere if $\kappa = -1$, a property equivalent to $\tilde{m}(u_0)$ being timelike; see Remark 2.5.3. Let \mathcal{P} denote the plane in (4.11) in which \tilde{m} lies, as specified in Remark 4.2.6. Since $(a, b, c) \in \mathcal{O}^-$, \mathcal{P} is timelike, and by Proposition 4.3.2 it contains \mathbf{e}_3 . Since $\langle \tilde{m}(u_0), \mathbf{e}_3 \rangle = 0$, then $\tilde{m}(u_0)$ must be timelike, as desired.

To prove item (5), let Ψ' denote an isometry of $\mathbb{M}^3(\kappa)$ that leaves Σ_0 invariant. Under this isometry, we must have $\Psi'(\Gamma) = \Gamma$, since the points of Γ represent the

middle points of the (intrinsic) geodesics $\Omega_j \cap \Sigma_0$ of Σ_0 . Therefore, the restriction of Ψ' to \mathbf{S} is a symmetry of Γ , and hence a composition \mathcal{T} of the symmetries Ψ_j with respect to Ω_j , by Proposition 4.4.4. If Ψ' takes each boundary component of Σ_0 to itself, we deduce then that $\Psi' = \mathcal{T}$. Otherwise $\Psi' = \Psi_{\mathbf{S}} \circ \mathcal{T}$, where $\Psi_{\mathbf{S}}$ is the symmetry with respect to \mathbf{S} (note that $\Psi_{\mathbf{S}}$ interchanges the boundary components of Σ_0). This proves item (5). \square

Theorem 4.5.1 motivates the next definition and consequence.

Definition 4.5.2. *Let $(a, b, c) \in \mathcal{W}$, where \mathcal{W} is the set in (3.33), and assume that (4.9) holds for $u = \tau$, where $\tau = \tau(a, b, c)$ is the value given by Proposition 3.4.5. If $\kappa = 1$, assume further that the fourth coordinate of $m(u)$ at $u = \tau$ does not vanish. Then, we define the height map $\mathfrak{h} = \mathfrak{h}(a, b, c)$ as the analytic function*

$$\mathfrak{h}(a, b, c) := m_3(\tau(a, b, c)),$$

where m_3 denotes the third coordinate of the center map $m(u)$ in Proposition 4.2.4; see also Remark 4.2.5.

Remark 4.5.3. *We note that the map $m(u)$ is defined up to a sign in the case $\kappa = 1$; see Proposition 4.2.4. In that case, we choose ϵ in (4.10) so that $m(u)$ lies in the half-space $\{x_4 > 0\}$.*

Corollary 4.5.4. *Let $(a, b, c) \in \mathcal{O}^- \cap \mathcal{W}$ so that $\Theta(a, b, c) = m/n \in \mathbb{Q}$, where $n \in \mathbb{N} \setminus \{0\}$. Assume that $\mathfrak{h}(a, b, c) = 0$. Then, choosing $u_0 = \tau$, both boundary components of the annulus Σ_0 in Theorem 4.5.1 intersect orthogonally the same umbilic 2-sphere \mathcal{Q} of $\mathbb{M}^3(\kappa)$; see also (2.35), (4.3).*

4.6 The case $a = 1$: rotational surfaces

In this section, we will study the set of surfaces $\Sigma(a, b, c)$ in Definition 4.2.2 with $a = 1$. According to Remark 4.2.3, the function $v \mapsto \rho(0, v)$ is the constant $\rho(0, v) \equiv -\log(2\mu c)$. Therefore, $\rho_v(0, v) \equiv 0$ and by uniqueness of the solution to the Cauchy problem for (4.2b) we have that $\rho = \rho(u)$, i.e., $\rho_v(u, v) \equiv 0$. It follows then by (4.4) that the coefficients of the fundamental forms I, II for Σ only depend on u , and so Σ is invariant under a 1-parameter group of ambient isometries of $\mathbb{M}^3(\kappa)$. Moreover, each curve $v \mapsto \psi(u, v)$ is an orbit of such 1-parameter group.

In our situation, $\Gamma(v) := \psi(0, v)$ is such an orbit, which actually lies in the totally geodesic surface $\mathbf{S} \subset \mathbb{M}^3(\kappa)$ in (4.12); see Lemma 4.3.1. Since Σ intersects \mathbf{S} or-

thogonally along $\Gamma(v)$, the geodesic curvature of $\Gamma(v)$ as a curve in \mathbb{S} is given by the principal curvature $\kappa_2(0, v)$, which by (4.5) is constant, and equal to $H - \mu c^2$.

Therefore, in the case $\kappa = 1$, Σ is a rotational CMC surface in \mathbb{S}^3 . The u -curves (resp. v -curves) of Σ correspond to the \mathfrak{s} -curves (resp θ -curves) in the parametrization $\psi(\mathfrak{s}, \theta)$ of rotational surfaces of Section 2.6.1. In this way, $\psi(u, 0)$ is a profile curve of Σ . The principal curvature $\kappa_1(u)$ associated to this profile curve $\psi(u, 0)$ is always positive, by (4.5). Thus, if $H > 0$, Σ must be the universal cover of either a flat torus or a spherical nodoid of \mathbb{S}^3 ; see (2.42) and Definition 2.6.2. Similarly, if $H = 0$, Σ covers a spherical catenoid or a Clifford torus.

Remark 4.6.1. *If $a = c = 1$, then $y'(0) = 0$ by (3.5), and so $y(u) \equiv 0$. By (4.2b), (4.3) and $\rho(0) = -\log(2\mu)$, it follows that $\rho(u) \equiv -\log(2\mu)$. In particular, the principal curvatures κ_1, κ_2 in (4.5) are constant. This implies that $a = c = 1$ corresponds to the case where Σ covers a flat CMC torus in \mathbb{S}^3 .*

In the case $\kappa = -1$, we have that Σ is a *generalized* rotational surface in \mathbb{H}^3 , i.e., it is invariant by either hyperbolic, elliptic or parabolic rotations in \mathbb{H}^3 . We will be interested in the elliptic case, i.e. the case where the orbits of these rotations are (compact) circles. This happens if and only if the absolute value of the geodesic curvature of the orbits is greater than 1. That is, if and only if

$$(H - \mu c^2)^2 > 1, \quad (4.22)$$

see (4.5). Thus, if (4.22) holds for our choice of (H, c) , then Σ will be a rotational surface in \mathbb{H}^3 with constant mean curvature $H > 1$. Again, since κ_1 is positive by (4.5) and describes the geodesic curvature of the profile curve of Σ , we deduce that Σ is a hyperbolic nodoid; see (2.42) and Definition 2.6.4. An equivalent form of (4.22) is

$$H < \frac{\mu}{2} \left(c^2 + \frac{1}{c^2} \right), \quad (4.23)$$

where we have used that $\mu^2 = H^2 - 1$ if $\kappa = -1$. This motivates the following definition.

Definition 4.6.2. *We let $\mathcal{R} \subset \mathbb{R}^3$ be the open subset of $\mathcal{O} \cap \{a = 1\}$ given by*

$$\mathcal{R} := \{(1, b, c) \in \mathcal{O} : (H - \mu c^2)^2 + \kappa > 0\}.$$

We note that \mathcal{R} is just $\mathcal{O} \cap \{a = 1\}$ if $\kappa = 1$, and that the inequality defining \mathcal{R} is (4.22) if $\kappa = -1$. Thus, from the discussion above we have:

Proposition 4.6.3. *Assume that $(1, b, c) \in \mathcal{R}$. Then, $\Sigma = \Sigma(1, b, c)$ is the universal cover of the (spherical or hyperbolic) nodoid ($H > 0$) or catenoid ($H = 0$) in $\mathbb{M}^3(\kappa)$ with neck curvature given by $\kappa = H - \mu c^2$.*

Remark 4.6.4. *If $(1, b, c) \in \mathcal{R} \cap \mathcal{O}^-$, then the rotation axis of $\Sigma(1, b, c)$ is the geodesic \mathcal{L} in Proposition 4.2.4. This follows from the fact that, in this case, $\Gamma(v) = \psi(0, v)$ is a (compact) circle, and any of the symmetries described in Proposition 4.3.2 must leave the center of $\Gamma(v)$ fixed, i.e. the center lies in the intersection of the symmetry planes Ω_j . Since both the rotation axis and Ω_j are orthogonal to \mathbf{S} , we conclude from there that the rotation axis agrees with $\mathcal{L} = \cap_{j \in \mathbb{Z}} \Omega_j$.*

It follows from Proposition 4.6.3 that the parameter c determines uniquely the immersion $\psi(u, v)$ that defines $\Sigma(1, b, c)$. On the other hand, the role of the parameter b is to determine the initial values (3.5) of system (3.2). More conceptually, since $\psi(u, v)$ is rotational, each curve $v \mapsto \psi(u, v)$ is a circle that can be seen as contained in infinitely many 2-dimensional totally umbilic surfaces $S[\tilde{m}(u), \tilde{d}(u)]$ of $\mathbb{M}^3(\kappa)$. The choice of b in $\Sigma(1, b, c)$ determines the values of $\tilde{m}(u), \tilde{d}(u)$ in this description.

4.7 The period map for rotational surfaces

In this section we will assume, as in Section 4.6, that $a = 1$, and keep the same notations. Therefore, $\rho = \rho(u)$, and Σ is the rotational example of Proposition 4.6.3. In particular $\kappa_2(0, v) = H - \mu c^2$.

As explained in Section 4.6, if $\kappa = 1$, the curve $\Gamma(v) = \psi(0, v)$ is a circle in the totally geodesic surface \mathbf{S} in (4.12). If $\kappa = -1$, $\Gamma(v)$ is a curve in \mathbf{S} of constant curvature $H - \mu c^2$. This curve will be a (compact) circle if and only if (4.22) holds, i.e., if and only if $(1, b, c) \in \mathcal{R}$ (see Definition 4.6.2). We also recall that the set \mathcal{O}^- and the period map $\Theta(a, b, c)$ were introduced in Definitions 4.3.3 and 4.4.2 respectively. We prove next:

Proposition 4.7.1. *Let $(1, b, c) \in \mathcal{R} \cap \mathcal{O}^-$. Then,*

$$\Theta(1, b, c) = \frac{-\sqrt{(H - \mu c^2)^2 + \kappa}}{\mu \sqrt{1 + (b + b^{-1})c^2 + c^4}}. \quad (4.24)$$

Proof. Consider the planar curve $\gamma(v) = \varphi_\kappa(\Gamma(v))$ in Definition 4.4.2. The metric

on $S \setminus \{-e_4\}$ can be written via the inverse stereographic map φ_κ^{-1} in (4.18) as

$$\varrho(dx^2 + dy^2), \quad \varrho := \frac{1}{(1 + \frac{\kappa}{4}(x^2 + y^2))^2}, \quad (4.25)$$

where (x, y) are Euclidean coordinates in \mathbb{R}^2 . From here and (4.4), we have

$$\|\gamma'\| = \frac{e^{\rho(0,v)}}{\sqrt{\varrho}}. \quad (4.26)$$

On the other hand, by standard formulas of conformally related Riemannian metrics, the geodesic curvature κ_Γ of $\Gamma(v)$ in S , i.e., the geodesic curvature of $\gamma(v)$ with respect to the metric (4.25), is related to the Euclidean geodesic curvature κ_γ of γ by

$$\kappa_\gamma = \frac{\langle \nabla \sqrt{\varrho}, \mathbf{n} \rangle}{\sqrt{\varrho}} + \sqrt{\varrho} \kappa_\Gamma, \quad (4.27)$$

where \mathbf{n} is the unit normal of γ in \mathbb{R}^2 , and both $\nabla, \langle \cdot, \cdot \rangle$ are Euclidean. Recall that

$$\kappa_\Gamma = \kappa_2(0, v) = H - \mu c^2 < 0.$$

Since $\Gamma(v)$ is a horizontal circle, its stereographic projection $\gamma(v)$ parametrizes a circle of a certain radius $r > 0$ in the plane (or in a disk of \mathbb{R}^2 , if $\kappa = -1$), which is negatively oriented since $\kappa_\Gamma < 0$. Along $\gamma(v)$ we have

$$\sqrt{\varrho} = \frac{1}{1 + \frac{\kappa}{4}r^2}, \quad \nabla \sqrt{\varrho} = -\frac{\kappa}{2(1 + \frac{\kappa}{4}r^2)^2} \gamma(v), \quad (4.28)$$

and $\mathbf{n} = \frac{1}{r} \gamma(v)$. Then, it follows from (4.27), (4.28) and $\kappa_\gamma = -1/r$ that

$$r = \frac{2}{\kappa} \left(H - \mu c^2 \pm \sqrt{(H - \mu c^2)^2 + \kappa} \right).$$

Here, we should recall that (4.22) holds when $\kappa = -1$, since $(1, b, c) \in \mathcal{R}$. Moreover, taking into account that $r > 0$ if $\kappa = 1$ and $r \in (0, 2)$ if $\kappa = -1$, we deduce that, actually,

$$r = \frac{2}{\kappa} \left(H - \mu c^2 + \sqrt{(H - \mu c^2)^2 + \kappa} \right). \quad (4.29)$$

We now compute the value of $\Theta(1, b, c)$ using (4.19). First note that, by (4.26),

(4.28) and $e^{\rho(0,v)} = \frac{1}{2\mu c}$, we have

$$\|\gamma'\| = \frac{1 + \frac{\kappa}{4}r^2}{2\mu c}.$$

Thus using that $\kappa_\gamma = -1/r$ and (3.37), we have from (4.19) that

$$\Theta(1, b, c) = -\frac{1 + \frac{\kappa}{4}r^2}{\mu r \sqrt{1 + (b + b^{-1})c^2 + c^4}}.$$

Using (4.29) in this expression, we obtain (4.24). \square

Remark 4.7.2. For any $p_0 = (1, b, c) \in \mathcal{R} \cap \mathcal{O}^-$, $c > 1$, a straightforward computation from (4.24) shows that the partial derivative $\Theta_c(p_0)$ does not vanish. By the implicit function theorem and the analyticity of $\Theta(a, b, c)$ (Proposition 4.4.3), it follows that the level set given by $\Theta(a, b, c) = \Theta_0$, where $\Theta_0 := \Theta(p_0)$, can be locally expressed around p_0 as the graph of a real analytic function $c = c^{\Theta_0}(a, b)$.

Similarly, if $p_0 \in \mathcal{R} \cap \mathcal{O}^-$, $b > 1$, an analogous computation shows that $\Theta_b(p_0) \neq 0$, so in this case we can locally express the level set $\Theta(a, b, c) = \Theta(p_0)$ as the graph of a function $b^{\Theta_0}(a, c)$.

For the rest of this section, it will be convenient to consider the parameters (r_1, r_3) in (3.26) instead of (b, c) . We recall that r_1, r_2, r_3 in (3.26) are the roots of the polynomial $g(x)$ in (3.24). Observe that, since $a = 1$, it holds $r_1 = r_2$; see (3.26). The map $(b, c) \mapsto (r_1, r_3)$ is a diffeomorphism from $\{(b, c) : b > 1, c > 1\}$ onto $\{(r_1, r_3) : r_1 < 0, r_3 > 1\}$ which extends homeomorphically to the boundary, so we can view $\Theta(1, b, c)$ as a map $\Theta(r_1, r_3)$. Using (3.26) and $\mu^2 = H^2 + \kappa$, the expression for $\Theta = \Theta(r_1, r_3)$ in (4.24) simplifies to

$$\Theta(r_1, r_3)^2 = \frac{\mu(2r_3 - 1) - H}{2\mu(r_3 - r_1)}. \quad (4.30)$$

This can be rewritten alternatively as

$$r_3 = \frac{\Theta^2}{\Theta^2 - 1}r_1 + \frac{H + \mu}{2\mu(1 - \Theta^2)} \quad (4.31)$$

For any fixed $\Theta = \Theta_0$, this equation represents the line with slope $\Theta_0^2/(\Theta_0^2 - 1)$ that passes through the point

$$p_0 := \left(\frac{H + \mu}{2\mu}, \frac{H + \mu}{2\mu} \right). \quad (4.32)$$

As an immediate consequence of (4.24) and (4.30), we have:

Corollary 4.7.3. $\Theta(1, b, c) \in (-1, 0)$ for any $(1, b, c) \in \mathcal{R} \cap \mathcal{O}^-$.

We next show that in Proposition 4.7.1 we can simply assume $(1, b, c) \in \mathcal{R}$.

Proposition 4.7.4. $\mathcal{R} \subset \mathcal{O}^-$.

Proof. Let $(1, b, c) \in \mathcal{R}$. Then, $\Sigma(1, b, c)$ is a rotational surface in $\mathbb{M}^3(\kappa)$ whose rotation axis is orthogonal to \mathbf{e}_2 . After a linear isometry of \mathbb{R}_κ^4 that fixes $\mathbf{e}_2, \mathbf{e}_3$, we can assume that this rotation axis is $\mathbb{M}^3(\kappa) \cap \{x_1 = x_2 = 0\}$. We now consider, as we did in Section 4.4, the stereographic projection φ_κ of $\mathbb{M}^3(\kappa)$ from $-\mathbf{e}_4$ to \mathbb{R}^3 , and the planar curve $\gamma(v) := \varphi_\kappa(\Gamma(v))$. Define next the number

$$\widehat{\Theta} := \frac{1}{\pi} \int_0^\sigma \kappa_\gamma ||\gamma'||| dv,$$

just as in (4.19). We use here the new notation $\widehat{\Theta}$, since Θ in (4.19) was only defined on \mathcal{O}^- ; nonetheless, the right hand side of (4.19) makes sense in our case. Moreover, the computations in Proposition 4.7.1 show that $\widehat{\Theta}$ is also given by the right hand side of (4.24).

In order to show that $(1, b, c) \in \mathcal{O}^-$ we must prove first that the vectors $\{\nu_0, \nu_1\}$ are linearly independent; see Definition 4.3.3. If ν_1 were collinear to ν_0 , then $\widehat{\Theta}$ would be an integer, since $\pi\widehat{\Theta}$ measures the variation of the unit tangent of $\gamma(v)$ along $[0, \sigma]$. But on the other hand, the computations in Corollary 4.7.3 using that $\widehat{\Theta}$ is given by (4.24) show that $\widehat{\Theta} \in (-1, 0)$. This shows that $(1, b, c) \in \mathcal{O}^-$ if $\kappa = 1$. In the case $\kappa = -1$, we also need to check that the plane $\Lambda := \text{span}\{\nu_0, \nu_1\}$ is spacelike. This condition holds because Λ is orthogonal to the rotation axis $\mathbb{M}^3(\kappa) \cap \{x_1 = x_2 = 0\}$ of $\Sigma(1, b, c)$. \square

4.8 Detecting critical rotational annuli

Throughout this section we will consider points of the form $(1, b, c) \in \mathcal{R} \cap \mathcal{W}$, and let $\Sigma = \Sigma(1, b, c)$ be the associated rotational H -surface in $\mathbb{M}^3(\kappa)$, see (3.33) and Proposition 4.6.3. Our objective in this section will be to find some special zeros of the map $\mathfrak{h}(1, b, c)$ introduced in Definition 4.5.2. These zeros will detect those rotational H -surfaces whose restriction to $u \in [-\tau, \tau]$ are free boundary in some geodesic ball (i.e. they cover critical nodoids or catenoids in $\mathbb{M}^3(\kappa)$). These special values where

$\mathfrak{h}(1, b, c) = 0$ will be used in Section 4.9 as bifurcation points in our parameter domain (a, b, c) in order to construct non-rotational free boundary CMC annuli.

Using (3.26), we can actually view $\Sigma = \Sigma(r_1, r_3)$ as depending on r_1, r_3 . We can then reparametrize the parameter domain $\mathcal{R} \cap \mathcal{W}$ in terms of (r_1, r_3) as

$$\widehat{\mathcal{W}} := \mathcal{R} \cap \mathcal{W} = \left\{ (r_1, r_3) \in \mathbb{R}^2 : r_1 \leq 0, r_3 > \max \left\{ \frac{(r_1 - 1)^2}{1 - 2r_1}, \frac{H + \mu}{2\mu} \right\} \right\}. \quad (4.33)$$

This follows directly from a computation using (3.26), the definition of \mathcal{W} in (3.33), Proposition 4.7.4 and (4.23). Note that if $\kappa = 1$, the maximum in (4.33) is always the first quantity, as

$$\frac{(1 - r_1)^2}{1 - 2r_1} \geq 1 > \frac{H + \mu}{2\mu},$$

since $\mu = \sqrt{H^2 + 1} > H$; see Figure 4.1.

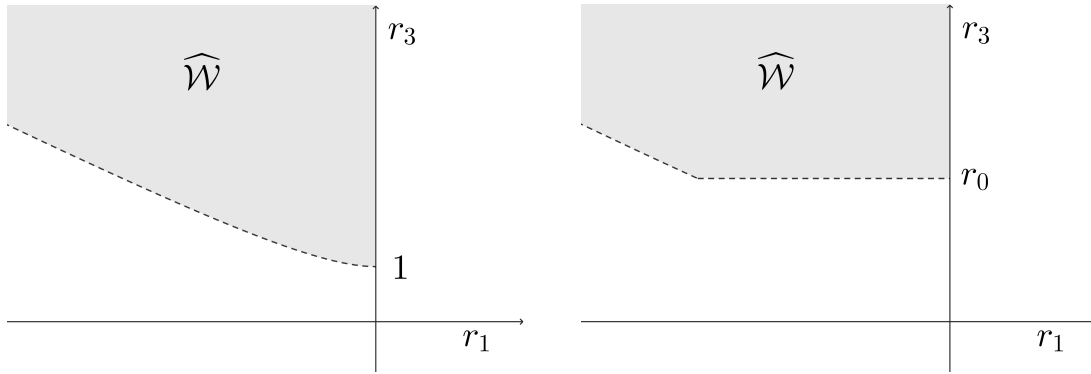


Figure 4.1: The parameter domain $\widehat{\mathcal{W}}$ in (4.33) for the cases $\kappa = 1$ (left) and $\kappa = -1$ (right). In the right picture, the value r_0 stands for $r_0 = \frac{H + \mu}{2\mu}$.

Similarly, we can write the functions $\tau(1, b, c)$ in Proposition 3.4.5 and $\mathfrak{h}(1, b, c)$ in Definition 4.5.2 as $\tau(r_1, r_3)$ and $\mathfrak{h}(r_1, r_3)$, respectively. Both of them are naturally defined in this way on $\widehat{\mathcal{W}}$, and are real analytic.

By Proposition 4.6.3, $\Sigma(r_1, r_3)$ corresponds to one of the catenoids or nodoids $\psi(\mathfrak{s}, \theta)$ in $\mathbb{M}^3(\kappa)$ studied in Section 2.6.1, whose profile curves were parametrized by arc-length, that is, $\|\psi_{\mathfrak{s}}\|^2 \equiv 1$.

If $\delta > 0$ denotes the parameter in Propositions 2.6.1 and 2.6.3 that defines $\psi(\mathfrak{s}, \theta)$, then it follows that the map $r_3 \mapsto \delta(r_3)$, where $r_3 > \max \left\{ 1, \frac{H + \mu}{2\mu} \right\}$, is real analytic and injective: indeed, note that the function $r_3 = r_3(c)$ in (3.26) gives a diffeomorphism between the intervals $r_3 \in (1, \infty)$ and $c \in (1, \infty)$. Moreover, the condition $r_3 > \frac{H + \mu}{2\mu}$ is imposed when $\kappa = -1$ to ensure that (4.22) holds. In particular, the parameter

$r_3 = r_3(c)$ determines the rotational surface $\Sigma(r_1, r_3)$ uniquely; see the discussion after Remark 4.6.4.

Let us also emphasize that, if $\kappa = 1$, the limit value $r_3 = 1$ corresponds to the case where $\Sigma(r_1, 1)$ covers a flat torus in \mathbb{S}^3 , as this implies $c = 1$; see Remark 4.6.1. Therefore, it follows from Remark 2.6.10 that $\delta(r_3)$ can be continuously extended to $r_3 = 1$, with value $\delta(1) = \frac{H+\mu}{2}$. Besides, since $\psi(\mathfrak{s}, \theta)$ is a parametrization by curvature lines of Σ , it is easy to see that the parameter u of Σ is linked to the arclength parameter \mathfrak{s} by $\mathfrak{s} = \mathfrak{s}(u)$, with

$$\mathfrak{s}'(u) = e^{\rho(u)}, \quad \mathfrak{s}(0) = 0. \quad (4.34)$$

Here, the condition $\mathfrak{s}(0) = 0$ comes from the fact that, in both parametrizations, the value 0 gives a point where the geodesic curvature of the profile curve has a maximum. In this way, the change of parameters $\mathfrak{s} = \mathfrak{s}(u)$ is real analytic also with respect to r_3 , and is independent from r_1 . This leads to the following definition.

Definition 4.8.1. We define $\tilde{u}(r_3)$ as $\tilde{u}(r_3) := u(\tilde{\mathfrak{s}}; r_3)$, where $\tilde{\mathfrak{s}} = \tilde{\mathfrak{s}}(\kappa, H, \delta(r_3))$ is defined in Theorem 2.6.9.

Remark 4.8.2. The map $r_3 \rightarrow \tilde{u}(r_3)$ is analytic for all $r_3 > \max\left\{1, \frac{H+\mu}{2\mu}\right\}$. Moreover, if $\kappa = 1$, $\tilde{u}(r_3)$ extends continuously to the limit value $r_3 = 1$, and

$$\tilde{u}(1) = 2\mu\tilde{\mathfrak{s}}\left(1, H, \frac{H+\mu}{2}\right) = \frac{\pi}{\sqrt{2}}\sqrt{\frac{\mu}{H+\mu}}.$$

This follows immediately from (2.50), (4.34) and the fact that $e^{\rho(u)} \equiv \frac{1}{2\mu}$ in this case.

Remark 4.8.3. Assume that $\Theta(r_1, r_3) = m/n \in \mathbb{Q} \cap (-1, 0)$, with $n \in \mathbb{N}$ and m/n irreducible. Choose $u_0 := \tilde{u}(r_3)$, and let $\Sigma_0 := \Sigma_0(1, b, c; u_0) \equiv \Sigma_0(r_1, r_3; u_0)$ be the compact H -annulus in $\mathbb{M}^3(\kappa)$ of Theorem 4.5.1. Then, by the definition of $\tilde{u}(r_3)$ and the previous discussion, we deduce that Σ_0 covers an embedded free boundary catenoid or nodoid $\mathfrak{N} = \mathfrak{N}(r_3)$ in $\mathbb{M}^3(\kappa)$. The value of r_3 determines the specific catenoid or nodoid (since it determines its neck curvature). Contrastingly, r_1 can be regarded as a free parameter in this description.

Let us be more specific about this covering property. Since the central planar geodesic $\Gamma := \mathbf{S} \cap \Sigma_0$ of Σ_0 has rotation index $m \in \mathbb{Z}^-$ (by Proposition 4.4.4), we observe that Σ_0 is a finite $(-m)$ -cover of \mathfrak{N} . In particular, if $\Theta(r_1, r_2) = -1/n$ for some $n \geq 2$, then Σ_0 is an embedding, since it is a trivial covering of the embedded compact annulus $\mathfrak{N} \subset \mathbb{M}^3(\kappa)$.

Remark 4.8.4. Following Definition 2.6.8, for every $u > 0$, let ζ_u denote the geodesic of $\mathbb{M}^3(\kappa)$ passing through the point $\psi(u, 0)$ with tangent vector $\psi_u(u, 0)$. According to item (2) in Theorem 2.6.9, we deduce the existence of a neighbourhood $\mathcal{I} \subset \mathbb{R}$ of $\tilde{u} = \tilde{u}(r_3)$ and an analytic map $\hat{p} = \hat{p}(u) : \mathcal{I} \rightarrow \mathbb{M}^3(\kappa)$ such that, for every $u \in \mathcal{I}$, $\hat{p}(u)$ is the unique intersection point between ζ_u and the geodesic \mathcal{L} in Proposition 4.2.4 in the half-space $\{x_4 > 0\}$. We recall that \mathcal{L} coincides with the rotation axis of the immersion; see Remark 4.6.4. Moreover, denoting by $\hat{p}_3(u)$ the third coordinate of \hat{p} , we have that $\hat{p}_3(\tilde{u}) > 0$, so $\hat{p}_3(u)$ is increasing near \tilde{u} .

Recall that we want to control the zeros of $\mathfrak{h}(r_1, r_3)$. The next proposition characterizes such zeros in terms of the function $\tilde{u}(r_3)$ in Definition 4.8.1.

Proposition 4.8.5. Following the above notations, let $(r_1, r_3) \in \widehat{\mathcal{W}}$ and assume that $\tau(r_1, r_3)$ lies in the interval \mathcal{I} in Remark 4.8.4. Then, the map $\mathfrak{h}(r_1, r_3)$ in Definition 4.5.2 is well defined and satisfies

$$\mathfrak{h}(r_1, r_3) = \hat{p}_3(\tau(r_1, r_3)), \quad (4.35)$$

where \hat{p}_3 denotes the third coordinate of \hat{p} ; see Remark 4.8.4. In particular, if $\tau(r_1, r_3) = \tilde{u}(r_3)$, then $\mathfrak{h}(r_1, r_3) = 0$.

Proof. By Remark 4.6.4, Proposition 4.3.2 and Proposition 4.7.4, we know that the rotation axis \mathcal{L} of $\Sigma(r_1, r_3)$ is contained in the 2-plane \mathcal{P} of \mathbb{R}_κ^4 where the map $\tilde{m}(u)$ takes its values; see Remark 4.2.6. Also, by continuity of the functions \tilde{u}, τ , we can define $\hat{p}(\tau)$ for all (r_1^0, r_3^0) close enough to (r_1, r_3) , where \hat{p} is given by Remark 4.8.4. By construction, $\hat{p}(u)$ lies in \mathcal{L} . In particular, both $\tilde{m}(\tau)$ and $\hat{p}(\tau)$ lie in \mathcal{P} .

Let now \mathcal{P}' denote the 2-plane of \mathbb{R}_κ^4 generated by $\psi(\tau, 0)$ and $\psi_u(\tau, 0)$, where $\tau = \tau(r_1, r_3)$. By definition, $\hat{p}(\tau) \in \mathcal{P}'$. And on the other hand, it follows from the definition of τ and (4.8) that $\tilde{m}(\tau) \in \mathcal{P}'$. Note also that $\mathcal{P} \neq \mathcal{P}'$, since $\psi(\tau, 0) \notin \mathcal{P}$, due to the fact that catenoids and nodoids in $\mathbb{M}^3(\kappa)$ do not touch their rotation axis, see Section 2.6. Thus, $\tilde{m}(\tau)$ and $\hat{p}(\tau)$ are collinear, since they both lie in the line $\ell := \mathcal{P} \cap \mathcal{P}'$ of \mathbb{R}_κ^4 . Depending on the value of the curvature κ , we deduce the following:

If $\kappa = 1$, then the value $m(\tau)$ in Proposition 4.2.4 is well defined, and $\ell \cap \mathbb{S}^3$ consists of the two antipodal points $\{m(\tau), -m(\tau)\}$. We had defined $m(u)$ so that it lies in the half-space $\{x_4 > 0\}$ (see Remark 4.5.3), so we deduce that necessarily

$$\hat{p}(\tau) = m(\tau). \quad (4.36)$$

We thus obtain (4.35) in this case.

Similarly, if $\kappa = -1$, then ℓ must be timelike, since it contains the point $\widehat{p}(\tau) \in \mathbb{H}^3$. In particular, $\widehat{m}(\tau) \in \ell$ is also timelike, so we can consider the rescaling $m(\tau) \in \mathbb{H}^3$ in (4.10). The intersection $\ell \cap \mathbb{H}^3$ consists of a single point, and so (4.36) holds again.

Finally, if $\tau(r_1, r_3) = \widetilde{u}(r_3)$ holds, then clearly

$$\mathfrak{h}(r_1, r_3) = \widehat{p}_3(\tau(r_1, r_3)) = \widehat{p}_3(\widetilde{u}(r_3)) = 0,$$

completing the proof of the Proposition. \square

The following result allows to find roots of $\mathfrak{h}(r_1, r_3)$ along curves in $\widehat{\mathcal{W}}$ joining two of the boundary curves of $\partial\widehat{\mathcal{W}}$. This can be seen as an adaptation of Proposition 3.6.5 in the current context.

Proposition 4.8.6. *Let $\Upsilon : [0, 1] \rightarrow \mathbb{R}^2$, $\Upsilon(r) = (r_1(r), r_3(r))$, be an analytic curve satisfying:*

1. $\Upsilon(r) \in \widehat{\mathcal{W}}$ for every $r \in [0, 1]$.
2. $\Upsilon(0) = (0, r_3(0))$.
3. $\Upsilon(1) = (\bar{r}_1, \bar{r}_3) \notin \widehat{\mathcal{W}}$, with

$$\bar{r}_3 = \frac{(\bar{r}_1 - 1)^2}{1 - 2\bar{r}_1}, \quad \bar{r}_3 > \max \left\{ 1, \frac{H + \mu}{2\mu} \right\}. \quad (4.37)$$

Then there exists some value $r^ \in (0, 1)$ such that $\mathfrak{h}(\Upsilon(r^*)) = 0$. Moreover, $\mathfrak{h}(r) := \mathfrak{h}(\Upsilon(r))$ changes sign at this point; specifically, $\mathfrak{h}(r) > 0$ for $r \in (r^* - \varepsilon, r^*)$ and $\mathfrak{h}(r) < 0$ for $r \in (r^*, r^* + \varepsilon)$, for some $\varepsilon > 0$.*

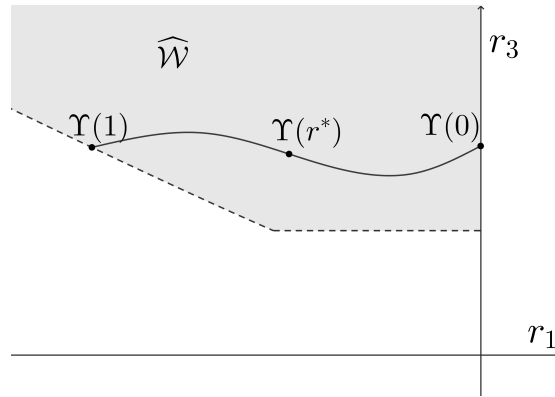


Figure 4.2: Example of a curve $\Upsilon(r)$ in the conditions of Proposition 4.8.6.

Proof. Let us consider the analytic function $f : [0, 1) \rightarrow \mathbb{R}$ defined as

$$f(r) := \tau(\Upsilon(r)) - \tilde{u}(r_3(r)) \equiv \tau(r) - \tilde{u}(r_3(r)).$$

Our goal will be to prove that f vanishes at some point $r^* \in (0, 1)$ and it changes sign. From this, we will conclude that $\mathfrak{h}(r)$ shows the same behaviour at that point.

We show first that $f(0) > 0$. Since $r_1 = 0$ at $\Upsilon(0)$, we see from Remark 3.4.1 that the solution $(s(\lambda), t(\lambda))$ to the system (3.23) associated to the parameters $(0, r_3(0))$ satisfies $t(\lambda) \equiv 0$, while $s(\lambda)$ oscillates between $s = 1$ and $s = r_3(0)$. According to (3.22), $z(u) \equiv 0$ while $y(u)$ is not constant. In fact, by Proposition 3.4.4, $y(u) > 0$ for all $u \in (0, u_1)$. By definition, τ is the first value for which $y(\tau) = z(\tau)$ (see Proposition 3.4.5), so in this case τ is the first positive root of $y(u)$, that is, $\tau(0, r_3(0)) = u_1(0, r_3(0))$. We will now show that $\tilde{u}(r_3(0)) < u_1(0, r_3(0))$. The curvature of the profile curve $u \mapsto \psi(u, 0)$ is $\kappa_1(u, 0) = H + \frac{1}{4\mu}e^{-2\rho(u)}$, by (4.5). By (4.2b) and $z(u) \equiv 0$, this curvature is strictly decreasing on the interval $u \in [0, u_1]$, and it actually has a local minimum at $u = u_1$. On the other hand, by Theorem 2.6.9 the principal curvature κ_1 is strictly decreasing on an interval $[0, u_0)$ containing \tilde{u} . So, we must have $\tilde{u}(r_3(0)) < u_1(0, r_3(0)) = \tau(0, r_3(0))$. As a consequence, $f(0) > 0$.

We will show next that $\lim_{r \rightarrow 1^-} f(r) < 0$. To start, note that the function $\tilde{u}(r_3(r))$ is positive by construction. Also, $\tilde{u}(r_3(r))$ can be defined and is analytic at $r = 1$ by the inequality in (4.37); see Remark 4.8.2. So, $\lim_{r \rightarrow 1^-} \tilde{u}(r_3(r)) = \tilde{u}(\bar{r}_3) > 0$. Now we claim that $\lim_{r \rightarrow 1^-} \tau(r) = 0$. Assume by contradiction that there exists a sequence $(r_n)_n \rightarrow 1$ of values in $(0, 1)$ such that $\lim \tau(r_n) =: L_0 > 0$. Let $(y_n(u), z_n(u))$ denote the solutions $(y(u), z(u))$ of (3.2), (3.5) associated to the parameters $\Upsilon(r_n)$, and $(y_0(u), z_0(u))$ be the corresponding solution for the limit case $\Upsilon(1)$. By definition of τ , we have that $y_n(u) > z_n(u)$ for all $u \in (0, \tau(r_n))$. By continuity of solutions of ODEs with respect to initial conditions and parameters, we deduce that $y_0(u) \geq z_0(u)$ for all $u \in [0, L_0]$. This leads to a contradiction, since the equality in (4.37) implies that $y_0(u) < z_0(u)$ for any $u > 0$ small enough; see Remark 3.4.7.

Therefore, the analytic function $f(r)$ changes sign on the interval $[0, 1)$. More specifically, there exists a value $r^* \in (0, 1)$ satisfying $f(r^*) = 0$, $f(r) > 0$ for $r \in (r^* - \varepsilon, r^*)$ and $f(r) < 0$ for $r \in (r^*, r^* + \varepsilon)$, for $\varepsilon > 0$ small enough.

Let us now study the function $\mathfrak{h}(r)$. We know that $\tau(r^*) = \tilde{u}(r_3(r^*))$, so by Proposition 4.8.5, $\mathfrak{h}(r^*) = 0$. In order to prove that $\mathfrak{h}(r)$ changes sign at r^* , consider $r \in (r^* - \varepsilon, r^*)$ for some $\varepsilon > 0$ small enough. Then, at the point $\Upsilon(r)$ we have $\tau > \tilde{u}$, since $f(r) > 0$. Thus, $\tau > \tilde{u}$ and by Remark 4.8.4 we have $\hat{p}_3(\tau) > \hat{p}_3(\tilde{u}) = 0$, since

$\widehat{p}(u)$ is strictly increasing near \widetilde{u} . Similarly, $\widehat{p}_3(\tau) < 0$ at $\Upsilon(r)$ for $r \in (r^*, r^* + \varepsilon)$. Now, using (4.36), this implies that $\mathfrak{h} = m_3(\tau)$ changes sign at $r = r^*$ along $\Upsilon(r)$. \square

We will next prove a further result that, in the spherical case $\kappa = 1$, will allow us to find roots of $\mathfrak{h}(r_1, r_3)$ along curves in $\widehat{\mathcal{W}}$ that start from the *vertex* $(r_1, r_3) = (0, 1)$; see Figure 4.1.

Lemma 4.8.7. *Let $\kappa = 1$. Given $l > 0$, consider the half-line given by*

$$L(r) := (r_1(r), r_3(r)) = (-r, lr + 1) \quad (4.38)$$

for all $r > 0$. Then, there exists $\lim_{r \rightarrow 0^+} \tau(L(r)) - \widetilde{u}(r_3(r)) > 0$. In particular,

$$\tau(L(r)) > \widetilde{u}(r_3(r))$$

for any $r > 0$ small enough.

Proof. Note that the expression in this directional limit makes sense, since $L(r) \in \widehat{\mathcal{W}}$ for $r > 0$ small enough. By Remark 4.8.2, we know that $\widetilde{u}(r_3(0)) = \widetilde{u}(1) < \pi$. We will now prove that $\lim_{r \rightarrow 0^+} \tau(L(r)) = \pi$, proving the lemma.

Let $r > 0$ such that $L(r) \in \widehat{\mathcal{W}}$, and define $\widehat{\tau}(r) := \lambda(\tau(L(r)))$, where $\lambda = \lambda(u)$ is the parameter used in the differential system (3.23), in which we recall that the polynomial $g(x)$ is given by (3.24) with roots (3.26). Equivalently, $\widehat{\tau}(r)$ can be defined as the first positive value for which

$$s(\widehat{\tau}(r); r) + t(\widehat{\tau}(r); r) = 1,$$

where by $s(\lambda; r)$, $t(\lambda; r)$ we denote the solutions of (3.23) for $(r_1(r), r_3(r))$. We now define the functions

$$S(\lambda; r) := \frac{s-1}{r_3(r)-1} = \frac{s-1}{lr}, \quad T(\lambda; r) := \frac{t}{r_1(r)} = -\frac{t}{r}. \quad (4.39)$$

In this way, $\widehat{\tau}(r)$ corresponds to the first value $\lambda > 0$ for which

$$F(\lambda; r) := lS(\lambda; r) - T(\lambda; r) \quad (4.40)$$

vanishes. From (3.23) and (3.24), (3.26), we deduce that $S(\lambda), T(\lambda)$ are solutions of

the differential system

$$\begin{cases} S'(\lambda)^2 = S(1-S)(1+rS)(1+r+rS)^2, & (S \geq 0), \\ T'(\lambda)^2 = rT(1-T)^2(1+rT)(1+lr+rT), & (T \geq 0), \end{cases} \quad (4.41)$$

with initial conditions

$$S(0; r) = T(0; r) = 0. \quad (4.42)$$

More specifically, since $r > 0$, we have that $s(\lambda; r)$ and $t(\lambda; r)$ are not constant. Thus, from (4.39), we see that $S(\lambda; r)$, $T(\lambda; r)$ are the unique non-constants solutions to (4.41)-(4.42). By differentiation of (4.41) and using (4.42), we obtain $2S''(0; r) = (1+r) > 0$ and $2T''(0; r) = r(1+lr) > 0$.

The system (4.41) depends analytically on the parameter r , and for the limit $r = 0$ case we can solve it directly. By the previous observations, we deduce that $S(\lambda; r)$ and $T(\lambda; r)$ converge analytically as $r \rightarrow 0$ to

$$S(\lambda; 0) = \frac{1 - \cos(\lambda)}{2}, \quad T(\lambda; 0) \equiv 0. \quad (4.43)$$

Let us prove that $\lim_{r \rightarrow 0^+} \widehat{\tau}(r) = 2\pi$. First, we show that $\limsup \widehat{\tau}(r) \leq 2\pi$. Let $\lambda_1(r) := \lambda(u_1(L(r)))$, see Proposition 3.4.4 for the definition of u_1 . Then, by (3.22), (4.39), $\lambda_1(r)$ is the first positive value for which $S(\lambda; r)$ vanishes. According to (4.41), this quantity is equal to

$$\lambda_1(r) = 2 \int_0^1 \frac{dS}{\sqrt{S(1-S)(lrS+1)(lrS+1+r)^2}},$$

which depends analytically on r , and $\lambda_1(0) = 2\pi$. Notice, on the other hand, that $\widehat{\tau}(r) \leq \lambda_1(r)$ for all $r > 0$, according to Proposition 3.4.5. Consequently,

$$\limsup \widehat{\tau}(r) \leq 2\pi.$$

We will now prove that $\delta := \liminf_{r \rightarrow 0^+} \widehat{\tau}(r) \geq 2\pi$. First, it follows by (4.41), (4.42) that $F(0; r) = F'(0; r) = 0$.

By definition of δ and $F(\lambda; r)$, there exists a sequence (λ_n, r_n) such that $\lambda_n \rightarrow \delta$, $r_n \rightarrow 0$ and $F(\lambda_n; r_n) = 0$ for all n , with $F(\lambda; r_n) \neq 0$ for all $\lambda \in (0, \lambda_n)$. By continuity of F , it follows that $F(\delta; 0) = 0$. By (4.43) and (4.40), we see that δ must be either 0 or 2π (recall that $\limsup \widehat{\tau}(r) \leq 2\pi$). Assume by contradiction that $\delta = 0$.

Since $F(0; r_n) = F'(0; r_n) = F(\lambda_n; r_n) = 0$ for all r_n , we deduce the existence of a sequence $\lambda_n^* \in (0, \lambda_n)$ such that $F''(\lambda_n^*; r_n) = 0$ for all n . Now, $\delta = 0$ by hypothesis, we have $\lambda_n^* \rightarrow 0$, and so $F''(0; 0) = 0$ by continuity. However, a direct computation using (4.40), (4.43) shows that $F''(0; 0) = \frac{l}{2} > 0$, a contradiction. In conclusion, $\liminf_{r \rightarrow 0^+} \widehat{\tau}(r) = \lim_{r \rightarrow 0^+} \widehat{\tau}(r) = 2\pi$.

Finally, to compute $\lim_{r \rightarrow 0^+} \tau(L(r))$, we just make use of the change of variables $u = u(\lambda)$ given by (3.25) and the fact that $s(\lambda; r), t(\lambda; r)$ converge uniformly to the constants 1 and 0 respectively; see Remark 3.4.1. This yields

$$\lim_{r \rightarrow 0^+} \tau(L(r)) = \lim_{r \rightarrow 0^+} \int_0^{\widehat{\tau}(r)} \frac{s(\lambda; r) - t(\lambda; r)}{2} d\lambda = \int_0^{2\pi} \frac{1 - 0}{2} d\lambda = \pi.$$

This completes the proof of Lemma 4.8.7. \square

4.9 Proof of the main theorems

In this section we will prove Theorems 4.1.1 and 4.1.2. The general idea behind these results is to study the rational level sets of the period map $\Theta(a, b, c) = \Theta_0 \in (-1, 0) \cap \mathbb{Q}$; see Definition 4.4.2. Suppose that for some parameters (a, b, c) in of these rational level sets we have that $\mathfrak{h}(a, b, c) = 0$ (see Definition 4.5.2). By Theorem 4.5.1, the associated surface Σ_0 is a compact annulus, and by Corollary 4.5.4, Σ_0 intersects orthogonally a certain totally umbilic sphere \mathcal{Q} of $\mathbb{M}^3(\kappa)$. Under certain conditions, we will be able to prove that Σ_0 is actually contained in the geodesic ball \mathbf{B} whose boundary is \mathcal{Q} , that is, Σ_0 is *free boundary* in \mathbf{B} . The embeddedness of Σ_0 will also be studied.

The results obtained in Section 4.8 can be applied to find roots of $\mathfrak{h}(a, b, c)$ when $a = 1$. In that case, the corresponding compact annuli $\Sigma_0(1, b, c; u_0)$ are pieces of nodoids or catenoids: see Section 4.6. Our goal now is to find new zeros of $\mathfrak{h}(a, b, c)$ with $a > 1$, which will correspond with non-rotational CMC annuli.

4.9.1 Proof of Theorem 4.1.1

The proof will consist of two steps. On the first one, we will show that for any $H \geq 0$, $\kappa = \pm 1$ such that $H^2 + \kappa > 0$, there are countably many values $\Theta_0 \in (-1, 0) \cap \mathbb{Q}$ such that the function $\mathfrak{h}(a, b, c)$ vanishes along an analytic curve $C(\eta) \subset \mathcal{W}$ on the level set given by $\Theta(a, b, c) = \Theta_0$. Then, on the second step, we will show that the family of surfaces $\Sigma_0 = \Sigma_0(\eta)$ associated to the curve $C(\eta)$ constitute examples of

free boundary H -annuli in $\mathbb{M}^3(\kappa)$.

For the **first step**, we distinguish two cases, depending on the sign of the quantity $8H^2 - \kappa$.

First step, case $8H^2 - \kappa > 0$. Let \mathcal{J} be the interval

$$\mathcal{J} = \begin{cases} \left(-\frac{1}{\sqrt{3}}, 0\right), & \text{if } \kappa = -1, \\ \left(-\frac{1}{\sqrt{3}}, -\sqrt{\frac{\mu-H}{2\mu}}\right), & \text{if } \kappa = 1, \end{cases} \quad (4.44)$$

where we recall that $\mu := \sqrt{H^2 + \kappa}$. Note that \mathcal{J} is indeed an interval when $\kappa = 1$, due to $8H^2 - \kappa > 0$. Given some $\Theta_0 \in \mathcal{J} \cap \mathbb{Q}$, consider the level set of the period map given by $\Theta(a, b, c) = \Theta_0$. On the plane $\{a = 1\}$, this level set can be expressed as (4.31) in terms of (r_1, r_3) given by (3.26), i.e., as the line

$$\Upsilon(r) := (r_1(r), r_3(r)) = \left(-r, \frac{\Theta_0^2}{1 - \Theta_0^2}r + \frac{H + \mu}{2\mu(1 - \Theta_0^2)}\right). \quad (4.45)$$

We now show that a segment of $\Upsilon(r)$ satisfies the properties listed in the statement of Proposition 4.8.6.

First, it is clear from (4.45) and $\Theta_0 \in \mathcal{J}$ that $\Upsilon(0) = (0, r_3(0)) \in \widehat{\mathcal{W}}$, i.e. the second condition of Proposition 4.8.6 holds. Also, $\Upsilon(r) \in \widehat{\mathcal{W}}$ for $r \geq 0$ small enough; see Figure 4.3.

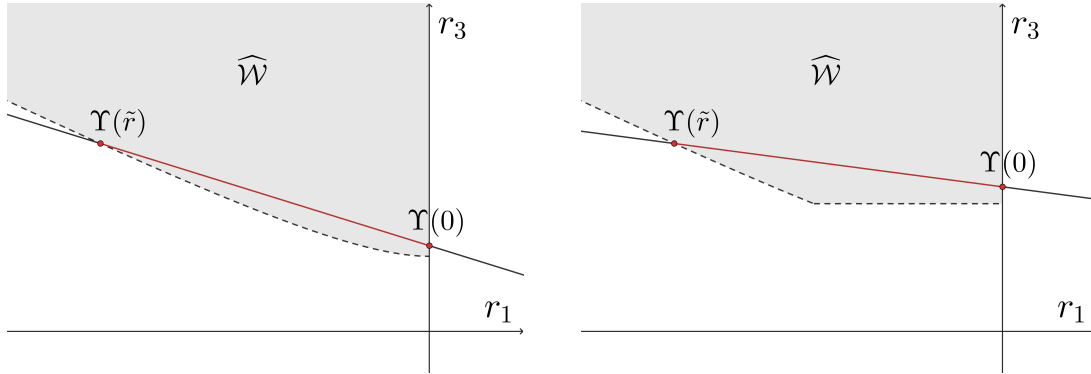


Figure 4.3: Level lines Υ of the period map on the parameter domain (r_1, r_3) for the cases $\kappa = 1$ (left) and $\kappa = -1$ (right). If $8H^2 - \kappa > 0$, there are infinitely many level lines for which a segment of Υ satisfies the hypotheses of Proposition 4.8.6.

On the other hand, $\Upsilon(r) \notin \widehat{\mathcal{W}}$ for r large enough; indeed, consider the inequality for r_3 in (4.33). It is clear that $r_3(r) > \frac{H+\mu}{2\mu}$ for any $r \geq 0$, since $\Upsilon(r)$ has negative

slope. However, we can prove that

$$r_3(r) < \mathcal{G}(r) := \frac{(r_1(r) - 1)^2}{1 - 2r_1(r)}$$

for r large enough. This follows directly from $\Theta_0^2 < 1/3$ (since $\Theta_0 \in \mathcal{J}$) and the inequalities

$$0 < r'_3(r) = \frac{\Theta_0^2}{1 - \Theta_0^2} < \frac{1}{2} = \lim_{r \rightarrow \infty} \mathcal{G}'(r).$$

As a consequence, there is a first value $\tilde{r} > 0$ such that $\Upsilon(\tilde{r}) \notin \widehat{\mathcal{W}}$, for which the equality in (4.37) is satisfied. Thus, the segment $\Upsilon(r) : [0, \tilde{r}] \rightarrow \mathbb{R}^2$ is in the conditions of Proposition 4.8.6, after the linear change $r \mapsto r/\tilde{r}$.

Thus, by Proposition 4.8.6, there exists $r^* > 0$ such that $\Upsilon(r^*) \in \widehat{\mathcal{W}}$, with $\mathfrak{h}(\Upsilon(r^*)) = 0$ and so that $\mathfrak{h}(\Upsilon(r))$ changes sign at r^* . Now, let $(1, b^*, c^*)$ be the point associated to $(r_1(r^*), r_3(r^*))$ by the change (3.26). Consider the function

$$g(a, b) := \mathfrak{h}(a, b, c^{\Theta_0}(a, b)), \quad (4.46)$$

defined on a neighbourhood of $(1, b^*) \in \mathbb{R}^2$, where $c^{\Theta_0}(a, b)$ is the analytic map defined in Remark 4.7.2, which parametrizes the level set $\Theta(a, b, c) = \Theta_0$ in a neighbourhood of $(1, b^*, c^*) \in \mathbb{R}^3$. We know by our previous discussion that $g(1, b^*) = 0$ and, moreover, that $b \mapsto g(1, b)$ changes sign at b^* , meaning that $g(1, b) > 0$ (resp. $g(1, b) < 0$) for $b \in (b^* - \varepsilon, b^*)$ (resp. $b \in (b^*, b^* + \varepsilon)$), for $\varepsilon > 0$ small enough. Since $g(a, b)$ is analytic, there exists a real analytic curve $\zeta(\eta) := (a(\eta), b(\eta))$, $\eta \in [0, \varepsilon_0)$ for a certain $\varepsilon_0 > 0$, satisfying $g(\zeta(\eta)) \equiv 0$ and $\zeta(0) = (1, b^*)$. This can be seen as a consequence of Lojasiewicz's Structure Theorem, which implies that if a non-constant real analytic function $f : U \subset \mathbb{R}^2 \rightarrow \mathbb{R}$ has a non-isolated zero at $p_0 \in U$, then the set $\{f = 0\}$ is, around p_0 , the union of a finite number of real analytic arcs meeting at p_0 ; see e.g. [52, Theorem 5.2.3]. Moreover, as $b \mapsto g(1, b)$ changes sign, then $a(\eta) > 1$ for all $\eta > 0$. We define then the curve

$$C(\eta) := (a(\eta), b(\eta), c^{\Theta_0}(\zeta(\eta))), \quad (4.47)$$

which by definition is contained in the level set $\Theta(a, b, c) = \Theta_0$, and satisfies $\mathfrak{h}(C(\mu)) \equiv 0$. Observe that we obtain a different curve $C(\eta)$ for every Θ_0 in the countable set $\mathcal{J} \cap \mathbb{Q}$. This concludes the proof of the **first step** in the case $8H^2 - \kappa > 0$.

First step, case $8H^2 - \kappa \leq 0$. This implies in particular that $\kappa = 1$, and so $\mu > H$.

Now, take any $l > 0$ such that $l < \frac{\mu-H}{\mu+H}$, and consider the line $L(r) := (-r, lr + 1)$. Also, for any

$$\Theta_0 \in \left(-\sqrt{\frac{\mu-H}{2\mu}}, -\sqrt{\frac{l}{1+l}} \right) \quad (4.48)$$

we consider the level line of the period map $\Upsilon = \Upsilon(r; \Theta_0)$ in (4.45). The conditions on Θ_0 in (4.48) imply that Υ and L meet at a point $L(\bar{r}) = \Upsilon(\bar{r})$, $\bar{r} = \bar{r}(\Theta_0) > 0$; see Figure 4.4. The value $L(\bar{r})$ depends analytically on Θ_0 , and for the limit case $\Theta_0 = -\sqrt{\frac{\mu-H}{2\mu}}$ it holds $\bar{r} = 0$, that is, L and Υ meet at $(r_1, r_3) = (0, 1)$.

Note also that, by Lemma 4.8.7, the inequality $\tau(L(r)) > \tilde{u}(lr + 1)$ holds for all $r > 0$ sufficiently close to zero. In particular, there exists a smaller interval

$$\mathcal{J} := \left(-\sqrt{\frac{\mu-H}{2\mu}}, \tilde{\Theta} \right)$$

such that, for all $\Theta_0 \in \mathcal{J}$:

1. The point $L(\bar{r})$ belongs to $\widehat{\mathcal{W}}$, and so $\tau(L(\bar{r}))$ is well defined.
2. The inequality $\tau(L(\bar{r})) > \tilde{u}(l\bar{r} + 1)$ is satisfied.

We now fix some $\Theta_0 \in \mathcal{J} \cap \mathbb{Q}$ and define $\tau(r) := \tau(\Upsilon(r))$, $\mathfrak{h}(r) := \mathfrak{h}(\Upsilon(r))$. We will prove that there exists a value $r^* \in (0, \bar{r})$ where $\tau(r^*) = \tilde{u}(r_3(r^*))$, with $r_3(r)$ as in (4.45), and so $\mathfrak{h}(r^*) = 0$.

By hypothesis, we know that $\Upsilon(\bar{r}) = L(\bar{r}) \in \widehat{\mathcal{W}}$, and in fact $\tau(\bar{r}) > \tilde{u}(r_3(\bar{r}))$, by item (2) above. Since $r_3(r)$ is strictly increasing with $r_3(0) < 1$ and $r_3(\bar{r}) > 1$, we can define $r_b := r_3^{-1}(1) \in (0, \bar{r})$. Moreover, $\Upsilon(r_b) = (-r_b, 1)$ does not lie in $\widehat{\mathcal{W}}$, since the inequality for r_3 in (4.33) does not hold at that point.

Consequently, there exists a certain interval $(r_c, \bar{r}] \subsetneq (r_b, \bar{r}]$ such that $\Upsilon(r) \in \widehat{\mathcal{W}}$ for all $r \in (r_c, \bar{r}]$, and $\Upsilon(r_c) \in \partial\widehat{\mathcal{W}}$; see Figure 4.4. By a similar argument to the one in the proof of Proposition 4.8.6, it is possible to check that $\lim_{r \rightarrow r_c^+} \tau(r) = 0$. On the other hand, $\tilde{u}(r_3(r))$ is a positive function defined at $r = r_c$, so

$$\lim_{r \rightarrow r_c^+} (\tau(r) - \tilde{u}(r_3(r))) = -\tilde{u}(r_3(r_c)) < 0.$$

In particular, there exists some $r^* \in (r_c, \bar{r})$ where $\tau(r^*) = \tilde{u}(r_3(r^*))$. In fact, since \tilde{u} and τ are analytic and they do not coincide, we can take r^* so that the function $f(r) := \tau(r) - \tilde{u}(r_3(r))$ changes sign at $r = r^*$, being negative (resp. positive) for any $r < r^*$ (resp. $r > r^*$) close enough to r^* .

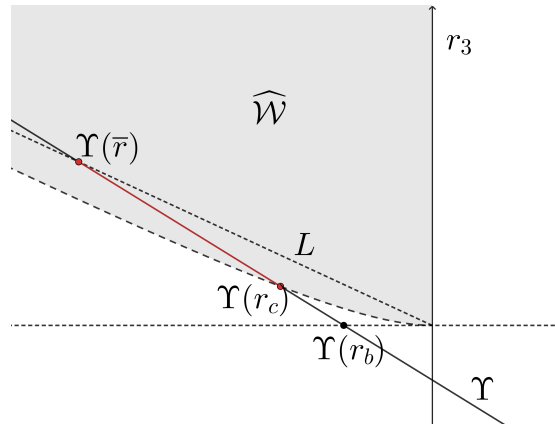


Figure 4.4: The level line Υ and the line L meet at a point $\Upsilon(\bar{r}) \in \widehat{\mathcal{W}}$.

From the definition of r^* and Proposition 4.8.5 it follows that $\mathfrak{h}(r^*) = 0$. In fact, since $f(r)$ changes sign at r^* , arguing as in the last part of the proof of Proposition 4.8.6, we deduce that $\mathfrak{h}(r)$ also changes sign. Now, let $(1, b^*, c^*) \in \mathcal{O}^-$ be the point associated with $(r_1(r^*), r_3(r^*))$ by (3.26). We deduce that the analytic function $b \mapsto g(1, b)$, with $g(a, b)$ given by (4.46), changes sign at $b = b^*$. Consequently, as explained in the proof of the case $8H^2 - \kappa > 0$ above, it follows from Lojasiewicz's Structure Theorem ([52, Theorem 5.2.3]) that there exists an analytic curve $\zeta(\eta) = (a(\eta), b(\eta))$ such that $g(\zeta(\eta)) \equiv 0$, $\zeta(0) = (1, b^*)$ and $a(\eta) > 1$ for $\eta > 0$. We deduce that the curve $C(\eta)$ defined as in (4.47), contained in the level set $\Theta(a, b, c) = \Theta_0$, satisfies $\mathfrak{h}(C(\mu)) \equiv 0$. We remark that we obtain (at least) one such curve for every Θ_0 in the countable set $\mathcal{J} \cap \mathbb{Q}$. This completes the **first step of the proof**.

So far, we have proved that for any values $H \geq 0$, $\kappa = \pm 1$ with $H^2 + \kappa > 0$, there is a countable number of curves $C_q := C_q(\eta) : [0, \varepsilon_0(q)) \rightarrow \mathcal{W} \cap \mathcal{O}^-$, each of them contained in the level set of the period map $\Theta(a, b, c) = q \in \mathcal{J} \cap \mathbb{Q} \subset (-1, 0) \cap \mathbb{Q}$, with the property that \mathfrak{h} vanishes identically along $C_q(\eta)$. Let us now define $\mathbb{A}_q = \mathbb{A}_q(\eta)$ as the compact annulus $\Sigma_0 = \Sigma_0(a, b, c; \tau(a, b, c))$ of Theorem 4.5.1 associated to the point $(a, b, c) = C_q(\eta)$. Our goal is to prove that $\mathbb{A}_q(\eta)$ satisfies each of the properties listed in Theorem 4.1.1.

Items (2) and (5) of Theorem 4.1.1 are a direct consequence of Theorem 4.5.1 and the fact that $a(\eta) > 1$ for all $\eta > 0$. Similarly, item (3) follows from Proposition 4.4.4, while item (4) is derived from Proposition 4.6.3 and Remark 4.8.3. Item (6) holds by construction, as any surface $\Sigma = \Sigma(a, b, c)$ has constant mean curvature H and is of Enneper type. Let us now prove item (1). Since \mathfrak{h} vanishes along the curve $C_q(\eta)$, we deduce by Corollary 4.5.4 that the annuli $\mathbb{A}_q(\eta)$ meet orthogonally a certain

totally umbilic 2-sphere $\mathcal{Q} = \mathcal{Q}(q, \eta)$ of $\mathbb{M}^3(\kappa)$ along their boundary. Let us denote by $\mathbf{B}(q, \eta)$ the geodesic ball of $\mathbb{M}^3(\kappa)$ whose boundary is the sphere $\mathcal{Q}(q, \eta)$; in the case $\kappa = 1$ there are two such balls, and we choose the one for which $\psi(0, 0) \in \mathbf{B}(q, \eta)$. For $\eta = 0$, we know that $\tau(C_q(0)) = \tilde{u}(C_q(0))$, so the compact nodoid or catenoid $\mathbb{A}_q(0)$ is one of the examples constructed in item 1 of Theorem 2.6.9. In particular, this rotational annulus is contained in $\mathbf{B}(q, 0)$. By real analyticity, we conclude that the (non-rotational) annuli $\mathbb{A}_q(\eta)$, $\eta \in (0, \varepsilon_0(q))$, will also be contained in their respective balls $\mathbf{B}(q, \eta)$, at least for a certain $\varepsilon_0(q) > 0$ small enough, so they constitute free boundary examples. This completes the proof of Theorem 4.1.1.

4.9.2 Proof of Theorem 4.1.2

We will now focus on level sets of the period map of the form $\Theta(a, b, c) = -1/n$, where $n \in \mathbb{N}$, $n \geq 2$. Suppose that either $\kappa = -1$ or $\kappa = 1$ and $H \geq \frac{1}{\sqrt{3}}$. Then, the inequality

$$\frac{\mu - H}{2\mu} \leq \frac{1}{n^2} \quad (4.49)$$

is satisfied for some $n \geq 2$. More specifically, if $\kappa = 1$ and $H \geq \frac{1}{\sqrt{3}}$, then (4.49) holds for a finite set of natural numbers, while if $\kappa = -1$ it is true for all $n \geq 2$. We will split our analysis into two cases, depending on whether the inequality (4.49) is strict or not.

Suppose first that (4.49) is strict for some $n \geq 2$. This means that we are in the case $8H^2 - \kappa > 0$ detailed in the proof of Theorem 4.1.1, and that $q_n := -1/n$ lies in the open interval \mathcal{J} defined in (4.44). By the proof of Theorem 4.1.1, we deduce that there is a curve $C_{q_n}(\eta) : [0, \varepsilon_0(n)) \rightarrow \mathcal{O}^-$, contained in the level set $\Theta(a, b, c) = q_n$, such that the associated annuli $\mathbb{A}_{q_n}(\eta)$ are free boundary in a geodesic ball $\mathbf{B}(q_n, \eta)$ of $\mathbb{M}^3(\kappa)$. It just remains to check the embeddedness of these examples, which will be studied below.

Suppose now that (4.49) holds for the equality case. In that situation, we cannot use Theorem 4.1.1 directly. By the equality in (4.49), and using (4.45), the level curve $\Theta(1, b, c) = q_n := -1/n$ is expressed in terms of (r_1, r_3) as

$$\Upsilon(r) := (r_1(r), r_3(r)) = \left(-r, \frac{r}{n^2 - 1} + 1 \right).$$

This is the equation of a line $L(r) := \Upsilon(r)$ that is in the conditions of Lemma 4.8.7, so for any $r > 0$ small enough, we have $\Upsilon(r) \in \widehat{\mathcal{W}}$ and $\tau(\Upsilon(r)) > \tilde{u}(r_3(r))$. However, it is possible to check that $\Upsilon(r) \notin \widehat{\mathcal{W}}$ for $r > 0$ large enough, by a similar argument

to the first step of the proof of Theorem 4.1.1. Also following the proof of that first step, we can deduce that there exists a point r^* where $\tilde{u}(r_3(r^*)) = \tau(\Upsilon(r^*))$, and so $\mathfrak{h}(\Upsilon(r^*)) = 0$. In fact, we can show that there is a real analytic curve $C_n(\eta)$ such that \mathfrak{h} vanishes identically along C_n , and from this we obtain a 1-parameter family of free boundary annuli $\mathbb{A}_n(\eta)$ that satisfies the properties stated in Theorem 4.1.1.

In conclusion, for any $n \geq 2$ such that (4.49) holds, there exists a 1-parameter family of immersed, free boundary annuli $\mathbb{A}_{q_n}(\eta)$. It just remains to prove that the annuli $\mathbb{A}_{q_n}(\eta)$, $\eta \in [0, \varepsilon_0(n))$, are embedded for some $\varepsilon_0(n) > 0$ small enough.

For every $\eta \in [0, \varepsilon_0(n))$, let us denote by $\psi_\eta(u, v)$ our usual parametrization by curvature lines of the compact annulus $\mathbb{A}_{q_n}(\eta)$. We know by Corollary 4.4.5 that

$$\psi_\eta(u, v) = \psi_\eta(u, v + 2n\sigma),$$

where $\sigma = \sigma(a, b, c)$ depends analytically on η . Identifying $(u, v) \sim (u, v + 2n\sigma)$ as usual (see Section 4.5), we can view ψ_η as a parametrization $\psi_\eta : [-\tau(\eta), \tau(\eta)] \times \mathbb{S}^1 \rightarrow \mathbb{A}_{q_n}(\eta)$ of $\mathbb{A}_{q_n}(\eta)$. Observe that for $\eta = 0$, the annulus $\mathbb{A}_{q_n}(0)$ is an embedding, since it is a trivial covering of a critical catenoid or nodoid \mathfrak{N} embedded in $\mathbb{M}^3(\kappa)$; see Remark 4.8.3. Thus, ψ_0 is injective.

Now, by the real analyticity of the family of compact annuli $\mathbb{A}_{q_n}(\eta)$, we deduce that for all η sufficiently close to zero, the parametrizations ψ_η are also injective, and so the annuli $\mathbb{A}_{q_n}(\eta)$ are embedded. This completes the proof of Theorem 4.1.2.

4.10 Embedded capillary minimal and CMC annuli in \mathbb{S}^3

In Theorem 4.1.2, we constructed embedded examples of non-rotational, free boundary CMC annuli in geodesic balls of \mathbb{H}^3 (for $H > 1$) and \mathbb{S}^3 (for $H \geq 1/\sqrt{3}$). In this section we will show that if we relax the free boundary condition to *capillarity*, then we can also find embedded non-rotational capillary CMC annuli in \mathbb{S}^3 for any $H \geq 0$.

Recall that a compact surface Σ in $\mathbb{M}^3(\kappa)$ is called a *capillary surface* in a geodesic ball $\mathbf{B} \subset \mathbb{M}^3(\kappa)$ if $\Sigma \subset \mathbf{B}$ intersects $\partial\mathbf{B}$ at a constant angle along $\partial\Sigma$. We prove next:

Theorem 4.10.1. *For any $H \geq 0$ and any $n \geq 2$ there exists a real analytic 2-parameter family of embedded capillary annuli $\mathbb{A}_n(a, \eta)$ with constant mean curvature H in a geodesic ball $\mathbf{B} = \mathbf{B}(n, a, \eta)$ of \mathbb{S}^3 , with a prismatic symmetry group of order $4n$.*

The rough idea behind this result is as follows: consider the level set of the period given by $\Theta(a, b, c) = -1/n$, and suppose that for some $(a, b, c) \in \mathcal{O}^-$ with $a > 1$ in this level set there exists a value $u^* > 0$ such that $\tilde{m}_3(u^*) = 0$, that is, the third coordinate of the map $\tilde{m}(u)$ in (4.8) vanishes. According to items (2), (4) and (5) of Theorem 4.5.1, the compact annulus $\Sigma_0(a, b, c; u^*)$ intersects along $\partial\Sigma_0$ at a constant angle a totally umbilic sphere \mathcal{Q} of \mathbb{S}^3 , and Σ_0 has a prismatic symmetry group of order $4n$. Consequently, it suffices to check that the annuli Σ_0 are embedded and contained in a geodesic ball \mathbf{B} of \mathbb{S}^3 whose boundary is \mathcal{Q} .

We will make use of the following lemma:

Lemma 4.10.2. *Suppose that for some $(a_0, b_0, c_0) \in \mathcal{O}^-$ there exists $u_0 > 0$ such that $\tilde{m}_3(u_0) = 0$. Then, there exists a neighbourhood \mathcal{V} of (a_0, b_0, c_0) and an analytic function $u^* = u^*(a, b, c) : \mathcal{V} \cap \mathcal{O}^- \rightarrow \mathbb{R}$ such that $u^*(a_0, b_0, c_0) = u_0$ and $\tilde{m}_3(u^*(a, b, c)) \equiv 0$.*

Proof. The lemma is a direct consequence of the implicit function theorem if we prove that $\tilde{m}'_3(u_0) \neq 0$. Assume by contradiction that $\tilde{m}'_3(u_0) = 0$. Since $\tilde{m}_3(u_0) = 0$ by hypothesis, we deduce from (2.37) that $\tilde{m}_3(u)$ vanishes identically. This is a contradiction, as (4.8) and the initial conditions in Remark 4.4.1 imply that $\tilde{m}_3(0) = -2$. \square

4.10.1 Proof of Theorem 4.10.1

Let $n \geq 2$ and $\kappa = 1$. We will distinguish two cases, depending on whether or not (4.49) holds.

Assume first that (4.49) holds, and consider the level set $\Theta(a, b, c) = -1/n =: \Theta_0$. Following the proof of Theorem 4.1.2 in Section 4.9.2, we know that there is a point $(1, b^*, c^*)$ in that level set such that $\mathfrak{h}(1, b^*, c^*) = m_3(\tau(1, b^*, c^*)) = 0$. By applying Lemma 4.10.2 with $u_0 = \tau(1, b^*, c^*)$, we deduce the existence of a function u^* defined on a neighbourhood \mathcal{V} of $(1, b^*, c^*)$ such that the map $\tilde{m}_3(u^*(a, b, c))$ vanishes identically. Now, consider the analytic function

$$(a, b) \mapsto u^*(a, b) := u^*(a, b, c^{\Theta_0}(a, b)),$$

where $c^{\Theta_0}(a, b)$ is the analytic map in Remark 4.7.2. Let $\mathbb{A}_n(a, b) \equiv \psi([-u^*, u^*] \times \mathbb{S}^1)$ be the compact annulus associated to the parameters $(a, b, c^{\Theta_0}(a, b))$, where we identify the points $(u, v) \sim (u, v + 2n\sigma)$ as in Corollary 4.4.5. By construction, any of these annuli meets a totally umbilic sphere $\mathcal{Q} = \mathcal{Q}(n, a, b)$ of \mathbb{S}^3 with constant angle along

its boundary $\partial\mathbb{A}_n(a, b)$, so in order to prove Theorem 4.10.1 we just need to check that the annuli $\mathbb{A}_n(a, b)$ are embedded and contained in a geodesic ball of \mathbb{S}^3 bounded by their corresponding sphere \mathcal{Q} . Notice that in Theorem 4.1.2 we already proved this for the annulus $\mathbb{A}_n(1, b^*)$, so by real analyticity, there is an open neighbourhood $G \subset \mathbb{R}^2$ of $(1, b^*)$ such that the annuli $\mathbb{A}_n(a, b)$ are also embedded and contained in a geodesic ball $\mathbf{B}(n, a, b)$ of \mathbb{S}^3 bounded by $\mathcal{Q}(n, a, b)$ for all $(a, b) \in G$. We also recall that there are two such geodesic balls in \mathbb{S}^3 ; we make the same choice for it that we did when proving Theorem 4.1.1.

Take next some $n \in \mathbb{N}$, $n \geq 2$, such that (4.49) does not hold and consider the level curve $\Theta(1, b, c) = \Theta_0 := -1/n$. In the (r_1, r_3) -coordinates, this curve is given by $\Upsilon(r)$ in (4.45), and so it meets the horizontal line $\{r_3 = 1\}$ at a certain point $\Upsilon(r_l) = (-r_l, 1)$, where $r_l > 0$. Let us see that $(1, b_l, c_l) \equiv \Upsilon(r_l)$ is in the conditions of Lemma 4.10.2.

Let Σ denote the rotational H -surface associated to $(r_1, r_3) = \Upsilon(r_l) \equiv (1, b_l, c_l)$; note that $c_l = 1$ since $r_3 = 1$, see (3.26). Thus, by Remark 4.6.1, Σ covers a flat CMC torus in \mathbb{S}^3 . Since $\Theta = -1/n$, we can consider for any $u_0 > 0$ the compact immersed H -annulus $\Sigma_0 = \Sigma_0(1, b_l, 1; u_0)$ as defined in Section 4.5, after the identification $(u, v) \sim (u, v + 2n\sigma)$. Under this identification, the v -curves $\psi(u_0, v) : \mathbb{S}^1 \rightarrow \mathbb{S}^3$ are injective parametrizations of circles.

We find next an explicit parametrization for the profile curve $\psi(u, 0)$ of Σ_0 , using the expression of the flat H -torus in \mathbb{S}^3 given in Remark 2.6.10 in terms of the parameters (\mathfrak{s}, θ) . To start, note that it holds $e^{\rho(u)} \equiv \frac{1}{2\mu}$ for Σ_0 due to $c = 1$, and so the reparametrization $u = u(\mathfrak{s})$ in (4.34) is just $u = 2\mu\mathfrak{s}$. In addition, the rotation axis of the flat torus in Remark 2.6.10 is $\mathbb{S}^3 \cap \{x_1 = x_2 = 0\}$, which agrees with the geodesic \mathcal{L} of \mathbb{S}^3 that contains the center map $m(u)$ of Σ ; see Remark 4.6.4. Thus, by (2.51), we see that the profile curve of Σ is

$$\psi(u, 0) = (\varrho_1, 0, \varrho_2 \sin(\varrho_1 u), \varrho_2 \cos(\varrho_1 u)), \quad (4.50)$$

where

$$\varrho_1 = \sqrt{\frac{\mu + H}{2\mu}}, \quad \varrho_2 = \sqrt{\frac{\mu - H}{2\mu}}.$$

Let $u_0 \in (0, \bar{u})$, where $\bar{u} := \pi/\varrho_1$. From the expression of the profile curve $\psi(u, 0)$ and the previous discussion, it follows that the parametrization $\psi : [-u_0, u_0] \times \mathbb{S}^1 \rightarrow \mathbb{S}^3$ of Σ_0 is injective, where we identify $(u, v) \sim (u, v + 2n\sigma)$ as usual. Moreover, Σ_0 is contained in the ball $B[\mathbf{e}_4, x_4(u_0)]$.

We now claim that there exists some $u_0 \in (0, \bar{u})$ such that $\tilde{m}_3(u_0) = 0$. To prove this, note first that $f(u) := -\langle \tilde{m}(u), e^{-\rho(u,0)} \psi_u(u, 0) \rangle$ is the constant $f(u) \equiv 2$; see (4.8). By (4.50),

$$\begin{aligned} f(0) &= -\langle \tilde{m}(0), e^{-\rho(0,0)} \psi_u(0, 0) \rangle = -\tilde{m}_3(0), \\ f(\bar{u}) &= -\langle \tilde{m}(\bar{u}), e^{-\rho(\bar{u},0)} \psi_u(\bar{u}, 0) \rangle = \tilde{m}_3(\bar{u}). \end{aligned}$$

We deduce that there is some $u_0 \in (0, \bar{u})$ for which $\tilde{m}_3(u_0) = 0$. So, by Lemma 4.10.2, there exists a function $u^*(a, b, c)$ defined on a neighbourhood of $(1, b_l, 1)$, with $u^*(1, b_l, 1) = u_0$ and $m_3(u^*(a, b, c)) \equiv 0$.

We consider the analytic function $u^*(a, c) := u^*(a, b^{\Theta_0}(a, c), c)$ and define for any (a, c) in a neighborhood of $(1, 1)$ the compact H -annuli

$$\mathbb{A}_n(a, c) := \Sigma_0(a, b^{\Theta_0}(a, c), c; u^*(a, c)),$$

where $b^{\Theta_0}(a, c)$ is the analytic map in Remark 4.7.2. By construction, $\mathbb{A}_n(a, c)$ meets a totally umbilic sphere $\mathcal{Q}(n, a, c)$ with constant angle along $\partial \mathbb{A}_n(a, c)$, according to Theorem 4.5.1. The annulus $\mathbb{A}_n(1, 1)$ is equal to $\Sigma_0(1, b_l, 1; u_0)$, which by our previous discussion, is embedded and contained in a geodesic ball of \mathbb{S}^3 bounded by $\mathcal{Q}(n, 1, 1)$. Consequently, there is a neighbourhood of $(1, 1)$ such that the annuli $\mathbb{A}_n(a, c)$ are embedded capillary CMC annuli in a geodesic ball of \mathbb{S}^3 bounded by $\mathcal{Q}(n, a, c)$. This completes the proof of Theorem 4.10.1.

4.11 Final notes

The existence of CMC tori immersed in \mathbb{R}^3 by Wente [75] and the studies by Abresch [1] and Walter [72, 73] in the 1980s was followed by a spectacular development of the theory of CMC tori in terms of integrable systems theory. In this line, the fundamental achievement was the “classification” of all CMC tori in the space forms \mathbb{R}^3 , \mathbb{S}^3 and \mathbb{H}^3 by Pinkall-Sterling [63] (in \mathbb{R}^3), Hitchin [40] (for minimal tori in \mathbb{S}^3) and then by Bobenko [7] (for CMC tori in \mathbb{S}^3 and \mathbb{H}^3), using algebro-geometric methods from integrable systems. In these theorems, CMC tori were shown to be determined by *finite type* solutions of the sinh-Gordon equation. The rough idea for this classification is that, for any natural $N \geq 1$, the space of type N sinh-Gordon solutions is finite dimensional, all CMC tori are of finite type, and they can be detected within their associated finite dimensional space by explicit closing conditions.

This classification did not detect the possible embeddedness of CMC tori in \mathbb{S}^3 (in \mathbb{R}^3 and \mathbb{H}^3 there are no closed embedded CMC surfaces, by Alexandrov's theorem). The proof that embedded CMC tori are rotational had to wait until the much more recent works of Brendle [6] and Andrews-Li [4], using different ideas.

There is a natural boundary version of the classification problem for CMC tori discussed above: to classify all free boundary CMC annuli in geodesic balls of $\mathbb{M}^3(\kappa) = \mathbb{R}^3, \mathbb{S}^3$ or \mathbb{H}^3 . Regarding this problem, there is an important analytic result by Kilian and Smith in [51]. Specifically, they proved that any capillary annulus of constant mean curvature H in a geodesic ball of $\mathbb{M}^3(\kappa)$, if $H^2 > \kappa$, comes from a finite type solution ω of the sinh-Gordon equation. This is a first step towards adapting to the free boundary case the classification theorems of CMC tori by Pinkall-Sterling, Hitchin and Bobenko [63, 40, 7].

The spherical curvature lines condition of our examples is very natural in the context of finite type solutions of the sinh-Gordon equation, since they correspond to solutions of type $N = 2$, see [63, 64, 76]. For $N > 2$ the construction method is much more complicated. In this sense, it is an interesting problem to construct a free boundary CMC annulus in a geodesic ball of $\mathbb{M}^3(\kappa)$ that is not foliated by spherical curvature lines, or to show that such an example cannot exist.

Regarding embeddedness, it is very natural to conjecture that the (spherical) critical catenoids are the only embedded free boundary minimal annuli in geodesic balls of \mathbb{S}^3 ; see [57, 60]. Note that Theorem 4.1.1 implies that the embeddedness assumption cannot be removed from this conjecture.

More generally, aligned with the Open Problem 3.8.1 for the Euclidean case, one could ask whether any embedded free boundary CMC annulus in a geodesic ball of $\mathbb{R}^3, \mathbb{S}^3$ or \mathbb{H}^3 should be foliated by spherical curvature lines. We note that the existence of an embedded free boundary minimal annulus with spherical curvature lines in a geodesic ball of \mathbb{S}^3 is also open (in \mathbb{R}^3 , the results in [29] show that these examples do not exist).

We also do not know if there exist continuous deformations of free boundary CMC annuli in a fixed geodesic ball of $\mathbb{R}^3, \mathbb{S}^3$ or \mathbb{H}^3 , with a fixed mean curvature H .

Chapter 5

Free boundary minimal annuli in hyperbolic balls

5.1 Summary and main result

In this chapter we prove the existence of infinitely many compact minimal annuli of Enneper type with free boundary in some geodesic ball of \mathbb{H}^3 , and a finite prismatic symmetry group of order $4n$. In particular, there exist free boundary minimal annuli in geodesic balls of \mathbb{H}^3 that are non-rotational. This chapter is based on [18].

We now introduce the main result in this chapter. We model the hyperbolic space as $\mathbb{H}^3 := \mathbb{M}^3(-1)$, where $\mathbb{M}^3(-1)$ is defined in Section 2.5.1. Then, it holds:

Theorem 5.1.1. *There exists an open interval $\mathcal{J} \subset \left(-\frac{1}{\sqrt{2}}, -\frac{1}{\sqrt{3}}\right)$ satisfying the following property: let $q \in \mathcal{J} \cap \mathbb{Q}$, which we express as an irreducible fraction $q = -m/n$, $m, n \in \mathbb{N}$. Then, there exists $\varepsilon_0 = \varepsilon_0(q)$ and a real analytic 1-parameter family $\{\mathbb{A}_q(\eta) : \eta \in [0, \varepsilon_0)\}$ of minimal compact annuli $\mathbb{A}_q(\eta)$ in \mathbb{H}^3 such that:*

1. *The annulus $\mathbb{A}_q(\eta)$ is free boundary in some geodesic ball $\mathbf{B} = \mathbf{B}(q, \eta) \subset \mathbb{H}^3$ whose geodesic center is $\mathbf{e}_4 = (0, 0, 0, 1) \in \mathbb{H}^3$.*
2. *$\mathbb{A}_q(\eta)$ is invariant under the symmetry with respect to the totally geodesic surface $\mathbf{S} := \{x_3 = 0\} \cap \mathbb{H}^3$ and also with respect to n totally geodesic surfaces which meet equiangularly along the geodesic $\mathcal{L} := \{x_1 = x_2 = 0\} \cap \mathbb{H}^3$.*
3. *The curve $\mathbb{A}_q(\eta) \cap \mathbf{S}$ of $\mathbb{A}_q(\eta)$ is a geodesic of $\mathbb{A}_q(\eta)$ with rotation index $-m$ in \mathbf{S} .*
4. *The annulus $\mathbb{A}_q(\eta)$ is of Enneper type.*

5. If $\eta > 0$, the annulus $\mathbb{A}_q(\eta)$ has a prismatic symmetry group of order $4n$. This group is generated by the isometries in item (2). In particular, $\mathbb{A}_q(\eta)$ is not rotational.
6. If $\eta = 0$, the annulus $\mathbb{A}_q(0)$ is an m -cover of a free boundary hyperbolic catenoid.

Structure of the chapter

We start by following a similar structure to the one presented in Chapter 4. In Section 5.2, we construct a family of analytic solutions $\omega(u, v)$ to the overdetermined system (2.14) for $H = 0$ and $B = \frac{1}{4}$, which depends on three parameters (a, b, κ) . This set of solutions induces a family of minimal surfaces $\psi(u, v) = \psi(u, v; a, b, \kappa)$, each of them immersed in a space form $\mathbb{M}^3(\kappa)$ of constant curvature κ . These immersions are conformally parametrized by curvature lines. Moreover, the v -lines $v \mapsto \psi(u_0, v)$ of the immersion are *spherical*, i.e., the immersions $\psi(u, v)$ are of Enneper type; see Definition 2.5.4. By Joachimsthal's theorem, the intersection angle of $\psi(u, v)$ with $\mathcal{Q}(u_0)$ is constant along the corresponding v -line.

A key difference between Chapter 4 and the current situation is that we now use κ , the sectional curvature of the ambient space, as a parameter in the construction. To do so, it will be crucial to use the model for the spaces $\mathbb{M}^3(\kappa)$ described in Section 2.5.1, since it allows us to connect the spherical and hyperbolic spaces in a way that the immersions $\psi(u, v; a, b, \kappa)$ can be viewed as analytic mappings from an open region of \mathbb{R}^5 into \mathbb{R}^4 .

The goal of Section 5.3 is to determine the symmetries of the surfaces $\psi(u, v)$. We will define a *period map* $\Theta = \Theta(a, b, \kappa)$ with the property that the v -lines of $\psi(u, v)$ are closed whenever Θ is a rational number. In such a case, the restriction $\Sigma_0 = \Sigma_0(a, b, \kappa; u_0)$ of $\psi(u, v)$ to a strip $[-u_0, u_0] \times \mathbb{R}$ covers a minimal annulus. By our study in Section 5.2, the boundary components of Σ_0 are contained in the totally umbilical surfaces $\mathcal{Q}(-u_0)$, $\mathcal{Q}(u_0)$, and the intersection angle is constant. In particular, if we find special parameters (a, b, κ) and $u_0 > 0$ such that:

- (i) the period $\Theta(a, b, \kappa)$ is rational,
- (ii) the surfaces $\mathcal{Q}(u_0)$ and $\mathcal{Q}(-u_0)$ are compact and coincide,
- (iii) the intersection angle with the immersion $\psi(u, v)$ is $\pi/2$,

then Σ_0 is a compact annulus whose boundary components meet orthogonally the geodesic sphere $S = \mathcal{Q}(u_0) = \mathcal{Q}(-u_0)$. If $\kappa \leq 0$, one can show that Σ_0 is con-

tained in the geodesic ball B bounded by S , i.e., Σ_0 is a free boundary annulus in B . So, the rest of the chapter is devoted to finding values (a, b, κ) , $u_0 > 0$ satisfying the properties listed above.

At the end of Section 5.3, we show that the immersions $\psi(u, v) = \psi(u, v; a, b, \kappa)$ associated to the parameter $a = 1$ are rotational. More specifically, they are *spherical, Euclidean or hyperbolic* catenoids, depending on the sign of the parameter κ ; see also Section 2.6. We know by our analysis in Section 2.6 that these rotational examples have a compact piece which is free boundary in some geodesic ball of $\mathbb{M}^3(\kappa)$. We emphasize that the analysis of these examples is fundamental, as our strategy to prove Theorem 5.1.1 is to detect free boundary rotational examples within the family of minimal surfaces foliated by spherical curvature lines, and find a non-rotational bifurcation from them.

In Section 5.4 we compute explicitly the period map $\Theta(a, b, \kappa)$ for values with $a = 1$. This allows us to determine the structure of the level sets of this map for values (a, b, κ) near $a = 1$. This is relevant since we aim to find immersions $\psi(u, v) = \psi(u, v; a, b, \kappa)$ for which the v -lines are closed (i.e., the immersion covers an annulus), a condition that is satisfied whenever the period map $\Theta(a, b, \kappa)$ is a rational number.

In Section 5.5, we find a map $\tau(a, b, \kappa) : \mathcal{W} \rightarrow (0, \infty)$ defined on an open region \mathcal{W} of the parameter space (a, b, κ) such that the immersion $\psi(u, v)$ meets orthogonally the totally umbilical surfaces $\mathcal{Q}(\tau)$, $\mathcal{Q}(-\tau)$ along the v -lines $u = \pm\tau$.

We now provide a geometric motivation for Section 5.6. We already know from Section 5.3 that if $a = 1$ and $\kappa = 0$, then $\psi(u, v)$ is a Euclidean catenoid which admits a free boundary piece in some geodesic ball. Our goal now is to detect this piece by using the map τ in Section 5.5. More specifically, for every b we know that the restriction $\Sigma_0(1, b, 0; \tau)$ covers a compact piece of a catenoid which intersects the spheres $\mathcal{Q}(\tau)$, $\mathcal{Q}(-\tau)$ orthogonally, where $\tau = \tau(1, b, 0)$. We will find a special b_0 such that the spheres $\mathcal{Q}(\tau)$, $\mathcal{Q}(-\tau)$ coincide.

The relevance of Section 5.6 is that it enables us to understand the condition $\mathcal{Q}(\tau) = \mathcal{Q}(-\tau)$ for values (a, b, κ) near $(1, b_0, 0)$. A simultaneous control of this property and the rationality of the period map (already studied in Section 5.4) is carried out in Section 5.7. There, we find a countable number of real analytic curves $\hat{\mu}_q$, $q \in \mathbb{Q}$, on the parameter space (a, b, κ) lying inside the region $\{a > 1, \kappa < 0\}$ and satisfying both properties, i.e., the period map Θ is constantly q along each curve $\hat{\mu}_q$, and the spheres $\mathcal{Q}(\tau)$, $\mathcal{Q}(-\tau)$ coincide. The annuli $\Sigma_0(a, b, \kappa; \tau)$ associated to the values (a, b, κ) in these curves are shown to be free boundary, proving Theorem 5.1.1.

5.2 A family of minimal immersions of Enneper type in

$$\mathbb{M}^3(\kappa)$$

The goal of this section is to construct a family of minimal immersions in the spaces $\mathbb{M}^3(\kappa)$, where $\kappa \in (-\frac{1}{4}, \frac{1}{4})$. These surfaces will be of Enneper type and without umbilical points. We will make use of Theorems 2.4.5 and 2.5.8 to create such examples. Throughout this chapter, the constant Q associated to the Hopf differential in Theorem 2.5.8 will be $Q = \frac{1}{2}$. We will also set $H = 0$, $A = \kappa$.

5.2.1 Constructing solutions to an overdetermined system

We start by defining an adequate parameter region and initial conditions for the system (2.14) that determines minimal surfaces of Enneper type in $\mathbb{M}^3(\kappa)$. Let $\mathcal{O} \subset \mathbb{R}^3$ be the parameter space

$$\mathcal{O} := \{(a, b, \kappa) : a, b \geq 1, 4|\kappa| < 1, -4\kappa a < b\}. \quad (5.1)$$

In particular, observe that $\kappa \in (-\frac{1}{4}, \frac{1}{4})$ from now on. For each $(a, b, \kappa) \in \mathcal{O}$, we define the constants

$$\mathcal{A} := \frac{1}{2} \left(a + \frac{1}{a} \right), \quad \mathcal{B} := \frac{1}{2} \left(b + \frac{4\kappa}{b} \right). \quad (5.2)$$

We also define the functions $\alpha(u) = \alpha(u; a, b, \kappa)$ and $\beta(u) = \beta(u; a, b, \kappa)$ as the unique solutions to the differential system

$$\begin{cases} \alpha'' = \hat{a}\alpha - 2\alpha^2\beta - 2\kappa\beta, \\ \beta'' = \hat{a}\beta - 2\alpha\beta^2 - \frac{1}{2}\alpha, \end{cases} \quad (5.3)$$

with initial conditions and $\hat{a} \in \mathbb{R}$ given by

$$\begin{aligned} \alpha(0) &= \beta(0) = 0, \\ 2\alpha'(0) &= \frac{1}{2} \left(b + \frac{4\kappa}{b} - 4\kappa a - \frac{4\kappa}{a} \right) = \mathcal{B} - 4\kappa\mathcal{A}, \\ 2\beta'(0) &= \frac{1}{2} \left(a + \frac{1}{a} - b - \frac{4\kappa}{b} \right) = \mathcal{A} - \mathcal{B}, \\ 4\hat{a} &= -\frac{4\kappa}{ab} - \frac{4\kappa a}{b} - \frac{b}{a} - ab + 4\kappa + 1 = -4\mathcal{A}\mathcal{B} + 4\kappa + 1. \end{aligned} \quad (5.4)$$

We note that (5.3) coincides with (2.17) under the substitution $A = \kappa$, $Q = \frac{1}{2}$. By

(5.4), the polynomial $p(x) \equiv p(0, x)$ in (2.24) admits the factorization

$$p(x) \equiv p(0, x) = -(x - a) \left(x - \frac{1}{a} \right) (4\kappa x + b) \left(x + \frac{1}{b} \right). \quad (5.5)$$

In particular, $p(x) \geq 0$ for every $x \in [\frac{1}{a}, a]$. Hence, it follows from Theorem 2.4.5 that for every $(a, b, \kappa) \in \mathcal{O}$ there exists a unique solution $\omega(u, v)$ to the overdetermined system

$$\Delta\omega + \kappa e^{2\omega} - \frac{1}{4}e^{-2\omega} = 0, \quad (5.6a)$$

$$2\omega_u = \alpha(u)e^\omega + \beta(u)e^{-\omega}, \quad (5.6b)$$

with $e^{\omega(0,0)} = \frac{1}{a}$.

Definition 5.2.1. We denote by $\omega(u, v) = \omega(u, v; a, b, \kappa)$ the solution to (5.6) constructed above.

We observe that, up to a linear change ($\omega \mapsto \omega + \vartheta_0$) and a homothety $(u, v) \mapsto (\vartheta_1 u, \vartheta_1 v)$, condition (5.6a) can be reduced to either the sinh-Gordon equation (when $\kappa > 0$), the cosh-Gordon equation (when $\kappa < 0$), or the Liouville equation (when $\kappa = 0$).

Remark 5.2.2. Let $X(u, v) := e^{\omega(u, v)}$. Arguing as in Remark 3.2.2, at $u = 0$ it holds

$$4X_v(0, v)^2 = p(X), \quad (5.7)$$

where $p(x)$ is given by (5.5). If $a = 1$, this implies that $X(0, v) \equiv 1$, a constant, so by (5.6b), we have that $\omega = \omega(u)$ only depends on u . Otherwise, if $a > 1$, $v \mapsto X(0, v)$ is a periodic function taking values on the interval $[\frac{1}{a}, a]$. In any case, $\omega(u, v)$ can always be defined on a maximal open strip $(u, v) \in \mathcal{D}$, where

$$\mathcal{D} := (-u_{\mathcal{D}}, u_{\mathcal{D}}) \times \mathbb{R}, \quad (5.8)$$

for some $u_{\mathcal{D}} \in (0, \infty]$.

Remark 5.2.3. As mentioned before, if $a = 1$ then $\omega = \omega(u)$ does not depend on v . In particular, (5.6a) reduces to a second order differential equation for $\omega(u)$ which yields a unique solution since $\omega(0) = \omega_u(0) = 0$; see (5.4), (5.6b). This equation only depends on κ , so ω is also independent of the parameter b in this particular case. The

differential equation (5.6a) admits a first integral, namely

$$\omega_u^2 + \kappa (e^{2\omega} - 1) + \frac{1}{4} (e^{-2\omega} - 1) = 0. \quad (5.9)$$

Since $\omega(0) = 0$, $\omega_{uu}(0) > 0$, it can be deduced from (5.9) that $\omega = \omega(u)$ attains its global minimum at $u = 0$.

An adaptation of Proposition 3.2.3 ensures that any solution $\omega(u, v)$ as in Definition 5.2.1 with $\kappa > 0$ is defined in \mathbb{R}^2 . However, when $\kappa \leq 0$, the pair $(\alpha(u), \beta(u))$ in (5.3) may explode in finite time, so $\omega(u, v)$ might not be globally defined.

We note that $\alpha(u), \beta(u)$ are anti-symmetric by (5.3) and (5.4). This implies, along with (5.6b), that

$$\omega(u, v) = \omega(-u, v). \quad (5.10)$$

We have an additional symmetry property:

Lemma 5.2.4. *For every $(a, b, \kappa) \in \mathcal{O}$ there exists a value $\sigma = \sigma(a, b, \kappa) > 0$ such that $v \mapsto \omega(0, v)$ is increasing in $v \in [0, \sigma]$ and*

$$\omega(u, j\sigma + v) = \omega(u, j\sigma - v) \quad (5.11)$$

for all $j \in \mathbb{Z}$. Moreover, $\sigma = \sigma(a, b, \kappa) : \mathcal{O} \rightarrow \mathbb{R}^+$ is analytic, and

$$\sigma(1, b, \kappa) = \frac{2\pi}{\sqrt{4\kappa + 2\mathcal{B} + 1}}. \quad (5.12)$$

Proof. The proof is a straightforward adaptation of the arguments in Proposition 3.3.1 and Remark 3.5.2. Specifically, if $a > 1$, $\sigma = \sigma(a, b, \kappa)$ is defined as the first positive value for which $v \mapsto X(0, v) = e^{\omega(0, v)}$ reaches its maximum, that is, $X(0, \sigma) = a$. In this way, (5.11) can be deduced using (5.6b).

By (5.7), we find the following expression for $\sigma(a, b, \kappa)$:

$$\sigma(a, b, \kappa) = \int_{a^{-1}}^a \frac{2}{\sqrt{p(x)}} dx. \quad (5.13)$$

The change of variables $x = h_a(t) := (a - a^{-1})t + a^{-1}$ allows us to rewrite the previous integral as

$$\sigma(a, b, \kappa) = \int_0^1 \frac{2}{\sqrt{t(1-t)} \sqrt{4\kappa h_a(t)^2 + (b + 4\kappa b^{-1})h_a(t) + 1}} dx.$$

This alternative expression is analytic in the whole space \mathcal{O} and for the limit value $a = 1$ it yields (5.12). \square

5.2.2 Construction of minimal immersions in $\mathbb{M}^3(\kappa)$

By Theorem 2.5.8, the functions $\omega(u, v) = \omega(u, v; a, b, \kappa)$ constructed in the previous section induce a family of minimal immersions $\psi(u, v) = \psi(u, v; a, b, \kappa)$ of Enneper type in $\mathbb{M}^3(\kappa)$ with first and second fundamental forms given by

$$I = e^{2\omega(u,v)} (du^2 + dv^2), \quad II = \frac{1}{2}(du^2 - dv^2). \quad (5.14)$$

Thus, the principal curvatures $\kappa_1 > \kappa_2$ satisfy

$$\kappa_1(u, v) = -\kappa_2(u, v) = \frac{1}{2}e^{-2\omega(u,v)}. \quad (5.15)$$

Definition 5.2.5. We denote by $\Sigma = \Sigma(a, b, \kappa)$ the surface given by the immersion $\psi(u, v)$ associated to the parameters $(a, b, \kappa) \in \mathcal{O}$.

Remark 5.2.6. By definition of the model spaces $\mathbb{M}^3(\kappa) \subset \mathbb{R}^4$ in Section 2.5.1, the immersions $\psi(u, v) : \mathcal{D} \rightarrow \mathbb{M}^3(\kappa)$ can be seen as \mathbb{R}^4 -valued maps. From this perspective, it follows from (2.32)-(2.33), (5.3)-(5.4) and (5.6) that the immersions $\psi(u, v; a, b, \kappa)$ depend analytically on the parameters (a, b, κ) .

By (5.6b), the immersions $\psi(u, v)$ are of Enneper type, that is, every v -line $v \mapsto \psi(u, v)$ lies in a certain totally umbilical surface $\mathcal{Q}(u) \subset \mathbb{M}^3(\kappa)$, and the intersection angle $\theta(u)$ between $\mathcal{Q}(u)$ and $\psi(u, v)$ is constant along each v -line. In particular, if $\kappa \neq 0$, we have $\mathcal{Q}(u) = S[\tilde{m}(u), \tilde{d}(u)]$, where $\tilde{m}(u), \tilde{d}(u)$ and $\theta(u)$ are related to the pair $(\alpha(u), \beta(u))$ by

$$\alpha(u) = -\frac{2\tilde{d}\kappa}{\sin \theta \sqrt{\langle \tilde{m}, \tilde{m} \rangle_\kappa - \kappa \tilde{d}^2}}, \quad \beta = -\cot \theta, \quad (5.16)$$

and

$$\tilde{m}(u) = -2e^{-\omega}\psi_u + 2\beta N + \alpha\psi, \quad (5.17)$$

see (2.35), (2.36). Alternatively, if $\kappa = 0$ but $\alpha(u) \neq 0$, $\mathcal{Q}(u)$ is a sphere of radius $R = R(u)$. In this case, $R(u)$ and the intersection angle $\theta(u)$ satisfy

$$R^2 = \frac{4 + 4\beta^2}{\alpha^2}, \quad \beta = -\cot \theta, \quad (5.18)$$

according to (2.12). Also, by (2.13), the center $\widehat{c}(u) \in \mathbb{M}^3(0)$ of the sphere $\mathcal{Q}(u)$ simplifies to

$$\widehat{c}(u) = \psi - \frac{2}{\alpha}\psi_u e^{-\omega} + \frac{2\beta}{\alpha}N. \quad (5.19)$$

Finally, if $\kappa = \alpha(u) = 0$, then $\mathcal{Q}(u)$ is a plane and the intersection angle θ is given as in (5.18).

According to Remark 2.5.3 and our previous discussion, for every $\kappa \in (-\frac{1}{4}, \frac{1}{4})$, the condition for $\mathcal{Q}(u)$ to be a sphere is that

$$\alpha(u)^2 + 4\kappa(1 + \beta(u)^2) > 0. \quad (5.20)$$

Remark 5.2.7. *If (5.20) holds for some $u_0 \in (-u_{\mathcal{D}}, u_{\mathcal{D}})$, there exists a neighbourhood I of u_0 such that $\mathcal{Q}(u)$ is a sphere for every $u \in I$. In such a case, if $\kappa \neq 0$, the map $\widetilde{m}(u)$ admits the rescaling*

$$m(u) := \epsilon \frac{-2e^{-\omega}\psi_u + 2\beta N + \alpha\psi}{\sqrt{\alpha^2 + 4\kappa(1 + \beta^2)}}, \quad (5.21)$$

where $\epsilon = \pm 1$ if $\kappa > 0$ and $\epsilon = \text{sgn}(\alpha)$ if $\kappa < 0$. In this way, $m(u) \in \mathbb{M}^3(\kappa)$ is the geodesic center of $\mathcal{Q}(u)$. We note that the map $m(u)$ is well defined when $\kappa = 0$, and in fact it coincides with the center function (5.19) under the choice $\epsilon = \text{sgn}(\alpha)$.

Remark 5.2.8. *In the conditions of the previous remark, assume further that $\alpha(u) \neq 0$. Then, choosing $\epsilon = \text{sgn}(\alpha)$ in (5.21), it follows that $m(u) = m(u; a, b, \kappa)$ is analytic as a function of both u and $(a, b, \kappa) \in \mathcal{O}$, as $\psi(u, v)$ and the pair $(\alpha(u), \beta(u))$ are. Note further that if $\kappa \leq 0$, then (5.20) automatically implies $\alpha(u) \neq 0$.*

Remark 5.2.9. *It follows from (2.32), (5.4) and (5.17) that the vectors $\widetilde{m}(0)$, $\widetilde{m}'(0)$ are linearly independent for all $(a, b, \kappa) \in \mathcal{O}$: indeed,*

$$\begin{aligned} \widetilde{m}(0) &= -2e^{-\omega(0,0)}\psi_u(0,0) = -2\mathbf{e}_3, \\ \widetilde{m}'(0) &= BN(0,0) + C\psi(0,0) = B\mathbf{e}_1 + C\mathbf{e}_4, \end{aligned} \quad (5.22)$$

where B, C are given by

$$\begin{aligned} B &= -\frac{1}{2} \left(a - \frac{1}{a} + 2\mathcal{B} \right), \\ C &= \frac{1}{4} \left(2\mathcal{B} - 4\kappa \left(a - \frac{1}{a} \right) \right). \end{aligned} \quad (5.23)$$

In particular, $\mathcal{P} := \text{span}\{\tilde{m}(0), \tilde{m}'(0)\} \subset \mathbb{R}_\kappa^4$ is a 2-dimensional linear subspace. Thus, by Proposition 2.5.10, we deduce that $\tilde{m}(u) \in \mathcal{P}$ for all u .

We note that if $\mathcal{Q}(u)$ is a 2-sphere, then its geodesic center $m(u)$ must belong to both $\mathbb{M}^3(\kappa)$ and \mathcal{P} , so in particular the set $\mathbb{M}^3(\kappa) \cap \mathcal{P}$ is not empty (and thus, a geodesic; see Remark 2.5.11). In the following lemma we explore the properties of this intersection.

Lemma 5.2.10. *Let \mathcal{P} be the plane in Remark 5.2.9 and \mathbf{S} be the totally geodesic surface*

$$\mathbf{S} := \mathbb{M}^3(\kappa) \cap \{x_3 = 0\}. \quad (5.24)$$

Then, $\mathcal{L} := \mathbb{M}^3(\kappa) \cap \mathcal{P}$ is a geodesic of $\mathbb{M}^3(\kappa)$ if and only if $\kappa \geq 0$, or $\kappa < 0$ and \mathcal{P} is timelike. In such a case, if $\kappa \leq 0$, then $\mathcal{L} \cap \mathbf{S}$ is a single point p , while for $\kappa > 0$ this intersection consists of two antipodal points $\{p, -p\}$. Moreover, \mathcal{L} is orthogonal to \mathbf{S} at p , and

$$p = -\frac{B\mathbf{e}_1 + C\mathbf{e}_4}{C^2 + \kappa B^2}, \quad (5.25)$$

where B, C are the constants in (5.23).

Proof. By (5.22), we can parametrize the plane \mathcal{P} as

$$\mathcal{P} = \{\vartheta_1\mathbf{e}_3 + \vartheta_2(B\mathbf{e}_1 + C\mathbf{e}_4) : \vartheta_1, \vartheta_2 \in \mathbb{R}\}, \quad (5.26)$$

with B, C as in (5.23). The assumption that \mathcal{P} is timelike for $\kappa < 0$ is equivalent to

$$C^2 + \kappa B^2 > 0. \quad (5.27)$$

Notice further that if $\kappa = 0$, then $C = b/4 \neq 0$. We deduce that if either $\kappa \geq 0$ or $\kappa < 0$ and (5.27) holds, the point p in (5.25) is well defined and belongs to $\mathbb{M}^3(\kappa) \cap \mathcal{P}$. In such a case, the (non-empty) set $\mathcal{L} = \mathcal{P} \cap \mathbb{M}^3(\kappa)$ must be a geodesic of $\mathbb{M}^3(\kappa)$; see Remark 2.5.11.

Conversely, assume that $\mathcal{L} = \mathcal{P} \cap \mathbb{M}^3(\kappa)$ is a geodesic. If $\kappa \geq 0$, we have nothing to prove, while if $\kappa < 0$, we have to show that \mathcal{P} is timelike. This is immediate: indeed, any $p_0 \in \mathcal{L} \subset \mathcal{P}$ must be timelike, since $p_0 \in \mathbb{M}^3(\kappa)$. Hence, \mathcal{P} is timelike.

Finally, notice that $\mathcal{L} \cap \mathbf{S} = \mathcal{P} \cap \{x_3 = 0\} \cap \mathbb{M}^3(\kappa)$. By (5.26), it is straightforward that $\mathcal{L} \cap \mathbf{S}$ is either the single point p in (5.25) for $\kappa \leq 0$ or the antipodal pair $\{p, -p\}$ when $\kappa > 0$. Furthermore, the vector \mathbf{e}_3 is tangent to both \mathcal{P} and $\mathbb{M}^3(\kappa)$ at the point p , so in particular \mathbf{e}_3 is tangent to \mathcal{L} at p . However, \mathbf{e}_3 is orthogonal to \mathbf{S} , so \mathcal{L} is orthogonal to \mathbf{S} at p . \square

5.3 Geometric properties of $\Sigma(a, b, \kappa)$

Let $\psi(u, v)$ denote the minimal immersion associated to $\Sigma(a, b, \kappa)$ for some $(a, b, \kappa) \in \mathcal{O}$ as defined in the previous section. The symmetries of $\psi(u, v)$ can be analyzed using the function $\omega(u, v)$ from Definition 5.2.1, following a procedure analogous to the one presented in Section 4.3.

Remark 5.3.1. *In analogy with Lemma 4.3.1, it can be shown using (5.10) that $\Sigma(a, b, \kappa)$ is symmetric with respect to the totally geodesic surface \mathbf{S} given by (5.24), and that (4.13) holds.*

By (5.11), we find more symmetries:

Proposition 5.3.2. *For every $(a, b, \kappa) \in \mathcal{O}$, the surface $\Sigma(a, b, \kappa)$ satisfies properties (1)-(5) of Proposition 4.3.2, where $\sigma = \sigma(a, b, \kappa)$ is the value in Lemma 5.2.4 and \mathcal{P} is given by Remark 5.2.9.*

Proof. A straightforward adaptation of the proof of Proposition 4.3.2 is valid for every $(a, b, \kappa) \in \mathcal{O}$ with $\kappa \neq 0$. In fact, the arguments in items (1)-(4) also apply when $\kappa = 0$, so we just need to show item (5) in the Euclidean case.

First, we note that both the planes Ω_j in item (1) and the line \mathcal{L} are orthogonal to \mathbf{S} ; see Lemma 5.2.10. In particular, \mathcal{L} is parallel to every Ω_j , so if we prove that the intersection $\mathcal{L} \cap \Omega_j$ is not empty, then $\mathcal{L} \subset \Omega_j$. We do this next.

By (5.4), it holds $\alpha'(0) = \frac{b}{4} > 0$, so $\alpha(u) \neq 0$. In particular, there exists $u_0 \in \mathbb{R}$ for which we can consider the center function $\widehat{c}(u) = m(u)$ in (5.21). By evaluating the right-hand side of (5.21) at the values $(u, v) = (u_0, j\sigma)$, it is possible to check that $m(u_0) \in \Omega_j$ for all $j \in \mathbb{Z}$. By construction, $m(u_0)$ also belongs to \mathcal{L} , and thus

$$\mathcal{L} \subset \bigcap_{j \in \mathbb{Z}} \Omega_j.$$

Now, by (4.15), the intersection $\bigcap_{j \in \mathbb{Z}} \Omega_j$ is an affine space of dimension at most one, so we deduce (4.16). \square

We will be interested in those surfaces $\Sigma(a, b, \kappa)$ for which (4.15) holds, as this allows us to identify \mathcal{L} with the intersection of the surfaces Ω_j .

Definition 5.3.3. *We define $\mathcal{O}^- \subset \mathcal{O}$ as the open subset for which the condition (4.15) holds.*

Remark 5.3.4. *It will later be shown that \mathcal{O}^- is not empty, as it contains every $(a, b, \kappa) \in \mathcal{O}$ with $a = 1$; see Proposition 5.4.2. In this set, the map $p = p(a, b, \kappa) : \mathcal{O}^- \rightarrow \mathbb{R}^4$ in (5.25) is well defined and analytic.*

5.3.1 The period map

Let $(a, b, \kappa) \in \mathcal{O}^-$, and consider the immersion $\psi(u, v)$ associated to $\Sigma(a, b, \kappa)$. We now want to determine the conditions under which the planar curve $v \mapsto \Gamma(v) := \psi(0, v)$ is closed, or equivalently, periodic. In order to do so, we need to study the behaviour of the period map introduced in Section 4.4 in the current context.

By Lemma 5.2.10 and the fact that $(a, b, \kappa) \in \mathcal{O}^-$, we know that $\mathcal{L} = \mathcal{P} \cap \mathbb{M}^3(\kappa)$ is a geodesic of $\mathbb{M}^3(\kappa)$ which meets \mathbf{S} in (5.24) at the point p in (5.25). Observe that there is a unique isometry in $\mathbb{M}^3(\kappa)$ which fixes the coordinates x_2, x_3 and sends p to $\mathbf{e}_4 \in \mathbb{M}^3(\kappa)$. This will modify the initial data for $\psi(0, 0)$ and $N(0, 0)$ in (2.32), but it will do so in an analytic way, since p is analytic; see Remark 5.3.4. In particular, this isometry sends \mathcal{L} to the geodesic $\{x_1 = x_2 = 0\} \cap \mathbb{M}^3(\kappa) \subset \mathbb{R}^4$.

Remark 5.3.5. *From now on, for every $(a, b, \kappa) \in \mathcal{O}^-$ we will make use of the aforementioned initial data for the surface $\Sigma(a, b, \kappa)$ instead of (2.32).*

Arguing as in Section 4.4, we will project the spaces $\mathbb{M}^3(\kappa)$, $\kappa \in (-\frac{1}{4}, \frac{1}{4})$ into \mathbb{R}^3 via the stereographic projection φ_κ , which is defined as the restriction to $\mathbb{M}^3(\kappa)$ of the map φ introduced in (4.18). For $\kappa > 0$, φ_κ sends $\mathbb{M}^3(\kappa) \setminus \{-\mathbf{e}_4\}$ to \mathbb{R}^3 . For $\kappa < 0$, φ_κ sends $\mathbb{M}^3(\kappa)$ to the Euclidean 3-ball B_κ of radius $\frac{2}{\sqrt{-\kappa}}$. Finally, for $\kappa = 0$, φ_0 reduces to the projection $\varphi(x_1, x_2, x_3, 1) = (x_1, x_2, x_3)$. In any case, φ_κ sends the surface \mathbf{S} to the plane $\{z = 0\}$ and the geodesic \mathcal{L} to the line $\{x = y = 0\}$, where (x, y, z) are the usual Euclidean coordinates on \mathbb{R}^3 .

Remark 5.3.6. *It follows from Definition 2.5.1 and (4.18) that the projections φ_κ are conformal for all $\kappa \in (-\frac{1}{4}, \frac{1}{4})$.*

As mentioned before, we are interested in studying the geometry and periodicity properties of the curve $\Gamma(v) = \psi(0, v)$. We will do so by using its stereographic projection into \mathbb{R}^3 , that is, $\gamma := \varphi_\kappa \circ \Gamma$. In particular, γ is contained in the plane $\{z = 0\} \subset \mathbb{R}^3$.

Definition 5.3.7. *For any $(a, b, \kappa) \in \mathcal{O}^-$, we define the period $\Theta = \Theta(a, b, \kappa)$ as*

$$\Theta := \frac{1}{\pi} \int_0^\sigma \kappa_\gamma ||\gamma'||| dv, \quad (5.28)$$

where $\sigma = \sigma(a, b, \kappa)$ is the value in Lemma 5.2.4.

Remark 5.3.8. *We recall that the value $\pi\Theta(a, b, \kappa)$ measures the variation of the unit tangent to $\gamma(v)$ along the interval $[0, \sigma]$. We also note that the map $\Theta(a, b, \kappa)$ is analytic in \mathcal{O}^- .*

Remark 5.3.9. *Under the assumption that $\Theta(a, b, \kappa) = m/n \in \mathbb{Q}$ with $n \in \mathbb{N} \setminus \{0\}$ and m/n irreducible, the same periodicity and symmetry properties established in Proposition 4.4.4 hold for the curve $\Gamma(v)$ in this new context. Specifically,*

$$\Gamma(v + 2n\sigma) = \Gamma(v).$$

Moreover, $\Gamma : [0, 2n\sigma] \rightarrow \mathbf{S}$ is a closed curve with rotation index $m \in \mathbb{Z}$, and when $a > 1$, the curve has a dihedral symmetry group D_n with $n \geq 2$.

Corollary 5.3.10. *Let $(a, b, \kappa) \in \mathcal{O}^-$ such that $\Theta(a, b, c) = m/n \in \mathbb{Q}$. Then, for any $u_0 \in (-u_{\mathcal{D}}, u_{\mathcal{D}})$, the v -line $v \mapsto \psi(u_0, v)$ is $2n\sigma$ -periodic, where σ is given by Lemma 5.2.4; see also (5.8).*

5.3.2 Constructing minimal annuli

We will now use the results of Proposition 5.3.2 and Remark 5.3.9 to construct a set of compact minimal annuli in $\mathbb{M}^3(\kappa)$ and determine their symmetries.

Definition 5.3.11. *For any $(a, b, \kappa) \in \mathcal{O}$ and $u_0 \in (0, u_{\mathcal{D}})$, we define $\Sigma_0(a, b, \kappa; u_0)$ as the restriction of the immersion $\psi(u, v)$ to the strip $[-u_0, u_0] \times \mathbb{R}$. By Corollary 5.3.10, if $\Theta(a, b, \kappa) = m/n \in \mathbb{Q}$, then Σ_0 is a compact minimal annulus under the identification $(u, v) \sim (u, v + 2n\sigma)$, where σ is given by Lemma 5.2.4.*

The symmetry properties of the annuli Σ_0 are made precise in the following result.

Theorem 5.3.12. *Let $(a, b, \kappa) \in \mathcal{O}^-$ so that $\Theta(a, b, \kappa) = m/n \in \mathbb{Q}$, where m, n are coprime integers. Then, for any $u_0 \in (0, u_{\mathcal{D}})$, the minimal annulus $\Sigma_0(a, b, \kappa; u_0)$ in Definition 5.3.11 satisfies:*

1. Σ_0 is invariant under the reflection with respect to the totally geodesic surface $\mathbf{S} \subset \mathbb{M}^3(\kappa)$ in (5.24) and also with respect to n totally geodesic surfaces $\Omega_j \subset \mathbb{M}^3(\kappa)$ which meet equiangularly along the geodesic \mathcal{L} of Lemma 5.2.10.
2. The boundary components of Σ_0 , given by the v -lines $\psi(u_0, v)$ and $\psi(-u_0, v)$, intersect the totally umbilical surfaces $\mathcal{Q}(u_0)$, $\mathcal{Q}(-u_0) \subset \mathbb{M}^3(\kappa)$ at a constant angle $\theta(u_0)$. Moreover, $\mathcal{Q}(u_0) = \Psi_{\mathbf{S}}(\mathcal{Q}(-u_0))$, where $\Psi_{\mathbf{S}}$ denotes the reflection with respect to \mathbf{S} .
3. Assume that $\beta(u_0) = 0$. Then, Σ_0 meets the surfaces $\mathcal{Q}(u_0)$, $\mathcal{Q}(-u_0)$ orthogonally.

4. Assume that $\tilde{m}_3(u_0) = 0$, where $\tilde{m}_3(u)$ denotes the third coordinate of the map $\tilde{m}(u)$ in (5.17). Then, $\mathcal{Q}(u_0) = \mathcal{Q}(-u_0)$, and in fact these surfaces are 2-spheres centered at $\mathbf{e}_4 \in \mathbb{M}^3(\kappa)$.
5. If $a > 1$, Σ_0 has a prismatic symmetry group of order $4n$, that is, $D_n \times \mathbb{Z}_2$. This group is generated by the reflections described in item (1). In particular, Σ_0 is not rotational.

Proof. The result follows from a straightforward adaptation of Theorem 4.5.1 to the current context. Here, we use the symmetry results for the surfaces $\Sigma(a, b, \kappa)$ given by Remark 5.3.1 and Proposition 5.3.2. \square

Remark 5.3.13. Let $(a, b, \kappa) \in \mathcal{O}^-$, $u_0 \in (0, u_{\mathcal{D}})$ such that $\Theta(a, b, \kappa) \in \mathbb{Q}$ and $\tilde{m}_3(u_0) = \beta(u_0) = 0$. If we further assume that $\kappa \leq 0$, then it is an immediate consequence of the maximum principle that the compact annulus $\Sigma_0 = \Sigma_0(a, b, \kappa; u_0)$ lies in the ball B bounded by the sphere $\mathcal{Q}(u_0)$, so it is actually free boundary in B .

5.3.3 The geometry of the surfaces $\Sigma(1, b, \kappa)$

We conclude this section by studying the surfaces associated to $(a, b, \kappa) \in \mathcal{O}$ in the special case $a = 1$. Recall that in this situation the function $\omega(u)$ only depends on u ; see Remark 5.2.2. Arguing as in Section 4.6, we see that Σ is invariant under a 1-parameter group \mathcal{G} of orientation-preserving ambient isometries of $\mathbb{M}^3(\kappa)$. In particular, the v -line $\Gamma(v) = \psi(0, v)$ corresponds to the orbit of $\psi(0, 0)$ under the action of \mathcal{G} . This curve is contained in the totally geodesic surface \mathbf{S} in (5.24). The geodesic curvature of Γ in \mathbf{S} is constant and coincides with $\kappa_2 \equiv -\frac{1}{2}$, as $\Sigma(1, b, \kappa)$ meets \mathbf{S} orthogonally; see (5.15) and Remark 5.3.1. Since \mathbf{S} is a surface of constant curvature κ , the curve Γ will be a circle (and hence, bounded) provided that $\kappa > -\frac{1}{4}$. This property holds by definition of the set \mathcal{O} ; see (5.1). These facts imply that \mathcal{G} must be a rotation group in $\mathbb{M}^3(\kappa)$, and so the immersions $\Sigma(1, b, \kappa)$ are catenoids in $\mathbb{M}^3(\kappa)$.

In Section 2.6.1, we studied the set of catenoids in $\mathbb{M}^3(\kappa)$ in terms of parametrizations $\psi(\mathfrak{s}, \theta)$. We determine next the relation between the parameters (u, v) and (\mathfrak{s}, θ) :

Lemma 5.3.14. *The parameters (\mathfrak{s}, θ) and (u, v) are related by a change of variables $\mathfrak{s} = \mathfrak{s}(u)$, $\theta = \theta(v)$. Moreover, $\mathfrak{s}'(u) = e^{\omega(u)}$ and $\mathfrak{s}(0) = 0$.*

Proof. By the discussion in Section 2.6.1, we know that the \mathfrak{s} -curves in $\psi(\mathfrak{s}, \theta)$ and the u -curves in $\psi(u, v)$ correspond to the profile curves of the rotational surfaces, so we can express $\mathfrak{s} = \mathfrak{s}(u)$. Moreover, by (5.14) and since \mathfrak{s} is the arc-length parameter,

it holds $\mathfrak{s}'(u) = e^{\omega(u)}$. Similarly, θ and v both represent the rotation parameter, so $\theta = \theta(v)$. Finally, the equality $\mathfrak{s}(0) = 0$ follows from the fact that the curvatures of the \mathfrak{s} -curve $\psi(\mathfrak{s}, 0)$ and the u -curve $\psi(u, 0)$ both attain their maximum value at the point $u = \mathfrak{s} = 0$; this follows from Propositions 2.6.1, 2.6.3, 2.6.5, equation (5.15) and Remark 5.2.3. \square

We note that the metrics $\omega(u)$ for $a = 1$ do not depend on the parameter b , according by Remark 5.2.3. Geometrically, this implies that for every b , the immersions $\Sigma(1, b, \kappa)$ yields the same catenoid in $\mathbb{M}^3(\kappa)$. The fact that the curvature at the *neck* of the catenoid is $\kappa_2(0, v) = -\frac{1}{2}$, along with (2.39) and (2.42), allows us to identify $\Sigma(1, b, \kappa)$ with the catenoid $\mathcal{S}(\kappa, 0, \frac{2}{1+4\kappa})$. In particular, the reparametrization $u(\mathfrak{s})$ only depends on κ , i.e., $u(\mathfrak{s}) = u(\mathfrak{s}; \kappa)$. This motivates the following definition:

Definition 5.3.15. *For every $\kappa \in (-\frac{1}{4}, \frac{1}{4})$, we denote by $\tilde{u} = \tilde{u}(\kappa)$ the value $\tilde{u} := u(\tilde{\mathfrak{s}}; \kappa)$, where $\tilde{\mathfrak{s}} = \tilde{\mathfrak{s}}(\kappa, 0, \frac{2}{1+4\kappa})$ is the free boundary value defined in Theorem 2.6.9.*

Remark 5.3.16. *We note that, by Theorem 2.6.9, the restriction of $\psi(u, v)$ to $[-\tilde{u}, \tilde{u}] \times \mathbb{R}$ yields an infinite cover of a compact, embedded free boundary catenoid. Thus, \tilde{u} is necessarily below the value $u_{\mathcal{D}}$ in (5.8).*

The rotation axis of the examples $\Sigma(1, b, \kappa)$, which we denote by $\mathcal{X} \subset \mathbb{M}^3(\kappa)$, is a geodesic pointwise fixed by any isometry of \mathcal{G} . This geodesic coincides with the set \mathcal{L} introduced in Lemma 5.2.10:

Proposition 5.3.17. *For any $(1, b, \kappa) \in \mathcal{O}$, the set \mathcal{L} in Lemma 5.2.10 is a geodesic. Moreover, \mathcal{L} coincides with the rotation axis \mathcal{X} of the surface $\Sigma(1, b, \kappa)$.*

Proof. By Lemma 5.2.10, we know that \mathcal{L} is a geodesic if $\kappa \geq 0$, while for $\kappa < 0$ we need to check that the plane \mathcal{P} is timelike. This is immediate by (5.26) since the vector $B\mathbf{e}_1 + C\mathbf{e}_4 = \frac{\mathcal{B}}{2}(\mathbf{e}_4 - 2\mathbf{e}_1) \in \mathcal{P}$ is timelike; see also (2.28).

Let us now prove that $\mathcal{L} = \mathcal{X}$. First, notice that the v -curve $\Gamma(v) = \psi(0, v)$ parametrizes a circle in $\mathbf{S} \subset \mathbb{M}^3(\kappa)$, so the map $v \mapsto \psi_v(0, v)$ is not constant. In particular, we can choose $\hat{\sigma} > 0$ such that the vectors $\hat{\nu}_0 := \psi_v(0, 0)$ and $\hat{\nu}_1 := \psi_v(0, \hat{\sigma})$ are linearly independent. More generally, we can define the vectors $\hat{\nu}_j := \psi_v(0, j\hat{\sigma})$, $j \in \mathbb{Z}$ and consider the totally geodesic surfaces $\hat{\Omega}_j \subset \mathbb{M}^3(\kappa)$ orthogonal to $\hat{\nu}_j$ at $\psi(0, j\hat{\sigma})$. Since the metric $\omega = \omega(u)$ does not depend on v , we can apply the arguments of the proof of Proposition 5.3.2 using $\hat{\sigma}, \hat{\nu}_j, \hat{\Omega}_j$ instead of σ, ν_j, Ω_j to prove that:

1. If $\hat{\Psi}_j$ is the reflection with respect to $\hat{\Omega}_j$, then

$$\psi(u, v + j\hat{\sigma}) = \hat{\Psi}_j(\psi(u, j\hat{\sigma} - v)).$$

2. The geodesic \mathcal{L} coincides with the intersection of the surfaces $\widehat{\Omega}_j$, that is,

$$\mathcal{L} = \bigcap_{j \in \mathbb{Z}} \widehat{\Omega}_j. \quad (5.29)$$

In particular, $\mathcal{L} \subset \mathbb{M}^3(\kappa)$ is the unique geodesic fixed pointwise by the isometries $\widehat{\Psi}_j$. These isometries must also fix the rotation axis \mathcal{X} of the surface, so necessarily $\mathcal{X} = \mathcal{L}$. \square

Remark 5.3.18. For every $u > 0$, let us denote by ζ_u the geodesic passing through the point $\psi(u, 0)$ with tangent vector $\psi_u(u, 0)$. Arguing as in Remark 4.8.4, we may define the function $\widehat{p} = \widehat{p}(u) : \mathcal{I} \rightarrow \mathbb{M}^3(\kappa)$ such that for every $u \in \mathcal{I}$, $\widehat{p}(u)$ is the unique intersection point between ζ_u and the axis \mathcal{X} , where $\mathcal{I} \subset \mathbb{R}$ is a neighbourhood of $\widetilde{u}(\kappa)$. In particular, $\widehat{p}_3(\widetilde{u}) = 0$ and $\widehat{p}'_3(\widetilde{u}) > 0$, where $\widehat{p}_3(u)$ denotes the third coordinate of $\widehat{p}(u)$.

5.4 The period map for rotational immersions

In this section we will obtain an explicit expression for the the period map $\Theta(a, b, \kappa)$ for every $(a, b, \kappa) \in \mathcal{O}$ with $a = 1$; see (5.1). In particular, we will show that every $(1, b, \kappa) \in \mathcal{O}$ belongs to \mathcal{O}^- and so $\Theta(1, b, \kappa)$ is indeed well defined. To achieve this purpose, we will adapt the results in Section 4.7 to our current context.

Proposition 5.4.1. Let $(1, b, \kappa) \in \mathcal{O}^-$. Then,

$$\Theta(1, b, \kappa) = -\frac{\sqrt{4\kappa + 1}}{\sqrt{4\kappa + 2\mathcal{B} + 1}}. \quad (5.30)$$

Proof. The proof is a straightforward adaptation of Proposition 4.7.1. Let $\psi(u, v)$ be the immersion associated to $\Sigma(1, b, \kappa)$ and φ_κ be the stereographic projection from $\mathbb{M}^3(\kappa) \setminus \{-e_4\}$ to \mathbb{R}^3 ; see the discussion after Remark 5.3.5. We can use the inverse map $\varphi_\kappa^{-1} = \varphi_\kappa^{-1}(x, y, z)$ to express the metric on $\mathbf{S} \setminus \{-e_4\}$ (where \mathbf{S} is given by (5.24)) as

$$\varrho(dx^2 + dy^2), \quad \varrho := \frac{1}{\left(1 + \frac{\kappa}{4}(x^2 + y^2)\right)^2}, \quad (5.31)$$

where (x, y) are the usual Euclidean coordinates on $\mathbb{R}^2 \equiv \mathbb{R}^3 \cap \{z = 0\}$, which

corresponds to $\varphi_\kappa^{-1}(\mathbf{S} \setminus \{-\mathbf{e}_4\})$. In particular, for the curve $\gamma = \varphi_\kappa \circ \Gamma$, it holds

$$\|\gamma'\| = \frac{e^{\omega(0,v)}}{\sqrt{\varrho}}. \quad (5.32)$$

Since the projection φ_κ is conformal (see Remark 5.3.6), we can relate the geodesic curvature κ_Γ of $\Gamma(v)$ in \mathbf{S} with the curvature κ_γ of the planar curve $\gamma(v)$ in \mathbb{R}^2 by

$$\kappa_\gamma = \frac{\langle \nabla \sqrt{\varrho}, \mathbf{n} \rangle}{\sqrt{\varrho}} + \sqrt{\varrho} \kappa_\Gamma, \quad (5.33)$$

where $\nabla, \langle \cdot, \cdot \rangle$, denote the usual Euclidean gradient and inner product respectively, while $\mathbf{n} = \mathbf{n}(v)$ is the unit normal of $\gamma(v)$. Since $\Gamma(v) \subset \mathbf{S}$ has constant negative geodesic curvature $\kappa_\Gamma \equiv -\frac{1}{2}$ (see Subsection 5.3.3), we deduce that its projection $\gamma(v)$ is a negatively oriented circle of some radius $r > 0$ in \mathbb{R}^2 . This circle must be centered at $(0, 0)$: indeed, $(0, 0) = \varphi_\kappa(\mathbf{e}_4)$, and by Proposition 5.3.17, the rotation axis \mathcal{X} of the immersion $\psi(u, v)$ coincides with the geodesic \mathcal{L} , which passes through \mathbf{e}_4 . In particular, along the curve $\gamma(v)$ we have that $\mathbf{n} = \frac{1}{r}\gamma(v)$, $\kappa_\gamma = -\frac{1}{r}$ and

$$\sqrt{\varrho} = \frac{1}{1 + \frac{\kappa}{4}r^2}, \quad \nabla \sqrt{\varrho} = -\frac{\kappa}{2(1 + \frac{\kappa}{4}r^2)^2} \gamma(v). \quad (5.34)$$

It follows then from (5.33) that r satisfies

$$r = \frac{4}{1 + \sqrt{1 + 4\kappa}}. \quad (5.35)$$

Hence, by definition of the period map, (5.12), (5.32), and having in mind that $e^{\omega(0,v)} \equiv 1$ if $a = 1$, we deduce (5.30). \square

Proposition 5.4.2. *Every $(a, b, \kappa) \in \mathcal{O}$ with $a = 1$ belongs to \mathcal{O}^- . Moreover, $\Theta(1, b, \kappa)$ takes values in $(-\frac{\sqrt{2}}{2}, 0)$.*

Proof. Let $(1, b, \kappa) \in \mathcal{O}$. We know that $\Sigma(1, b, \kappa)$ is a catenoid whose rotation axis \mathcal{X} coincides with the geodesic \mathcal{L} of Lemma 5.2.10; see Proposition 5.3.17. Following the discussion at the beginning of Section 5.3.1, there exists a unique isometry in $\mathbb{M}^3(\kappa)$ which fixes the coordinates x_2, x_3 and sends the point p in (5.25) to \mathbf{e}_4 . We apply this isometry and consider the stereographic projection φ_κ given by (4.18). Setting $\Gamma(v) = \psi(0, v)$ and $\gamma = \varphi_\kappa \circ \Gamma$, we can define the value

$$\widehat{\theta} := \frac{1}{\pi} \int_0^\sigma \kappa_\gamma \|\gamma'\| dv. \quad (5.36)$$

If $(1, b, \kappa)$ belonged to \mathcal{O}^- , then $\widehat{\theta}$ would coincide with the period map $\Theta(1, b, \kappa)$. In any case, the integral in (5.36) is well defined, and $\pi\widehat{\theta}$ measures the variation of the angle of the unit tangent vector of $\gamma(v)$ from $v = 0$ to $v = \sigma$. In fact, applying the same computations as in Proposition 5.4.1 we obtain that the value $\widehat{\theta}$ also satisfies (5.30). In particular, it holds $\widehat{\theta} \in \left(-\frac{\sqrt{2}}{2}, 0\right)$.

So, it remains to show that $(1, b, \kappa)$ belongs to \mathcal{O}^- . For this, we prove that the vectors $\nu_0 = \psi_v(0, 0)$, $\nu_1 = \psi_v(0, \sigma)$ satisfy (4.15). First, we note that ν_0, ν_1 are not collinear: otherwise, $\widehat{\theta}$ should be an integer. This shows (4.15) provided that $\kappa \geq 0$. If $\kappa < 0$, we also need to check that the plane $\Lambda_0 := \text{span}\{\nu_0, \nu_1\}$ is spacelike. Observe that both ν_0, ν_1 are orthogonal to the vectors $\widetilde{m}(0), \widetilde{m}'(0)$ which span the plane \mathcal{P} in Remark 5.2.9, so $\Lambda_0^\perp = \mathcal{P}$. Now, since $\mathcal{L} = \mathcal{X}$ is a geodesic, we deduce by Lemma 5.2.10 that \mathcal{P} is timelike, so Λ_0 must be spacelike. \square

Remark 5.4.3. Let $(1, b, \kappa) \in \mathcal{O}$ and $\Theta_0 := \Theta(1, b, \kappa)$. Assume further that $\Theta_0 \in \mathbb{Q}$ and express Θ_0 as an irreducible fraction $\Theta_0 = -m/n$, $m, n \in \mathbb{N}$. Then, the annulus $\Sigma_0(1, b, \kappa; u_0)$ is an m -cover of a piece of a catenoid under the identification $(u, v) \sim (u, v + 2n\sigma)$; see Definition 5.3.11.

Remark 5.4.4. Let $(1, b_0, \kappa_0) \in \mathcal{O}$ and $\Theta_0 := \Theta(1, b_0, \kappa_0)$. By (5.30) it follows that the partial derivative $\frac{\partial \Theta}{\partial b}(1, b_0, \kappa_0)$ is strictly positive. Since the map $\Theta(a, b, \kappa)$ is analytic, we deduce by the implicit function theorem that the level set $\Theta(a, b, \kappa) = \Theta_0$ can be expressed locally around $(1, b_0, \kappa_0)$ as a graph $b^{\Theta_0} = b^{\Theta_0}(a, \kappa)$. If $a = 1$, we can use (5.2) and (5.30) to compute $b^{\Theta_0}(1, \kappa)$ explicitly:

$$b^{\Theta_0}(1, \kappa) = \frac{1}{2\Theta_0^2} \left((1 + 4\kappa)(1 - \Theta_0^2) + \sqrt{(1 + 4\kappa)^2(1 - \Theta_0^2)^2 - 16\Theta_0^4\kappa} \right). \quad (5.37)$$

5.5 The map $\tau(a, b, \kappa)$

Let $(a, b, \kappa) \in \mathcal{O}$. Our goal in this section is to determine whether for some $u_0 \in (0, u_{\mathcal{D}})$ the piece $\Sigma_0(a, b, \kappa; u_0)$ in Definition 5.3.11 meets the totally umbilical surfaces $\mathcal{Q}(-u_0)$, $\mathcal{Q}(u_0)$ orthogonally along its boundary components. According to Theorem 5.3.12, this will happen if the function $\beta(u) = \beta(u; a, b, \kappa)$ in (5.16) vanishes at $u = u_0$.

The main result of this section is Proposition 5.5.8, which states that there exists a subset $\mathcal{W}_1 \subset \mathcal{O}$ and an analytic map $\tau(a, b, \kappa) : \mathcal{W}_1 \rightarrow \mathbb{R}^+$ such that the first positive

root of $\beta(u) = \beta(u; a, b, \kappa)$ is attained at $u = \tau$. In order to do so, we will adapt the arguments from Section 3.4 to this new setting.

In order to prove the existence of the map $\tau(a, b, \kappa)$, we will study the differential system (5.3). This system admits a first integral that can be obtained by a classical Hamilton-Jacobi procedure; see [76, pp. 9-14]. More specifically, if $\kappa \geq 0$, consider the change of variables

$$\begin{aligned}\alpha\beta &= s + t - 2\sqrt{\kappa}, \\ -st &= \left(\alpha/2 - \sqrt{\kappa}\beta\right)^2,\end{aligned}\tag{5.38}$$

where we set $s \geq t$. We can express the pair (s, t) explicitly as

$$\begin{aligned}s &= \sqrt{\kappa} + \frac{\alpha\beta}{2} + \frac{1}{2}\sqrt{(2\sqrt{\kappa} + \alpha\beta)^2 + (\alpha - 2\sqrt{\kappa}\beta)^2}, \\ t &= \sqrt{\kappa} + \frac{\alpha\beta}{2} - \frac{1}{2}\sqrt{(2\sqrt{\kappa} + \alpha\beta)^2 + (\alpha - 2\sqrt{\kappa}\beta)^2}.\end{aligned}\tag{5.39}$$

If $(\alpha(u), \beta(u))$ is a solution of (5.3) with initial conditions (5.4), then $(s, t) = (s(\lambda), t(\lambda))$ satisfies the following first order system of differential equations:

$$\begin{cases} s'(\lambda)^2 &= s(s - 2\sqrt{\kappa})g(s), \\ t'(\lambda)^2 &= t(t - 2\sqrt{\kappa})g(t), \end{cases}\tag{5.40}$$

where $\lambda = \lambda(u)$ satisfies

$$2u'(\lambda) = s(\lambda) - t(\lambda) \geq 0\tag{5.41}$$

and $g(x)$ is the third-order polynomial given by

$$g(x) = -x^3 + (\hat{a} + 3\sqrt{\kappa})x^2 + (\mathcal{K}_1 - 2\hat{a}\sqrt{\kappa} - 2\kappa)x + \frac{1}{4}\mathcal{K}_2,\tag{5.42}$$

where $\mathcal{K}_1, \mathcal{K}_2$ are the constants in (2.25), (2.26) under the assumption that $A = \kappa$, $Q = \frac{1}{2}$; see the discussion at the beginning of Section 5.2. For every $(a, b, \kappa) \in \mathcal{O}$, the polynomial $g(x)$ has three real roots $\hat{r}_1 \leq \hat{r}_2 \leq 0 < \hat{r}_3$ satisfying

$$\begin{aligned}\hat{r}_1 &= \frac{-4\kappa + 4a\sqrt{\kappa}b - a^2b^2}{4ab} = -\frac{(ab - 2\sqrt{\kappa})^2}{4ab}, \\ \hat{r}_2 &= \frac{-4a^2\kappa + 4a\sqrt{\kappa}b - b^2}{4ab} = -\frac{(2a\sqrt{\kappa} - b)^2}{4ab}, \\ \hat{r}_3 &= \frac{4\kappa + 4\sqrt{\kappa} + 1}{4} = \frac{(2\sqrt{\kappa} + 1)^2}{4}.\end{aligned}\tag{5.43}$$

An alternative version of this change of variables can also be obtained for $\kappa < 0$, although in this case the corresponding functions (s, t) are expected to take complex values, so the Hamilton-Jacobi procedure does not yield significative information. For this reason, we will derive the information we need for the case $\kappa < 0$ by means of a careful analysis of the situation for $\kappa \geq 0$.

5.5.1 Case $\kappa > 0$

We set $\lambda = \lambda(u)$ in (5.41) so that $\lambda(0) = 0$. According to (5.39), the initial conditions $\alpha(0) = \beta(0) = 0$ imply that $s(0) = 2\sqrt{\kappa}$, $t(0) = 0$. Hence, the function $s(\lambda)$ will oscillate in the interval $[2\sqrt{\kappa}, \hat{r}_3]$ with a period $2\hat{\mathcal{M}} > 0$. The behaviour of the function $t(\lambda)$ depends on the values of the roots (5.43):

1. If $\hat{r}_1 < \hat{r}_2 < 0$, $t(\lambda)$ will be oscillating in $[\hat{r}_2, 0]$ with a certain period $2\hat{\mathcal{N}} > 0$.
2. If $\hat{r}_1 = \hat{r}_2 < 0$, $t(\lambda)$ decreases for all $\lambda > 0$, converging to the limit value \hat{r}_2 as $\lambda \rightarrow \infty$.
3. Finally, if $\hat{r}_2 = 0$, then $t(\lambda) \equiv 0$.

By (5.40), the half-periods $\hat{\mathcal{M}}, \hat{\mathcal{N}}$ can be computed in terms of the following integrals, provided that $\hat{r}_2 < 0$:

$$\begin{aligned}\hat{\mathcal{M}} &= \int_{2\sqrt{\kappa}}^{\hat{r}_3} \frac{dz}{\sqrt{-z(z-2\sqrt{\kappa})(z-\hat{r}_1)(z-\hat{r}_2)(z-\hat{r}_3)}}, \\ \hat{\mathcal{N}} &= \int_{\hat{r}_2}^0 \frac{dz}{\sqrt{-z(z-2\sqrt{\kappa})(z-\hat{r}_1)(z-\hat{r}_2)(z-\hat{r}_3)}}.\end{aligned}\tag{5.44}$$

Observe that the integral for $\hat{\mathcal{M}}$ always converges, while $\hat{\mathcal{N}} < \infty$ if and only if $\hat{r}_1 < \hat{r}_2$.

Lemma 5.5.1. *Suppose that $\hat{r}_2 < 0$. Then, $\hat{\mathcal{M}} < \hat{\mathcal{N}}$.*

Proof. We know that, by (5.43), $\hat{r}_1 \leq \hat{r}_2$ and $2\sqrt{\kappa} < \hat{r}_3$. Applying the change of variables $z = 2\sqrt{\kappa}x$ in (5.44), we can rewrite these integrals as

$$\begin{aligned}\hat{\mathcal{M}} &= (2\sqrt{\kappa})^{-\frac{3}{2}} \int_1^{\hat{r}_3} \frac{dx}{\sqrt{-x(x-1)(x-r_1)(x-r_2)(x-r_3)}}, \\ \hat{\mathcal{N}} &= (2\sqrt{\kappa})^{-\frac{3}{2}} \int_{r_2}^0 \frac{dx}{\sqrt{-x(x-1)(x-r_1)(x-r_2)(x-r_3)}},\end{aligned}\tag{5.45}$$

where $r_i := \frac{1}{2\sqrt{\kappa}}\hat{r}_i$. We note that, up to a common factor $(2\sqrt{\kappa})^{-\frac{3}{2}}$, the values $\hat{\mathcal{M}}, \hat{\mathcal{N}}$ in (5.45) coincide with \mathcal{M}, \mathcal{N} in (3.27), (3.28) for constants $r_1 \leq r_2 < 0 < 1 < r_3$.

Thus, following the same argument as in the proof of Lemma 3.4.3, we conclude that $\widehat{\mathcal{M}} < \widehat{\mathcal{N}}$, as claimed. \square

The inequality of the previous lemma allows us to define the map u_1 introduced in Proposition 3.4.4 in this context.

Proposition 5.5.2. *Let $(a, b, \kappa) \in \mathcal{O} \cap \{\kappa > 0\}$. Then, there exists a value $u_1 > 0$ such that the functions $\widehat{y}(u) := \alpha(u)/2 + \sqrt{\kappa}\beta(u)$ and $\widehat{z}(u) := \alpha(u)/2 - \sqrt{\kappa}\beta(u)$ satisfy:*

1. $\widehat{y}(u) > 0$ for all $u \in (0, u_1)$, and $\widehat{y}(u_1) = 0$.
2. If $\mathcal{B} > 2\sqrt{\kappa}\mathcal{A}$, then $\widehat{z}(u)$ is positive on $(0, u_1]$, where \mathcal{A} and \mathcal{B} are defined in (5.2). In the limit case $\mathcal{B} = 2\sqrt{\kappa}\mathcal{A}$, $\widehat{z}(u) \equiv 0$.

Additionally, the map $u_1(a, b, \kappa) : \mathcal{O} \cap \{\kappa > 0\} \rightarrow \mathbb{R}^+$ is analytic.

Proof. We first rewrite system (5.3) for (α, β) in terms of $(\widehat{y}, \widehat{z})$ as above, as follows:

$$\begin{cases} \widehat{y}'' &= \widehat{a}\widehat{y} - \widehat{y}\left(\sqrt{\kappa} + \frac{1}{\sqrt{\kappa}}(\widehat{y}^2 - \widehat{z}^2)\right), \\ \widehat{z}'' &= \widehat{a}\widehat{z} + \widehat{z}\left(\sqrt{\kappa} - \frac{1}{\sqrt{\kappa}}(\widehat{y}^2 - \widehat{z}^2)\right). \end{cases} \quad (5.46)$$

The initial conditions (5.4) are given in this situation by $\widehat{y}(0) = \widehat{z}(0) = 0$ and

$$\widehat{y}'(0) = \left(\frac{1}{2} - \sqrt{\kappa}\right) \left(\frac{\mathcal{B} + 2\sqrt{\kappa}\mathcal{A}}{2}\right), \quad \widehat{z}'(0) = \left(\frac{1}{2} + \sqrt{\kappa}\right) \left(\frac{\mathcal{B} - 2\sqrt{\kappa}\mathcal{A}}{2}\right). \quad (5.47)$$

It is easy to check that $\widehat{y}(u)$ (resp. $\widehat{z}(u)$) vanishes if and only if $s(\lambda) = 2\sqrt{\kappa}$ (resp. $t(\lambda) = 0$). Since $\widehat{y}(0) = 0$, $\widehat{y}'(0) > 0$, there exists a first positive root u_1 of $\widehat{y}(u)$, corresponding to the point at which $\lambda(u_1) = 2\widehat{\mathcal{M}}$; see (5.44).

To prove (2), observe that for $\mathcal{B} = 2\sqrt{\kappa}\mathcal{A}$ it holds $\widehat{z}(0) = \widehat{z}'(0) = 0$, and so $\widehat{z} \equiv 0$. On the other hand, if $\mathcal{B} > 2\sqrt{\kappa}\mathcal{A}$, then $\widehat{z}(0) = 0$, $\widehat{z}'(0) > 0$ and therefore $\widehat{z}(u)$ is positive in $(0, u_2)$, where u_2 satisfies $\lambda(u_2) = 2\widehat{\mathcal{N}}$; see (5.44). Since in this case $\widehat{r}_1 \leq \widehat{r}_2 < 0$, Lemma 5.5.1 gives that $u_1 < u_2$: indeed, $\lambda(u)$ is strictly increasing due to (5.41) and the fact that for $\kappa > 0$ it holds $s(\lambda) - t(\lambda) \geq 2\sqrt{\kappa} > 0$. This proves item (2), as $u_1 = \lambda^{-1}(2\widehat{\mathcal{M}}) < \lambda^{-1}(2\widehat{\mathcal{N}}) = u_2$.

Let us finally show that $u_1 = u_1(a, b, \kappa)$ is an analytic function. Since $\alpha(u) = \alpha(u; a, b, \kappa)$ and $\beta(u) = \beta(u; a, b, \kappa)$ are analytic and $u_1 > 0$ is by definition the first root of $\widehat{y}(u)$, it suffices to show that $\widehat{y}'(u_1) \neq 0$ and apply the implicit function theorem. This is immediate: assume by contradiction that $\widehat{y}'(u_1) = 0$. From the fact that $\widehat{y}(u_1) = 0$ and (5.46), it would follow that $\widehat{y}(u) \equiv 0$, which is impossible. \square

The function $u_1(a, b, \kappa)$ will be key to finding the first positive root $\tau = \tau(a, b, \kappa)$ of the function $\beta(u)$. Let

$$\mathcal{W}_0 := \{(a, b, \kappa) \in \mathcal{O} : \mathcal{A} > \mathcal{B} \geq 2\sqrt{\kappa}\mathcal{A}, 0 < \kappa < 1/4\}. \quad (5.48)$$

Remark 5.5.3. *The restrictions on the definition of \mathcal{W}_0 are motivated by the following fact: if $(a, b, \kappa) \in \mathcal{W}_0$ then by (5.4) and (5.47) we have that $\alpha'(0), \beta'(0) > 0$ and $\mathcal{Z}'(0) \geq 0$.*

Proposition 5.5.4. *For any $(a, b, \kappa) \in \mathcal{W}_0$, the function $\beta(u)$ has a first positive root $\tau \in (0, u_1]$, where $\tau = u_1$ if and only if $\mathcal{B} = 2\sqrt{\kappa}\mathcal{A}$. Additionally, the map $\tau(a, b, \kappa) : \mathcal{W}_0 \rightarrow \mathbb{R}^+$ is analytic.*

Proof. Consider the function

$$f(\lambda) := s(\lambda) + t(\lambda) - 2\sqrt{\kappa}. \quad (5.49)$$

By (5.38), $f(\lambda)$ coincides with the product $\alpha(u)\beta(u)$. It is then straightforward that $f(0) = 0$ and $f(\lambda) > 0$ for $\lambda > 0$ small enough, since $\alpha(u), \beta(u)$ are positive for small u ; see Remark 5.5.3.

We will now prove that $f(\lambda)$ has a first positive root $\lambda^* \in (0, 2\widehat{\mathcal{M}}]$, and denote by τ the value in the variable u corresponding to λ^* . By (5.38), we would have that either $\alpha(\tau) = 0$ or $\beta(\tau) = 0$. We will show that the latter case always holds, and so τ is the first root of $\beta(u)$. We will split our analysis into two cases, depending on whether the inequality $\mathcal{B} \geq 2\sqrt{\kappa}\mathcal{A}$ is strict or not.

Assume first that $\mathcal{B} = 2\sqrt{\kappa}\mathcal{A}$. Since $a, b \geq 1$, this implies that $b = 2a\sqrt{\kappa}$, and by (5.43), $\widehat{r}_2 = 0$. The function $t(\lambda)$ is constantly zero, and so $f(\lambda)$ reduces to $s(\lambda) - 2\sqrt{\kappa}$. Since $2\widehat{\mathcal{M}}$ is the first positive value for which $s(\lambda) = 2\sqrt{\kappa}$, we deduce that $\lambda^* = 2\widehat{\mathcal{M}}$, so τ exists and coincides with $u_1 > 0$; see the proof of Proposition 5.5.2. Now, by (5.38), $\alpha(\tau)\beta(\tau) = 0$ and $\alpha(\tau)/2 = \sqrt{\kappa}\beta(\tau)$, so $\alpha(\tau) = \beta(\tau) = 0$ and τ is the first positive root of both functions.

Let us now show that τ is analytic in this case. It suffices to check that $\beta'(\tau) \neq 0$. This is immediate by the first integral (2.25) and the fact that $\alpha(\tau) = \beta(\tau) = 0$, as $0 \neq \alpha'(0)\beta'(0) = \alpha'(\tau)\beta'(\tau)$, so necessarily $\beta'(\tau) \neq 0$.

We now assume that $\mathcal{B} > 2\sqrt{\kappa}\mathcal{A}$. Hence, $b > 2\sqrt{\kappa}a$, and so $\widehat{r}_2 < 0$. In that case, $t(\lambda)$ will take values in the interval $[\widehat{r}_2, 0]$. If $\widehat{r}_1 = \widehat{r}_2$, $t(\lambda)$ never vanishes for $\lambda > 0$, while if $\widehat{r}_1 < \widehat{r}_2$, $t(\lambda)$ will have a first positive root at $\lambda = 2\widehat{\mathcal{N}} > 2\widehat{\mathcal{M}}$. In any case, we see that $f(2\widehat{\mathcal{M}}) = t(2\widehat{\mathcal{M}}) < 0$, so $f(\lambda)$ must have a first positive root $\lambda^* \in (0, 2\widehat{\mathcal{M}})$.

As before, this implies the existence of a first value $\tau > 0$ for which either $\alpha(\tau) = 0$ or $\beta(\tau) = 0$. Observe also that by Proposition 5.5.2, $z(u)$ is positive for all $u \in (0, u_1]$, so $0 < \widehat{z}(\tau) = \alpha(\tau)/2 - \sqrt{\kappa}\beta(\tau)$. Now, $\alpha(\tau), \beta(\tau) \geq 0$, so necessarily $\beta(\tau) = 0$ and $\alpha(\tau) > 0$.

We will finally show that τ is analytic in this case. Assume by contradiction that $\beta'(\tau) = 0$. Notice that $\beta''(\tau) = -\frac{\alpha(\tau)}{2} < 0$. This indicates that $\beta(u)$ has a local maximum at $u = \tau$, but this is impossible since $\beta(u) > \beta(\tau) = 0$ for $u \in (0, \tau)$. Hence, $\beta'(\tau) \neq 0$, and so τ is analytic in \mathcal{W}_0 by the implicit function theorem. \square

5.5.2 Case $\kappa = 0$

So far, the map $\tau(a, b, \kappa)$ is just defined on the set \mathcal{W}_0 in (5.48). We now aim to extend this map for points (a, b, κ) with $\kappa = 0$. To do so, we will make use again of the change of variables (5.38). The system (5.40) for the case $\kappa = 0$ was previously studied by Wente [76, Section IV] and Fernández, Hauswirth, Mira [29, Section 3], and it exhibits a different behaviour with respect to the case $\kappa > 0$. We summarize it in the next lemma:

Lemma 5.5.5. ([29]) *Let $\kappa = 0$ and $(s(\lambda), t(\lambda))$ be a solution of (5.40). Assume that for some $\lambda_0 \in \mathbb{R}$ it holds $s(\lambda_0) \in (0, \widehat{r}_3]$, $t(\lambda_0) \in [\widehat{r}_2, 0)$ and $t(\lambda)$ is decreasing at $\lambda = \lambda_0$. Then,*

1. *The function $s(\lambda)$ takes values in $(0, \widehat{r}_3]$ for all λ . More specifically, $s(\lambda)$ is increasing until reaching \widehat{r}_3 and then decreases, satisfying $\lim_{\lambda \rightarrow \pm\infty} s(\lambda) = 0$.*
2. *The function $t(\lambda)$ takes values in $[\widehat{r}_2, 0)$, and $\lim_{\lambda \rightarrow -\infty} t(\lambda) = 0$.*
3. *If $\widehat{r}_1 = \widehat{r}_2$, $t(\lambda)$ is decreasing for all λ , and $\lim_{\lambda \rightarrow \infty} t(\lambda) = \widehat{r}_2$.*
4. *Otherwise, if $\widehat{r}_1 < \widehat{r}_2$, then $t(\lambda)$ reaches the minimum \widehat{r}_2 and then it is increasing, with $\lim_{\lambda \rightarrow \infty} t(\lambda) = 0$.*

Proof. Notice that the roots $\widehat{r}_1, \widehat{r}_2, \widehat{r}_3$ of $g(x)$ in (5.43) satisfy $\widehat{r}_1 \leq \widehat{r}_2 < 0 < \widehat{r}_3 = \frac{1}{4}$, where the equality $\widehat{r}_1 = \widehat{r}_2$ holds if and only if $a = 1$. The polynomial $g(x)$ in (5.40) is nonnegative on $(-\infty, \widehat{r}_1] \cup [\widehat{r}_2, 0) \cup (0, \widehat{r}_3]$. In particular, under the hypotheses of the lemma, $s(\lambda)$ must take values in $(0, \widehat{r}_3]$ for all λ while $t(\lambda)$ does so in $[\widehat{r}_2, 0)$. The monotonicity and limit properties of $s(\lambda), t(\lambda)$ are straightforward from (5.40). \square

Remark 5.5.6. Any solution $(s(\lambda), t(\lambda))$ of (5.40) in the conditions of Lemma 5.5.5 induces by (5.38) a solution $(\epsilon\alpha(u), \epsilon\beta(u))$, of (5.3) (defined up to a sign $\epsilon = \pm 1$). Notice, however, that this solution is not defined for all $u \in \mathbb{R}$: if $\hat{r}_1 < \hat{r}_2$, $u'(\lambda) = \frac{s-t}{2}$ converges to zero exponentially as $\lambda \rightarrow \pm\infty$, so the domain of the induced solution is some interval $I := (u_m, u_M)$. By (5.38), we deduce that $\alpha(u) \neq 0$ for $u \in I$, but $\alpha(u_m) = \alpha(u_M) = 0$. On the other hand, if $\hat{r}_1 = \hat{r}_2$, then $s - t$ converges to 0 when $\lambda \rightarrow -\infty$ and to $-\hat{r}_2 > 0$ as $\lambda \rightarrow \infty$. In this case, the induced solution is defined on an interval $u \in (u_m, \infty)$.

Conversely, let $(\alpha(u), \beta(u)) : I \rightarrow \mathbb{R}^2$ be any solution of (5.3) with initial conditions (5.4), where $I := (0, u_M)$ is the maximal interval in which $\alpha(u)$ does not vanish. For u_0 small enough, $\alpha(u_0)$ and $\beta(u_0)$ are close to zero, so the corresponding values (s, t) obtained by the change (5.39) will be in the conditions of Lemma 5.5.5. The limit $\lambda \rightarrow -\infty$, in which s, t converge to zero, corresponds to the limit value $u = 0$ in the system $(\alpha(u), \beta(u))$. If $\hat{r}_1 = \hat{r}_2$, then $I = (0, \infty)$, while for $\hat{r}_1 < \hat{r}_2$ the value $u_M < \infty$ corresponds to the first positive root of $\alpha(u)$.

As we explained previously, our main objective is to extend analytically the map τ defined in \mathcal{W}_0 (5.48) for values with $\kappa = 0$. As an intermediate step, we must also extend the map u_1 of Proposition 5.5.2.

Proposition 5.5.7. The function u_1 defined in Proposition 5.5.2 can be extended analytically to the set $\mathcal{O} \cap \{a > 1, \kappa = 0\}$. In particular, if $\kappa = 0$, $u_1 = u_1(a, b, 0)$ corresponds to the first root of $\alpha(u)$.

Proof. Let $(a, b, \kappa) \in \mathcal{O} \cap \{a > 1, \kappa = 0\}$. Then, the function $\hat{y}(u)$ coincides with $\alpha(u)/2$, so we just need to study the first root of $\alpha(u)$, in case it exists. Since $a > 1$, we know that $\hat{r}_1 < \hat{r}_2$ (see (5.43)), and by Remark 5.5.6, $\alpha(u)$ has a first root $u_M = u_M(a, b)$. Hence, $u_1(a, b, 0) \equiv u_M(a, b)$. Let us now show that this extension is analytic. We claim that $\alpha'(u_1) \neq 0$: suppose otherwise that $\alpha'(u_1) = 0$. Since $\alpha(u_1) = 0$, using (5.3) we deduce that $\alpha(u) \equiv 0$, which is impossible as $\alpha'(0) > 0$; see (5.4). By the implicit function theorem, the map $u_1(a, b, \kappa)$ extends analytically to $\mathcal{O} \cap \{a > 1, \kappa = 0\}$, as we wanted to prove. \square

We will now extend the map $\tau(a, b, \kappa)$ of Proposition 5.5.4:

Proposition 5.5.8. The map $\tau = \tau(a, b, \kappa) > 0$ defined in Proposition 5.5.4 can be extended analytically to the set

$$\mathcal{W}_1 := \{(a, b, \kappa) \in \mathcal{O} : \mathcal{A} > \mathcal{B} \geq 2\sqrt{\kappa}\mathcal{A}, 0 \leq \kappa < 1/4\}. \quad (5.50)$$

In particular, $\tau(a, b, \kappa) > 0$ and $\beta(\tau(a, b, \kappa)) = 0$ for all $(a, b, \kappa) \in \mathcal{W}_1$.

Proof. Note that \mathcal{W}_1 is exactly \mathcal{W}_0 in (5.48) plus the boundary component of \mathcal{W}_0 in which $\kappa = 0$. Therefore, to prove this result, we only need to show that $\tau(a, b, \kappa)$ can be analytically extended for these boundary values. We will split the proof into two cases, depending on whether $a > 1$ or $a = 1$.

Let $(a_0, b_0, 0) \in \mathcal{W}_1$ with $a_0 > 1$. Since $\mathcal{W}_1 \subset \overline{\mathcal{W}_0}$, we can define

$$\rho_0 := \liminf_{(a,b,\kappa) \rightarrow (a_0,b_0,0)} \tau(a, b, \kappa).$$

This limit exists and it is finite, since $0 < \tau(a, b, \kappa) \leq u_1(a, b, \kappa)$ for all $(a, b, \kappa) \in \mathcal{W}_0$ and $u_1(a_0, b_0, 0) < \infty$; see Proposition 5.5.7. Notice further that ρ_0 is a root of $\beta(u; a_0, b_0, 0)$: indeed, consider a sequence (a_n, b_n, κ_n) converging to $(a_0, b_0, 0)$ and such that $\tau_n := \tau(a_n, b_n, \kappa_n)$ converges to ρ_0 . By continuity,

$$\beta(\rho_0; a_0, b_0, 0) = \lim_{n \rightarrow \infty} \beta(\tau_n; a_n, b_n, \kappa_n) = 0.$$

We also claim that $\rho_0 > 0$: otherwise, since

$$\beta(0; a_n, b_n, \kappa_n) = \beta(\tau_n; a_n, b_n, \kappa_n) = 0,$$

there would exist some $\xi_n \in (0, \tau_n)$ such that $\beta'(\xi_n; a_n, b_n, \kappa_n) = 0$. If $\rho_0 = \lim \tau_n = 0$, then the sequence $\{\xi_n\}_n$ would also converge to zero, and hence $\beta'(0; a_0, b_0, 0) = 0$, which is impossible by definition of \mathcal{W}_1 ; see (5.4) and (5.50). As a consequence, $\rho_0 > 0$, so $\beta(u; a_0, b_0, 0)$ necessarily admits a first positive root $\tau = \tau(a_0, b_0, 0) \in (0, \rho_0]$. In particular, $\tau(a_0, b_0, 0) \leq \rho_0 \leq u_1(a_0, b_0, 0)$.

For the case $a = 1$, we consider the function $f(\lambda)$ defined in (5.49). We recall that $f(\lambda)$ coincides with the product $\alpha(u)\beta(u)$ by (5.38). Since $\alpha(0)\beta(0) = 0$ but $\alpha(u)\beta(u) > 0$ for small positive values of u , we deduce that $f(\lambda)$ is positive for λ negative and large enough. In this case, it holds $\widehat{r}_1 = \widehat{r}_2 < 0$, so $\lim_{\lambda \rightarrow \infty} f(\lambda) = \lim_{\lambda \rightarrow \infty} t(\lambda) = \widehat{r}_2 < 0$. In particular, $f(\lambda)$ changes sign, so it must have a first root $\lambda^* \in \mathbb{R}$. Let τ be the value in the variable u corresponding to λ^* . By (5.38) and the fact that $s(\lambda^*), t(\lambda^*) \neq 0$, we conclude that $\alpha(\tau) \neq 0$, so $\beta(\tau) = 0$. Moreover, since λ^* is the first root of $f(\lambda)$, τ must be the first (positive) root of $\beta(u)$.

Let us now show that $\tau = \tau(a, b, \kappa)$ is analytic in \mathcal{W}_1 . We already proved this in \mathcal{W}_0 , so we only need to consider those points in \mathcal{W}_1 with $\kappa = 0$. As we have done before, it suffices to check that $\beta'(\tau) \neq 0$ and apply the implicit function theorem.

Assume by contradiction that $\beta'(\tau) = 0$. If $a = 1$ or $a > 1$ and $\tau < u_1$, then, by (5.3), $\beta''(\tau) = -\frac{\alpha(\tau)}{2} < 0$. This implies that β has a maximum at τ , which is impossible since $\beta(u) > \beta(\tau) = 0$ for all $u \in (0, \tau)$. In particular, $\beta'(\tau) < 0$. Finally, if $a > 1$ and $\tau = u_1$, then $\alpha(\tau) = \beta(\tau) = 0$. Using the first integral (2.25) of the system (α, β) , we deduce that $\alpha'(\tau)\beta'(\tau) = \alpha'(0)\beta'(0) \neq 0$, so in particular $\beta'(\tau) \neq 0$. \square

Remark 5.5.9. *In the previous proposition we showed that if $a = 1$ and $\kappa = 0$, then τ corresponds to the first root λ^* of the function $f(\lambda)$ in (5.49), and that $\alpha(\tau) > 0$, $\beta'(\tau) < 0$.*

Remark 5.5.10. *The analyticity of $\tau(a, b, \kappa)$ on \mathcal{W}_1 implies that $\tau(a, b, \kappa)$ is defined and analytic on a larger open set $\mathcal{W} \subset \mathcal{O}$ which contains \mathcal{W}_1 . In particular \mathcal{W} extends into the region $\{\kappa < 0\} \cap \mathcal{O}$; see Figure 5.1.*

Let us also remark that $\beta(\tau(a, b, \kappa)) \equiv 0$ for all $(a, b, \kappa) \in \mathcal{W}$: indeed, this equality holds on \mathcal{W}_1 , so by analyticity it extends to \mathcal{W} . Hence, by (5.16), (5.18) we deduce that the surfaces $\Sigma_0(a, b, \kappa; \tau(a, b, \kappa))$ intersect orthogonally the spheres $\mathcal{Q}(\pm\tau)$ for all $(a, b, \kappa) \in \mathcal{W}$; see Definition 5.3.11.

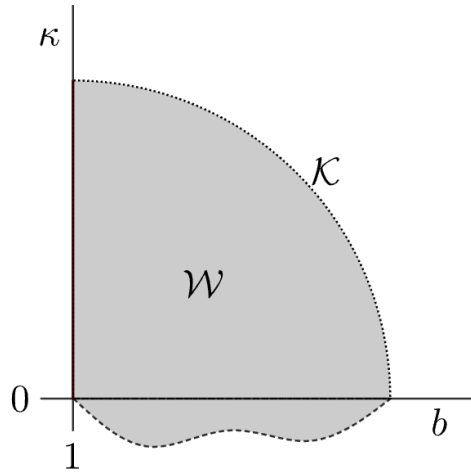


Figure 5.1: The open set $\mathcal{W} \subset \mathcal{O}$ in Remark 5.5.10. The boundary component of \mathcal{W} in the quadrant $\{b > 1, \kappa \geq 0\}$ represents the set \mathcal{T} in (5.51).

Lemma 5.5.11. *Let $(a_0, b_0, \kappa_0) \in \mathcal{T}$, where*

$$\mathcal{T} := \{(a, b, \kappa) \in \partial\mathcal{W}_1 : \mathcal{A} = \mathcal{B}, 0 \leq \kappa < 1/4\}. \quad (5.51)$$

Then, $\lim_{n \rightarrow \infty} \tau(a_n, b_n, \kappa_n) = 0$ for any sequence $\{(a_n, b_n, \kappa_n)\}_n \subset \mathcal{W}_1$ converging to (a_0, b_0, κ_0) .

Proof. Let us denote by $(\alpha_0(u), \beta_0(u))$ the solution to (5.3) associated to the parameters $(a_0, b_0, \kappa_0) \in \mathcal{T}$, and by $(\alpha_n(u), \beta_n(u))$, $n \in \mathbb{N}$, the corresponding solutions for $(a_n, b_n, \kappa_n) \in \mathcal{W}_1$. Moreover, let $\tau_n := \tau(a_n, b_n, \kappa_n) > 0$. To prove this lemma, it suffices to show that the value $\tau_0 := \limsup_{n \rightarrow \infty} \tau_n$ is zero, so assume by contradiction that $\tau_0 > 0$. By definition, $\tau_n > 0$ is the first positive root of $\beta_n(u)$. In fact, $\beta_n(u) > 0$ for every $u \in (0, \tau_n)$, since $\beta'_n(0) > 0$. By continuity of the solutions to (5.3) with respect to the parameters (a, b, κ) , it follows that $\beta_0(u) \geq 0$ for every $u \in [0, \tau_0]$. However, this is impossible: by (5.3), (5.4) and (5.51), we have that $\beta_0(0) = \beta'_0(0) = \beta''_0(0) = 0$ but $\beta'''_0(0) = -\frac{\alpha'_0(0)}{2} < 0$, so $\beta_0(u)$ must be negative for $u > 0$ small enough. \square

Remark 5.5.12. Let $(a, b, \kappa) \in \mathcal{W}$, where \mathcal{W} is defined in Remark 5.5.10. It remains to show that the value $\tau(a, b, \kappa) > 0$ in Remark 5.5.10 is below $u_{\mathcal{D}}$ in (5.8). The study of this property will be postponed until Section 5.7.3.

5.6 Detecting the Euclidean free boundary catenoid

Let $a = 1$, $\kappa = 0$. The goal of this section is to detect some $b_0 > 1$ such that the surface $\Sigma_0(1, b_0, 0; \tau)$ covers a Euclidean catenoid with free boundary in a ball, where $\tau := \tau(1, b_0, 0)$; see Definition 5.3.11 and Proposition 5.5.8. According to Theorem 2.6.9 and Definition 5.3.15, this happens if $\tau(1, b_0, 0)$ satisfies the condition

$$\tau(1, b_0, 0) = \tilde{u}(0). \quad (5.52)$$

We recall that when $a = 1$, the surfaces $\Sigma(1, b, \kappa)$ are independent of b , i.e., they all represent the same catenoid in $\mathbb{M}^3(\kappa)$; see the discussion after Lemma 5.3.14. In particular, for $\kappa = 0$, $\Sigma(1, b, 0)$ is a Euclidean catenoid of neck curvature $\frac{1}{2}$. We will devote the rest of this section to prove that

$$\tau(1, 1, 0) > \tilde{u}(0) > 0 = \lim_{b \rightarrow 2^-} \tau(1, b, 0). \quad (5.53)$$

In particular, this implies the existence of $b_0 \in (1, 2)$ such that (5.52) holds. The limit in the right-hand side of (5.53) is immediate: indeed, the point $(1, 2, 0) \in \mathcal{O}$ belongs to the set \mathcal{T} in Lemma 5.5.11, so $\lim_{b \rightarrow 2^-} \tau(1, b, 0) = 0$; see (5.2). Hence, it remains to show the first inequality of (5.53). This will be achieved in Theorem 5.6.9, and the rest of the section is devoted to proving that result. It will be necessary to study the geometry of the catenoid $\Sigma(1, b, 0)$ as well as the system $(\alpha(u), \beta(u))$ in (5.3) for the

parameters $(a, b, \kappa) = (1, 1, 0) \in \mathcal{O}$. We do this next.

5.6.1 The case $(1, 1, 0) \in \mathcal{O}$

We fix the parameters $(a, b, \kappa) = (1, 1, 0)$, and consider the solution $(s(\lambda), t(\lambda))$ to (5.40). The roots of the polynomial $g(x)$ satisfy $-\hat{r}_1 = -\hat{r}_2 = \hat{r}_3 = 1/4$, that is,

$$g(x) = -(x + 1/4)^2(x - 1/4), \quad (5.54)$$

see (5.43). If we define the variables $S = 4s$, $T = 4t$, $\eta = \lambda/8$, (5.40) reduces to

$$\begin{cases} S'(\eta)^2 &= S^2(1 - S)(S + 1)^2, \\ T'(\eta)^2 &= T^2(1 - T)(T + 1)^2. \end{cases} \quad (5.55)$$

This system was previously studied in [29, Section 4]. The following result is a straightforward consequence of [29, Theorem 4.2] and its proof:

Theorem 5.6.1. ([29, Theorem 4.2]). *The function $f(\lambda) = s(\lambda) + t(\lambda)$ in (5.49) has a first root λ^* satisfying*

$$\mathcal{F}(4s(\lambda^*)) = -1 \quad (5.56)$$

and $s'(\lambda^*) < 0$, where $\mathcal{F}(x) := H(x)H(-x)$, being

$$H(x) := \frac{1 + \sqrt{1 - x}}{1 - \sqrt{1 - x}} \left(\frac{\sqrt{2} - \sqrt{1 - x}}{\sqrt{2} + \sqrt{1 - x}} \right)^{\frac{1}{\sqrt{2}}}.$$

Lemma 5.6.2. *Let $(\alpha(u), \beta(u))$ be the solution to (5.3)-(5.4) for $(a, b, \kappa) = (1, 1, 0)$, and $\tau_1 := \tau(1, 1, 0)$. Then, $\alpha'(\tau_1) < 0$.*

Proof. Let $(s(\lambda), t(\lambda))$ be the solution to (5.40) for $(1, 1, 0) \in \mathcal{O}$. By Remark 5.5.9, τ_1 corresponds to the first root λ^* of the function $f(\lambda) = s(\lambda) + t(\lambda)$, and $\alpha(\tau_1) > 0$. Now, by (5.38), $\alpha^2 = -4st$, so differentiating with respect to u at τ_1 ,

$$\alpha(\tau_1)\alpha'(\tau_1) = -2\lambda'(\tau_1)(s'(\lambda^*)t(\lambda^*) + s(\lambda^*)t'(\lambda^*)) = 2\lambda'(\tau_1)s(\lambda^*)(s'(\lambda^*) - t'(\lambda^*)),$$

where we use $s(\lambda^*) = -t(\lambda^*)$. Since $\alpha(\tau_1), \lambda'(\tau_1), s(\lambda^*) > 0$, it suffices to prove that

$$s'(\lambda^*) - t'(\lambda^*) < 0. \quad (5.57)$$

Let $s^* := s(\lambda^*) = -t(\lambda^*)$. We know that $t(\lambda)$ is decreasing so $t'(\lambda^*) < 0$. Moreover, $s^* \in (0, 1/4]$; see Remark 5.5.6. By Theorem 5.6.1, it also holds that $s'(\lambda^*) < 0$, which by (5.40) and (5.54) implies that $s^* \neq 1/4$. Hence, (5.57) is equivalent to

$$1 > \frac{t'(\lambda^*)}{s'(\lambda^*)} = \frac{\sqrt{g(-s^*)}}{\sqrt{g(s^*)}}.$$

It is immediate to check that $g(x) > g(-x)$ for all $x \in (0, 1/4)$, so we deduce (5.57).

□

5.6.2 The orthogonal radius

As we mentioned at the beginning of this section, for every $b \geq 1$ the surface $\Sigma = \Sigma(1, b, 0)$ represents the same catenoid. In fact, the immersion $\psi(u, v; 1, b, 0)$ does not depend on b either, according by Remark 5.2.3. In this particular situation, we can compute $\psi(u, v)$ explicitly. First, we identify $\mathbb{M}^3(0) = \mathbb{R}^4 \cap \{x_4 = 1\}$ with \mathbb{R}^3 . Under this identification, the rotation axis \mathcal{X} of the catenoid is just the x_3 -axis. The initial conditions in Remark 5.3.5 for the immersion are then

$$\psi(0, 0) = 2\mathbf{e}_1, \quad \psi_u(0, 0) = \mathbf{e}_3, \quad \psi_v(0, 0) = -\mathbf{e}_2, \quad N(0, 0) = \mathbf{e}_1, \quad (5.58)$$

where $\{\mathbf{e}_1, \mathbf{e}_2, \mathbf{e}_3\}$ denotes the canonical basis of \mathbb{R}^3 . It is immediate by (5.9) that $e^{\omega(u)} = \cosh\left(\frac{u}{2}\right)$. Since the u -curve $\psi(u, 0)$ is the profile curve of the catenoid and v is the rotation parameter, we deduce that

$$\begin{aligned} \psi(u, v) &= \left(2 \cosh\left(\frac{u}{2}\right) \cos\left(\frac{v}{2}\right), -2 \cosh\left(\frac{u}{2}\right) \sin\left(\frac{v}{2}\right), u \right), \\ N(u, v) &= \left(\operatorname{sech}\left(\frac{u}{2}\right) \cos\left(\frac{v}{2}\right), -\operatorname{sech}\left(\frac{u}{2}\right) \sin\left(\frac{v}{2}\right), -\tanh\left(\frac{u}{2}\right) \right). \end{aligned} \quad (5.59)$$

We now introduce the following concept.

Definition 5.6.3. For every $u_0 > 0$, we define the **orthogonal radius** $R_\perp = R_\perp(u_0) > 0$ as the radius of the unique ball $B_\perp = B_\perp(u_0) \subset \mathbb{R}^3$ which intersects the Euclidean catenoid $\psi(u, v)$ in (5.59) orthogonally along the v -line $\psi(u_0, v)$; see Figure 5.2.

Remark 5.6.4. It follows from the definition of orthogonal radius that the centers $\hat{c}_\perp(u)$ of the balls $B_\perp(u)$ must lie in the rotation axis \mathcal{X} of the catenoid; see Figure 5.2. These centers are given by

$$\hat{c}_\perp(u) = \psi(u, 0) - R_\perp(u) e^{-\omega(u)} \psi_u(u, 0). \quad (5.60)$$

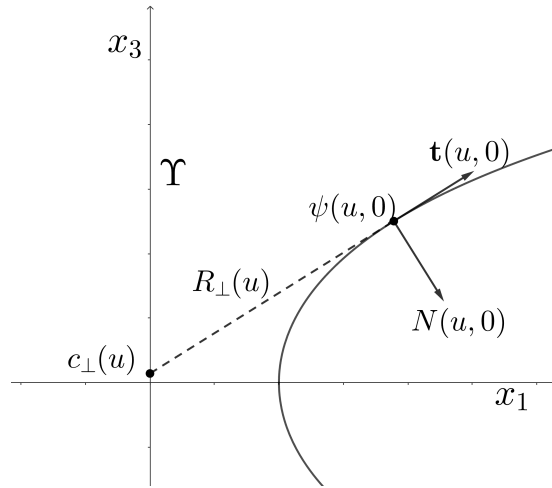


Figure 5.2: Geometric interpretation of the orthogonal radius. Here, $\mathbf{t}(u, 0)$ denotes the unit tangent vector $e^{-\omega(u)}\psi_u(u, 0)$.

The study of the orthogonal radius will be key to prove (5.53), as we will see in Theorem 5.6.9.

Lemma 5.6.5. *The orthogonal radius satisfies the following properties:*

1. $\lim_{u \rightarrow 0^+} R_\perp(u) = \lim_{u \rightarrow \infty} R_\perp(u) = \infty$.
2. $R_\perp(u)$ is strictly decreasing in $(0, u^*]$ and strictly increasing in $[u^*, \infty)$, where $u^* := 2 \operatorname{arcsinh}(1)$.
3. $u^* < \tilde{u}(0) < \hat{u}$, where $\tilde{u}(0)$ is given by Definition 5.3.15, and $\hat{u} := 2 \operatorname{arcsinh}(2)$.

Proof. We first obtain an explicit expression for the orthogonal radius. Indeed, for each $u > 0$, $R_\perp(u) > 0$ is the unique value for which the right-hand side of (5.60) lies in the x_3 -axis. A straightforward computation using (5.59) allows us to deduce that

$$\begin{aligned} \hat{c}_\perp(u) &= \left(0, 0, u - 2 \coth \left(\frac{u}{2}\right)\right), \\ R_\perp(u) &= 2 \coth \left(\frac{u}{2}\right) \cosh \left(\frac{u}{2}\right). \end{aligned} \tag{5.61}$$

Items (1) and (2) of the lemma are then immediate. Let us prove item (3). By definition, $\tilde{u}(0)$ is a value in which the piece of catenoid $\Sigma_0(1, b, 0; \tilde{u}(0))$ is free boundary in a ball; see Theorem 2.6.9. By construction, this ball must be exactly $B_\perp(\tilde{u}(0))$, so necessarily $\hat{c}_\perp(\tilde{u}(0)) = (0, 0, 0)$. In particular, we deduce by (5.61) that $\tilde{u}(0)$ is a root of

$$G(u) := u - 2 \coth \left(\frac{u}{2}\right). \tag{5.62}$$

Observe that $G(u)$ is strictly increasing, so $\tilde{u}(0)$ is actually the unique root of this function. Since $G(u^*) = 2 \operatorname{arcsinh}(1) - 2\sqrt{2} < 0$ and $G(\hat{u}) = 2 \operatorname{arcsinh}(2) - \sqrt{5} > 0$, we deduce that $u^* < \tilde{u}(0) < \hat{u}$, proving item (3). \square

Remark 5.6.6. *Since the map $R_\perp(u)$ is increasing for $u \in [u^*, \infty)$, it holds*

$$R_\perp(\tilde{u}(0)) < R_\perp(\hat{u}) = 5. \quad (5.63)$$

Corollary 5.6.7. *Let $u_0 > 0$ such that $R_\perp(u_0) > R_\perp(\tilde{u}(0))$ and $R'_\perp(u_0) > 0$. Then, $u_0 > \tilde{u}(0)$.*

Proof. Since $R'_\perp(u_0) > 0$, we deduce by the previous lemma that u_0 belongs to the interval (u^*, ∞) , in which R_\perp is strictly increasing. The value $\tilde{u}(0)$ also lies in this interval, and due to the fact that $R_\perp(u_0) > R_\perp(\tilde{u}(0))$, it holds $u_0 > \tilde{u}(0)$. \square

Our next goal is to show that the value $u_0 = \tau(1, 1, 0)$ is in the conditions of Corollary 5.6.7, from which we will prove (5.53).

Lemma 5.6.8. *Let $\tau_1 = \tau(1, 1, 0)$. Then, $R'_\perp(\tau_1) > 0$.*

Proof. Let $R = R(u)$ denote the radius of the sphere $\mathcal{Q}(u)$ in (5.18). At $u = \tau_1$, the sphere $\mathcal{Q}(\tau_1)$ intersects the v -line $\psi(\tau_1, v)$ orthogonally, so

$$R(\tau_1) = R_\perp(\tau_1) \quad (5.64)$$

by definition of orthogonal radius. We will now prove that

$$R'_\perp(\tau_1) \geq R'(\tau_1) > 0, \quad (5.65)$$

from which the lemma follows. First, by (5.18),

$$R'(\tau_1) = \left(\frac{2\sqrt{1+\beta^2}}{\alpha} \right)' \Big|_{u=\tau_1} = \left(\frac{2}{\alpha} \right)' \Big|_{u=\tau_1} = -\frac{2\alpha'(\tau_1)}{\alpha^2(\tau_1)}, \quad (5.66)$$

where we have used that $\beta(\tau_1) = 0$ and $\alpha(\tau_1) > 0$; see Remark 5.5.9. By Lemma 5.6.2 we conclude that $R'(\tau_1) > 0$.

Let us now prove that $R'_\perp(\tau_1) \geq R'(\tau_1)$. To do so, for any $u > 0$ we will compute the first component of $\psi(u, 0)$, i.e. $\langle \psi(u, 0), \mathbf{e}_1 \rangle$ in two different ways. Here, $\langle \cdot, \cdot \rangle$ denotes the usual Euclidean product in \mathbb{R}^3 and $\mathbf{e}_1 = (1, 0, 0)$. First, we use the fact that $\hat{c}_\perp(u)$ lies in the rotation axis \mathcal{X} , so $\langle \hat{c}_\perp(u), \mathbf{e}_1 \rangle = 0$. In particular, by (5.59) and (5.60),

$$\langle \psi(u, 0), \mathbf{e}_1 \rangle = \langle \psi(u, 0) - \widehat{c}_\perp(u), \mathbf{e}_1 \rangle = R_\perp(u) \tanh\left(\frac{u}{2}\right) > 0. \quad (5.67)$$

We can apply a similar trick by using the center map $\widehat{c}(u)$ in (5.19) instead, yielding

$$\langle \psi(u, 0), \mathbf{e}_1 \rangle = \langle \psi(u, 0) - \widehat{c}(u), \mathbf{e}_1 \rangle = \frac{2}{\alpha(u)} \tanh\left(\frac{u}{2}\right) - \frac{2\beta(u)}{\alpha(u)} \operatorname{sech}\left(\frac{u}{2}\right). \quad (5.68)$$

Now, the expressions in (5.67) and (5.68) must coincide, so

$$R_\perp(u) = \frac{2}{\alpha(u)} - \frac{2\beta(u)}{\alpha(u) \sinh\left(\frac{u}{2}\right)}. \quad (5.69)$$

Since $\beta(\tau_1) = 0$ but $\beta'(\tau_1) < 0$ (see Remark 5.5.9), it follows that $\beta(u) < 0$ for every $u > \tau_1$ close enough to τ_1 . In particular, from (5.69) it holds $R_\perp(\tau_1) = \frac{2}{\alpha(\tau_1)}$ while $R_\perp(u) > \frac{2}{\alpha(u)}$ for $u > \tau_1$. Along with (5.66), this implies that

$$R'_\perp(\tau_1) \geq \left(\frac{2}{\alpha}\right)' \Big|_{u=\tau_1} = R'(\tau_1) > 0.$$

This proves (5.65) and the lemma. \square

We finally prove (5.53), the main result of this section.

Theorem 5.6.9. *Let $\tau_1 = \tau(1, 1, 0)$. Then, $\tau_1 > \widetilde{u}(0)$.*

Proof. It is an immediate consequence of Corollary 5.6.7 and Lemma 5.6.8 once we prove that $R_\perp(\tau_1) > R_\perp(\widetilde{u}(0))$. We first note that the function $\mathcal{F}(x)$ in Theorem 5.6.1 satisfies

$$-1 = \mathcal{F}(4s(\lambda^*)) = \mathcal{F}(2\alpha(\tau_1)) = \mathcal{F}\left(\frac{4}{R(\tau_1)}\right) = \mathcal{F}\left(\frac{4}{R_\perp(\tau_1)}\right). \quad (5.70)$$

The first equality follows from the statement of Theorem 5.6.1. For the second equality, we use (5.38) and the fact that λ^* corresponds to the value τ_1 in the variable u ; see Remark 5.5.9. Finally, the third and fourth equalities are a consequence of (5.18), Remark 5.5.9 and (5.64). Now, it is not hard to prove that the function $\mathcal{F}(x)$ is strictly increasing. This implies, by (5.63), that

$$\mathcal{F}\left(\frac{4}{R_\perp(\widetilde{u}(0))}\right) > \mathcal{F}\left(\frac{4}{5}\right).$$

Observe that $\mathcal{F}\left(\frac{4}{5}\right) \approx -0.862875 > -1$. Hence, by (5.70), it follows that

$$\mathcal{F}\left(\frac{4}{R_{\perp}(\tilde{u}(0))}\right) > -1 = \mathcal{F}\left(\frac{4}{R_{\perp}(\tau_1)}\right).$$

By the monotonicity of $\mathcal{F}(x)$, we deduce that $R_{\perp}(\tau_1) > R_{\perp}(\tilde{u}(0))$, as we wanted to prove. \square

Corollary 5.6.10. *Let $\hat{f} : \mathcal{W} \cap \{a = 1\} \rightarrow \mathbb{R}$ be the analytic map*

$$\hat{f}(b, \kappa) := \tau(1, b, \kappa) - \tilde{u}(\kappa), \quad (5.71)$$

where \mathcal{W} is the open set in Remark 5.5.10. Then, there exists an analytic regular curve $\mu \subset \mathbb{R}^2$ contained in the region $\{b > 1, \kappa \leq 0\} \subset \mathbb{R}^2$ such that $\hat{f}(b, \kappa)$ vanishes along μ . This curve can be locally expressed as a graph over κ , i.e., there exists some $\kappa_0 < 0$ and an analytic function $b_{\mu}(\kappa)$ defined on $(\kappa_0, 0)$ satisfying

$$\mu \equiv \mu(\kappa) = (b_{\mu}(\kappa), \kappa).$$

Furthermore, the function $b \mapsto \hat{f}(b, \kappa)$ changes sign at $b = b_{\mu}(\kappa)$, meaning that $\hat{f}(b, \kappa) > 0$ (resp. $\hat{f}(b, \kappa) < 0$) for $b < b_{\mu}(\kappa)$ (resp. $b > b_{\mu}(\kappa)$). In other words, the sign of $\hat{f}(b, \kappa)$ coincides with that of $b_{\mu}(\kappa) - b$ locally around μ .

Proof. From (5.53), it follows that $\hat{f}(1, 0) > 0$ and that $\hat{f}(b, 0) < 0$ for every $b < 2$ close enough to 2. Hence, there exists some $b_0 \in (1, 2)$ with $\hat{f}(b_0, 0) = 0$ and such that $b \mapsto \hat{f}(b, 0)$ changes sign at $b = b_0$. The existence of the curve μ and its properties then follow from Lojasiewicz's Structure Theorem [52, Theorem 5.2.3]. \square

5.7 Proof of the main theorem

In Corollary 5.6.10, we proved the existence of a curve $\mu : (\kappa_0, 0) \rightarrow \mathcal{W} \cap \{a = 1\}$,

$$\mu(\kappa) = (b_{\mu}(\kappa), \kappa),$$

along which $\tau(1, b_{\mu}(\kappa), \kappa) = \tilde{u}(\kappa)$. According to Definition 5.3.15, this means that for every $\kappa \in (\kappa_0, 0)$, the surface $\Sigma_0(1, b_{\mu}(\kappa), \kappa; \tau)$ is a hyperbolic free boundary catenoid, where $\tau = \tau(1, b_{\mu}(\kappa), \kappa)$; see also Theorem 2.6.9. We now aim to construct non-rotational free boundary annuli. To achieve this purpose, we first recall that the surfaces $\Sigma_0(a, b, \kappa; u_0)$ with $a > 1$ are (non-rotational) annuli provided that $\Theta(a, b, \kappa) \in \mathbb{Q}$; see

Corollary 5.3.10. This property will be studied in Section 5.7.1. In Section 5.7.2 we will introduce a *height map* $\mathfrak{h} := \mathfrak{h}(a, b, \kappa)$ whose zeros are related with the free boundary property. Finally, in Section 5.7.3, we will prove Theorem 5.1.1.

5.7.1 The curve μ and the period map

We will now study some properties of the curve μ described above and its relation with the level sets of period map $\Theta(a, b, \kappa)$ for $a = 1$; see Section 5.4.

Lemma 5.7.1. *Let $a = 1$ and $\Theta_0 \in \left(-\frac{1}{\sqrt{2}}, -\frac{1}{\sqrt{3}}\right)$. Then, there exists some $\kappa_1 \in (0, \frac{1}{4})$ such that the point $(1, b^{\Theta_0}(1, \kappa), \kappa)$ lies in \mathcal{W}_1 for every $\kappa \in [0, \kappa_1)$ and to \mathcal{T} for $\kappa = \kappa_1$, where \mathcal{W}_1 and \mathcal{T} are defined in (5.50) and (5.51), and $b^{\Theta_0}(1, \kappa)$ is given by (5.37).*

Proof. Let $a = 1$ and $\kappa \in [0, 1/4)$. From (5.2), (5.50) it follows that $(1, b, \kappa) \in \mathcal{O}$ belongs to \mathcal{W}_1 if and only if $b < \widehat{b}(\kappa)$, and $(1, b, \kappa) \in \mathcal{T}$ if and only if $b = \widehat{b}(\kappa)$, where $\widehat{b}(\kappa) := 1 + \sqrt{1 - 4\kappa} \geq 1$. By (5.37),

$$\begin{aligned} b^{\Theta_0}(1, 0) &= \frac{1 - \Theta_0^2}{\Theta_0^2} < 2 = \widehat{b}(0), \\ b^{\Theta_0}\left(1, \frac{1}{4}\right) &= \frac{1 - \Theta_0^2}{\Theta_0^2} + \frac{\sqrt{1 - 2\Theta_0^2}}{\Theta_0^2} > 1 = \widehat{b}\left(\frac{1}{4}\right), \end{aligned}$$

which implies the existence of some $\kappa_1 \in (0, 1/4)$ such that $(1, b^{\Theta_0}(1, \kappa), \kappa)$ lies in \mathcal{W}_1 for $\kappa \in [0, \kappa_1)$ and to \mathcal{T} for $\kappa = \kappa_1$. \square

Lemma 5.7.2. *Let $a = 1$ and consider the curve $\mu(\kappa) = (b_\mu(\kappa), \kappa)$, $\kappa \in (\kappa_0, 0)$, introduced in Corollary 5.6.10. Then, the period map is not constant along $\mu(\kappa)$.*

Proof. Assume by contradiction that the period map is constant along μ , that is, it holds $\Theta(1, b_\mu(\kappa), \kappa) \equiv \Theta_0$. This means that $\mu(\kappa)$ coincides with the level curve $\kappa \mapsto (b^{\Theta_0}(1, \kappa), \kappa)$ in (5.37) for $\kappa \in (\kappa_0, 0)$. Observe that, since $\mu(0) = (b_0, 0)$ with $b_0 \in (1, 2)$, (5.30) shows that $\Theta_0 \in \left(-\frac{1}{\sqrt{2}}, -\frac{1}{\sqrt{3}}\right)$. Now, let

$$g(\kappa) := \widehat{f}(b^{\Theta_0}(1, \kappa), \kappa), \quad (5.72)$$

where $\widehat{f}(b, \kappa)$ is defined in (5.71). Note that $g(\kappa)$ is analytic for $\kappa \in (\kappa_0, \kappa_1)$, where $\kappa_1 > 0$ is defined in Lemma 5.7.1. It is clear that for $\kappa \in (\kappa_0, 0)$, $g(\kappa) = \widehat{f}(\mu(\kappa)) = 0$,

so by analyticity, $g(\kappa) \equiv 0$ for all $\kappa \in (\kappa_0, \kappa_1)$. However, this leads to a contradiction:

$$0 = \lim_{\kappa \rightarrow \kappa_1} g(\kappa) = \lim_{\kappa \rightarrow \kappa_1} \tau(1, b^{\Theta_0}(1, \kappa), \kappa) - \tilde{u}(\kappa) = -\tilde{u}(\kappa_1) < 0,$$

where in the last inequality we use the fact that $(1, b^{\Theta_0}(1, \kappa_1), \kappa_1) \in \mathcal{T}$ and Lemma 5.5.11. This contradiction proves Lemma 5.7.2. \square

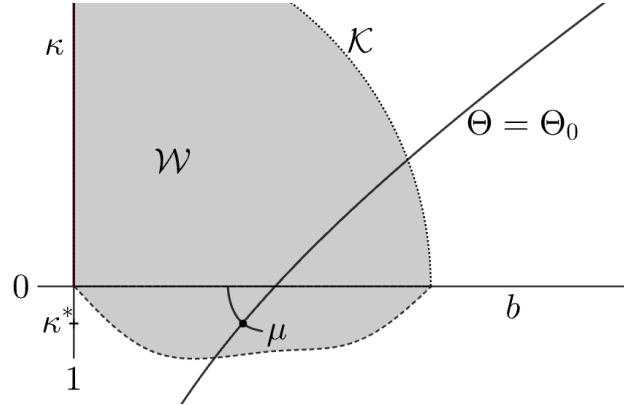


Figure 5.3: Level curve $\Theta = \Theta_0$ on the plane $\{a = 1\}$ for $\Theta_0 \in \left(-\frac{1}{\sqrt{2}}, -\frac{1}{\sqrt{3}}\right)$. This level set and the curve μ intersect at a point $\mu(\kappa^*) \in \mathcal{W}$ with $\kappa^* < 0$.

Proposition 5.7.3. *There exists an interval $\mathcal{J} \subset \left(-\frac{1}{\sqrt{2}}, -\frac{1}{\sqrt{3}}\right)$ such that, for every $\Theta_0 \in \mathcal{J}$, it holds $b^{\Theta_0}(1, \kappa^*) = b_\mu(\kappa^*)$ for some $\kappa^* = \kappa^*(\Theta_0) < 0$. Moreover, $\kappa \mapsto b_\mu(\kappa) - b^{\Theta_0}(1, \kappa)$ changes sign at $\kappa = \kappa^*$; see Figure 5.3.*

Proof. The result is a consequence of Remark 5.4.4 and Lemma 5.7.2. Indeed, consider a closed interval $I := [\kappa_a, \kappa_b] \subset (\kappa_0, 0)$. Let $\Theta_m < \Theta_M$ be the minimum and maximum of the (non-constant) function $\kappa \mapsto \Theta(1, b_\mu(1, \kappa), \kappa)$ on I , and $\kappa_c, \kappa_d \in I$ be values in which the minimum and maximum are attained, respectively. Then, for every $\Theta_0 \in \mathcal{J} := (\Theta_m, \Theta_M)$,

$$\begin{aligned} 0 < \Theta_0 - \Theta_m &= \Theta(1, b^{\Theta_0}(1, \kappa_c), \kappa_c) - \Theta(1, b_\mu(\kappa_c), \kappa_c) \\ &= \frac{\partial \Theta}{\partial b}(1, \xi, \kappa_c)(b^{\Theta_0}(1, \kappa_c) - b_\mu(\kappa_c)), \end{aligned}$$

by the mean value theorem, where $\frac{\partial \Theta}{\partial b}$ denotes the partial derivative of Θ with respect to b . This derivative is positive, so $b^{\Theta_0}(1, \kappa_c) > b_\mu(\kappa_c)$; see Remark 5.4.4. An analogue computation using $\Theta_0 - \Theta_M$ shows that $b^{\Theta_0}(1, \kappa_d) < b_\mu(\kappa_d)$. As a consequence, there exists some κ^* between κ_c and κ_d satisfying the properties listed in the proposition. \square

Corollary 5.7.4. *With the notations of Proposition 5.7.3, for every $\Theta_0 \in \mathcal{J}$, the function $g(\kappa)$ in (5.72) changes sign at $\kappa^* < 0$.*

Proof. By definition of κ^* , it holds

$$b^{\Theta_0}(1, \kappa^*) = b_\mu(\kappa^*),$$

so $g(\kappa^*) = \widehat{f}(b_\mu(\kappa^*), \kappa^*) = 0$. From Corollary 5.6.10 we deduce that $b \mapsto \widehat{f}(b, \kappa)$ changes sign at $b = b_\mu(\kappa)$, i.e., the sign of $\widehat{f}(b, \kappa)$ coincides with that of $b_\mu(\kappa) - b$ locally around μ . Now, since $b_\mu(\kappa) - b^{\Theta_0}(1, \kappa)$ changes sign at $\kappa = \kappa^*$, so does $g(\kappa)$. \square

5.7.2 The height map

We now define the following map, which aims to detect those surfaces $\Sigma_0(a, b, \kappa; \tau)$ which are free boundary in a ball.

Definition 5.7.5. *Let $(a, b, \kappa) \in \mathcal{W}$ and suppose that for $\tau = \tau(a, b, \kappa)$, it holds (5.20) and $\alpha(\tau) \neq 0$, where τ and \mathcal{W} are given by Proposition 5.5.8 and Remark 5.5.10 respectively. We then define the height map as the analytic function*

$$\mathfrak{h}(a, b, \kappa) := m_3(\tau(a, b, \kappa)),$$

where m_3 is the third coordinate of the center map $m(u)$ in (5.21); see Remarks 5.2.7 and 5.2.8.

Let $(a, b, \kappa) \in \mathcal{W} \cap \mathcal{O}^-$ with $\kappa < 0$. According to Corollary 5.3.10 and Remark 5.3.13, if $\mathfrak{h}(a, b, \kappa) = 0$ and $\Theta(a, b, \kappa) \in \mathbb{Q}$, then $\Sigma_0(a, b, \kappa; \tau)$ is a free boundary minimal annulus in some geodesic ball of $\mathbb{M}^3(\kappa)$, where $\tau = \tau(a, b, \kappa)$. This motivates the study of the roots of the function $\mathfrak{h}(a, b, \kappa)$. The following lemma relates \mathfrak{h} with the map \widehat{p} in Remark 5.3.18:

Lemma 5.7.6. *Let $(1, b, \kappa) \in \mathcal{W}$ with $\kappa < 0$ and $\widehat{p}(u) : \mathcal{I} \subset \mathbb{R} \rightarrow \mathcal{X}$ be the map in Remark 5.3.18. If $\tau(1, b, \kappa)$ lies in \mathcal{I} , then the height map $\mathfrak{h}(1, b, \kappa)$ is well defined and satisfies*

$$\mathfrak{h}(1, b, \kappa) = \widehat{p}_3(\tau(1, b, \kappa)). \quad (5.73)$$

Proof. Let $\tau = \tau(1, b, \kappa)$. We will prove that the center map $m(u) = m(u; 1, b, \kappa)$ is well defined at $u = \tau$, i.e., the condition (5.20) is satisfied; see Remark 5.2.8. In fact, we will show that $m(\tau) = \widehat{p}(\tau)$, from which (5.73) follows.

Let $\tilde{m}(u)$ be the map in (5.17). For every u , $\tilde{m}(u)$ lies in the timelike plane

$$\mathcal{P} = \{x_1 = x_2 = 0\},$$

see Remark 5.3.5 and Proposition 5.4.2. Recall that this plane intersects $\mathbb{M}^3(\kappa)$ along the geodesic \mathcal{L} , which coincides with the rotation axis of the surface $\Sigma(1, b, \kappa)$; see Proposition 5.3.17.

Now, let $u = \tau$. Using (5.17) and the definition of the map τ , it follows that $\tilde{m}(\tau)$ belongs to the timelike plane P_0 spanned by $\psi(\tau, 0)$ and $\psi_u(\tau, 0)$. We will now prove that $P_0 \cap \mathcal{P}$ is a timelike line in \mathbb{R}_κ^4 , which implies by Remarks 5.2.7 and 5.2.8 that $m(u)$ is well defined and analytic, i.e., $\tilde{m}(u)$ admits a rescaling which belongs to $\mathbb{M}^3(\kappa)$.

We note that $P_0 \cap \mathbb{M}^3(\kappa)$ is a geodesic of $\mathbb{M}^3(\kappa)$ which must coincide with ζ_τ ; see Remark 5.3.18. We know that ζ_τ and the rotation axis of the catenoid meet at a unique point $\hat{p}(\tau)$ in the half space $\{x_4 > 0\}$. This implies that $P_0 \cap \mathcal{P}$ is a timelike line in which $\tilde{m}(\tau)$ lies. In fact, the rescaling $m(\tau)$ of $\tilde{m}(\tau)$ must be $\hat{p}(\tau)$, as we wanted to prove. \square

Proposition 5.7.7. *With the notations of Proposition 5.7.3, for each $\Theta_0 \in \mathcal{J}$, the function*

$$\tilde{g}(\kappa) := \mathfrak{h}(1, b^{\Theta_0}(1, \kappa), \kappa)$$

is well defined on a neighbourhood of κ^ and changes sign at that point.*

Proof. We first show that the function $\tilde{g}(\kappa)$ is well defined. By Corollary 5.7.4, it holds $\tilde{u}(\kappa^*) = \tau(1, b^{\Theta_0}(1, \kappa^*), \kappa^*)$. In particular, for values of κ near κ^* , $\tau = \tau(1, b^{\Theta_0}(1, \kappa), \kappa)$ will be close to $\tilde{u}(\kappa)$, and so τ will belong to the interval \mathcal{I} in Remark 5.3.18. By Lemma 5.7.6, $\tilde{g}(\kappa)$ is well defined on a neighbourhood of κ^* .

In order to prove the proposition, we will show that the signs of $\tilde{g}(\kappa)$ and $g(\kappa)$ defined in (5.72) coincide on a neighbourhood of κ^* and then apply Corollary 5.7.4. To simplify notation, let $\tau = \tau(1, b^{\Theta_0}(1, \kappa), \kappa)$ and $\tilde{u} = \tilde{u}(\kappa)$. By (5.73) and the definition of $\tilde{g}(\kappa)$, it holds $\tilde{g}(\kappa) = \hat{p}_3(\tau)$. Since the function $\hat{p}_3(u)$ is strictly increasing and $\hat{p}_3(\tilde{u}) = 0$, the sign of $\hat{p}_3(\tau)$ coincides with that of $\tau - \tilde{u} = g(\kappa)$, as we wanted to show; see Remark 5.3.18. In particular, note that $\tilde{g}(\kappa^*) = g(\kappa^*) = 0$. \square

5.7.3 Proof of Theorem 5.1.1

Fix $q \in \mathcal{J} \cap \mathbb{Q}$ and define

$$\mathfrak{G}(a, \kappa) := \mathfrak{h}(a, b^q(a, \kappa), \kappa), \tag{5.74}$$

where $b^q(a, \kappa)$ is the function in Remark 5.4.4 for $\Theta_0 = q$ and \mathcal{J} is the interval in Proposition 5.7.3. Observe that if $a = 1$, $\mathfrak{G}(1, \kappa) = \tilde{\mathfrak{g}}(\kappa)$. By Proposition 5.7.7, $\mathfrak{G}(a, \kappa)$ is well defined and analytic on a neighbourhood of $(a, \kappa) = (1, \kappa^*)$, and $\kappa \mapsto \mathfrak{G}(1, \kappa)$ changes sign at κ^* . Hence, applying Lojasiewicz's Structure Theorem [52, Theorem 5.2.3] to the map $\mathfrak{G}(a, \kappa)$, it follows that there exists $\varepsilon_0 = \varepsilon_0(q)$ and a curve $\hat{\mu}_q : [0, \varepsilon_0) \rightarrow \mathbb{R}^2$, $\hat{\mu}_q(\eta) := (a(\eta), \kappa(\eta))$, satisfying $\mathfrak{G}(\hat{\mu}_q(\eta)) \equiv 0$ for all $\eta \geq 0$. Moreover, $\hat{\mu}_q(0) = (1, \kappa^*)$ and $a(\eta) > 1$ for every $\eta > 0$ and $\kappa(\eta) < 0$.

Consider the 1-parameter family of surfaces

$$\Sigma_q(\eta) := \Sigma_0(a(\eta), b^q(a(\eta), \kappa(\eta)), \kappa(\eta); \tau(\eta)), \quad (5.75)$$

where $\tau(\eta) = \tau(a(\eta), b^q(a(\eta), \kappa(\eta)), \kappa(\eta))$; see Definition 5.3.11. We note that for every $\eta \geq 0$ close enough to zero, $\tau(\eta)$ is below the value $u_{\mathcal{D}} = u_{\mathcal{D}}(\eta)$ in (5.8), so that $\Sigma_q(\eta)$ is well defined: indeed, this property holds at $\eta = 0$, as $a(0) = 1$ and $\tau(0) = \tilde{u}(\kappa(0)) < u_{\mathcal{D}}(0)$; see Remark 5.3.16. Now, by the analyticity of the immersions $\psi(u, v) = \psi(u, v; \eta)$ associated the family of surfaces $\Sigma_q(\eta)$ with respect to the parameter η , we deduce that necessarily $\tau(\eta) < u_{\mathcal{D}}(\eta)$ for $\eta \geq 0$ sufficiently small.

Let us express the rational number q as an irreducible fraction $q = -m/n$, $m, n \in \mathbb{N}$. From Corollary 5.3.10 it follows that the surfaces $\Sigma_q(\eta)$ are compact minimal annuli once we identify $(u, v) \sim (u, v + 2n\sigma)$, where $\sigma = \sigma(a(\eta), b^q(a(\eta), \kappa(\eta)), \kappa(\eta))$ depends analytically on η . Moreover, by definition of τ and since the height map \mathfrak{h} vanishes along the parameters associated to $\Sigma_q(\eta)$, it follows from Remark 5.3.13 that each of these annuli is free boundary in some geodesic ball $B = B(q, \eta)$ of $\mathbb{M}^3(\kappa(\eta))$. Furthermore, the following properties are satisfied:

- (i) The balls $B(q, \eta)$ are centered at $\mathbf{e}_4 \in \mathbb{M}^3(\kappa(\eta))$ by item (4) of Theorem 5.3.12.
- (ii) Each annulus $\Sigma_q(\eta)$ is invariant under the symmetry with respect to the totally geodesic surface $\mathbf{S} \subset \mathbb{M}^3(\kappa(\eta))$, and also with respect to the n totally geodesic surfaces $\Omega_j \subset \mathbb{M}^3(\kappa(\eta))$ which meet equiangularly along \mathcal{L} . This follows from item (1) of Theorem 5.3.12.
- (iii) The rotation index of the planar geodesic $\Sigma_q(\eta) \cap \mathbf{S}$ is $-m$; see Remark 5.3.9.
- (iv) The annuli $\Sigma_q(\eta)$ are of Enneper type; see the discussion at the beginning of Section 5.2.2.

- (v) If $\eta > 0$, then $a(\eta) > 1$, and so the annulus $\Sigma_q(\eta)$ has a prismatic symmetry group of order $4n$; see item (5) of Theorem 5.3.12.
- (vi) For $\eta = 0$ it holds $a(\eta) = 1$, so the annulus $\Sigma_q(0)$ is an m -cover of a free boundary hyperbolic catenoid. This follows from the discussion in Subsection 5.3.3 and Remark 5.3.9.

We will now define the set of annuli $\mathbb{A}_q(\eta) \subset \mathbb{H}^3$ in Theorem 5.1.1. First, recall that for every $\kappa < 0$, $\mathbb{M}^3(\kappa) \subset \mathbb{R}_\kappa^4$ is a hyperbolic space of sectional curvature κ ; see Remark 2.5.2. In fact, the linear change $x_4 \mapsto x_4/\sqrt{-\kappa}$ yields an isometry between $\mathbb{M}^3(\kappa)$ and the three-dimensional hyperboloid model $\mathbb{H}^3(\kappa) \subset \mathbb{L}^4$ of curvature κ , that is,

$$\mathbb{H}^3(\kappa) = \{(x_1, x_2, x_3, x_4) \in \mathbb{L}^4 : x_1^2 + x_2^2 + x_3^2 - x_4^2 = 1/\kappa, x_4 > 0\}.$$

Now, a homothety of ratio $\sqrt{-\kappa}$ in Lorentz space \mathbb{L}^4 sends the hyperboloid $\mathbb{H}^3(\kappa)$ to the usual hyperbolic space $\mathbb{H}^3 \subset \mathbb{L}^4$ of curvature -1 . We then define $\mathbb{A}_q(\eta) \subset \mathbb{H}^3$ as the image of the annulus $\Sigma_q(\eta)$ under the isometry and homothety that sends the space $\mathbb{M}^3(\kappa(\eta))$ to \mathbb{H}^3 . By the properties (I)-(VI) of the annuli $\Sigma_q(\eta)$ listed above, it is immediate to check that the surfaces $\mathbb{A}_q(\eta)$ are free boundary minimal annuli in geodesic balls of \mathbb{H}^3 satisfying items (1)-(6) of Theorem 5.1.1. This completes the proof.

5.8 Final notes

The theory of free boundary minimal surfaces in geodesic balls of hyperbolic 3-space is still undeveloped. The examples that we have produced in Theorem 5.1.1 are the first ones other than totally geodesic disks and free boundary hyperbolic catenoids. In particular, no embedded examples other than the rotational ones have been constructed yet.

It is natural to expect that some of the methods used to construct free boundary minimal surfaces in the Euclidean unit ball, such as min-max techniques (see for example [10, 11, 30, 31, 50]), could be applied in \mathbb{H}^3 .

In [29, Theorem 1.2], it was proved that any embedded, free boundary minimal annulus in the Euclidean unit ball foliated by spherical curvature lines must be the critical catenoid. This result relies on a theorem by Seo [65]. The study carried out in this chapter leads us to believe that there are no embedded, non-rotational free boundary minimal annuli in geodesic balls of \mathbb{H}^3 foliated by spherical curvature lines. This

supports the validity of the \mathbb{H}^3 -version of the critical catenoid conjecture, proposed by Medvedev [60].

We also emphasize that the annuli constructed in Theorem 5.1.1 are free boundary in *some* geodesic balls of \mathbb{H}^3 . In other words, we do not prescribe the radius of the ball in our construction. We do not know whether non-rotational free boundary minimal annuli exist on *any* geodesic ball of \mathbb{H}^3 .

The problem of finding free boundary CMC annuli with mean curvature $H \in (0, 1]$ in geodesic balls of \mathbb{H}^3 remains unexplored. For the case $H \in (0, 1)$ it is likely that the deformation idea that we used for $H = 0$ still holds, and this would create free boundary CMC annuli of Enneper type. This happens because the Gauss equation for CMC surfaces in \mathbb{H}^3 with $H \in [0, 1)$ is, up to conformal reparametrization, the cosh-Gordon equation, and so most of our study for the case $H = 0$ could also be applied there.

The case $H = 1$ is special in this context. It corresponds to the so-called *Bryant surfaces*, which have been studied in detail for many years, motivated by [8]. These surfaces are locally isometric to minimal surfaces in \mathbb{R}^3 , and admit a Weierstrass-type representation based on the fact that the so-called *hyperbolic Gauss map* of the surface is conformal when $H = 1$. In particular, the Gauss equation is given, in this situation, by the Liouville equation, and many of the analytic aspects in the study of minimal surfaces of Enneper type in \mathbb{R}^3 studied in [76] or [29] can be applied to Bryant surfaces. In particular, one expects to have a nice, more explicit theory of Enneper type surfaces in \mathbb{H}^3 when $H = 1$ than for the rest of values of H .

In Chapter 4 we showed that there exist CMC annuli of Enneper type that are free boundary and embedded in some geodesic ball of \mathbb{H}^3 , for every $H > 1$. This makes the limit case $H = 1$ specially interesting in what regards embeddedness. We expect that there will exist free boundary $H = 1$ surfaces of Enneper type in some geodesic balls of \mathbb{H}^3 , but that they will never be embedded.

Chapter 6

Capillary minimal annuli in \mathbb{B}^3

6.1 Summary and main results

In this chapter, we construct, for any $n \in \mathbb{N}$, $n \geq 2$, a real analytic family $\mathcal{F} := \{\mathbb{A}_n(a) : a \in (0, 1)\}$ of embedded capillary minimal annuli in the unit ball \mathbb{B}^3 of \mathbb{R}^3 , with a prismatic symmetry group of order $4n$; see Figures 1.3, 1.4. These annuli interpolate between a compact piece of a catenoid (as $a \rightarrow 1$) and a necklace of n vertical disks meeting tangentially along the equator of $\partial\mathbb{B}^3$ (as $a \rightarrow 0$). As an application, we construct non-radial annular regions $\Omega \subset \mathbb{S}^2$ that admit solutions to $\Delta u + 2u = 0$ in Ω with constant Dirichlet and Neumann conditions along $\partial\Omega$. This chapter is based on [17].

We first state the result regarding the existence of the family of embedded capillary minimal annuli in \mathbb{B}^3 .

Theorem 6.1.1. *Let $n \in \mathbb{N}$, $n \geq 2$. Then, there exists a real analytic 1-parameter family $\{\mathbb{A}_n(a) : a \in (0, 1]\}$ of capillary minimal annuli in $\mathbb{B}^3 \subset \mathbb{R}^3$ satisfying the following properties:*

- (1) *Each $\mathbb{A}_n(a)$ is symmetric with respect to the horizontal plane $\{x_3 = 0\}$ and also with respect to n vertical planes which meet equiangularly along the x_3 -axis.*
- (2) *If $a = 1$, $\mathbb{A}_n(a)$ is a piece of a capillary catenoid in \mathbb{B}^3 .*
- (3) *If $a \in (0, 1)$, $\mathbb{A}_n(a)$ has a prismatic symmetry group generated by the isometries in item (1). In particular, $\mathbb{A}_n(a)$ is not rotational.*
- (4) *Each $\mathbb{A}_n(a)$ is a radial graph over the origin of \mathbb{R}^3 . Consequently, $\mathbb{A}_n(a)$ is an embedded minimal annulus.*

- (5) $\mathbb{A}_n(a)$ converges as $a \rightarrow 0$ to a chain of n vertical disks meeting tangentially along the equator $\{x_3 = 0\} \cap \partial\mathbb{B}^3$. In particular, if $n = 2$, $\mathbb{A}_2(a)$ converges to a double cover of a vertical equatorial disk.

This theorem extends a previous result by Fernández, Hauswirth and Mira [29]. More precisely, they showed the existence of the annuli $\mathbb{A}_n(a)$ in Theorem 6.1.1 for values of the parameter a near 1, that is, their examples are close to catenoids. In the present work, we analyze the global behaviour of the family $\mathbb{A}_n(a)$ for all $a \in (0, 1)$. We show that each annulus in this family is embedded, and describe the limit surfaces $\mathbb{A}_n(a)$ as $a \rightarrow 0$.

The proof method used in Theorem 6.1.1 also provides partial control on the contact angles of the capillary annuli $\mathbb{A}_n(a)$ with $\partial\mathbb{B}^3$. Specifically, we prove:

Theorem 6.1.2. *There exist $\vartheta_0, \vartheta_1 \in (0, \pi/2)$ such that:*

1. *For every $\theta \in (0, \vartheta_0)$, there exists a non-rotational embedded minimal annulus $\mathbb{A}_n(a)$ which intersects $\partial\mathbb{B}^3$ with contact angle θ .*
2. *Similarly, given any $\theta \in (\vartheta_1, \frac{\pi}{2})$, we can find a non-rotational embedded minimal annulus $\mathbb{A}_2(a)$ with $n = 2$ meeting $\partial\mathbb{B}^3$ with angle θ .*

Let us recall the critical catenoid conjecture (see Conjecture 1.3), which states that the critical catenoid is the unique embedded minimal annulus which meets $\partial\mathbb{B}^3$ with constant intersection angle $\theta = \frac{\pi}{2}$. As an immediate corollary of Theorem 6.1.2, we deduce that such a result does not hold for a range of angles θ below the critical value $\frac{\pi}{2}$.

Corollary 6.1.3. *There exists $\vartheta_1 \in (0, \frac{\pi}{2})$ such that for every $\theta \in (\vartheta_1, \frac{\pi}{2})$, there exist embedded, non-rotational minimal annuli which intersect $\partial\mathbb{B}^3$ with constant angle θ .*

We now present a brief outline of the chapter. In Section 6.2 we construct a 2-parameter family of minimal surfaces $\Sigma = \Sigma(a, b)$ of Enneper type in \mathbb{R}^3 . These examples were already studied by Fernández, Hauswirth and Mira [29], but we consider an alternative parametrization here that suits our purposes better. One of the key differences in the present work is that we use the constant Q associated to the Hopf differential as a parameter. In this way, totally geodesic examples appear naturally in the construction. This is essential, as we expect to detect families of capillary annuli which converge to a chain of (planar) disks; see Theorem 6.1.1.

In Section 6.3, we study the symmetries of the surfaces $\Sigma(a, b)$. We also introduce the period map $\Theta = \Theta(a, b)$, whose rational values detect when a certain surface

$\Sigma(a, b)$ is an annulus. This allows us to define, for every $n \geq 2$, a 1-parameter family of capillary minimal annuli in some ball of \mathbb{R}^3 . In Section 6.4, we show that these annuli are embedded. The proof of Theorem 6.1.1 is then almost direct; the remaining details are studied in Section 6.5.1. In that section, we also prove Theorem 6.1.2.

The goal of Section 6.6 is to provide a proof of some technical lemmas needed throughout Section 6.4. Finally, in Section 6.7, we use the set of minimal annuli in Theorem 6.1.1 to construct a family of solutions to the overdetermined problem (1.5). These solutions provide counterexamples to a conjecture by Souam [70] (see Conjecture 1.5).

6.2 A family of minimal immersions of Enneper type in \mathbb{R}^3

The goal of this section is to construct a 2-parameter family of minimal immersions of Enneper type in \mathbb{R}^3 . Up to a reparametrization and homothety in \mathbb{R}^3 , these examples coincide with those obtained by Fernández, Hauswirth and Mira [29, Theorem 1.3]. However, the parametrization considered here will be more convenient for our purposes. To do so, we will study a set of solutions to the overdetermined system (2.14) in the particular case $A = 0$. The constant Q associated to the Hopf differential will be used as a parameter in the construction. This will allow us to consider totally geodesic examples in a natural way within the construction.

6.2.1 A set of solutions to (2.14)

We will now construct a two-parameter family of solutions to (2.14) under the assumption that $A = 0$. We consider the parameter space $\mathcal{O} \subset \mathbb{R}^2$ given by

$$\mathcal{O} := \{(a, b) : a \in [0, 1], b \in (0, \infty)\}. \quad (6.1)$$

For every $(a, b) \in \mathcal{O}$, we define the pair $\alpha(u) = \alpha(u; a, b)$ and $\beta(u) = \beta(u; a, b)$ as the unique solutions to the system

$$\begin{cases} \alpha'' = \hat{a}\alpha - 4Q\alpha^2\beta, \\ \beta'' = \hat{a}\beta - 4Q\alpha\beta^2 - Q\alpha \end{cases} \quad (6.2)$$

with the following initial conditions and constants $\hat{a}, Q \in \mathbb{R}$:

$$\begin{aligned} \alpha(0) = \beta(0) = 0, \quad \alpha'(0) = \frac{1}{4}, \quad \beta'(0) = \frac{1}{4b}(a^2b^2 + b^2 - 1), \\ \hat{a} = -\frac{1}{4}(-a^2b^2 + a^2 + 1), \quad Q = \frac{a^2b}{2}. \end{aligned} \quad (6.3)$$

Under these initial conditions, the polynomial $p(x) = p(0, x)$ in (2.24) admits the following factorization:

$$p(x) = -(x-1)(x-a^2)(x+a^2b^2), \quad (6.4)$$

which satisfies $p(x) \geq 0$ for every $x \in [a^2, 1]$. By Theorem 2.4.5 and Remark 2.4.6, we deduce for every $(a, b) \in \mathcal{O} \cap \{a > 0\}$ the existence of a unique solution $\omega(u, v) = \omega(u, v; a, b)$ to the overdetermined system (2.14) with $A = 0$, $Q = \frac{a^2b}{2} > 0$ and $\omega(0, 0) = 0$.

Remark 6.2.1. Let $(a, b) \in \mathcal{O}$ with $a = 0$. We note that the converse implication of Theorem 2.4.5 also holds in the limit case $Q = \frac{a^2b}{2} = 0$, i.e., any solution (α, β) to (6.2) induces a solution $\omega(u, v) = \omega(u, v; 0, b)$ to (2.14) in the particular case $Q = 0$.

Remark 6.2.2. Let $X(u, v) := e^{\omega(u, v)}$, and assume that $a > 0$. At $u = 0$, we have by (2.23) that

$$4X_v(0, v)^2 = p(x), \quad (6.5)$$

where $p(x)$ is the polynomial in (6.4). Thus, we deduce that the function $v \mapsto \omega(0, v)$ satisfies:

1. If $a \in (0, 1)$, then $\omega(0, v)$ is periodic and takes values on the interval $[a^2, 1]$.
2. If $a = 1$, then $\omega(0, v) \equiv 0$. In particular, by (2.14b), $\omega = \omega(u)$ only depends on u .

By the previous remark and (2.14b), it is clear that for $a > 0$, the solutions $\omega(u, v)$ to (2.14) are defined at least on an open strip

$$\mathcal{D} = (-u_{\mathcal{D}}, u_{\mathcal{D}}) \times \mathbb{R}. \quad (6.6)$$

Regarding the limit case $a = 0$, we can explicitly compute $\omega(u, v)$, as we will see in Section 6.2.3.

Remark 6.2.3. *Arguing as in Proposition 3.2.3, it is possible to show that u_D coincides with the first positive root of $\alpha(u)$, if it exists. In case $\alpha(u) > 0$ for all $u > 0$, then $\omega(u, v)$ is defined on \mathbb{R}^2 .*

We will now study the symmetries of the functions $\omega(u, v)$. According to (6.3), it follows that the pairs $(\alpha(u), \beta(u))$ solving (6.2) are antisymmetric. Thus, by (2.14b), we deduce that

$$\omega(u, v) = \omega(-u, v). \quad (6.7)$$

If $a > 0$ we can also find a value $\sigma = \sigma(a, b)$ as we did in Proposition 3.3.1.

Lemma 6.2.4. *There exists an analytic function $\sigma(a, b) \in \mathcal{O} \cap \{a > 0\}$ such that*

$$\omega(u, j\sigma + v) = \omega(u, j\sigma - v) \quad (6.8)$$

for every $v \in \mathbb{R}$. In particular, it holds

$$\omega(u, v) = \omega(u, v + 2\sigma).$$

If $a \in (0, 1)$, then σ is given by

$$\sigma(a, b) = \int_{a^2}^1 \frac{2}{\sqrt{p(x)}} dx, \quad (6.9)$$

where $p(x)$ is the polynomial in (6.4). In the particular case $a = 1$, it holds

$$\sigma(1, b) = \frac{2\pi}{\sqrt{1+b^2}}. \quad (6.10)$$

Moreover, for every $b_0 > 0$,

$$\lim_{(a,b) \rightarrow (0,b_0)} \sigma(a, b) = \infty. \quad (6.11)$$

Proof. Assume first that $a \in (0, 1)$. Then, it follows from (6.5) and the expression of $p(0, x)$ in (6.4) that $v \mapsto e^{\omega(0,v)}$ (and thus, $\omega(0, v)$) is 2σ -periodic and takes values on the interval $[a^2, 1]$, where $\sigma = \sigma(a, b)$ satisfies (6.9). Moreover, it holds

$$\omega(0, j\sigma + v) = \omega(0, j\sigma - v)$$

for every $v \in \mathbb{R}$ and $j \in \mathbb{Z}$. In particular, by using (2.14b), it is possible to deduce (6.8). By applying the change of variables $x = h_a(t) = (1 - a^2)t + a^2$ in (6.9), we

obtain that

$$\sigma(a, b) = \int_0^1 \frac{2}{\sqrt{t(1-t)}\sqrt{h_a(t) + a^2b^2}} dt. \quad (6.12)$$

This expression is well defined and analytic for $a = 1$, and in fact $\sigma(1, b)$ satisfies (6.10).

Finally, the limit (6.11) is a straightforward consequence of the monotone convergence theorem: indeed, if $0 < a_0 < a_1$, then $h_{a_0}(t) + a_0^2b^2 < h_{a_1}(t) + a_1^2b^2$ for all $t \in [0, 1]$, and moreover $\lim_{a \rightarrow 0} h_a(t) + a^2b^2 = t$. Thus, by (6.12),

$$\lim_{(a,b) \rightarrow (0,b_0)} \sigma(a, b) = \int_0^1 \frac{2dt}{t\sqrt{1-t}} = \infty.$$

□

6.2.2 The induced minimal immersions

Let $(a, b) \in \mathcal{O}$. By Theorem 2.4.4 and Remark 6.2.1, it follows that the function $\omega(u, v) = \omega(u, v; a, b)$ constructed in Section 6.2.1 induces a minimal immersion $\psi(u, v) = \psi(u, v; a, b)$ in \mathbb{R}^3 with first and second fundamental forms given by

$$I = e^{2\omega}(du^2 + dv^2), \quad II = \frac{a^2b}{2}(du^2 - dv^2).$$

In particular, $\psi(u, v)$ is either totally geodesic (if $a = 0$) or has no umbilical points (if $a > 0$).

Definition 6.2.5. We will denote by $\Sigma = \Sigma(a, b)$ the surface associated to the immersion $\psi(u, v) = \psi(u, v; a, b)$.

Remark 6.2.6. It is clear that the immersions $\psi(u, v) = \psi(u, v; a, b)$ depend analytically on the parameters $(a, b) \in \mathcal{O}$.

We note that $\psi(u, v)$ is of Enneper type, so that every v -line $v \mapsto \psi(u, v)$ lies in a certain sphere or plane $\mathcal{Q}(u)$ of \mathbb{R}^3 . By Proposition 2.4.3, if $\alpha \neq 0$ the radii and contact angles with Σ of \mathcal{Q} satisfy

$$R^2 = \frac{4 + 4\beta^2}{\alpha^2}, \quad \tan \theta = -\frac{1}{\beta}, \quad (6.13)$$

and the center function $\widehat{c}(u)$ simplifies to

$$\widehat{c}(u) = \psi - \frac{2}{\alpha}\psi_u e^{-\omega} + \frac{2\beta}{\alpha}N. \quad (6.14)$$

Finally, if $\alpha(u) = 0$, the v -line $\psi(u, v)$ is planar.

We showed in Proposition 2.4.7 that the center function $\widehat{c}(u)$ takes values on a line L . Arguing as in Lemma 3.2.7 of Chapter 3, the following result can be deduced:

Lemma 6.2.7. *There exists a line $L \subset \mathbb{R}^3$ such that $\widehat{c}(u)$ lies in L for every $u \in (-u_{\mathcal{D}}, u_{\mathcal{D}})$ satisfying $\alpha(u) \neq 0$; see (6.6)). Moreover, L is orthogonal to the horizontal plane $\{x_3 = 0\}$, and*

$$\widehat{c}(u) = 2 \frac{\alpha'(0)}{\alpha(u)} \mathbf{e}_3 = \frac{1}{2\alpha(u)^2} \mathbf{e}_3 \quad (6.15)$$

6.2.3 The limit case $a = 0$

We will now study the surfaces $\Sigma(0, b)$ associated to the limit values $(0, b) \in \mathcal{O}$. We know that these immersions are totally geodesic since their Hopf differential is zero, so they are (pieces of) planes. Nevertheless, it will be of interest for our purposes to explicitly compute their parametrizations $\psi(u, v)$.

First, we will look at the functions $\omega(u, v) = \omega(u, v; 0, b)$. By (6.2)-(6.3), it is straightforward to deduce that

$$\begin{aligned} \alpha(u; 0, b) &= \frac{1}{2} \sin\left(\frac{u}{2}\right), \\ \beta(u; 0, b) &= \frac{b^2 - 1}{2b} \sin\left(\frac{u}{2}\right). \end{aligned} \quad (6.16)$$

By (6.4), (6.5) and the initial condition $e^{\omega(0,0)} = 1$, it is possible to obtain $v \mapsto e^{\omega(0,v)}$, yielding

$$e^{\omega(0,v)} = \frac{2}{1 + \cosh\left(\frac{v}{2}\right)}.$$

Now, for every fixed $v_0 \in \mathbb{R}$, we use (2.14b) and (6.16) to compute $u \mapsto \omega(u, v)$, obtaining

$$e^{\omega(u,v)} = \frac{2}{\cos\left(\frac{u}{2}\right) + \cosh\left(\frac{v}{2}\right)}. \quad (6.17)$$

We note that $\omega(u, v)$ is a real analytic function in $\mathbb{R}^2 \setminus \mathcal{Z}$, where \mathcal{Z} is the discrete set

$$\mathcal{Z} = \{(2\pi + 4k\pi, 0) : k \in \mathbb{Z}\}.$$

Moreover, $\omega(u, v)$ does not depend on b . In particular, the maximal open strip in which $\omega(u, v)$ is well defined is given by

$$\mathcal{D} = (-2\pi, 2\pi) \times \mathbb{R}.$$

We will now explicitly compute the immersion $\psi(u, v) : \mathcal{D} \subset \mathbb{R}^2 \rightarrow \mathbb{R}^3$. First, we recall that the Hopf differential Qdz^2 vanishes, so $\psi(u, v)$ must be a piece of a plane. More specifically, by (2.9), $\psi(u, v)$ must be the vertical plane $\{x_1 = 0\}$. Since $\psi(u, v)$ is conformal and well defined on \mathcal{D} , it follows from (2.9) that the map $\Psi : \mathcal{D} \rightarrow \mathbb{C}$ given by

$$\Psi(u + iv) := \psi_3(u, v) - i\psi_2(u, v) \quad (6.18)$$

is holomorphic, where ψ_2, ψ_3 denote the second and third coordinates of $\psi(u, v)$. Using the initial conditions (2.9), the Gauss-Weingarten equations (2.10), as well as (6.17), it is possible to compute the u -line $u \mapsto \psi(u, 0)$, obtaining

$$\begin{aligned} \psi_2(u, 0) &= 0, \\ \psi_3(u, 0) &= 4 \tan\left(\frac{u}{4}\right), \end{aligned}$$

This means by (6.18) that $\Psi(u) = \psi_3(u, 0) = 4 \tan\left(\frac{u}{4}\right)$. Now, since $\Psi(u + iv)$ is holomorphic, we deduce that

$$\Psi(u + iv) = 4 \tan\left(\frac{u + iv}{4}\right) = \frac{4 \sin\left(\frac{u}{2}\right)}{\cos\left(\frac{u}{2}\right) + \cosh\left(\frac{v}{2}\right)} + i \frac{4 \sinh\left(\frac{v}{2}\right)}{\cos\left(\frac{u}{2}\right) + \cosh\left(\frac{v}{2}\right)}.$$

In particular,

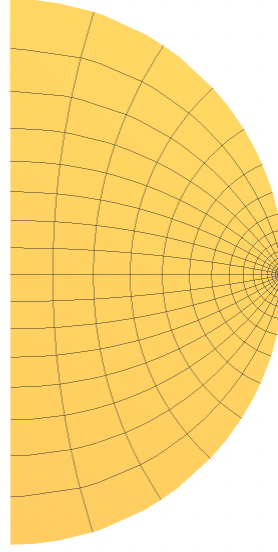
$$\begin{aligned} \psi_2(u, v) &= -\frac{4 \sinh\left(\frac{v}{2}\right)}{\cos\left(\frac{u}{2}\right) + \cosh\left(\frac{v}{2}\right)} \\ \psi_3(u, v) &= \frac{4 \sin\left(\frac{u}{2}\right)}{\cos\left(\frac{u}{2}\right) + \cosh\left(\frac{v}{2}\right)} \end{aligned} \quad (6.19)$$

It follows from (6.19) that the restriction of $\psi(u, v)$ to $[-\pi, \pi] \times [0, \infty)$ yields a conformal parametrization of the set $S \subset \{x_1 = 0\}$ given by

$$S := \{(0, x_2, x_3) : x_2^2 + x_3^2 \leq 16, 0 \leq x_2 < 4\}. \quad (6.20)$$

In other words, S is a vertical half-disk of radius 4 centered at the origin minus the boundary point $(0, 4, 0)$; see Figure 6.1.

Remark 6.2.8. Let $\eta(u) := u/\pi$ and $x(v) := e^{\omega(0, v)}$. It follows from (6.5) and the expression of $p(0, x)$ in (6.4) that $x(v)$ provides a diffeomorphism between $v \in [0, \infty)$ and $x \in (0, 1]$, with $\lim_{v \rightarrow \infty} x(v) = 0$. In particular, if we consider the immersion $\tilde{\psi}(\eta, x) : [-1, 1] \times (0, 1] \rightarrow \mathbb{R}^3$ given by the reparametrization $(u, v) \rightarrow (\eta, x)$, then we deduce from (6.19) that $\psi(\eta, x)$ can be continuously extended to every value $(\eta, 0)$,

Figure 6.1: Half disk S in (6.20).

$\eta \in [-1, 1]$, yielding

$$\tilde{\psi}(\eta, 0) = (0, 4, 0).$$

In particular, the image of $[-1, 1] \times [0, 1]$ via $\tilde{\psi}(\eta, x)$ is the half-disk $S \cup \{(0, 4, 0)\}$; see (6.20).

6.2.4 The limit case $a = 1$: catenoids

We will finish this section by studying the surfaces $\Sigma(1, b)$, i.e., the case $a = 1$. By Remark 6.2.2, $\omega = \omega(u)$ does not depend on v , which implies that $\Sigma(1, b)$ must be rotational. The v -line $\psi(0, v)$, contained in the horizontal plane $\{x_3 = 0\}$, is a geodesic of $\Sigma(1, b)$ with constant curvature $\kappa_2(0, v) \equiv -\frac{b}{2} < 0$. This implies that $\Sigma(1, b)$ is a catenoid whose *neck* is a circle of radius $\frac{2}{b}$. The profile curve of the catenoid is given by the u -curve $\psi(u, 0)$. We finally note that the rotation axis \mathcal{X} of Σ coincides with the line L in Lemma 6.2.7: indeed, every v -line $\psi(u_0, v)$ parametrizes a horizontal circle C_{u_0} . Thus, if any of these v -lines is contained in a sphere $\mathcal{Q}(u_0)$, then the center $\hat{c}(u_0)$ of the sphere must be contained in the vertical line passing through the center of the circle C_{u_0} . The rotation axis \mathcal{X} of the catenoid is also a vertical line passing through the center of C_{u_0} , so $L = \mathcal{X}$, as claimed.

6.3 The period map

Let $(a, b) \in \mathcal{O}$ with $a > 0$, and consider the immersion $\psi(u, v)$ associated to $\Sigma(a, b)$. Due to the properties (6.7), (6.8) of $\omega(u, v)$, we deduce several symmetries of $\Sigma(a, b)$.

Proposition 6.3.1. *Let $(a, b) \in \mathcal{O}$ such that $a > 0$. Then, the surface $\Sigma(a, b)$ satisfies the following properties:*

- (1) $\Sigma(a, b)$ is symmetric with respect to the horizontal plane $\{x_3 = 0\}$.
- (2) For every $j \in \mathbb{Z}$, let Ω_j be the vertical plane orthogonal to $\psi_v(0, j\sigma)$ at $\psi(0, j\sigma)$, where $\sigma(a, b)$ is given by Lemma 6.2.4. Then, $\Sigma(a, b)$ is symmetric with respect to Ω_j .
- (3) The angle between consecutive planes Ω_j, Ω_{j+1} is independent of j . This angle coincides with the variation of the unit tangent of the planar curve $v \mapsto \psi(0, v)$ between $v = 0$ and $v = \sigma$, given by

$$\chi(a, b) = -\frac{a^2 b}{2} \int_0^\sigma e^{-\omega(0, v)} dv. \quad (6.21)$$

- (4) The image of the function $\chi(a, b)$ is the interval $(-\pi, 0)$.

Proof. The proof of items (1), (2) and (3) is a straightforward adaptation of the corresponding arguments in Remark 3.2.6 and Proposition 3.3.1, where we make use of the symmetries (6.7) and (6.8), so it just remains to prove item (4). Suppose first that $a = 1$. Then, we know by Remark 6.2.2 that $\omega(u)$ does not depend on v , so in particular $\omega(0) = 0$. Thus, by (6.10) and (6.21) we obtain

$$\chi(1, b) = -\frac{b\pi}{\sqrt{1+b^2}}. \quad (6.22)$$

In particular, $\chi(1, b) \in (-\pi, 0)$. Let us assume then that $a \in (0, 1)$. Considering the change of variables $x = X(0, v) = e^{\omega(0, v)}$ in (6.21) and using (6.5), we get

$$\chi(a, b) = -\int_{a^2}^1 \frac{a^2 b}{x \sqrt{p(x)}} dx, \quad (6.23)$$

where we recall that $p(x)$ is the polynomial in (6.4). It is easy to see that the partial derivative $\frac{\partial \chi}{\partial b}(a, b)$ is strictly negative, and that $\lim_{b \rightarrow 0} \chi(a, b) = 0$ for each fixed a . We

will now prove that

$$\lim_{b \rightarrow \infty} \chi(a, b) = - \int_{a^2}^1 \frac{a}{x \sqrt{(1-x)(x-a^2)}} dx = -\pi, \quad (6.24)$$

showing that $\chi(a, b) \in (-\pi, 0)$ in this case. We will use the residue theorem for that purpose. Let $f(z)$ be the function

$$f(z) := \frac{a}{z \sqrt{(1-z)(z-a^2)}},$$

where the square root $z \mapsto \sqrt{z}$ is defined so that it is holomorphic on \mathbb{C} minus the half line $\{x \in \mathbb{R} : x \leq 0\}$. Thus, $f(z)$ is meromorphic on $\mathbb{C} \setminus [a^2, 1]$ with a pole at $z = 0$. Let Ξ_n be the path in Figure 6.2. For every n , Ξ_n consists of a curve $\Xi_n^{(1)}$ enclosing the interval $[a^2, 1]$ and a circle $\Xi_n^{(2)}$ of radius n . By the residue theorem, it holds

$$\int_{\Xi_n} f(z) dz = 2\pi i \operatorname{Res}(f, 0) = 2\pi.$$

On the other hand, by taking limits as $n \rightarrow \infty$,

$$\begin{aligned} \lim_{n \rightarrow \infty} \int_{\Xi_n^{(1)}} f(z) dz &= 2 \int_{a^2}^1 \frac{a}{x \sqrt{(1-x)(x-a^2)}} dx, \\ \lim_{n \rightarrow \infty} \int_{\Xi_n^{(2)}} f(z) dz &= 0, \end{aligned}$$

so we conclude that

$$\int_{a^2}^1 \frac{a}{x \sqrt{(1-x)(x-a^2)}} dx = \frac{1}{2} \int_{\Xi_n} f(z) dz = \pi,$$

completing the proof of item (4). □

As in previous chapters, we introduce the period map $\Theta(a, b) : \mathcal{O} \cap \{a > 0\} \rightarrow \mathbb{R}$ as the analytic function

$$\Theta(a, b) = \frac{1}{\pi} \chi(a, b) = -\frac{a^2 b}{2\pi} \int_0^\sigma e^{-\omega(0, v)} dv. \quad (6.25)$$

We are interested in those values $(a, b) \in \mathcal{O}$ for which $\Theta(a, b) = -\frac{m}{n}$, $m, n \in \mathbb{N}$, as they will be associated to annular examples. We study this property next.

Theorem 6.3.2. *Let $(a, b) \in \mathcal{O}$, $a > 0$ such that $\Theta(a, b) = -m/n \in (-1, 0)$, with*

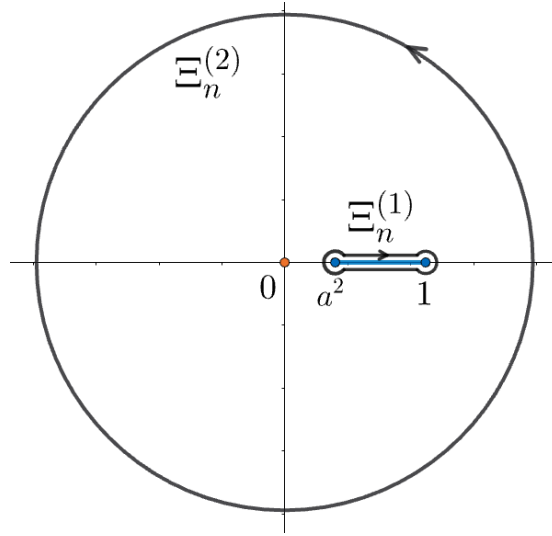


Figure 6.2: Integration path Ξ_n for the function $f(z)$.

$m, n \in \mathbb{N}$ and m/n irreducible. Given $u_0 \in (0, u_D)$, where u_D is given by (6.6), we define the surface $\Sigma_0 = \Sigma_0(a, b; u_0)$ as the restriction of $\psi(u, v)$ to $[-u_0, u_0] \times [-n\sigma, n\sigma]$. In this way, Σ_0 can be seen as a compact annulus under the identification $(u, v) \sim (u, v + 2n\sigma)$. Then, the following conditions hold:

1. Σ_0 is symmetric with respect to the horizontal plane $\{x_3 = 0\}$ and also with respect to n equiangular vertical planes that intersect along the line L in Lemma 6.2.7.
2. The closed planar geodesic $\Gamma(v) := \psi(0, v) : [-n\sigma, n\sigma] \rightarrow \{x_3 = 0\}$ has rotation index $-m$.
3. Assume that u_0 satisfies $\widehat{c}_3(u_0) = 0$, where \widehat{c}_3 is the third coordinate of the center function. Then, $\mathcal{Q}(u_0)$ is a sphere and Σ_0 is a capillary minimal annulus in the ball B bounded by $\mathcal{Q}(u_0)$. Moreover, Σ_0 meets $\mathcal{Q}(u_0)$ with angle θ , where $\tan \theta = -\frac{1}{\beta(u_0)}$.
4. If $a \in (0, 1)$, Σ_0 has a prismatic symmetry group of order $4n$, generated by the isometries in item (1). In particular, Σ_0 is not rotational.
5. If $a = 1$, Σ_0 is an m -cover of a rotational piece of a catenoid, and the vertical line L coincides with the rotation axis of the catenoid.

Proof. The fact that Σ_0 is an annulus and the proof of items (1) and (2) is a straightforward adaptation of Corollary 3.3.3. Regarding item (3), it follows by the symmetry

of Σ with respect to $\{x_3 = 0\}$ that $\widehat{c}_3(u_0) = \widehat{c}_3(-u_0) = 0$. In particular, the spheres $\mathcal{Q}(u_0), \mathcal{Q}(-u_0)$ coincide. The boundary components of the annulus Σ_0 lie on these spheres. It then follows by the maximum principle and the compactness of Σ_0 that the annulus Σ_0 must lie in the interior of the ball B bounded by $\mathcal{Q}(u_0)$. The fact that Σ_0 is capillary in B and the expression for the contact angle follows from (6.13). Finally, the proof of items (4) and (5) are analogous to items (5) and (6) in Proposition 3.6.3.

□

We conclude this section by studying the following property regarding the period map (6.25).

Lemma 6.3.3. *The period map $\Theta(a, b)$ in (6.25) can be continuously extended to $a = 0$, with*

$$\Theta(0, b) = -\frac{2}{\pi} \arctan(b) \quad (6.26)$$

Proof. Let $a \in (0, 1)$ and consider the change of variables $x = \frac{1}{h_a(t)}$ in (6.25), where $h_a(t) := (\frac{1}{a^2} - 1)t + 1$. This yields

$$\Theta(a, b) = -\frac{1}{\pi} \int_0^1 \frac{b\sqrt{(1-a^2)t + a^2}}{\sqrt{t(1-t)(b^2(1-a^2)t + a^2b^2 + 1)}} dt \quad (6.27)$$

This expression is well defined and continuous at the limit value $a = 0$, and in fact

$$\Theta(0, b) = -\frac{1}{\pi} \int_0^1 \frac{b}{\sqrt{(1-t)(b^2t + 1)}} dt = -\frac{2}{\pi} \arctan(b),$$

proving the lemma. □

Remark 6.3.4. *Let $(a, b) \in \mathcal{O} \cap \{a > 0\}$. It follows from the proof of Proposition 6.3.1 and (6.25) that the partial derivative $\frac{\partial \Theta}{\partial b}(a, b)$ is strictly negative. Thus, for every $q \in (-1, 0)$, we can express the level sets $\Theta(a, b) = q = -m/n$ as the graphs of analytic functions $b_q = b_q(a)$, $a \in (0, 1]$, with*

$$b_q(1) = \frac{m}{\sqrt{n^2 - m^2}}.$$

Moreover, these graphs can be continuously extended to the limit value $a = 0$, satisfying

$$b_q(0) = -\tan\left(\frac{m\pi}{2n}\right).$$

Moreover, it holds $b_q(a) > b_{q'}(a)$ for every $q < q'$ and $a \in [0, 1]$.

6.4 The embeddedness property

Fix $n \in \mathbb{N}$, $n \geq 2$. We will next define a family of capillary minimal annuli $\Sigma(a)$ in certain balls of \mathbb{R}^3 . This family will depend on the parameter $a \in (0, 1]$ in (6.1). We will show that each annulus within this family is embedded. Then, in Section 6.4.2, we will show that as $a \rightarrow 0$, the annuli $\Sigma(a)$ converge to a configuration of n capillary vertical flat disks.

6.4.1 The family of embedded capillary annuli

We first introduce following two preliminary lemmas, whose proofs will be postponed to Section 6.6.

Lemma 6.4.1. *For every $(a, b) \in \mathcal{O}$ there exists a value $u^* = u^*(a, b) \in (0, u_D)$ such that $\widehat{c}_3(u) < 0$ for every $u \in (0, u^*)$ and $\widehat{c}_3(u^*) = 0$, where $\widehat{c}_3(u)$ denotes the third coordinate of the center function. Moreover, the map $u^* : \mathcal{O} \rightarrow \mathbb{R}$ is analytic, and $u^*(0, b) = \pi$.*

Remark 6.4.2. *From now on, we will modify the initial conditions for $\psi(0, 0)$ in (2.9) by making a horizontal translation so that L coincides with the x_3 -axis. In this way, $\widehat{c}(u) = \widehat{c}_3(u)\mathbf{e}_3$, and $\widehat{c}(u^*)$ lies in the origin of \mathbb{R}^3 .*

Lemma 6.4.3. *Assume that $(a, b) \in \mathcal{O} \cap \{a > 0\}$ satisfies $\Theta(a, b) = -\frac{1}{n}$ with $n \in \mathbb{N}$, $n \geq 2$. Then, $\alpha(u) > 0$ and $\beta(u) < 0$ for every $u \in (0, u^*]$. Moreover, $\beta'(0) < 0$.*

We also introduce the following concept.

Definition 6.4.4. *Let $\gamma(v) : \mathbb{S}^1 \rightarrow \mathbb{R}^2$ a closed regular planar curve. We will say that $\gamma(v)$ is locally convex if its curvature $\kappa(v)$ has a definite sign, i.e., either $\kappa \geq 0$ or $\kappa \leq 0$ for all $v \in \mathbb{S}^1$. In particular, if $\kappa(v)$ never vanishes, we will say that $\gamma(v)$ is strictly locally convex.*

Remark 6.4.5. *It is well known that a locally convex curve with rotation index 1 must be embedded.*

Let $n \in \mathbb{N}$ with $n \geq 2$, and set $q := -\frac{1}{n}$. For every $a \in (0, 1]$, we consider the function $b_q(a)$ associated to the level set $\Theta(a, b) = -\frac{1}{n}$; see Remark 6.3.4. We then define the 1-parameter family of annuli $\Sigma(a)$ as

$$\Sigma(a) := \Sigma_0(a, b_q(a); u^*(a)), \quad (6.28)$$

where Σ_0 is defined in Theorem 6.3.2 and $u^*(a) := u^*(a, b_q(a))$ is given by Lemma 6.4.1. These examples can be seen as the restriction of the corresponding immersions $\psi(u, v) = \psi(u, v; a)$ to the annuli

$$\mathcal{D}_a := [-u^*(a), u^*(a)] \times [-n\sigma(a), n\sigma(a)], \quad (6.29)$$

where we have identified the points $(u, v) \sim (u, v + 2n\sigma(a))$. According to Remark 6.4.2, every $\Sigma(a)$ is a capillary annulus in some ball centered at the origin. We also define $\Upsilon_a^+(v)$, $\Upsilon_a^-(v)$ as the boundary curves $\Upsilon_a^+(v) = \psi(u^*, v)$ and $\Upsilon_a^-(v) = \psi(-u^*, v)$. Finally, we denote by $\Upsilon_a^0(v)$ the projection of any of the curves $\Upsilon_a^+(v)$ or $\Upsilon_a^-(v)$ onto the horizontal plane $\{x_3 = 0\}$.

Proposition 6.4.6. *Let $a \in (0, 1]$. Then, the following conditions hold:*

- (1) *Let $\psi_3(u, v)$ be the third coordinate of the immersion $\psi(u, v) = \psi(u, v; a)$. Then, $\psi_3(u^*, v)$ is positive for all $v \in [-n\sigma, n\sigma]$.*
- (2) *The third coordinate of the Gauss map, denoted by $N_3(u, v) = N_3(u, v; a)$, is negative for all $(u, v) \in (0, u^*] \times [-n\sigma, n\sigma]$.*
- (3) *The closed curve $\Upsilon_a^0(v)$ is strictly locally convex. In particular, Υ_a^0 is embedded, and so are the boundary curves Υ_a^+ , Υ_a^- of $\Sigma(a)$.*

Proof. Let (P) denote the properties (1)-(3) of the statement. Assume by contradiction that (P) does not hold for every $a \in (0, 1]$, and define

$$\mathcal{T} := \{a \in (0, 1] : \text{(P) holds for } \Sigma(a)\}.$$

Note that, by hypothesis, $\mathcal{T} \neq (0, 1]$, so we can define

$$a^* := \sup((0, 1] \setminus \mathcal{T}).$$

We will next show the following claim:

Claim 6.4.7. *The following properties hold:*

- (i) $1 \in \mathcal{T}$. In particular, $\mathcal{T} \neq \emptyset$.
- (ii) \mathcal{T} is an open set.
- (iii) $a^* \in \mathcal{T}$.

The properties above lead to a contradiction: indeed, since \mathcal{T} is a non-empty open set, it follows that $a^* < 1$ and $a^* \notin \mathcal{T}$. However, this is impossible by item (III) of the claim. Thus, $\mathcal{T} = (0, 1]$, proving the proposition. It remains to prove Claim 6.4.7. We do this next.

Let us show item (I) of the claim. Since $a = 1$, the annulus $\Sigma(1)$ is a capillary piece of a catenoid which is symmetric with respect to the horizontal plane $\{x_3 = 0\}$. The upper boundary component of the catenoid is a horizontal circle lying in the horizontal plane given by $\{x_3 = \psi_3(u^*, 0)\}$, where $\psi_3(u^*, 0) > 0$. In particular, $\psi_3(u^*, v) \equiv \psi_3(u^*, 0) > 0$ and the projection $\Upsilon_a^0(v)$ is a circle, so Υ_a^0 is trivially a strictly convex curve. This shows that items (1) and (3) of (P) hold. Finally, item (2) holds since $N(u, v)$ represents the *outer* normal vector of the catenoid. This follows since the curvature $\kappa_2(0, v)$ at the *neck* of the catenoid is negative; see Section 6.2.4 and Figure 6.3.

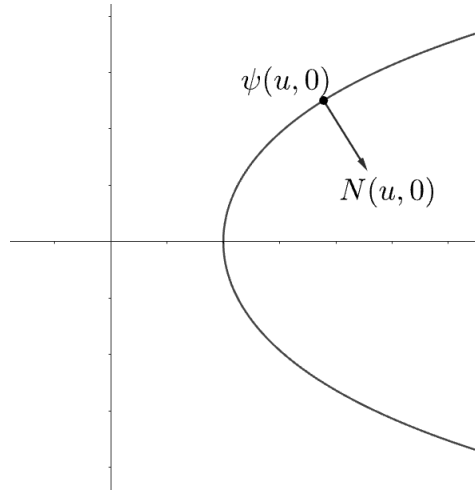


Figure 6.3: The catenoid $\Sigma(1)$.

We will now show that \mathcal{T} is an open set. Let $a_0 \in \mathcal{T}$. Then, $v \mapsto \psi_3(u^*, v; a_0)$ and the curvature of the closed curve $\Upsilon_{a_0}^0(v)$ (if oriented properly) are strictly positive functions for all $v \in [-n\sigma, n\sigma]$. By continuity, these properties must hold on a neighbourhood of a_0 , i.e., items (1) and (3) of (P) are satisfied for a near a_0 . Let us now prove that (2) also holds. First, it is clear by (2.9) and (2.10) that $N_3(0, v; a) \equiv 0$ and that $(N_3)_u(0, v; a) < 0$ for all $v \in [-n\sigma, n\sigma]$ and $a \in (0, 1]$. In particular, there exists a neighbourhood I of a_0 and $\varepsilon > 0$ such that $N_3(u, v; a) < 0$ for $(u, v) \in (0, \varepsilon] \times [-n\sigma, n\sigma]$ and $a \in I$. Now, by hypothesis, $N_3(u, v; a_0) < 0$ for all $(u, v) \in [\varepsilon, u^*] \times [-n\sigma, n\sigma]$, so this inequality must also hold on a (maybe smaller)

neighbourhood I' of a_0 . In particular, property (2) also holds for every a near a_0 , showing that \mathcal{T} must be an open set.

Let us finally prove item (III) of the claim. By definition of a^* , every $a \in (a^*, 1]$ satisfies (P). In particular, by continuity, the surface $\Sigma(a^*)$ has the following properties, which we denote by (P'):

- (1') $\psi_3(u^*, v) \geq 0$ for all $v \in [-n\sigma, n\sigma]$.
- (2') $N_3(u, v) \leq 0$ for all $(u, v) \in (0, u^*] \times [-n\sigma, n\sigma]$.
- (3') The curve $\Upsilon_a^0(v)$ is locally convex in the set of its regular points.

The properties (P') could be seen as a *weak* version of (P). However, we will show that (P') implies (P), proving Claim 6.4.7.

Let us first show that item (1) of (P) holds for the annulus $\Sigma(a^*)$. Assume by contradiction that there exists $v_0 \in [-n\sigma, n\sigma]$ such that $\psi_3(u^*, v_0) = 0$. Let $\psi(u, v)$ be the immersion associated to this surface, and consider the annular domain

$$\mathcal{D}_{a^*}^+ := [0, u^*] \times [-n\sigma, n\sigma], \quad (6.30)$$

where we identify $(u, v) \sim (u, v + 2n\sigma)$. Since $\psi(u, v)$ is a conformal parametrization of a minimal surface, the coordinate $\psi_3(u, v)$ is harmonic, and it is not constant, as $(\psi_3)_u(0, 0) > 0$; see (2.9). Now, we note that $\psi_3(0, v) \equiv 0$, while $\psi_3(u^*, v) \geq 0$. By the strong maximum principle and the hypothesis that $\psi_3(u^*, v_0) = 0$, we deduce that the partial derivative $(\psi_3)_u(u^*, v_0)$ is strictly negative. Now, by (6.14) and $\widehat{c}_3(u^*) = 0 = \psi_3(u^*, v_0)$, it follows

$$0 = -\frac{2}{\alpha(u^*)}(\psi_3)_u(u^*, v_0)e^{-\omega(u^*, v_0)} + \frac{2\beta(u^*)}{\alpha(u^*)}N_3(u^*, v_0).$$

This leads to a contradiction, since $\alpha(u^*) > 0$, $\beta(u^*) < 0$ while $(\psi_3)_u(u^*, v_0) < 0$ and $N_3(u^*, v_0) \leq 0$; see also Lemma 6.4.3.

We will now show that item (2) of (P) holds for $\Sigma(a^*)$. Assume by contradiction that there exists $(u_0, v_0) \in (0, u^*] \times [-n\sigma, n\sigma]$ such that $N_3(u_0, v_0) = 0$. We first note that the third coordinate of the Gauss map $N_3(u, v)$ is a Jacobi function, that is, it satisfies the partial differential equation

$$\Delta N_3 + 2Q^2 e^{-2\omega} N_3 = 0.$$

This condition implies that $N_3(u, v)$ cannot vanish at any point (u_0, v_0) with $u_0 \in$

$(0, u^*)$: in such a case, (u_0, v_0) would be a local maximum, and a Jacobi function cannot have maxima at points where it vanishes. Thus, necessarily $u_0 = u^*$. We will now see that this cannot happen either.

Let \mathcal{C} be the convex set $\mathcal{C} := \mathcal{C}_0 \times \mathbb{R}$, where \mathcal{C}_0 is the (convex) planar region bounded by the curve $\Upsilon_{a^*}^0$. We observe that, by construction, both boundary components of the annulus $\Sigma(a^*)$ lie in $\partial\mathcal{C}$. Thus, by the convex hull property for minimal surfaces, $\Sigma(a^*) \subset \mathcal{C}$. Let us define P as the vertical plane passing through $\psi(u^*, v_0)$ with normal vector $N^* := N(u^*, v_0)$. We note that P is tangent to \mathcal{C} at the point $\psi(u^*, v_0)$, so by convexity \mathcal{C} lies in one side of P . We next define the function $f(u, v) : \mathcal{D}_{a^*}^+ \rightarrow \mathbb{R}$ as

$$f(u, v) := \langle \psi(u, v) - \psi(u^*, v_0), N^* \rangle.$$

Geometrically, $f(u, v)$ measures the (signed) orthogonal distance from $\psi(u, v)$ to the plane P . Since $\psi(u, v)$ is a conformal parametrization of a minimal surface, it follows that $f(u, v)$ is a harmonic function. Now, since $\Sigma(a^*)$ is contained in \mathcal{C} , which lies in one side of P , we deduce that $f(u, v)$ does not change sign. However, since $f(u^*, v_0) = 0$, and

$$f_u(u^*, v_0) = \langle \psi_u(u^*, v_0), N^* \rangle = 0,$$

we deduce from the maximum principle that $f \equiv 0$, that is, $\Sigma(a^*)$ is contained in P . This leads to a contradiction, as $\Sigma(a^*)$ is not totally geodesic. Thus, it holds $N_3(u, v) < 0$ for all $(u, v) \in (0, u^*] \times [-n\sigma, n\sigma]$.

We will finally show that property (3) of (P) holds for $\Sigma(a^*)$, completing the proof of Claim 6.4.7 and the proposition. A normal vector to $\Upsilon_{a^*}^0(v)$ (not necessarily unitary) is given by

$$\mathbf{n}(v) = (-(\psi_2)_v(u^*, v), (\psi_1)_v(u^*, v)), \quad (6.31)$$

where $\psi_i(u, v)$, $i = 1, 2$, denote the first and second coordinate functions of $\psi(u, v)$. We note that the norm of \mathbf{n} coincides with that of the tangent vector $(\Upsilon_{a^*}^0)_v$. Thus, in order to show that $\Upsilon_{a^*}^0$ is regular and strictly locally convex, it suffices to show that $v \mapsto \langle (\Upsilon_{a^*}^0)_{vv}(v), \mathbf{n}(v) \rangle$ never vanishes, so that the curvature of $\Upsilon_{a^*}^0$ has a definite sign. We also note that

Now, by (2.10), it follows

$$\langle (\Upsilon_{a^*}^0)_{vv}(v), \mathbf{n}(v) \rangle = -\omega_u \langle \psi_u^0(u^*, v), \mathbf{n} \rangle - Q \langle N^0(u^*, v), \mathbf{n} \rangle, \quad (6.32)$$

where $\psi_u^0(u^*, v)$ and $N^0(u^*, v)$ denote the horizontal projections of $\psi_u(u^*, v)$ and $N(u^*, v)$ respectively, and we recall that $Q > 0$; see (6.3). Now, by (6.31) and since

$\{e^{-\omega}\psi_u, e^{-\omega}\psi_v, N\}$ defines an orthonormal frame, we deduce that

$$\langle \psi_u^0(u^*, v), \mathbf{n} \rangle = -e^{2\omega} N_3(u^*, v), \quad \langle N^0(u^*, v), \mathbf{n} \rangle = (\psi_3)_u(u^*, v).$$

Thus, using these expressions and (2.14b), we obtain that

$$\begin{aligned} \langle (\Upsilon_{a^*}^0)_{vv}(v), \mathbf{n}(v) \rangle &= \omega_u e^{2\omega} N_3(u^*, v) - Q(\psi_3)_u(u^*, v) \\ &= \frac{\alpha}{2} e^{3\omega} N_3(u^*, v) + Q\beta e^\omega N_3(u^*, v) - Q(\psi_3)_u(u^*, v) \quad (6.33) \\ &< Qe^\omega (\beta N_3(u^*, v) - e^{-\omega}(\psi_3)_u(u^*, v)), \end{aligned}$$

where for the last inequality we use that $\alpha(u^*) > 0$ and that $N_3(u^*, v) < 0$; see Lemma 6.4.3 and item (2) of (P). Now, using (6.14) and the fact that $\widehat{c}_3(u^*) = 0$,

$$\beta(u^*)N_3(u^*, v) - e^{-\omega}(\psi_3)_u(u^*, v) = -\frac{\alpha}{2}\psi_3(u^*, v) < 0. \quad (6.34)$$

Thus, from (6.32), (6.33) and (6.34),

$$\langle (\Upsilon_{a^*}^0)_{vv}(v), \mathbf{n}(v) \rangle < Qe^\omega (\beta N_3(u^*, v) - e^{-\omega}(\psi_3)_u(u^*, v)) < 0,$$

showing that $\Upsilon_{a^*}^0$ is strictly convex. This completes the proof of Claim 6.4.7 and hence Proposition 6.4.6. \square

We next show that the annuli $\Sigma(a)$ have positive support function.

Lemma 6.4.8. *In the conditions of Proposition 6.4.6, for every $a \in (0, 1]$, let $\mathcal{H}(u, v)$ denote the support function associated to $\psi(u, v)$, that is,*

$$\mathcal{H}(u, v) := \langle \psi(u, v), N(u, v) \rangle \quad (6.35)$$

Then, $\mathcal{H}(u, v) > 0$ for all $(u, v) \in \mathcal{D}_a$; see (6.29).

Proof. By the symmetry of $\psi(u, v)$ with respect to the horizontal plane $\{x_3 = 0\}$, it follows that $\mathcal{H}(u, v) = \mathcal{H}(-u, v)$. Thus, it suffices to prove the result for $(u, v) \in [0, u^*] \times [-n\sigma, n\sigma]$. We assume first that $u > 0$. By (6.14) and Remark 6.4.2, it follows that

$$\mathcal{H} = \langle \psi, N \rangle = \widehat{c}_3 N_3 - \frac{2\beta}{\alpha}. \quad (6.36)$$

We deduce from Lemmas 6.4.1 and 6.4.3 that $\widehat{c}_3(u) \leq 0$, $\beta(u) < 0$ and $\alpha(u) > 0$ for every $u \in (0, u^*]$. Moreover, by Proposition 6.4.6, $N_3(u, v) < 0$ for $(u, v) \in (0, u^*] \times [-n\sigma, n\sigma]$. Thus, by (6.36), we deduce that $\mathcal{H}(u, v) > 0$ for $(u, v) \in (0, u^*] \times$

$[-n\sigma, n\sigma]$.

Finally, regarding the limit value $u = 0$, by continuity of \mathcal{H} , it holds

$$\mathcal{H}(0, v) = \lim_{u \rightarrow 0^+} \mathcal{H}(u, v) \leq \lim_{u \rightarrow 0^+} -2 \frac{\beta(u)}{\alpha(u)} = -2 \frac{\beta'(0)}{\alpha'(0)}.$$

Now, by (6.3) and Lemma 6.4.3, we know that $\alpha'(0) = \frac{1}{4}$, $\beta'(0) < 0$, so $\mathcal{H}(0, v) > 0$, as we wanted to show. \square

The following result states that for every $a \in (0, 1]$, the annulus $\Sigma(a)$ can be expressed as a radial graph with respect to the origin, i.e., it admits a parametrization $\Psi_a(\mathbf{p}) : \mathcal{A} \subset \mathbb{S}^2 \rightarrow \mathbb{R}^3$ defined over an annular domain \mathcal{A} of \mathbb{S}^2 satisfying $\Psi_a(\mathbf{p}) = f(\mathbf{p})\mathbf{p}$, where $\mathbf{p} \in \mathbb{S}^2$ and $f(\mathbf{p}) : \mathcal{A} \rightarrow (0, \infty)$ is a real-valued positive function.

Proposition 6.4.9. *For every $a \in (0, 1]$, the annulus $\Sigma(a)$ is a radial graph with respect to the origin of \mathbb{R}^3 . In particular, $\Sigma(a)$ is an embedded minimal surface.*

Proof. Let $\psi(u, v) = \psi(u, v; a)$ denote the immersion associated to $\Sigma(a)$, $a \in (0, 1]$. Showing that $\Sigma(a)$ is a radial graph is equivalent to proving that the map $F_a(u, v) : \mathcal{D}_a \rightarrow \mathbb{S}^2$ given by

$$F_a(u, v) := \frac{\psi(u, v; a)}{|\psi(u, v; a)|} \quad (6.37)$$

defines a diffeomorphism between \mathcal{D}_a and an annular domain in \mathbb{S}^2 ; see (6.29).

The strategy to prove this result is as follows: assume first that $F_1(u, v)$ for $a = 1$ defines a diffeomorphism between \mathcal{D}_1 and an annular domain \mathcal{A}_1 in \mathbb{S}^2 ; we will show this fact at the end of the proof. Since the maps $F_a(u, v)$ depend analytically on the parameter a , this will actually prove that F_a is a diffeomorphism onto some annulus \mathcal{A}_a for every a in some maximal interval $(a_0, 1]$, $a_0 \geq 0$. Suppose by contradiction that a_0 were strictly greater than zero, that is, F_{a_0} is no longer a diffeomorphism but every F_a with $a > a_0$ is. This implies that one of the following conditions must hold:

- (1) $F_{a_0}(u, v)$ is not a *local* diffeomorphism, that is, there exists $p_0 = (u_0, v_0) \in \mathcal{D}_{a_0}$ such that the differential $d(F_{a_0})_{p_0}$ is not injective.
- (2) One of the boundary curves of \mathcal{A}_{a_0} , given by $v \mapsto F_{a_0}(u^*, v)$ and $v \mapsto F_{a_0}(-u^*, v)$, is not injective.
- (3) The boundary curves of \mathcal{A}_{a_0} meet each other at some point in \mathbb{S}^2 .

Let us study item (1). Given any $a \in (0, 1]$ and $p \in \mathcal{D}_a$, it is easy to show that the differential $d(F_a)_p$ is injective if and only if the support function \mathcal{H} in (6.35) does not

vanish at p . As we saw in Lemma 6.4.8, the support function never vanishes for the annuli $\Sigma(a)$, so item (1) cannot hold.

We will now examine items (2) and (3). By Proposition 6.4.6, we know that the boundary curves $\Upsilon_{a_0}^+(v) = \psi(u^*, v; a_0)$, $\Upsilon_{a_0}^-(v) = \psi(-u^*, v; a_0)$ are injective. Moreover, $\Upsilon_{a_0}^+$ lies in the half-space $\{x_3 > 0\}$. Since $\Upsilon_{a_0}^-$ is the reflection of $\Upsilon_{a_0}^+$ with respect to the plane $\{x_3 = 0\}$, we deduce that $\Upsilon_{a_0}^- \subset \{x_3 < 0\}$. In particular, $\Upsilon_{a_0}^+ \cap \Upsilon_{a_0}^- = \emptyset$. Now, both boundary components $\Upsilon_{a_0}^+(v)$ and $\Upsilon_{a_0}^-(v)$ lie on a sphere of radius $R^* := R(u^*)$ centered at the origin. Thus,

$$F_{a_0}(\pm u^*, v) = \frac{\Upsilon_{a_0}^\pm(v)}{R^*},$$

i.e., $F_{a_0}(\pm u^*, v)$ is just a rescaling of $\Upsilon_{a_0}^\pm$. We then deduce that the curves $v \mapsto F_{a_0}(\pm u^*, v)$ are injective and do not meet each other, showing that items (2) and (3) cannot hold, thus reaching a contradiction. As a consequence, $a_0 = 0$, so every map $F_a(u, v)$, $a \in (0, 1]$, in (6.37) defines a diffeomorphism onto its image \mathcal{A}_a . This completes the proof of the proposition once we show that $F_1(u, v)$ is a diffeomorphism. We do this next.

Let $a = 1$. We know that $\Sigma(1)$ is a piece of a catenoid whose neck curvature depends on the value $b = b_q(1)$. Arguing as in the beginning of Section 5.6.2, we find that the immersion $\psi(u, v) = \psi(u, v; 1)$ and its Gauss map $N(u, v) = N(u, v; 1)$ are given by

$$\begin{aligned} \psi(u, v) &= \frac{2}{b} \left(\cosh\left(\frac{bu}{2}\right) \cos\left(\frac{bv}{2}\right), -\cosh\left(\frac{bu}{2}\right) \sin\left(\frac{bv}{2}\right), \frac{bu}{2} \right), \\ N(u, v) &= \left(\operatorname{sech}\left(\frac{bu}{2}\right) \cos\left(\frac{bv}{2}\right), -\operatorname{sech}\left(\frac{bu}{2}\right) \sin\left(\frac{bv}{2}\right), -\tanh\left(\frac{bu}{2}\right) \right). \end{aligned} \quad (6.38)$$

It can be shown from (6.37) and (6.38) that there exists $\bar{u} > 0$ such that $u \mapsto F_1(u, v)$ is injective on a maximal interval $[-\bar{u}, \bar{u}]$ for every $v \in [-n\sigma, n\sigma]$. More precisely, \bar{u} is given by the implicit equation

$$\frac{b\bar{u}}{2} \tanh\left(\frac{b\bar{u}}{2}\right) = 1.$$

In particular, $F_1(u, v) : [-\bar{u}, \bar{u}] \times [-n\sigma, n\sigma]$ defines a diffeomorphism onto an annular domain in \mathbb{S}^2 under the identification $(u, v) \sim (u, v + 2n\sigma)$. On the other hand, it can be shown that the support function $\mathcal{H}(u, v)$ in (6.35) is positive for all $(u, v) \in (-\bar{u}, \bar{u}) \times [-n\sigma, n\sigma]$, and $\mathcal{H}(-\bar{u}, v) = \mathcal{H}(\bar{u}, v) = 0$. This allows us to deduce using

Lemma 6.4.8 that $u^* < \bar{u}$, and thus $\mathcal{D}_1 \subset (-\bar{u}, \bar{u}) \times [-n\sigma, n\sigma]$. Hence, $F_1(u, v)$ is injective in \mathcal{D}_1 , so it defines a diffeomorphism onto its image, as we wanted to show. We note that, up to an homothety, the restriction of $\psi(u, v)$ to $[-\bar{u}, \bar{u}] \times [-n\sigma, n\sigma]$ gives a parametrization of the critical catenoid. \square

6.4.2 The limit $a = 0$

Our goal in this section is to study the limit of the annuli $\Sigma(a)$ given by (6.28) as a converges to zero. In what follows, let $\psi(u, v; a)$ denote the immersion associated to the annulus $\Sigma(a)$. The fact that the value $\sigma = \sigma(a)$ introduced in Lemma 6.2.4 diverges as $a \rightarrow 0$ makes the analysis of the convergence of the annuli $\Sigma(a)$ involved, even though we can explicitly compute the immersion $\psi(u, v; 0)$, as seen in Section 6.2.3.

Definition 6.4.10. *Given $a \in (0, 1]$, we define the surface $\tilde{\Sigma} = \tilde{\Sigma}(a)$ as the restriction of the immersion $\psi(u, v; a)$ to the set $[-u^*(a), u^*(a)] \times [0, \sigma(a)]$.*

Remark 6.4.11. *By Proposition 6.3.1, it follows that the annulus $\Sigma(a)$ in (6.28) can be obtained as the orbit of $\tilde{\Sigma}(a)$ under the action of the dihedral group D_{2n} generated by rotations of angle $\frac{2\pi}{n}$ about the x_3 -axis and the vertical reflection with respect to the plane $\{x_2 = 0\}$.*

Since the value $\sigma(a)$ diverges as $a \rightarrow 0$, we will consider a new pair of parameters (η, x) instead of (u, v) . More precisely, we define $\eta = \eta(u)$ as $\eta(u) := u/u^*(a)$, and $x = x(v)$ as

$$x(v) := \frac{e^{\omega(0,v)} - a^2}{1 - a^2}. \quad (6.39)$$

Throughout this section, we will denote by $\tilde{\psi}(\eta, x) = \tilde{\psi}(\eta, x; a)$ the immersion associated to $\tilde{\Sigma}(a)$ in the new parameters (η, x) . Due to (6.5) and the expression of $p(x)$ in (6.4), it follows that $x(v)$ provides a diffeomorphism between $v \in [0, \sigma(a)]$ and $x \in [0, 1]$. In this way, the surface $\tilde{\Sigma}(a)$ can be seen as the restriction of $\tilde{\psi}(\eta, x; a)$ to the set $[-1, 1] \times [0, 1]$. We will next prove that this restriction of $\tilde{\psi}(\eta, x; a)$ converges uniformly as $a \rightarrow 0$ to the parametrization of the vertical half-disk of radius 4 in Remark 6.2.8; see Proposition 6.4.12.

Proposition 6.4.12. *Up to a translation in the x_1 -direction, the family of immersions*

$$\tilde{\psi}(\eta, x; a) : [-1, 1] \times [0, 1] \rightarrow \mathbb{R}^3$$

converge uniformly as $a \rightarrow 0$ to the parametrization of the vertical half-disk of radius 4 given by Remark 6.2.8.

Proof. Let $\psi(u, v) = \psi(u, v; a)$ be the immersion associated to $\tilde{\Sigma}(a)$ in the parameters (u, v) , and denote by $\psi(u, v; 0)$ be the immersion in Section 6.2.3. For simplicity, we will assume throughout this proof that the initial conditions for $\psi(u, v)$ satisfy (2.9), so that $\psi(0, 0) = (0, 0, 0)$. Moreover, let

$$X(u, v; a) := e^{\omega(u, v; a)} \quad (6.40)$$

and denote by $\tilde{X}(\eta, x; a)$ the function (6.40) in the parameters (η, x) .

First, by Remark 6.2.6 and (6.39), it is clear that the immersions $\psi(u, v; a)$ converge uniformly on compact subsets to the limit immersion $\psi(u, v; 0)$. In the parameters (η, x) , this implies that for every $\varepsilon > 0$, $\tilde{\psi}(\eta, x; a)$ converges uniformly to $\tilde{\psi}(\eta, x; 0)$ on the compact set $[-1, 1] \times [\varepsilon, 1]$. Let us assume the following claims, which will be proven later in the section:

Claim 6.4.13. *The function $\tilde{X}(\eta, x; a) : [-1, 1] \times [0, 1] \times [0, 1] \rightarrow [0, \infty)$ is continuous at every point $(\eta, 0; 0)$, $\eta \in [-1, 1]$. Moreover,*

$$\tilde{X}(\eta, 0; 0) \equiv 0.$$

Claim 6.4.14. *There exists a continuous function $f(x) : [0, 1] \rightarrow \mathbb{R}$ such that $f(0) = 0$ and*

$$\int_0^x \frac{2((1 - a^2)x' + a^2)}{\sqrt{(1 - x')x'((1 - a^2)x' + a^2(1 + b^2))}} dx' < f(x) \quad (6.41)$$

for all $a \in [0, 1]$, $b > 0$.

Let us now show the uniform convergence of the function $\tilde{\psi}(\eta, x; a)$. Assume by contradiction that there exists $\delta > 0$ and a sequence $\{(\eta_k, x_k; a_k)\}_k$ with $a_k \rightarrow 0$ such that

$$\left\| \tilde{\psi}(\eta_k, x_k; a_k) - \tilde{\psi}(\eta_k, x_k; 0) \right\| > \delta \quad (6.42)$$

for all $k \in \mathbb{N}$.

First, the uniform convergence of $\tilde{\psi}(\eta, x; a)$ on every set $[-1, 1] \times [\varepsilon, 1]$ with $\varepsilon > 0$

implies that necessarily x_k must converge to 0 as $k \rightarrow \infty$. We note that

$$\begin{aligned} \left\| \tilde{\psi}(\eta_k, x_k; a_k) - \tilde{\psi}(\eta_k, x_k; 0) \right\| &\leq \left\| \tilde{\psi}(\eta_k, x_k; a_k) - \tilde{\psi}(0, 0; a_k) \right\| \\ &\quad + \left\| \tilde{\psi}(0, 0; a_k) - \tilde{\psi}(0, 0; 0) \right\| \\ &\quad + \left\| \tilde{\psi}(0, 0; 0) - \tilde{\psi}(\eta_k, x_k; 0) \right\| \end{aligned} \quad (6.43)$$

We will now show that each of the three terms in the right-hand side of (6.43) can be bounded by $\delta/3$ for large values of k , reaching a contradiction with (6.42). Regarding the third term

$$\left\| \tilde{\psi}(0, 0; 0) - \tilde{\psi}(\eta_k, x_k; 0) \right\|, \quad (6.44)$$

we know by Remark 6.2.8 that $\tilde{\psi}(\eta, 0; 0) \equiv \tilde{\psi}(0, 0; 0)$ for all $\eta \in [-1, 1]$. Thus, it is clear that (6.44) converges to zero as $k \rightarrow \infty$, so for k sufficiently large we can ensure that

$$\left\| \tilde{\psi}(0, 0; 0) - \tilde{\psi}(\eta_k, x_k; 0) \right\| < \frac{\delta}{3}. \quad (6.45)$$

Let us now consider the second term,

$$\left\| \tilde{\psi}(0, 0; a_k) - \tilde{\psi}(0, 0; 0) \right\|.$$

We know by the discussion before Claim 6.4.13 that for every $x_0 > 0$, $\tilde{\psi}(0, x_0; a_k)$ converges to $\tilde{\psi}(0, x_0; 0)$ as $k \rightarrow \infty$, so in particular for large k it holds

$$\left\| \tilde{\psi}(0, x_0; a_k) - \tilde{\psi}(0, x_0; 0) \right\| < \frac{\delta}{9}. \quad (6.46)$$

We also note that

$$\left\| \tilde{\psi}(0, x_0; a) - \tilde{\psi}(0, 0; a) \right\| = \left\| \int_0^{x_0} \tilde{\psi}_x(0, x'; a) dx' \right\| \leq \int_0^{x_0} \left\| \tilde{\psi}_x(0, x'; a) \right\| dx' \quad (6.47)$$

for all a . Now, by (6.5) and (6.39), it is possible to prove that the integral

$$\int_0^{x_0} \left\| \tilde{\psi}_x(0, x') \right\| dx'$$

coincides with the left-hand side of (6.41). Thus, according to Claim 6.4.14, if we take x_0 close enough to zero so that $f(x_k) < \frac{\delta}{9}$ and k large so that (6.46) holds, we conclude

that

$$\begin{aligned}
\left\| \tilde{\psi}(0, 0; a_k) - \tilde{\psi}(0, 0; 0) \right\| &\leq \left\| \tilde{\psi}(0, 0; a_k) - \tilde{\psi}(0, x_0; a_k) \right\| \\
&+ \left\| \tilde{\psi}(0, x_0; a_k) - \tilde{\psi}(0, x_0; 0) \right\| \\
&+ \left\| \tilde{\psi}(0, x_0; 0) - \tilde{\psi}(0, 0; 0) \right\| < 2f(x_0) + \frac{\delta}{9} < \frac{\delta}{3}.
\end{aligned} \tag{6.48}$$

Let us finally study the first term of (6.43). We note that

$$\begin{aligned}
\left\| \tilde{\psi}(\eta_k, x_k; a_k) - \tilde{\psi}(0, 0; a_k) \right\| &\leq \left\| \tilde{\psi}(\eta_k, x_k; a_k) - \tilde{\psi}(0, x_k; a_k) \right\| \\
&+ \left\| \tilde{\psi}(0, x_k; a_k) - \tilde{\psi}(0, 0; a_k) \right\| =: A_1 + A_2.
\end{aligned} \tag{6.49}$$

Regarding the term A_1 , since $\|\tilde{\psi}_\eta(\eta, x; a)\| = u^*(a)\tilde{X}(\eta, x; a)$, it holds

$$\begin{aligned}
A_1 &= \left\| \tilde{\psi}(\eta_k, x_k; a_k) - \tilde{\psi}(0, x_k; a_k) \right\| \\
&\leq \int_0^{\eta_k} \left\| \tilde{\psi}_\eta(\eta, x_k; a_k) \right\| d\eta \\
&= u^*(a_k) \int_0^{\eta_k} \tilde{X}(\eta, x_k; a_k) d\eta.
\end{aligned} \tag{6.50}$$

In particular, by Claim 6.4.13, we can take k sufficiently large so that the inequality

$$u^*(a_k) \int_0^{\eta_k} \tilde{X}(\eta, x_k; a_k) d\eta < \frac{\delta}{6} \tag{6.51}$$

holds.

It just remains to consider the term A_2 in (6.49). We can argue as we did in the inequality (6.48) using Claim 6.4.14 to show that, for k large enough so that x_k is sufficiently close to zero,

$$A_2 = \left\| \tilde{\psi}(0, x_k; a_k) - \tilde{\psi}(0, 0; a_k) \right\| < \frac{\delta}{6}. \tag{6.52}$$

Thus, by (6.51), (6.52),

$$\left\| \tilde{\psi}(\eta_k, x_k; a_k) - \tilde{\psi}(0, 0; a_k) \right\| < \frac{\delta}{3}. \tag{6.53}$$

So, by (6.42), (6.45), (6.48), (6.53),

$$\delta < \left\| \tilde{\psi}(\eta_k, x_k; a_k) - \tilde{\psi}(\eta_k, x_k; 0) \right\| < \delta,$$

reaching a contradiction. This completes the proof of Proposition 6.4.12. \square

Proof of Claim 6.4.13. First, by (6.39), we have that

$$\tilde{X}(0, x; a) = (1 - a^2)x + a^2. \quad (6.54)$$

Thus, by (2.14b) and having in mind that $u = u^*\eta$, it follows that for every $x \in [0, 1]$, $\tilde{X}(\eta, x; a)$ can be obtained by solving the differential equation

$$2\tilde{X}_\eta = u^*(\alpha(u^*\eta)\tilde{X}^2 + Q\beta(u^*\eta)), \quad (6.55)$$

with initial condition on $\eta = 0$ given by (6.54). We recall that the solutions (α, β) to (6.2) depend on the parameter a . It is clear by (6.54)-(6.55) and the analysis carried out in Section 6.2.3 that $\tilde{X}(\eta, x; a)$ depends continuously on the parameter a , even at the limit value $a = 0$. In particular, if $x = a = 0$, it is immediate by (6.54)-(6.55) and the fact that $Q = 0$ that $\tilde{X}(\eta, 0; 0) \equiv 0$, completing the proof of the claim. \square

Proof of Claim 6.4.14. We note that

$$\frac{(1 - a^2)x + a^2}{\sqrt{(1 - a^2)x + a^2(1 + b^2)}} < 1,$$

so we can bound the integral in (6.41) as

$$\int_0^x \frac{2((1 - a^2)x' + a^2)}{\sqrt{(1 - x')x'((1 - a^2)x' + a^2(1 + b_q(a)^2))}} dx' < \int_0^x \frac{2}{\sqrt{(1 - x')x'}} dx' =: f(x).$$

It can be checked that $f(x) = 2(\arcsin(2x - 1) + \frac{\pi}{2})$, which clearly satisfies $f(0) = 0$, completing the proof of the claim. \square

As an immediate corollary of Remark 6.4.11 and Proposition 6.4.12, we deduce the following:

Corollary 6.4.15. *The annuli $\Sigma(a)$ in (6.28) converge as $a \rightarrow 0$ to a configuration of n equiangular vertical disks of radius 4.*

Remark 6.4.16. *We note that a configuration of n disks of radius 4 as in Corollary 6.4.15 is capillary in a ball B_R of radius $R = \frac{4}{\sin(\frac{\pi}{n})}$. These disks meet B_R with a contact angle $\theta = \pi/n$. This coincides with the expressions for the radius $R(u)$ and contact angle $\theta(u)$ at $u = u^*(0) = \pi$; see (6.13), (6.16) and Lemma 6.4.1.*

6.5 Proof of the main theorems

6.5.1 Proof of Theorem 6.1.1

Fix $n \geq 2$. Given any $a \in (0, 1]$, we consider the annulus $\Sigma(a)$ in (6.28). We know that $\Sigma(a)$ is capillary in some ball B_a centered at the origin with radius $R = R(u^*(a))$ given by (6.13). We can then define the annulus $\mathbb{A}_n(a)$ as $\Psi_a(\Sigma(a))$, where $\Psi_a : \mathbb{R}^3 \rightarrow \mathbb{R}^3$ is the homothety that sends the ball B_a to the unit ball.

It is clear that every $\mathbb{A}_n(a)$ is a capillary minimal annulus in the unit ball. These surfaces are in the conditions of Theorem 6.1.1: indeed, items (1), (2) and (3) follow immediately from Theorem 6.3.2. Similarly, item (4) is a direct consequence of Proposition 6.4.9, while item (5) can be deduced from our previous analysis in Section 6.4.2.

6.5.2 Proof of Theorem 6.1.2

Let $n \in \mathbb{N}$, $n \geq 2$. Given any $a \in [0, 1]$, let $\theta_{a,n}$ denote the contact angle between the annulus $\mathbb{A}_n(a)$ defined in the previous section and the unit ball. By (6.13), this value can be expressed in terms of $\beta(u)$ and the map u^* in Lemma 6.4.1 as

$$\theta_{a,n} = -\arctan\left(\frac{1}{\beta_{a,n}}\right), \quad \beta_{a,n} := \beta(u^*(a)), \quad (6.56)$$

where $u^*(a) = u^*(a, b_q(a))$, $q = -1/n$ and $b_q(a)$ is given by Remark 6.3.4. Denote by ϑ_m, ϑ_M the values

$$\vartheta_m := \min\{\theta_{0,n}, \theta_{1,n}\}, \quad \vartheta_M := \max\{\theta_{0,n}, \theta_{1,n}\}.$$

It is clear by continuity of the family of surfaces $\mathbb{A}_n(a)$ that for every angle $\theta \in (\vartheta_m, \vartheta_M)$ there exists at least one annulus $\mathbb{A}_n(a)$, $a \in (0, 1)$, that meets $\partial\mathbb{B}$ with angle θ . We can compute explicitly the values $\theta_{0,n}$ for every $n \geq 2$: indeed, by (6.16), Lemma 6.4.1 and (6.26), we conclude that

$$\theta_{0,n} = \frac{\pi}{n}. \quad (6.57)$$

We can now show item (2) of Theorem 6.1.2. First, $\theta_{0,2} = \frac{\pi}{2}$, while by (6.56) and Lemma 6.4.3, we conclude that $\beta_{1,2} < 0$, so $\vartheta_1 := \theta_{1,2} \in (0, \pi/2)$. Thus, for any angle $\theta \in (\vartheta_1, \pi/2)$ we can find a non-rotational capillary annulus $\mathbb{A}_2(a)$, $a \in (0, 1)$ meeting

$\partial\mathbb{B}^3$ with angle θ .

We next prove item (1) of the theorem. This will be a consequence of the following proposition, which will be proven below:

Proposition 6.5.1. *There exists $n_0 \in \mathbb{N}$ such that for every $n \geq n_0$, the intervals $(\theta_{1,n}, \theta_{0,n})$ and $(\theta_{1,n+1}, \theta_{0,n+1})$ overlap. Moreover, $\lim_{n \rightarrow \infty} \theta_{i,n} = 0$ for $i = 0, 1$.*

Assume for one moment that Proposition 6.5.1 holds, and let $\vartheta_0 := \theta_{0,n_0}$. Then,

$$(0, \vartheta_0) \subset \bigcup_{n \geq n_0} (\theta_{1,n}, \theta_{0,n}).$$

In particular, for every $\theta \in (0, \vartheta_0)$ we can always find some annulus $\mathbb{A}_n(a)$, $n \geq n_0$, $a \in (0, 1)$ which meets $\partial\mathbb{B}^3$ with angle θ , showing item (1) of Theorem 6.1.2 and completing the proof of this result. It remains to show Proposition 6.5.1, which we do next.

Proof of Proposition 6.5.1. We will compute the limit of the quotient $\frac{\beta_{1,n}}{\beta_{0,n}}$ as $n \rightarrow \infty$, and show that it is greater than 1. Moreover, we will show that the limit of the quotients $\frac{\beta_{0,n}}{\beta_{0,n+1}}, \frac{\beta_{1,n}}{\beta_{1,n+1}}$ is exactly 1. This will prove that, for n large, $\beta_{1,n} < \beta_{0,n}$ and that $\beta_{1,n+1} < \beta_{0,n}$. Since the values $\beta_{i,n}$ are negative by Lemma 6.4.3, the intervals $(\beta_{1,n}, \beta_{0,n})$, $(\beta_{1,n+1}, \beta_{0,n+1})$ overlap for sufficiently large n . The proposition then follows from (6.56).

We fix $a = 1$, that is, $b = 2Q$, and define $\tilde{\beta}(u) := -2Q\beta(u) = -b\beta(u)$. We can then rewrite (2.17) as

$$\begin{aligned} \alpha'' &= \hat{a}\alpha + 2\alpha^2\tilde{\beta}, \\ \tilde{\beta}'' &= \hat{a}\tilde{\beta} + 2\alpha\tilde{\beta}^2 + 2Q^2\alpha. \end{aligned} \tag{6.58}$$

From the initial conditions (6.3) we deduce that

$$\begin{aligned} \alpha'(0) &= \frac{1}{4}, \\ \hat{a} &= -\frac{1}{4}(-b^2 + 2), \\ \tilde{\beta}'(0) &= \frac{1}{4}(1 - 2b^2). \end{aligned} \tag{6.59}$$

We note that (6.58)-(6.59) depends analytically on b , even at $b = 0$. This case is of interest for our purposes, as $b_q(1) = \frac{1}{n^2-1}$ converges to zero as $n \rightarrow \infty$; see Remark 6.3.4. We can explicitly solve the system in this limit situation: indeed, (6.58)-(6.59) is symmetric with respect to the change $(\alpha, \tilde{\beta}) \rightarrow (\tilde{\beta}, \alpha)$. Thus, $\alpha(u; 1, 0) = \tilde{\beta}(u; 1, 0) = y(u)$, where $y(u)$ is the function given by the initial conditions $y(0) = 0$, $y'(0) = 1/4$

and

$$y'' = -\frac{1}{2}y + 2y^3.$$

We can explicitly compute $y(u)$, obtaining

$$y(u) = \frac{e^u - 1}{2(e^u + 1)}.$$

This allows us to compute the third coordinate of the center function, $\widehat{c}_3(u)$, explicitly. Indeed, we know that $\widehat{c}'_3 = 1/(2y^2)$ by (6.15), and that $\widehat{c}_3(u)$ is antisymmetric. This implies that

$$\widehat{c}_3(u) = 2 \left(u - \frac{4}{e^u - 1} - 2 \right).$$

We note that $\lim_{u \rightarrow 0^+} \widehat{c}_3(u) = -\infty$. Clearly, $\widehat{c}_3(u)$ has a unique positive root $u^* \approx 2.39936$. We can estimate $\widetilde{\beta}(u^*; 1, 0) = y(u^*)$ as $\widetilde{\beta}(u^*; 1, 0) \approx 0.416778$. Let us then compute the limit of the quotient $\frac{\beta_{1,n}}{\beta_{0,n}}$ as $n \rightarrow \infty$. We already know that $\beta_{0,n} = -\frac{1}{\tan(\pi/n)}$, while for $\beta_{1,n}$ we will make use of $y(u)$ and the fact that $b_q(1) = \frac{1}{\sqrt{n^2-1}}$, $q = -\frac{1}{n}$; see Remark 6.3.4. This yields

$$\lim_{n \rightarrow \infty} \frac{\beta_{1,n}}{\beta_{0,n}} = \lim_{n \rightarrow \infty} \frac{\widetilde{\beta}(u^*; 1, b_q(1))}{b_q(1) \cot\left(\frac{\pi}{n}\right)} = \pi y(u^*) \approx 1.30935,$$

where we make use of the fact that $\lim_{n \rightarrow \infty} b_q(1) = 0$. A similar argument shows that

$$\lim_{n \rightarrow \infty} \frac{\beta_{0,n}}{\beta_{0,n+1}} = \lim_{n \rightarrow \infty} \frac{\beta_{1,n}}{\beta_{1,n+1}} = 1,$$

as we wanted to prove. □

6.6 Preliminary lemmas

We will devote this section to proving Lemmas 6.4.1 and 6.4.3. In order to do so, we first need to study the solutions (α, β) to (6.2), (6.3). We recall that this system admits a first integral that can be obtained via a Hamilton-Jacobi procedure, and in particular we can study the solutions to (6.2) in terms of the system (s, t) that has been presented in previous chapters. We summarize the behaviour of this system next.

6.6.1 The system (s, t)

Throughout this section, let $(a, b) \in \mathcal{O} \cap \{a > 0\}$ so that the constant Q in (6.3) is positive. We consider the change of variables

$$\begin{aligned} Q\alpha\beta &= s + t, \\ Q^2\alpha^2 &= -st. \end{aligned} \tag{6.60}$$

This defines a diffeomorphism between the open quadrant $\{(s, t) : s > 0, t < 0\}$ and the half-plane $\{(\alpha, \beta) : \alpha > 0\}$ which extends homeomorphically onto the boundary. Thus, setting $s \geq t$, the pair (s, t) satisfies

$$\begin{aligned} s &= \frac{Q\alpha}{2} \left(\beta + \sqrt{4 + \beta^2} \right), \\ t &= \frac{Q\alpha}{2} \left(\beta - \sqrt{4 + \beta^2} \right). \end{aligned} \tag{6.61}$$

It can be shown that if $(\alpha(u), \beta(u))$ is a solution to (6.2), (6.3), then $(s, t) = (s(\lambda), t(\lambda))$ must be a solution to

$$\begin{cases} s'^2(\lambda) &= s^2 g(s), \\ t'^2(\lambda) &= t^2 g(t), \end{cases} \tag{6.62}$$

where $u = u(\lambda)$ satisfies

$$2u'(\lambda) = s(\lambda) - t(\lambda) \geq 0, \tag{6.63}$$

and $g(x)$ is the third-order polynomial

$$g(x) = -(x - r_1)(x - r_2)(x - r_3) \tag{6.64}$$

where $r_1 \leq r_2 < 0 < r_3$ are given by

$$r_1 = -\frac{1}{4}, \quad r_2 = -\frac{a^2}{4}, \quad r_3 = \frac{a^2 b^2}{4}. \tag{6.65}$$

Remark 6.6.1. *Arguing as in Section 5.5.2, we have that the properties stated in Lemma 5.5.5 and Remark 5.5.6 hold in this case, where the roots \hat{r}_i are substituted by r_i in (6.65). In particular, we deduce that for every $(a, b) \in \mathcal{O} \cap \{0 < a < 1\}$ there*

exists $u_M = u_M(a, b)$ such that the function $u(\lambda)$ in (6.63) satisfies

$$\lim_{\lambda \rightarrow -\infty} u(\lambda) = 0, \quad \lim_{\lambda \rightarrow \infty} u(\lambda) = u_M.$$

Moreover, $\alpha(u) > 0$ for all $u \in (0, u_M)$ and $\alpha(u_M) = 0$. In the limit case $a = 1$, it holds $\lim_{\lambda \rightarrow \infty} u(\lambda) = \infty$ and $\alpha(u) > 0$ for all $u \in (0, \infty)$.

Lemma 6.6.2. Let (s, t) be a solution to (6.62) associated to a solution (α, β) to (6.2), (6.3) and $a \in (0, 1)$. Let $\lambda_w, \lambda_f \in \mathbb{R}$ be the values for which $s(\lambda_w) = r_3$, $t(\lambda_f) = r_2$. Then, $\lambda_w < \lambda_f$; see Figure 6.4.

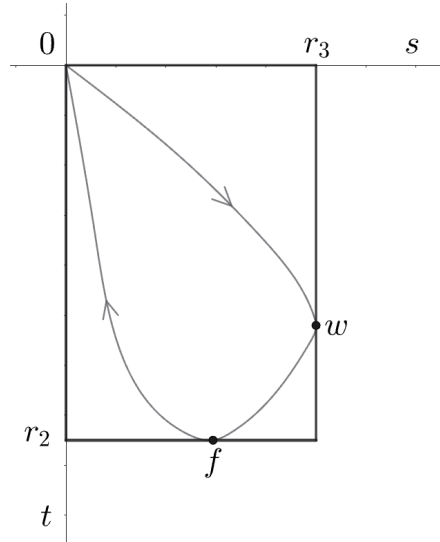


Figure 6.4: Orbit of the solution $(s(\lambda), t(\lambda))$ in Lemma 6.6.2. The value w corresponds with the point $(s(\lambda_w), t(\lambda_w))$ at which $s(\lambda_w) = r_3$. Similarly, f represents the point $(s(\lambda_f), t(\lambda_f))$, where $t(\lambda_f) = r_2$.

Proof. We first deduce from (6.61) that

$$\lim_{\lambda \rightarrow -\infty} \frac{s(\lambda)}{t(\lambda)} = \lim_{u \rightarrow 0^+} \frac{\beta(u) + \sqrt{4 + \beta(u)^2}}{\beta(u) - \sqrt{4 + \beta(u)^2}} = -1. \quad (6.66)$$

For all $\lambda \leq \min\{\lambda_w, \lambda_f\}$, we define the function

$$\mathcal{G}(\lambda) := \int_{s(\lambda)}^{r_3} \frac{dx}{x\sqrt{g(x)}} + \int_{r_2}^{t(\lambda)} \frac{dx}{x\sqrt{g(x)}}.$$

It can be deduced from (6.62) that the function $\mathcal{G}(\lambda)$ is constant. In fact, it holds

$$\mathcal{G}(\lambda) \equiv (\lambda_w - \lambda) + (\lambda - \lambda_f) = \lambda_w - \lambda_f. \quad (6.67)$$

We aim to show that $\lambda_w < \lambda_f$. To do so, we will prove that $\lim_{\lambda \rightarrow -\infty} \mathcal{G}(\lambda) < 0$. First, let $\lambda < 0$ be negative and large enough so that $s(\lambda) < -r_2$. This value must exist as $\lim_{\lambda \rightarrow -\infty} s(\lambda) = 0$. We may then rewrite $\mathcal{G}(\lambda)$ as

$$\mathcal{G}(\lambda) = \int_{s(\lambda)}^{r_3} \frac{dx}{x\sqrt{g(x)}} + \int_{r_2}^{-s(\lambda)} \frac{dx}{x\sqrt{g(x)}} + \int_{-s(\lambda)}^{t(\lambda)} \frac{dx}{x\sqrt{g(x)}} = \mathcal{G}_1(\lambda) + \mathcal{G}_2(\lambda), \quad (6.68)$$

where

$$\mathcal{G}_1(\lambda) := \int_{s(\lambda)}^{r_3} \frac{dx}{x\sqrt{g(x)}} + \int_{r_2}^{-s(\lambda)} \frac{dx}{x\sqrt{g(x)}}, \quad \mathcal{G}_2(\lambda) := \int_{-s(\lambda)}^{t(\lambda)} \frac{dx}{x\sqrt{g(x)}}.$$

We will now prove that $\lim_{\lambda \rightarrow -\infty} \mathcal{G}_1(\lambda) < 0$ and that $\lim_{\lambda \rightarrow -\infty} \mathcal{G}_2(\lambda) = 0$. We will deal first with the limit involving $\mathcal{G}_2(\lambda)$. Let $\lambda < 0$ be negative and large enough so that not only $s(\lambda) < -r_2$, but also $t(\lambda) > r_2/2$. We note by (6.64) that there exists a constant $M > 0$ such that $\frac{1}{\sqrt{g(x)}} < M$ for all $x \in (r_2/2, 0)$. Thus, we may bound $\mathcal{G}_2(\lambda)$ as

$$|\mathcal{G}_2(\lambda)| \leq M \left| \int_{-s(\lambda)}^{t(\lambda)} \frac{dx}{x} \right| = M \left| \log \left(-\frac{t(\lambda)}{s(\lambda)} \right) \right|.$$

By (6.66), we deduce

$$\lim_{\lambda \rightarrow -\infty} \mathcal{G}_2(\lambda) = 0. \quad (6.69)$$

We will now compute the limit regarding $\mathcal{G}_1(\lambda)$ by using Cauchy's theorem. Let $h(z)$ be the complex function

$$h(z) := \frac{i}{\sqrt{z - r_1} \sqrt{z - r_2} \sqrt{z - r_3}},$$

where we define the square root $z \rightarrow \sqrt{z}$ so that it is holomorphic on $\mathbb{C} \setminus \{z \in \mathbb{R} : z \leq 0\}$. This implies that $h(z)$ is defined and holomorphic on $\mathbb{C} \setminus ((-\infty, r_1] \cup [r_2, r_3])$. In particular, $h(z)$ is not defined on $z = 0$. However, we can compute the limits of $h(z)$ as z approaches $z = 0$ on the upper and lower half-planes $\mathbb{C}^+ := \{z \in \mathbb{C} : \text{Im}(z) > 0\}$,

$\mathbb{C}^- := \{z \in \mathbb{C} : \text{Im}(z) < 0\}$, respectively. This leads to

$$h_0^+ := \lim_{\substack{z \rightarrow 0 \\ z \in \mathbb{C}^+}} h(z) = \frac{1}{\sqrt{r_1 r_2 r_3}}, \quad h_0^- := \lim_{\substack{z \rightarrow 0 \\ z \in \mathbb{C}^-}} h(z) = -\frac{1}{\sqrt{r_1 r_2 r_3}} = -h_0^+. \quad (6.70)$$

Let λ_0 such that $s_0 := s(\lambda_0) < -r_2$. For every $n \in \mathbb{N}$ such that $n > |r_i|, i = 1, 2, 3$, let Ξ_n be the family of integration paths in Figure 6.5. That is, Ξ_n is the union of the circle arc $\Xi_n^{(1)}$ of radius n centered at $z = 0$, the curves $\Xi_n^{(2)}, \Xi_n^{(3)}, \Xi_n^{(4)}$ around the intervals $(-\infty, r_1], [r_2, -s_0]$ and $[s_0, r_3]$ and the arcs $\Xi_n^{(5)}, \Xi_n^{(6)}$ of the circle of radius s_0 centered at $z = 0$. We assume that the paths $\Xi_n^{(2)}, \Xi_n^{(3)}, \Xi_n^{(4)}$ are chosen so that they converge to their corresponding intervals as $n \rightarrow \infty$. Now, since the function $h(z)/z$ is holomorphic on $\mathbb{C} \setminus ((-\infty, r_1] \cup [r_2, r_3])$, it holds

$$\int_{\Xi_n} \frac{h(z)}{z} dz = 0.$$

On the other hand, if we integrate on each of the paths $\Xi_n^{(i)}, i = 1, \dots, 6$,

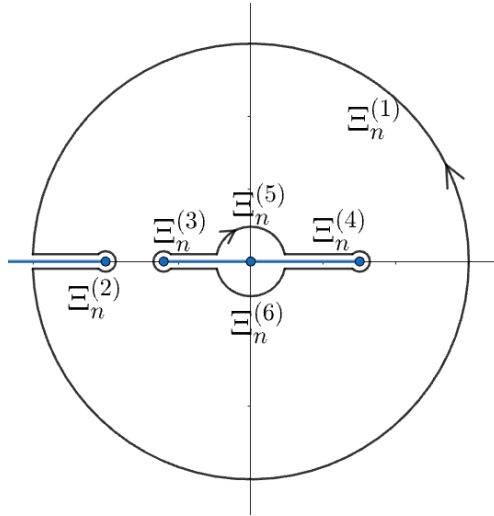


Figure 6.5: Integration path Ξ_n for the function $h(z)/z$.

$$\begin{aligned} \lim_{n \rightarrow \infty} \int_{\Xi_n^{(1)}} \frac{h(z)}{z} dz &= 0, \\ \lim_{n \rightarrow \infty} \int_{\Xi_n^{(2)}} \frac{h(z)}{z} dz &= -2 \int_{-\infty}^{r_1} \frac{dx}{x \sqrt{g(x)}} = \mathcal{C} > 0, \\ \lim_{n \rightarrow \infty} \int_{\Xi_n^{(3)}} \frac{h(z)}{z} dz &= 2 \int_{r_2}^{-s_0} \frac{dx}{x \sqrt{g(x)}} < 0, \end{aligned}$$

$$\begin{aligned}
\lim_{n \rightarrow \infty} \int_{\Xi_n^{(4)}} \frac{h(z)}{z} dz &= 2 \int_{s_0}^{r_3} \frac{dx}{x \sqrt{g(x)}} > 0, \\
\lim_{n \rightarrow \infty} \int_{\Xi_n^{(5)}} \frac{h(z)}{z} dz &= - \int_0^\pi \frac{s_0 i e^{it} h(s_0 e^{it})}{s_0 e^{it}} dt = -i \int_0^\pi h(s_0 e^{it}) dt, \\
\lim_{n \rightarrow \infty} \int_{\Xi_n^{(6)}} \frac{h(z)}{z} dz &= -i \int_\pi^{2\pi} h(s_0 e^{it}) dt,
\end{aligned}$$

where $\mathcal{C} > 0$ is a positive constant. This leads to

$$2\mathcal{G}_1(\lambda_0) = i \int_0^\pi h(s(\lambda_0)e^{it}) dt + i \int_\pi^{2\pi} h(s(\lambda_0)e^{it}) dt - \mathcal{C}. \quad (6.71)$$

This identity holds for every λ_0 such that $s(\lambda_0) < -r_2$. We note that \mathcal{C} is a positive constant independent of λ_0 . Thus, we may take limit as $\lambda_0 \rightarrow -\infty$ in (6.71). Since $\lim_{\lambda_0 \rightarrow -\infty} s(\lambda_0) = 0$, we deduce using (6.70) that

$$\begin{aligned}
\lim_{\lambda_0 \rightarrow -\infty} \mathcal{G}_1(\lambda_0) &= \lim_{\lambda_0 \rightarrow -\infty} \frac{1}{2} \left(i \int_0^\pi h(s(\lambda_0)e^{it}) dt + i \int_\pi^{2\pi} h(s(\lambda_0)e^{it}) dt - \mathcal{C} \right) \\
&= \frac{1}{2} \left(i \int_0^\pi h_0^+ dt + i \int_\pi^{2\pi} h_0^- dt - \mathcal{C} \right) = -\frac{\mathcal{C}}{2} < 0.
\end{aligned} \quad (6.72)$$

Combining (6.67), (6.68), (6.69) and (6.72), we deduce

$$\lambda_w - \lambda_f = \lim_{\lambda \rightarrow -\infty} \mathcal{G}(\lambda) = \lim_{\lambda \rightarrow -\infty} \mathcal{G}_1(\lambda) + \mathcal{G}_2(\lambda) = -\frac{\mathcal{C}}{2} < 0,$$

so $\lambda_w < \lambda_f$, as we wanted to show. □

Remark 6.6.3. If $a = 1$, then $t(\lambda)$ is decreasing for all $\lambda \in \mathbb{R}$, with $\lim_{\lambda \rightarrow \infty} t(\lambda) = r_2$. Nevertheless, $s(\lambda)$ attains the maximum $s(\lambda) = r_3$ in finite time. In particular, the value λ_w in the previous lemma is well defined in this case.

Lemma 6.6.4. Let $(a, b) \in \mathcal{O} \cap \{a > 0\}$ such that $\beta'(0) \leq 0$. Then $\beta(u) < 0$ for all $u \in (0, u_M)$. Moreover, if $a = 1$, $\beta(u) < 0$ for all $u \in (0, \infty)$; see Remark 6.6.1.

Proof. Let $f(\lambda) : \mathbb{R} \rightarrow \mathbb{R}$ be the function

$$f(\lambda) := s(\lambda) + t(\lambda). \quad (6.73)$$

By (6.60), $f(\lambda)$ corresponds to the product $\alpha(u)\beta(u)Q$ in the variable u . By Remark 6.6.1, we have that the sign of $f(\lambda)$ coincides with that of $\beta(u) = \beta(u(\lambda))$. So, if

$\beta'(0) < 0$, then it holds $f(\lambda) < 0$ for λ negative and large enough. The same holds if $\beta'(0) = 0$, as $\beta''(0) = 0$, $\beta'''(0) = -2Q\alpha'(0) < 0$.

Assume by contradiction that either $\beta(u)$ vanishes at some first value $u_0 \in (0, u_M)$ if $a < 1$ or at some $u_0 \in (0, \infty)$ if $a = 1$. This implies that $f(\lambda)$ should vanish at some $\lambda_0 \in \mathbb{R}$. Since $f(\lambda) < 0$ for λ negative and large enough, then it should hold $f'(\lambda_0) \geq 0$, that is,

$$s'(\lambda_0) + t'(\lambda_0) \geq 0. \quad (6.74)$$

According to Lemma 6.6.2, if $a < 1$ we need to study three cases depending on whether $\lambda_0 \in (-\infty, \lambda_w]$, $\lambda_0 \in [\lambda_w, \lambda_f]$ or $\lambda_0 \in [\lambda_f, \infty)$. For the limit $a = 1$, it suffices to consider the cases $\lambda_0 \in (-\infty, \lambda_w]$ and $\lambda_0 \in [\lambda_w, \infty)$ instead. In what follows, we set $s_0 := s(\lambda_0) = -t(\lambda_0)$, where $s_0 \in (0, \frac{a^2 b^2}{4}]$.

We first consider the case $\lambda_0 \in (-\infty, \lambda_w]$. Then, it holds $s'(\lambda_0) \geq 0$, $t'(\lambda_0) < 0$. Hence, (6.74) is equivalent to

$$g(s_0) \geq g(-s_0), \quad (6.75)$$

where $g(x)$ is the polynomial in (6.64). However, (6.75) cannot hold due to (6.3) and the assumption that $\beta'(0) \leq 0$. Thus, $f(\lambda) < 0$ for all $\lambda \leq \lambda_w$.

Let us assume then that $\lambda_0 \in (\lambda_w, \lambda_f]$ if $a < 1$ or $\lambda_0 \in (\lambda_w, \infty)$ if $a = 1$. In either case, for every λ in this interval we have that both $s(\lambda)$ and $t(\lambda)$ are decreasing, so $f'(\lambda) \leq 0$. Since $f(\lambda_w) < 0$, we conclude that $f(\lambda)$ is necessarily negative in this interval. This already shows the lemma for the case $a = 1$.

Finally, we consider the case $\lambda_0 \in [\lambda_f, \infty)$, $a < 1$. We have that $s(\lambda)$ is decreasing but $t(\lambda)$ is increasing. Consequently, we can deduce from (6.62) the following: let $\bar{\lambda} \in (-\infty, \lambda_w)$ be the unique value such that $s(\bar{\lambda}) = s(\lambda_f)$. Then, it holds

$$\begin{aligned} s(\lambda_f + \lambda) &= s(\bar{\lambda} - \lambda), \\ t(\lambda_f + \lambda) &< t(\bar{\lambda} - \lambda), \end{aligned}$$

for all $\lambda > 0$ by the uniqueness of solutions to (6.62); see also Figure 6.6. In particular, $f(\lambda_f + \lambda) < f(\bar{\lambda} - \lambda) < 0$, so $f(\lambda)$ does not vanish. This shows the lemma for the case $a < 1$ and concludes the proof. \square

6.6.2 Proof of preliminary lemmas

Proof of Lemma 6.4.1. We know by (6.15) and the fact that $\alpha(0) = 0$ that the third coordinate $\widehat{c}_3(u)$ of the center function is strictly increasing, and $\lim_{u \rightarrow 0^+} \widehat{c}_3(u) = -\infty$.

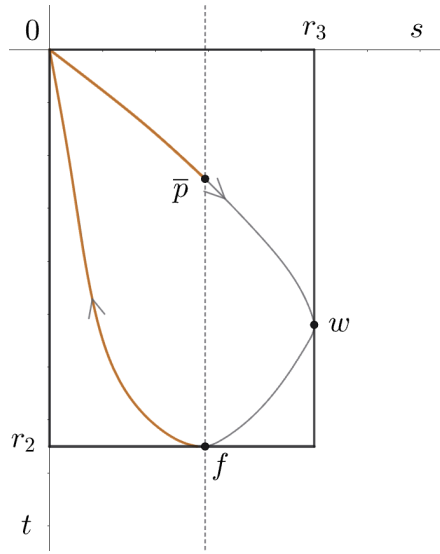


Figure 6.6: Solution $(s(\lambda), t(\lambda))$ with $a < 1$. The points \bar{p}, w, f are given by $\bar{p} = (s(\bar{\lambda}), t(\bar{\lambda}))$, $w = (s(\lambda_w), t(\lambda_w))$, $f = (s(\lambda_f), t(\lambda_f))$. The upper orange curve represents the trajectory $(s(\lambda), t(\lambda))$ for $\lambda < \bar{\lambda}$, while the lower one represents it for $\lambda > \lambda_f$.

If $a \in (0, 1)$, then we know that there exists a first positive value $u_M > 0$ for which $\alpha(u_M) = 0$, so in particular $\lim_{u \rightarrow u_M^-} \widehat{c}_3(u) = \infty$, deducing the existence of u^* in this case; see also Remark 6.6.1. The fact that $u^* < u_D$ is an immediate consequence of Remark 6.2.3.

Let us now assume that $a = 1$. In this case, the function $\alpha(u)$ does not vanish on the interval $(0, \infty)$. However, by (6.60) and Remark 6.6.1, we deduce that

$$\lim_{u \rightarrow \infty} \alpha(u) = \lim_{\lambda \rightarrow \infty} \frac{\sqrt{-s(\lambda)t(\lambda)}}{Q} = 0,$$

as $s(\lambda)$ converges to zero and $t(\lambda)$ is bounded. Thus, there exists $M > 0$ such that $|\alpha(u)| < M$ on $(0, \infty)$. Given any $u_0 > 0$, it follows from (6.15) that

$$\begin{aligned} \lim_{u \rightarrow \infty} \widehat{c}_3(u) &= \widehat{c}_3(u_0) + \lim_{u \rightarrow \infty} \int_{u_0}^u \frac{1}{2\alpha^2} du' \\ &> \widehat{c}_3(u_0) + \lim_{u \rightarrow \infty} \int_{u_0}^u \frac{1}{2M^2} du' = \infty. \end{aligned}$$

Consequently, we deduce the existence of u^* in this case. The fact that $u^* < u_D$ is again a consequence of Remark 6.2.3.

If $a = 0$, we can explicitly compute the third coordinate of $\widehat{c}(u)$; see (6.14), (6.19).

This yields

$$\widehat{c}_3(u) = 2 \left(\tan\left(\frac{u}{4}\right) - \cot\left(\frac{u}{4}\right) \right),$$

which has a first positive root at $u^* = \pi$. This value is below the value $u_{\mathcal{D}} = 2\pi$ obtained in Section 6.2.3.

Finally, the analyticity of the map $u^* : \mathcal{O} \rightarrow (0, \infty)$ follows from the implicit function theorem, (6.14) and (6.15), as $\widehat{c}'_3(u^*) > 0$. \square

Proof of Lemma 6.4.3. Let $n \in \mathbb{N}$, $n \geq 2$, and $q := -\frac{1}{n}$. The result is an immediate consequence of Remark 6.6.3 and Lemma 6.6.4 once we show that for every $a \in (0, 1]$ it holds that the value $\beta'(0) = \beta'(0; a, b)$ associated to the pair $(a, b_q(a))$ is negative. We will next prove that

$$\Theta\left(a, \frac{1}{\sqrt{a^2 + 1}}\right) < -\frac{1}{2} \leq -\frac{1}{n} = \Theta(a, b_q(a)). \quad (6.76)$$

In particular, since the derivative $\frac{\partial \Theta}{\partial b}$ is strictly negative, we deduce that $b_q(a) < \frac{1}{\sqrt{a^2 + 1}}$ for all $a \in (0, 1]$. It is then straightforward from (6.3) that $\beta'(0; a, b_q(a)) < 0$, proving the lemma.

We will now prove (6.76). Let $F : (0, 1) \rightarrow \mathbb{R}$ be the function

$$F(a) := \Theta\left(a, \frac{1}{\sqrt{a^2 + 1}}\right). \quad (6.77)$$

Now, for every $a \in (0, 1)$, consider the function

$$j(a, x) = \sqrt{\frac{(1 - a^2)x + a^2}{(1 - a^2)x + 2a^2 + 1}}.$$

Then, it follows from (6.27) that

$$F(a) = -\frac{1}{\pi} \int_0^1 \frac{j(a, x)}{\sqrt{x(1-x)}} dx = -\frac{1}{\pi} \int_0^1 \frac{j(a, 1-x)}{\sqrt{x(1-x)}} dx,$$

where in the second equality we use the change of variables $\tilde{x} = 1 - x$. This allows us to rewrite $F(a)$ as

$$F(a) = -\frac{1}{2\pi} \int_0^1 \frac{j(a, x) + j(a, 1-x)}{\sqrt{x(1-x)}} dx. \quad (6.78)$$

Let $k(a, w) := j\left(a, \frac{w+1}{2}\right)$. Applying the change of variables $w = 2x - 1$ in (6.78), we

obtain

$$F(a) = -\frac{1}{2\pi} \int_{-1}^1 \frac{k(a, w) + k(a, -w)}{\sqrt{1-w^2}} dw. \quad (6.79)$$

We will now show that $k_a(a, w) + k_a(a, -w) > 0$ for all $a \in (0, 1)$, $w \in [-1, 1]$, $w \neq 0$, where k_a denotes the partial derivative with respect to a . Setting $A := \frac{1-a^2}{2}$, $B := \frac{1+a^2}{2}$, we conclude that

$$k(a, w) = \sqrt{\frac{Aw + B}{Aw + 3B}},$$

so

$$\begin{aligned} k_a(a, w) + k_a(a, -w) &= -\frac{aw}{(3B + Aw)^{\frac{3}{2}} \sqrt{Aw + B}} + \frac{aw}{(3B - Aw)^{\frac{3}{2}} \sqrt{B - Aw}} \\ &= aw \left(\frac{1}{(3B - Aw)^{\frac{3}{2}} \sqrt{B - Aw}} - \frac{1}{(3B + Aw)^{\frac{3}{2}} \sqrt{B + Aw}} \right). \end{aligned}$$

Since the function $u \mapsto k(a, w) + k(a, -w)$ is symmetric, it suffices to show that

$$k_a(a, w) + k_a(a, -w) > 0$$

for $u > 0$. This holds trivially, as $A, B > 0$ and

$$(3B + Aw)^{\frac{3}{2}} \sqrt{B + Aw} > (3B - Aw)^{\frac{3}{2}} \sqrt{B - Aw}.$$

Since $k_a(a, w) + k_a(a, -w) > 0$, we conclude from (6.79) $a \mapsto F(a)$ is a strictly decreasing function. Thus, $F(a) < F(0)$ for all $a \in (0, 1]$, and we arrive at

$$\Theta \left(a, \frac{1}{\sqrt{a^2 + 1}} \right) < \Theta(0, 1) = -\frac{1}{2},$$

see (6.26). This shows (6.76) and the lemma. \square

6.7 An application to an overdetermined problem in \mathbb{S}^2

In this last section, we will use the examples of embedded annuli constructed in Theorem 6.1.1 to obtain a wide family of non-radial solutions to an overdetermined problem

in \mathbb{S}^2 . More precisely, let us consider the following overdetermined problem in \mathbb{S}^2 :

$$\begin{cases} \Delta w + 2w = 0 & \text{in } \Omega \subset \mathbb{S}^2, \\ w = c, \quad \frac{\partial w}{\partial \nu} = d & \text{on } \partial\Omega, \end{cases} \quad (6.80)$$

for some constants $c, d \in \mathbb{R}$, where Ω is a smooth domain in \mathbb{S}^2 , and $\frac{\partial w}{\partial \nu}$ denotes the outer normal derivative.

Let $n \in \mathbb{N}$, $n \geq 2$. We will now construct a 1-parameter family $\{\Omega_n(a)\}_{a \in (0,1)}$ of non-rotational annular domains in \mathbb{S}^2 and non-zero constants $c = c(a, n) > 0$, $d = d(a, n) < 0$ for which (6.80) can be solved; see Figures 1.5, 1.6. Specifically, we prove the following:

Theorem 6.7.1. *For any $n \geq 2$ there exists a real analytic family of regular annular domains $\{\Omega_n(a)\}_{a \in (0,1)}$, $\Omega_n(a) \subset \mathbb{S}^2$, with the following properties:*

1. *There exist $c = c(a, n) > 0$, $d = d(a, n) < 0$ such that the problem (6.80) admits a solution on $\Omega_n(a)$.*
2. *The corresponding solution $w : \Omega_n(a) \rightarrow \mathbb{R}$ satisfies $w \geq c(a, n)$.*
3. *If $a \in (0, 1)$, the domains $\Omega_n(a)$ have a finite prismatic symmetry group of order $2n$, generated by the reflection with respect to the equator $\mathbb{S}^2 \cap \{x_3 = 0\}$, and with respect to n equiangular vertical geodesics of \mathbb{S}^2 . Moreover, the associated solution u to (6.80) is invariant by all these symmetries. In particular, the domains $\Omega_n(a)$ and their solutions are not radially symmetric.*
4. *For $a = 1$, the domain $\Omega_n(1)$ is a rotational band of constant width δ_n around the equator of \mathbb{S}^2 , and u depends solely on the distance to the equator.*
5. *When $a \rightarrow 0$, the domains $\Omega_n(a)$ converge to a chain of n spherical caps tangent along the equator.*

We emphasize that problem (6.80) is actually a 1-parameter family of non-equivalent problems, namely, we can assume $c^2 + d^2 = 1$ after applying the linear change

$$w \mapsto \frac{1}{c^2 + d^2} w. \quad (6.81)$$

When $d = 0$, Souam proved in [70] that (6.80) never has a solution. When $c = 0$ and Ω is an annular domain, this problem can be shown to be equivalent to the *critical*

catenoid conjecture; see Conjecture 1.3. We prove as a consequence of Theorems 6.1.2 and 6.7.1 that near these two limit situations, the problem (6.80) always admits non-radial solutions.

Theorem 6.7.2. *There exist non-rotational annular domains in \mathbb{S}^2 solving (6.80) with $c = \cos \theta$ and $d = -\sin \theta$ for any $\theta \in (0, \pi/2)$ close enough to 0 or to $\pi/2$. More specifically:*

1. *There exists some $\vartheta_0 \in (0, \pi/2)$ such that for any $\theta \in (0, \vartheta_0)$, there is some domain $\Omega_n(a)$ in Theorem 6.7.1 that solves problem (6.80) for $c = \cos \theta$, $d = -\sin \theta$.*
2. *Similarly, there exists $\vartheta_1 \in (0, \pi/2)$ such that for any $\theta \in (\vartheta_1, \pi/2)$ there is some value $a \in (0, 1)$ so that the domain $\Omega_2(a)$ in Theorem 6.7.1 solves problem (6.80) for $c = \cos \theta$, $d = -\sin \theta$.*

The relationship between Theorems 6.1.1 and 6.7.1 relies on a classical connection between minimal surfaces and solutions to the partial differential equation

$$\Delta w + 2w = 0 \quad \text{in } \Omega \subset \mathbb{S}^2, \quad (6.82)$$

which we specify next.

Theorem 6.7.3 ([71]). *Let $\psi : \Omega \subset \mathbb{S}^2 \rightarrow \mathbb{R}^3$ be a minimal surface parametrized by its Gauss map, that is, $N(\mathbf{p}) = \mathbf{p}$. Then, the support function $w(\mathbf{p}) : \Omega \rightarrow \mathbb{R}$, given by*

$$w(\mathbf{p}) = \langle \psi(\mathbf{p}), \mathbf{p} \rangle,$$

satisfies (6.82).

Assume further that the minimal surface is capillary in a ball B_R with contact angle θ , where B_R is a ball of radius R centered at the origin. Then, the support function solves the overdetermined system (6.80) for some constants $c, d \in \mathbb{R}$.

Fix $n \geq 2$ and let $a \in (0, 1]$. We aim to use the examples of capillary annuli $\mathbb{A}_n(a)$ obtained in Theorem 6.1.1 to construct a set of solutions to the overdetermined problem (6.80). We recall that, up to an homothety, these surfaces are given by $\Sigma(a)$ in (6.28). In order to achieve this goal, we need to reparametrize the immersions $\psi(u, v) = \psi(u, v; a)$ associated to $\Sigma(a)$ in terms of their respective Gauss maps $N(u, v) = N(u, v; a)$. In particular, we need to show that each $N(u, v; a)$ is a diffeomorphism onto its image. We do this next.

Proposition 6.7.4. *With the previous notations, let $\Omega_n(a) \subset \mathbb{S}^2$ denote the image of the domain \mathcal{D}_a in (6.29) via the Gauss map $N(u, v) = N(u, v; a)$. Then,*

$$N(u, v) : \mathcal{D}_a \rightarrow \Omega_n(a)$$

is a diffeomorphism for all $a \in (0, 1]$. In particular, $\Omega_n(a)$ is an annular domain in \mathbb{S}^2 .

Proof. We will follow a similar strategy to the one in Proposition 6.4.9. The result is trivial in the limit case $a = 1$: indeed, $\Sigma(a)$ is a (piece of) catenoid, so its Gauss map is injective; see (6.38). Moreover, the image of any set $[-u_0, u_0] \times [-n\sigma, n\sigma]$ via $N(u, v; 1)$ clearly defines an annular domain in \mathbb{S}^2 . In particular, the restriction of $N(u, v; 1)$ to \mathcal{D}_1 defines a diffeomorphism onto $\Omega_n(1)$. This actually proves that there exists a maximal interval $(a_0, 1]$, $a_0 \geq 0$, such that every $N(u, v; a)$ is a diffeomorphism onto $\Omega_n(a)$ for $a \in (a_0, 1]$.

Suppose by contradiction that $a_0 > 0$, that is, $N(u, v; a_0)$ is no longer a diffeomorphism but every $N(u, v; a)$ with $a > a_0$ is. Thus, one of the following properties must hold:

- (1) $N(u, v; a_0)$ is not a local diffeomorphism, that is, there exists $p_0 = (u_0, v_0)$ such that $d(N(u, v; a_0))_{p_0}$ is not injective.
- (2) The boundary curves of $\Omega_n(a_0)$, given by $v \mapsto N(u^*, v)$, $v \mapsto N(-u^*, v)$, meet each other at some point in \mathbb{S}^2 .
- (3) One of the boundary curves of $\Omega_n(a_0)$ is not embedded.

We will now show that none of these conditions hold. First, it follows by (2.10) that the partial derivatives N_u, N_v are linearly independent if $a > 0$, as $Q > 0$ in this case, so $N(u, v; a_0)$ cannot satisfy (1).

Regarding the second property, we first note that since the annulus $\Sigma(a)$ is symmetric with respect to the horizontal plane $\{x_3 = 0\}$, it follows that the Gauss map $N(u, v; a_0)$ is also symmetric with respect to this plane. As a consequence, the boundary component $v \mapsto N(-u^*, v; a_0)$ is the reflection with respect to $\{x_3 = 0\}$ of $v \mapsto N(u^*, v; a_0)$. We proved in item (2) of Proposition 6.4.6 that the v -line $N(u^*, v; a_0)$ lies in the lower half-sphere $\mathbb{S}^2 \cap \{x_3 < 0\}$. Hence, $N(-u^*, v; a_0)$ will lie in the upper half-sphere $\mathbb{S}^2 \cap \{x_3 > 0\}$, so the boundary components of $\Omega_n(a_0)$ cannot meet each other. In particular, condition (2) cannot be satisfied.

Let us finally show that the third condition does not hold either. By the symmetry with respect to the plane $\{x_3 = 0\}$, it suffices to check that $v \mapsto N(u^*, v; a_0)$ is

injective. Let $\gamma(v)$ denote the projection of $v \mapsto N(u^*, v; a_0)$ onto the horizontal plane $\{x_3 = 0\}$. We will now show that $\gamma(v)$ is a strictly locally convex curve, which by Remark 6.4.5 implies that $\gamma(v)$ (and thus, $N(u^*, v; a_0)$) is embedded.

First, we know by Proposition 6.4.6 that the planar curve $\Gamma_{a_0}^0(v)$, given by the horizontal projection of $v \mapsto \psi(u^*, v; a_0)$, is strictly locally convex. This means that the product

$$\langle (\Gamma_{a_0}^0)_{vv}(v), \mathbf{n}(v) \rangle,$$

where $\mathbf{n}(v)$ is given by (6.31), never vanishes. Now, it follows from (2.10) that

$$\gamma'(v) = Qe^{-2\omega(u^*, v)}(\Gamma_{a_0}^0)_v(v). \quad (6.83)$$

This allows us to deduce several properties: first, $\gamma'(v)$ never vanishes, so $\gamma(v)$ is a regular curve. Since $\gamma'(v)$ is collinear with $(\Gamma_{a_0}^0)_v(v)$, the vector $\mathbf{n}(v)$ is orthogonal to $\gamma'(v)$. In particular, by differentiating (6.83) with respect to v , we see that

$$\langle \gamma''(v), \mathbf{n}(v) \rangle = Qe^{-2\omega(u^*, v)} \langle (\Gamma_{a_0}^0)_{vv}(v), \mathbf{n} \rangle \neq 0,$$

so $\gamma(v)$ is strictly locally convex. Consequently, the curve $v \mapsto N(u^*, v; a)$ is injective, completing the proof of the proposition. \square

We are now in conditions of proving the main results of this section, Theorems 6.7.1 and 6.7.2.

6.7.1 Proof of Theorem 6.7.1

Let $n \in \mathbb{N}$, $a \in (0, 1]$. By Proposition 6.7.4, the Gauss map $N(u, v; a) : \mathcal{D}_a \rightarrow \Omega_n(a)$ associated to the surface $\Sigma(a)$ in (6.28) is a diffeomorphism. In particular, we may reparametrize the immersion $\psi(u, v; a)$ in terms of its Gauss map, that is, $\tilde{\psi}(\mathbf{p}) := \psi(N^{-1}(\mathbf{p}))$. We can then consider the support function $w(\mathbf{p}) : \Omega_n(a) \subset \mathbb{S}^2 \rightarrow \mathbb{R}$, $w(\mathbf{p}) = w(\mathbf{p}; a, n)$ given by

$$w(\mathbf{p}) = \langle \tilde{\psi}(\mathbf{p}), \mathbf{p} \rangle. \quad (6.84)$$

We now recall that the annulus $\Sigma(a)$ in (6.28) is capillary in a ball centered at the origin. As a direct consequence of Theorem 6.7.3, we deduce that the function (6.84) yields a solution to the overdetermined system (6.80) on the annular domain $\Omega_n(a)$. Moreover, by combining (6.14), the definition of $u(\mathbf{p})$ in (6.84) and using the fact that $\widehat{c}(u^*(a)) = 0$, we deduce that the constants $c = c(a, n)$, $d = d(a, n)$ associated to this

solution can be expressed as

$$c(a, n) = -\frac{2\beta(u^*)}{\alpha(u^*)}, \quad d(a, n) = -\frac{2}{\alpha(u^*)}. \quad (6.85)$$

We note that the outer normal derivative $\frac{\partial w}{\partial \nu}$ in (6.80) is given by

$$\langle \psi(u^*, v), \psi_u(u^*, v) e^{-\omega(u^*, v)} \rangle,$$

see (2.10).

Let us now prove that the set of solutions $u(\mathbf{p}; a, n)$ and domains $\Omega_n(a)$ satisfy the properties in Theorem 6.7.1. Item (1) is direct from (6.85) and Lemma 6.4.3. Item (3) and (4) follow from the symmetry properties of the annuli $\Sigma(a)$; see Theorem 6.1.1 and its proof in Section 6.4.

Let us now prove item (2). It was shown in Lemma 6.4.8 that the support function $u(\mathbf{p}; a, n)$ associated to the annulus $\Sigma(a)$ is positive. Thus, it is immediate from (6.82) that $u(\mathbf{p}; a, n)$ cannot have local minima in the interior of $\Omega_n(a)$. Hence, for every $\mathbf{p}_0 \in \Omega_n(a)$,

$$u(\mathbf{p}_0) \geq \min_{\mathbf{p} \in \Omega_n(a)} u(\mathbf{p}) = \min_{\mathbf{p} \in \partial\Omega_n(a)} u(\mathbf{p}) = c(a, n).$$

Finally, regarding item (5), arguing as in Sections 6.2.3, 6.4.2, it is possible to show that the image of the set $[-u^*(a), u^*(a)] \times [0, 2\sigma(a)]$ via the Gauss map $N(u, v; a)$ converges as $a \rightarrow 0$ to a geodesic disk in \mathbb{S}^2 which is symmetric with respect to the horizontal geodesic $\mathbb{S}^2 \cap \{x_3 = 0\}$. Consequently, by the symmetry properties of the surfaces $\Sigma(a)$, it follows that the image of the annuli \mathcal{D}_a in (6.29) via $N(u, v; a)$ converge to a chain of n vertical geodesic disks as $a \rightarrow 0$. This completes the proof of the theorem.

6.7.2 Proof of Theorem 6.7.2

Given any $n \geq 2$, $a \in (0, 1]$, we normalize the function $u(\mathbf{p}; a, n)$ as in (6.81) so that the corresponding constants $c(a, n)$, $d(a, n)$ in (6.80) can be expressed as $c = \cos \theta$, $d = -\sin \theta$ for some $\theta = \theta(a, n)$. By (6.85), we deduce that

$$\tan \theta = -\frac{d}{c} = -\frac{1}{\beta(u^*(a))}.$$

It follows from (6.56) that the value $\theta(a, n)$ coincides with the contact angle $\theta_{a,n}$ associated to the capillary annulus $\mathbb{A}_n(a)$; see Section 6.5.2. Thus, the statements in

Theorem 6.7.2 are an immediate consequence of Theorem 6.1.2.

6.8 Final notes

Theorem 6.1.2 proves that there exist embedded capillary minimal annuli in \mathbb{B}^3 for intersection angles $\theta \in (0, \pi/2)$ arbitrarily close to 0 and to $\pi/2$. However, it does not prove that there exist such examples for *any* angle $\theta \in (0, \pi/2)$. More specifically, for each $n \geq 2$, the intersection angles $\theta_{a,n}$ of the capillary minimal annuli $\mathbb{A}_n(a)$ of Theorem 6.1.1 cover some interval $I_n \subset \mathbb{R}$, and so, the set of angles of our examples is the union of all such intervals. These intervals I_n can be numerically described in an accurate way, since our construction process is reasonably explicit (although depending on elliptic integrals). For example, these numerical computations show that ϑ_0 in Theorem 6.1.2 is given by $\vartheta_0 = \theta_{0,4} = \frac{\pi}{4}$, and that $\vartheta_1 = \theta_{1,2} \equiv 1.191692$. Nonetheless, these numerical simulations also show two *gaps* in the set $(0, \pi/2) \setminus \bigcup_n I_n$; see Figure 6.7. That is, the capillary minimal annuli $\mathbb{A}_n(a)$ constructed in Theorem 6.1.1 do not cover all possible intersection angles $\theta \in (0, \pi/2)$. This leaves open the possibility that, for some values $\theta \neq \pi/2$, the only embedded capillary minimal annuli in \mathbb{B}^3 with intersection angle θ are pieces of catenoids.

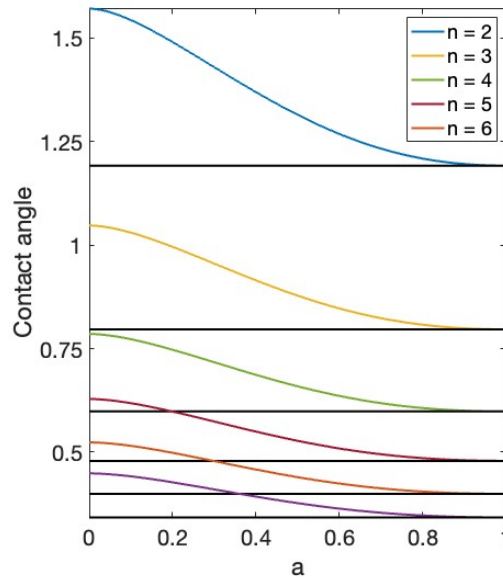


Figure 6.7: Numerical computations of the contact angles between the capillary annuli $\mathbb{A}_n(a)$ and $\partial\mathbb{B}^3$ for different values of n . For $n \geq 4$, the contact angles of consecutive families of annuli overlap.

Also regarding uniqueness, it is natural to ask whether *any* embedded capillary minimal annulus in \mathbb{B}^3 must be one of the annuli $\mathbb{A}_n(a)$ of Theorem 6.1.1. This problem was formulated in [29], and it can be seen as a generalization of the critical catenoid conjecture. We note that, by [29], any embedded free boundary minimal annulus in \mathbb{B}^3 foliated by spherical curvature lines must be the critical catenoid.

The construction method presented in Theorem 6.1.1 has some clear advantages with respect to the one developed originally by Fernández, Hauswirth and Mira in [29], even when considering immersed free boundary minimal annuli. Indeed, in [29] it was proved that there exist free boundary minimal annuli immersed in \mathbb{B}^3 that are very close to the universal cover of the critical catenoid. The method in [29] also allowed to check existence by an intermediate value argument for some particular rational periods, e.g. for a period $3/5$, but it did not supply a complete description of the space of such free boundary minimal annuli. It was conjectured in [29] that there exists a certain number $P^* \approx 0.6662 < \frac{2}{3}$ such that any rational number in the interval $(\frac{1}{2}, P^*)$ is the period of some free boundary minimal annulus in \mathbb{B}^3 , and that all free boundary examples in [29] belong to the same real analytic family.

The technique introduced in the proof of Theorem 6.1.1 can be used to prove this conjecture. Specifically:

Theorem 6.8.1. *Denote $\mathcal{J} := (\frac{1}{2}, P^*) \subset (\frac{1}{2}, \frac{2}{3})$, where $P^* \approx 0.6662$ is the value described above. Then, there exists a real analytic family of minimal surfaces in \mathbb{R}^3 , $\{\Sigma^\nu : \nu \in \mathcal{J}\}$, diffeomorphic to a strip $[0, 1] \times \mathbb{R}$, with the following properties.*

1. *The boundary components $\partial\Sigma_1^\nu, \partial\Sigma_2^\nu$ of Σ^ν both lie in $\partial\mathbb{B}^3$, and Σ^ν intersects $\partial\mathbb{B}^3$ orthogonally along them.*
2. *For any $\nu = m/n \in \mathbb{Q} \cap \mathcal{J}$, the strip Σ^ν covers an immersed free boundary minimal annulus in \mathbb{B}^3 with a prismatic symmetry group of order $4n$, and such that the rotation index of the planar geodesic $\Sigma^\nu \cap \{x_3 = 0\}$ is $-m$.*
3. *As $\nu \rightarrow P^*$, the strip Σ^ν converges to the universal cover of the critical catenoid.*
4. *As $\nu \rightarrow 1/2$, the strip Σ^ν converges to a collection of infinitely many flat vertical disks equiangularly distributed in a tangential way along the equator $\partial\mathbb{B}^3 \cap \{x_3 = 0\}$.*

In [43], Kapouleas and McGrath constructed immersed free boundary minimal annuli in \mathbb{B}^3 following a desingularization procedure starting from a collection of flat vertical disks joined by necks of half-catenoids. It is not clear from their construction

if these examples are part of the family of minimal annuli with spherical curvature lines constructed by Fernández, Hauswirth and Mira in [29]. Theorem 6.8.1 does not clarify this completely, but it shows that there exist examples within the general family of surfaces with spherical curvature lines in [29] that have the exact geometric behaviour as the ones in [43]. So, it is strongly expected that the examples of free boundary minimal annuli in \mathbb{B}^3 constructed in [43] lie in the family given by Theorem 6.8.1 above, and correspond to examples with ν close to $1/2$.

The topic of embedded capillary minimal surfaces in \mathbb{B}^3 is still undeveloped. For instance, there are no known examples, other than the free boundary ones, with a topological type different from a disk or an annulus. In this sense, it seems interesting to try to construct this type of examples by using min-max theory, in analogy with the free boundary case [10, 11, 30, 31, 50].

We finally discuss the overdetermined problem for $\Delta u + 2u = 0$ in \mathbb{S}^2 studied in Section 6.7. Our Theorem 6.7.1 presents new features with respect to previous existence results for overdetermined elliptic problems. To explain this, it is interesting to compare it with two relevant recent works on the topic.

One is the work [28] by Fall, Mindlind and Werth explained in the introduction, where they construct Schiffer ring domains in \mathbb{S}^2 . The second one is the paper [25] by Enciso, Fernández, Ruiz and Sicbaldi, where they construct non-rotational ring domains in \mathbb{R}^2 admitting Neumann eigenfunctions that are constant on each boundary component. These works rely on Crandall-Rabinowitz bifurcation with respect to some radial solution of the corresponding equation $\Delta u + \lambda u = 0$. In particular, the ring domains constructed in these papers must be close enough to a radial annulus.

In contrast, the Schiffer-Robin annuli in \mathbb{S}^2 that we construct in Theorem 6.7.1 are not subject to that limitation. Even though they can indeed be seen as bifurcation branches of radial annuli, we can furthermore control their existence throughout the complete space of solutions, until reaching the singular configuration of tangent vertical geodesic disks of \mathbb{S}^2 on the other side of this space. In particular, these annuli are in general far away from radial ones. This novelty seems interesting for other overdetermined problems, since it might indicate the general behavior of bifurcation branches from radial annuli.

The shape of the space of ring domains $\Omega_n(a) \subset \mathbb{S}^2$ for each fixed n resembles the geometry of Delaunay hypersurfaces, i.e., rotational CMC hypersurfaces in \mathbb{R}^n . The space of such hypersurfaces interpolates between a cylinder and a chain of tangent spheres along the rotation axis. In this sense, our annuli in Theorem 6.7.1 can also be seen as *desingularizations* of a singular configuration of tangent geodesic disks in \mathbb{S}^2 .

Regarding Souam's conjecture (see Conjecture 1.5), it is interesting to find counterexamples beyond the ring domains $\Omega_n(a) \subset \mathbb{S}^2$ in Theorem 6.7.1; e.g., domains with a more complicated topology. For smooth annular regions Ω in \mathbb{S}^2 , it is natural to conjecture that if the overdetermined problem (6.80) can be solved in $\Omega \subset \mathbb{S}^2$, then Ω must be radial or one of the ring domains $\Omega_n(a)$.

Bibliography

- [1] U. Abresch, Constant mean curvature tori in terms of elliptic functions, *J. Reine Angew. Math.* **394** (1987), 169–192.
- [2] F. Almgren, Some interior regularity theorems for minimal surfaces and an extension of Bernstein’s theorem, *Ann. Math.* **84** (1966), 277–292.
- [3] L. Ambrozio, I. Nunes, A gap theorem for free boundary minimal surfaces in the three-ball, *Comm. Anal. Geom.* **29** (2021), 283–292.
- [4] B. Andrews, H. Li, Embedded constant mean curvature tori in the 3-sphere, *J. Diff. Geom.* **99** (2015), 169–189.
- [5] R. Bettiol, P. Piccione, B. Santoro, Deformations of free boundary CMC hypersurfaces, *J. Geom. Anal.* **27** (2017), 3254–3284.
- [6] S. Brendle, Embedded minimal tori in \mathbb{S}^3 and the Lawson conjecture, *Acta Math.* **211** (2013), 177–190.
- [7] A. Bobenko, All constant mean curvature tori in \mathbb{R}^3 , \mathbb{S}^3 , \mathbb{H}^3 in terms of theta-functions, *Math. Ann.* **290** (1991), 209–245.
- [8] R.L. Bryant, Surfaces of mean curvature one in \mathbb{H}^3 , *Astérisque*, 154-155 (1987), 321–347.
- [9] C. A. T. Cardona, Non-existence of free boundary minimal Möbius bands in the unit three-ball, *Proc. Amer. Math. Soc.* **153** (2025), 2185-2198.
- [10] A. Carlotto, G. Franz, M.B. Schulz, Free boundary minimal surfaces with connected boundary and arbitrary genus. *Cambridge J. Math.* **10** (2022), 835–857.
- [11] A. Carlotto, M.B. Schulz, D. Wiygul, Infinitely many pairs of free boundary minimal surfaces with the same topology and symmetry group, *Mem. Amer. Math. Soc.*, to appear, arXiv:2205.04861.

- [12] M.P. do Carmo, *Differential Geometry of Curves and Surfaces* Prentice Hall (1976).
- [13] M.P. do Carmo, M. Dajczer, Rotation hypersurfaces in spaces of constant curvature, *Trans. Amer. Math. Soc.* **277** (1983), 685–709.
- [14] M.P. Cavalcante, D.F. de Oliveira, Index estimates for free boundary constant mean curvature surfaces, *Pacific J. Math.* **305** (2020), 153–163.
- [15] A. Cerezo, Free boundary minimal annuli in geodesic balls of \mathbb{H}^3 , preprint (2025), arXiv:2502.20303.
- [16] A. Cerezo, Free boundary saddle disks and Möbius bands immersed in the unit ball, in preparation (2025).
- [17] A. Cerezo, I. Fernández, P. Mira, Annular solutions to the partitioning problem in a ball, *J. Reine Angew. Math.*, to appear, arXiv:2212.07986.
- [18] A. Cerezo, I. Fernández, P. Mira, Free boundary CMC annuli in spherical and hyperbolic balls. *Calc. Var.* **64**, 37 (2025).
- [19] A. Cerezo, I. Fernández, P. Mira, Schiffer-Robin ring domains in the 2-sphere, in preparation (2025).
- [20] R. Courant, The existence of minimal surfaces of given topological structure under prescribed boundary conditions, *Acta Math.* **72** (1940), 51–98.
- [21] G. Darboux, *Leçons sur la théorie générale des surfaces*, Vol. III, Gautier-Villars, Paris (1995).
- [22] B. Devyver, Index of the critical catenoid, *Geom. Dedicata* **199** (2019), 355–371.
- [23] H. Dobriner, Die Flächen Constanter Krümmung mit einem System Sphärischer Krümmungslinien dargestellt mit Hilfe von Theta Functionen Zweier Variabeln, *Acta Math.* 9 (1886), 73-104.
- [24] H. Dobriner, Die Minimal Flächen mit einem System Sphärischer Krümmungslinien, *Acta Math.* 10 (1887), 145-152.
- [25] A. Enciso, M. Fernández, D. Ruiz, P. Sicbaldi, A Schiffer-type problem for annuli with applications to stationary planar Euler flows. *Duke Math. J.*, 174 (6) (2025), 1151-1208.

- [26] A. Enneper, Untersuchungen über die Flächen mit planen und sphärischen Krümmungslinien, *Abh. Königl. Ges. Wissensch. Göttingen* 23 (1878) and 24 (1880).
- [27] J.M. Espinar, D. Marín, An overdetermined eigenvalue problem and the Critical Catenoid conjecture, preprint, arXiv:2310.06705.
- [28] M. M. Fall, I. A. Minlend T. Weth, The Schiffer problem on the cylinder and on the 2-sphere, *J. Eur. Math. Soc.* (2025).
- [29] I. Fernández, L. Hauswirth, P. Mira, Free boundary minimal annuli immersed in the unit ball, *Arch. Rational Mech. Anal.* **247** (2023), 108.
- [30] G. Franz, D. Ketover, M.B. Schulz: Genus one critical catenoid, preprint (arxiv: 2409.12588).
- [31] G. Franz, M.B. Schulz: Topological control for min-max free boundary minimal surfaces, preprint (arxiv: 2307.00941).
- [32] A. Fraser, Extremal Eigenvalue Problems and Free Boundary Minimal Surfaces in the Ball, in: *Geometric Analysis, Lecture Notes in Mathematics* **2263**, Springer.
- [33] A. Fraser, M. Li, Compactness of the space of embedded minimal surfaces with free boundary in three-manifolds with nonnegative Ricci curvature and convex boundary, *J. Differential Geom.* **96** (2014), 183–200.
- [34] A. Fraser, R. Schoen, The first Steklov eigenvalue, conformal geometry, and minimal surfaces, *Adv. Math.* **226** (2011), 4011–4030.
- [35] A. Fraser, R. Schoen, Sharp eigenvalue bounds and minimal surfaces in the ball, *Invent. Math.* **203** (2016), 823–890.
- [36] A. Folha, F. Pacard, T. Zolotareva, Free boundary minimal surfaces in the unit 3-ball, *Manuscripta Math.* **154** (2017), 359–409.
- [37] J. A. Gálvez, P. Mira, M. P. Tassi, Analytic saddle spheres in \mathbb{S}^3 are equatorial, *Math. Ann.* 389, 3865–3884 (2024).
- [38] J. Guo, G. Wang, C. Xia, Stable capillary hypersurfaces supported on a horosphere in the hyperbolic space, *Adv. Math.* **409** (2022), 108641.
- [39] Y. He, Constant Mean Curvature Surfaces bifurcating from Nodoids, PhD dissertation, Technische Universität Darmstadt (2012).

- [40] N. Hitchin, Harmonic maps from a 2-torus to the 3-sphere, *J. Diff. Geom.* **31** (1990), 627–710.
- [41] H. Hopf, *Differential Geometry in the Large, volume 1000 of Lecture Notes in Math.* Springer-Verlag (1989).
- [42] H. Hopf, Über Flächen mit einer Relation zwischen den Hauptkrümmungen, *Math. Nachr.* **4** (1951), 232–249.
- [43] N. Kapouleas, P. McGrath, Free boundary minimal annuli immersed in the unit 3-ball, preprint (2022), arXiv:2212.09680.
- [44] N. Kapouleas, P. McGrath, Generalizing the Linearized Doubling approach, I: General theory and new minimal surfaces and self-shrinkers, *Cambridge J. Math.* **11** (2023), 299–439.
- [45] N. Kapouleas, M. Li, Free boundary minimal surfaces in the unit three-ball via desingularization of the critical catenoid and the equatorial disc, *J. Reine Angew. Math.* **776** (2021), 201–254.
- [46] N. Kapouleas, D. Wiygul, Free boundary minimal surfaces with connected boundary in the 3-ball by tripling the equatorial disc, *J. Differential Geom.*, **123** (2023), 311–362.
- [47] N. Kapouleas, J. Zou, Free Boundary Minimal surfaces in the Euclidean Three-Ball close to the boundary, preprint, arXiv:2111.11308.
- [48] M. Karpukhin, R. Kusner, P. McGrath, D. Stern, Embedded minimal surfaces in S^3 and B^3 via equivariant eigenvalue optimization, preprint, arXiv:2402.13121.
- [49] M. Karpukhin, D. Stern, From Steklov to Laplace: free boundary minimal surfaces with many boundary components, *Duke Math. J.*, **173** (2024) 1557–1629.
- [50] D. Ketover, Free boundary minimal surfaces of unbounded genus, preprint, arXiv:1612.08691.
- [51] M. Kilian, G. Smith, On the elliptic sinh-Gordon equation with integrable boundary conditions, *Nonlinearity*, **34** (2021), 5119.
- [52] S.G. Krantz, H.R. Parks, A primer of real analytic functions, Birkhäuser Advanced Texts, Basler Lehrbücher, 1992.

- [53] S. Kumaresan, J. Prajapat, Serrin's result for hyperbolic space and sphere, *Duke Math. J.* **91** (1998), 17–28.
- [54] H.B. Lawson, Complete minimal surfaces in \mathbb{S}^3 , *Ann. of Math.*, **92** (1970) 335–374.
- [55] M. Li, Free boundary minimal surfaces in the unit ball: recent advances and open questions. In: Proceedings of the International Consortium of Chinese Mathematicians, 2017 (First Annual Meeting), International Press of Boston, Inc., pp. 401–436 (2020).
- [56] H. Li, C. Xiong, A gap theorem for free boundary minimal surfaces in geodesic balls of hyperbolic space and hemisphere, *J. Geom. Anal.* **28** (2018), 3171–3182.
- [57] V. Lima, A. Menezes, Eigenvalue problems and free boundary minimal surfaces in spherical caps, preprint (2023), arXiv:2307.13556.
- [58] R. Mazzeo, F. Pacard, Bifurcating nodoids. In Topology and geometry: commemorating SISTAG, Contemporary Mathematics, vol. 314 (American Mathematical Society, Providence, RI, 2002), 169–186.
- [59] P. McGrath, A characterization of the critical catenoid, *Indiana Univ. Math. J.* **67** (2018), 889–897.
- [60] V. Medvedev, On free boundary minimal submanifolds in geodesic balls in \mathbb{H}^n and \mathbb{S}_+^n , *Math. Z.* **310**, 10 (2025).
- [61] S.H. Min, K. Seo, Free boundary constant mean curvature surfaces in a strictly convex three-manifold. *Ann. Global Anal. Geom.* **61** (2022), 621–639.
- [62] J.C.C. Nitsche, Stationary partitioning of convex bodies, *Arch. Rat. Mech. Anal.* **89** (1985), 1–19.
- [63] U. Pinkall, I. Sterling, On the classification of constant mean curvature tori, *Ann. Math.* **130** (1989), 407–451.
- [64] U. Pinkall, I. Sterling, Computational aspects of soap bubble deformations, *Proc. Amer. Math. Soc.* **118** (1993), 571–576.
- [65] D.H. Seo, Sufficient symmetry conditions for free boundary minimal annuli to be the critical catenoid, preprint, arXiv:2112.11877.

- [66] A. Ros, R. Souam, On stability of capillary surfaces in a ball, *Pacific J. Math.* **178** (1997), 345–361.
- [67] A. Ros, E. Vergasta, Stability for hypersurfaces of constant mean curvature with free boundary, *Geom. Dedicata* **56** (1995) 19–33.
- [68] M. Ruivo de Oliveira, New free boundary minimal annuli of revolution in the 3-sphere, preprint (2024), arXiv:2404.12304.
- [69] M.B. Schulz, *Geometric Analysis Gallery*. URL: <https://mbschulz.github.io>. Last visited on July, 2025.
- [70] R. Souam, Schiffer’s Problem and an isoperimetric inequality for the first buckling eigenvalue of domains on \mathbb{S}^2 , *Ann. Global Anal. Geom.* **27** (2005), 341–354.
- [71] R. Souam, On stability of stationary hypersurfaces for the partitioning problem for balls in space forms, *Math. Z.* **224** (1997), 195–208.
- [72] R. Walter, Explicit examples to the H -problem of Heinz Hopf, *Geom. Dedicata* **23** (1987), 187–213.
- [73] R. Walter, Constant mean curvature tori with spherical curvature lines in noneuclidean geometry, *Manuscripta Math.* **63** (1989), 343–363.
- [74] G. Wang, C. Xia, Uniqueness of stable capillary hypersurfaces in a ball. *Math. Ann.* **374** (2019), 1845–1882.
- [75] H.C. Wente, Counterexample to a conjecture of H. Hopf, *Pacific J. Math.* **121** (1986), 193–243.
- [76] H.C. Wente, Constant mean curvature immersions of Enneper type, *Mem. Amer. Math. Soc.* **478** (1992).
- [77] H.C. Wente, Tubular capillary surfaces in a convex body. Advances in geometric analysis and continuum mechanics, Edited by P. Concus and K. Lancaster, International Press 1995, 288–298.
- [78] S.T. Yau, Problem section, in *Seminar on differential geometry*, Ann. of Math. Stud. **102**, Princeton Univ. Press, Princeton, 1982, 669–706.